Copyright Warning & Restrictions

The copyright law of the United States (Title 17, United States Code) governs the making of photocopies or other reproductions of copyrighted material.

Under certain conditions specified in the law, libraries and archives are authorized to furnish a photocopy or other reproduction. One of these specified conditions is that the photocopy or reproduction is not to be "used for any purpose other than private study, scholarship, or research." If a, user makes a request for, or later uses, a photocopy or reproduction for purposes in excess of "fair use" that user may be liable for copyright infringement,

This institution reserves the right to refuse to accept a copying order if, in its judgment, fulfillment of the order would involve violation of copyright law.

Please Note: The author retains the copyright while the New Jersey Institute of Technology reserves the right to distribute this thesis or dissertation

Printing note: If you do not wish to print this page, then select "Pages from: first page # to: last page #" on the print dialog screen

THE EFFECT OF ULTRASONIC VIBRATIONS ON HETEROGENEOUS CATALYSIS

BY

WILLIAM LINTNER, JR.

A DISSERTATION

PRESENTED IN PARTIAL FULFILLMENT OF

THE REQUIREMENTS FOR THE DEGREE

OF

DOCTOR OF ENGINEERING SCIENCE

AT

NEWARK COLLEGE OF ENGINEERING

Newark, New Jersey
1973

ABSTRACT

The effect of ultrasonic vibrations on the vapor phase decomposition of cumene to benzene and propylene was investigated employing silica-aluminum cracking catalyst.

The catalytic reactor consisted of a 1 cm. diameter stainless steel tube containing a 20 in. long preheater and a 4 in. long catalyst chamber. The catalyst bed was irradiated from above by means of an ultrasonic horn which transmitted acoustical energy directly into the vapor.

The reactor was run at temperatures of 650°F. and 1050°F., frequencies of 26,000 cps and 39,000 cps, feed rates of 20 to 600 gms./hr., power outputs of 0.5 to 1.3 watts/cm.^{2}, and catalyst loadings of approximately 1 to 6 grams.

At temperatures and flow rates where external bulk diffusion controlled the rate of reaction, the application of ultrasound resulted in increases in the mass transfer coefficient up to 40%. In the area where surface reaction and internal pore diffusion controlled, the combined catalyst effectiveness factor - surface reaction rate constant was increased by up to 160%.

Confidence intervals were calculated for the coefficients of the equations expressing log k_g as a function of T and log $\mathcal{E}Lk_2$ as a function of $\frac{1}{T}$. The analysis of

variance indicated that the increases in mass transfer coefficients and combined catalyst effectiveness factor - surface reaction rate constants were significant at ultrasonic frequencies of 39,000 cps. The increases obtained between frequencies of 26,000 cps and no ultrasound were of lesser significance.

It is postulated that ultrasound causes acoustic streaming within the reactor tube and catalyst pores, resulting in higher transport rates caused by the combined effect of diffusion and forced convection as compared to the effect of diffusion alone in the absence of ultrasound. In addition, acoustic energy may cause localized heating within the catalyst bed, thereby increasing the rate of surface reaction.

APPROVAL OF DISSERTATION

THE EFFECT OF ULTRASONIC VIBRATIONS

ON HETEROGENEOUS CATALYSIS

BY

WILLIAM LINTNER, JR.

FOR

DEPARTMENT OF CHEMICAL ENGINEERING

NEWARK COLLEGE OF ENGINEERING

BY

FACULTY COMMITTEE

APPROVED: _____ CHAIRMAN

_____

_____

_____

_____

NEWARK, NEW JERSEY

JUNE, 1973

ACKNOWLEDGMENTS

Many people have given assistance and guidance to the author during almost four years of investigation and it is almost impossible to acknowledge them all. However, the author thanks particularly his advisor, Dr. Deran Hanesian, for his most valuable help from inception to completion of this work.

The author also expresses his sincere appreciation to Mr. Arnold Stewart, Mr. Gerard Gilkie and Mr. James Nickolson of Macrosonic International, and Dr. Carl Bertsch, formerly of Newark College of Engineering, for their advice in designing the experimental equipment.

He also acknowledges the aid of Mr. Donald Friedeman in constructing the equipment, and the generosity of Dr. Dimitrios Tassios for lending his gas chromatograph for the analytical work. He further acknowledges the generous assistance of Mr. Richard Robertson for helping him employ the computer program for correlation of data.

The author is deeply grateful to his wife, Doris, for typing this dissertation and to his son, William, who inked most of the data curves.

Finally, the author especially thanks his company, L & L Chemical Construction & Engineering Co., for granting him a leave of absence in order to fulfill his residency requirement, and du Pont for their fellowship which helped immensely with the financial burden.

TABLE OF CONTENTS

TABLE OF CONTENTS (continued)

TABLE OF CONTENTS (continued)

LIST OF FIGURES

LIST OF FIGURES (continued)

LIST OF TABLES

CHAPTER I

INTRODUCTION

Purpose and Scope of Investigation

Considerable information is available in the literature concerning the use of ultrasonic vibrations as an analytical tool and as a source of energy. Although most earlier references describe the passive applications of ultrasound, whereby the propagation characteristics of the sound wave are employed, the field has recently expanded into active applications of acoustical energy. These active applications now include the effect of ultrasonic vibrations on chemical reactions. Although considerable information is available concerning sonochemical reactions, much of the data and results are contradictory and almost all the experimentation deals with uncatalyzed liquid phase reactions.

It therefore appeared to this author that because of the paucity of quantitative data a most interesting and challenging research would be the study of the effect of ultrasonic vibrations on heterogeneous catalysis, or more specifically, the effect of ultrasound on the catalytic cracking of cumene.

Selection of system. The cumene system was selected for this study because of the following reasons:

1. Thermal cracking of cumene is negligible at the temperatures employed (650°-1050°F.).
2. The reaction is essentially clean with a minimum production of side products.
3. The reaction mechanism was determined by Garver[22] in 1955 and published in his Doctoral Thesis, thus providing an experimental base.
4. One literature reference published by Zhorov[97] in 1967 indicates that ultrasound effects the rate of this reaction, thereby providing this author with some indication of success.

Investigation plan. The plan of the investigation was to repeat some of Garver's work to obtain a firm basis for the reaction mechanism in the absence of ultrasound, and then to apply acoustical energy to the reaction and attempt to determine the following effects:

1. The effect of ultrasound on the rate of reaction.
2. The effect of ultrasound on the kinetic rate constant and the external diffusion coefficient.

Literature Survey

Early references. Literature references to ultrasonic vibrations, or more accurately acoustical energy, occur as early as 1927. At that time, Wood[92] developed a piezoelectric oscillator of quartz which produced frequencies up to 300,000 cps. It is now possible to produce frequencies

of over 9 x 10^{10} cps. Frequency ranges between 20,000 and 10^{9} cps are referred to as ultrasonic and ranges above 10^{9} cps are referred to as hypersonic. This investigation deals with the ultrasonic range between 20,000 and 50,000 cps.

Classification of acoustical energy. Acoustical energy is generally classified according to its application. Passive applications include those by which the propagation characteristics of the sound wave are employed and active applications are those by which the sound is used as a source of energy. Greguss[26] has classified several applications of acoustical energy according to the frequency employed. This classification is shown in Table 1. It is interesting to note that when Greguss prepared this summary in 1963, sonochemical effects were limited to liquid phase investigations only.

In addition to frequency, the second important variable in the study of acoustical energy is sound intensity.[71] The intensity of audible sound lies between 10^{-16} and 10^{-4} watts/cm.^{2}, with the latter value being the threshold of pain. Sound intensities of 120,000 watts/cm.^{2} at a frequency of 500,000 cps have been produced in liquids at the Moscow Acoustical Institute. However, the intensities most frequently applied in sonochemical research are those between 1 and 10 watts/cm.^{2} Peak intensities of up

TABLE 1

APPLICATIONS OF ACOUSTICAL ENERGY

Passive Applications	Physical State of Matter	Frequency cps
1. Theoretical solid state research	Solid	10^9-10^{11}
2. Computers	Solid	10^7-10^9
3. Non-destructive testing	Solid	10^5-10^8
4. Medical diagnostics	Solid and Liquid	10^5-10^7
5. Viscoelastic research	Solid	up to 10^6
6. Seismic research	Solid	up to 10^4
7. Measurements, remote control	Liquid and Gas	10^5-10^9
8. Flow measurements	Liquid	10^3-10^5
9. Viscosity measurements	Liquid	10^3-10^5
10. Level determinations	Liquid	10^5-10^7

TABLE 1 (continued)

APPLICATIONS OF ACOUSTICAL ENERGY

Active Applications	Physical State of Matter	Frequency cps
1. Effect on alloys	Solid and Liquid	up to 10^5
2. Fatigue research	Solid	up to 10^5
3. Colloid chemistry	Solid, Liquid and Gas	up to 10^6
4. Therapeutical applications	Solid and Liquid	10^5-10^7
5. Boiler scale prevention	Liquid	10^4-10^5
6. Effect on combustion processes	Gas	up to 10^4
7. Biochemical effects	Liquid	10^5-10^7
8. Sonochemical effects	Liquid	up to 10^8

to 1.3 watts/cm.^{2} were studied in this investigation because this was the limitation of the equipment employed.

Liquid phase reactions. Many investigations have been reported in the literature describing the effect of ultrasound on liquid phase chemical reactions, but, unfortunately, much of this work has led to erroneous conclusions and contradictory results. For example, Shaw[73] reported in 1967 that ultrasound caused scissions of the polymer chain in polysiloxane solutions. He further found that doubling the acoustic intensity at 20,000 cps doubled the degradation rate. Porter[58] confirmed this observation that same year when he reported that the average molecular weight of polyisobutylene dissolved in trichlorobenzene was decreased from 466,000 to 20,600 by irradiation with ultrasound. Peacocke[54] explained this phenomenum in 1968 as a result of his studies of the effect of ultrasound on such linear macromolecules as DNA by stating that the degradation is caused by stresses resulting from the relative movement of the macromolecule and the solvent molecule.

In contradiction to these observations, Makeeva[40] reported in 1967 that polyvinyl chloride prepared by the bulk polymerization of vinyl chloride and exposed to ultrasound had a higher molecular weight and fewer branches. Heymach[28] appeared to add to the confusion

when he reported that cavitation resulting from the application of intense acoustical energy selectively degraded polymers by fracturing longer chains at a faster rate than shorter chains. He concluded that ultrasonic irradiation may be a means of sharpening molecular weight distributions.

Effect on reaction rates. In addition to experimentation in the area of polymers and polymerization, many investigators were interested in the effect of ultrasound on reaction rates. Since it was early in the study of this new form of energy, most investigators made no attempt to explain the individual effects of intensity and frequency. For example, in 1965 Mario[44] reported that the reaction kinetics of the hydrolysis of aspirin are pseudo first order with or without ultrasound. He found that the reaction rate was increased with the application of ultrasound.

In 1966, Manu[42] reported that ultrasound at 1,000,000 cps and 4 to 12 watts/cm.^{2} increased the reaction rate of the oxidation of the aldehyde group in glucose. In 1968, Stolyarov[77] noted that ultrasound at frequencies of 20,000 to 100,000 cps increased the oxidation rate of aluminum in water at 90°F. During that same year, Prakash[61] showed that the rate of production of iodine from cesium iodide increased with the appli-

cation of ultrasound at frequencies of 1,000,000 cps and intensities of 1.4 to 2.4 watts/cm.^{2} In 1969, Kowalska[34] noted that ultrasonic irradiation increased the oxidation rate of divalent iron to trivalent iron by 300%.

Acoustic intensity and frequency effect. As more information became available describing the effect of ultrasound on reaction kinetics, investigators became more concerned with the specific effects of intensity and frequency. Most available data indicate that increasing intensity increases the reaction rate, but the data concerning the effect of frequency on reaction rate is highly contradictory. During his study of complex ethers in 1966, Zilberg[98] found that ultrasonic intensity increased the reaction rate but frequency variations between 300,000 and 1,000,000 cps had no effect. Prakash[60] observed that increasing the intensity increased the sonochemical decomposition of $C_2H_2Br_4$. Rice[66], Sergeeva[72], Suess[78] and Geissler[23] all independently confirmed the observation that increasing ultrasonic intensity increases the reaction rate. In 1967, Chen[10] reported that the reaction rate of the hydrolysis of methyl acetate with HCl catalyst increased with increasing ultrasonic intensity, but that variations in frequency had no effect, thus confirming Zilberg's work. However, in 1968, Saracco[68] completed his study of the hydrogenation of olive oil in

cyclohexane with Raney nickel catalyst and ultrasound. He discovered that the reaction rate reached a maximum with increasing intensity and then decreased at any frequency. He further observed that maximum reaction rates were obtained at frequencies of 500,000 cps. Finally, Paryjczak[53] reported that the zero order rate constant for the sono-oxidation of $FeCl_2$ decreased with increasing frequency.

Theory developments. In spite of these contradictory conclusions, many investigators attempted to develop theories to explain the sonochemical effect. In 1950, Weissler[91] proposed that the chemical reaction rate under the influence of ultrasound is a function of the sound intensity, duration of exposure, pressure, temperature and volume. In 1965, Nosov[49] added the proposal that intramolecular rearrangements and cavitation are the effects of the application of ultrasound to chemical reactions. He further stated that electrical discharges occur within the cavitation bubbles which ionize the solvent and solutes, producing highly reactive free radicals. Fogler[19] agreed with the theory that cavitation increases reaction rates as a result of his experimentation with the liquid phase hydrolysis of methyl acetate. Currell[13] produced acetylene by the ultrasonic cleavage of cyclohexanol. His results were also consistent with the theory that the

sonochemical reaction takes place within the cavitation bubbles. Kessler[32] was able to promote the chemical decomposition of tetralin and methyl naphthalene by ultrasonic irradiation at frequencies of 80,000 cps. Griffing[27] finally proposed that ultrasound causes cavitation and luminescence simultaneously. Luminescence may be caused by electrical charges within the cavitation bubble or by extremely high temperatures within the bubble. The cavitation bubbles then act as hot spots which may promote or enhance chemical reactions.

Prakash[60] found that the sonochemical decomposition of $C_2H_2Br_4$ increases with increasing ultrasonic intensity. He theorized that ultrasonic energy caused the formation of free radicals within the cavitation bubble. Tuchel[86] concurred with the free radical theory as a result of his experimentation with potassium iodide solution oxidations irradiated with ultrasound at frequencies of 870,000 cps. In 1968, Margulis[43], Maltsev[41] and Tuxzynski[87] independently arrived at the conclusion that reaction rate enhancement is due to the formation of free radicals within the cavitation holes.

In addition to the hot spot and free radical theories associated with the cavitation phenomenon, some investigators proposed other theories to explain the effect of ultrasound on the rate of chemical reactions. For example,

Vladar[89] continuously produced $Ca(OH)_2$ from pure $CaCO_3$ and CO_2 in a tubular reactor and found that ultrasound increased the rate of carbonation. He theorized that the ultrasonic energy reduced the particle size of the solids resulting in a higher reaction rate. Gindis[24] studied the effect of ultrasound on the electrochemical oxidation of K_2MnO_4 to $KMnO_4$ at frequencies of 20,000 cps and 25 to 30 watts/liter. He found that the degree of oxidation at the anode was increased by 10% to 65% and concluded that ultrasound increased the current efficiency of the electrolyte by that amount. Needham[48] applied ultrasound to aspirin in ethanol-water solution and found that although the same reaction order was maintained, the rate of degradation increased. Needham theorized that ultrasound lowered the activation energy, increased the rate of molecular collisions, and increased the rate of movement of the products away from each other.

Diffusion theory. In 1968, Belov[3] proposed that ultrasound causes higher reaction rates by acceleration of diffusional processes. In 1969, Kowalska[34], as a result of his studies of the application of ultrasonic fields to the oxidation of Fe^{++} to Fe^{+++}, also concluded that ultrasound decreases the thickness of the diffusion layer. This work, in addition to other confirming evidence, led this author to believe that ultrasound would effect the

rate of diffusion controlled solid-catalyzed gaseous reactions.

Catalyst activity. During the time when many investigators were studying the effect of ultrasound on uncatalyzed liquid phase reactions, some scientists experimented with the effect of ultrasound on catalysts. For example, Berger[4] regenerated some catalysts at 900° to 1000°C. in the presence of ultrasound at 20 to 100 watts/cm.^{2} and found that the catalytic activity was enhanced. Slaczka[75] irradiated nickel and cobalt catalysts with ultrasound during their preparation by the reduction of oxylates and found that their catalytic activity were increased. He concluded that the ultrasonic energy at frequencies of 25,000 cps and 0.3 watts/cm.^{2} caused an increase in the number of crystal defects, thus enhancing the activity. In 1960, Jones[30] fastened one end of a bundle of catalytically coated wires to an ultrasonic driver while the other end was suspended in a reactor. He noted that the catalytic activity was enhanced for the preparation of ammonia from nitrogen and hydrogen when ultrasonic energy at frequencies of 500 to 300,000 cps was applied.

Gas phase reactions. In 1967, Zhorov[97] studied the effect of ultrasound on the catalytic cracking of cumene. Zhorov proposed that the rate of reaction was controlled

by the diffusion rate of the reactants and products to and from the catalyst surface. He discovered that the diffusion rate, and hence the rate of reaction, could be increased by the application of ultrasonic vibrations.

Zhorov's equipment consisted of a continuous reactor in which he placed 7.9 gms. of aluminum-silicate catalyst. Cumene was fed into the reactor at a feed rate of 3.0 $\frac{\text{gm moles}}{\text{hr.}}$ ($W/F_{A_o} = 9{,}468 \frac{\text{gm cat-sec.}}{\text{gm mole}}$) and cracked at 878°F. The reactor was operated without ultrasound for the first half hour and then ultrasonic energy was applied for the second half hour at a frequency of 20,000 cps and an amplitude of 5 to 6 microns.

Analysis of the liquid product (a mixture of cumene and benzene) indicated that the concentration of benzene increased by 20% as a result of the application of ultrasound. This result serves as the basis for this author's research.

Reaction mechanism. Before any attempt is made to isolate the effect of ultrasound on the catalytic cracking of cumene, it is necessary to first determine the reaction mechanism of this system in the absence of ultrasonic energy. Considerable work was completed in this area from 1949 through 1967 by such investigators as Greensfelder[25], Topchieva[82,83], Corrigan[12], Rase[64], Garver[22], Panchenkov[50], Perrin[55], Zhorov[95,96,97], Pansing[51] and Spozhakina[76]. One of the

most complete investigations was published by Garver in his Doctoral Dissertation of 1955. Garver determined that the reaction mechanism for the cracking of cumene on silica-alumina catalyst at 850°F., 950°F. and 1050°F. was single site with surface reaction controlling and propylene not adsorbed. His experimentation also lead to the determination of the reaction rate constants.

This author's plan was to extend the work of Zhorov into a more detailed quantitative study of the effect of ultrasound on the solid catalyzed cumene reaction employing Garver's work as the basic starting point. This detailed investigation had never been studied previously as witnessed by the absence of published information concerning the effect of ultrasound on solid-catalyzed gaseous reactions.

Discussion

Ultrasound may increase the rate of a heterogeneous solid catalyzed gas reaction by one or more of the following methods.

1. Increase the number of active sites on the catalyst surface.
2. Increase the rate of diffusional processes:
    A. External bulk diffusion
    B. Internal pore diffusion
3. Decrease the reaction activation energy.
4. Increase the surface reaction rate.

5. Increase the pressure at the mouth of the catalyst pore by the application of acoustic energy.
6. Develop localized thermal effects by the application of ultrasonic energy.

Internal pore diffusion, the surface reaction rate and the number of active sites are described in a single constant, $\epsilon L k_2$, the reaction rate constant. If ultrasonic energy affects any of these three parameters and the data fit the reaction rate model at high flow rates, then $\epsilon L k_2$ can be calculated.

External bulk diffusion is proportional to the mass transfer coefficient, k_g. At low flow rates, mass transfer controls the rate of reaction, and therefore the effect of ultrasound on k_g can be measured at low flow rates.

Acoustic pressure can be calculated and, in fact, the variations in pressure at the mouth of the catalyst pore as a result of the application of ultrasonic energy will be shown to be negligible for the power employed in this investigation.

Localized hot spots on the surface of the catalyst will result in increased surface reaction rate constants and reaction rates. Quantitative measurements of this phenomenon are not possible in this investigation, but these thermal effects will also manifest themselves in $\epsilon L k_2$, a measurable quantity.

CHAPTER II

THEORY

Continuous Reaction Model

In solid-catalyzed gas-phase reactions, reaction occurs at the gas-solid interfaces. These interfaces lie on the external surface of the catalyst particle and also on the internal surfaces within the catalyst pore. The overall rate of reaction depends upon the availability of these surfaces to the reactants.

For the continuous reaction model, it is assumed that the reaction mechanism consists of seven distinct processes with the rate of reaction controlled by the slowest process.

These processes are described in detail in Appendices III through VII and briefly outlined below.

1. Gas film diffusion of reactants.
2. Pore diffusion of reactants.
3. Adsorption of reactants.
4. Surface reaction
5. Desorption of products.

6. Pore diffusion of products.

7. Gas film diffusion of products.

Gas film diffusion. Gas film diffusion of reactants and products is handled mathematically as a single simple diffusion process. The equation describing this process is as follows:

$$r_A = \frac{p_T k_g a}{RT} \ln \left[\frac{1+Y_{A_b}}{1+Y_{A_s}} \right] \qquad (1)$$

r_A = gm moles cumene diffusing toward catalyst surface per second per gm. catalyst, $\frac{\text{gm moles}}{\text{gm-sec.}}$

p_T = total pressure, atm.

k_g = mass transfer coefficient, $\frac{\text{cm.}}{\text{sec.}}$

$= \frac{D_{AB}}{\delta_f}$

D_{AB} = diffusivity of cumene in cumene, benzene and propylene, $\frac{\text{cm.}^2}{\text{sec.}}$

δ_f = thickness of stagnant gas film between main gas stream and external surface of catalyst, cm.

a = superficial surface area of catalyst, $\frac{\text{cm.}^2}{\text{gm.}}$

R = 82.06 $\frac{\text{cm.}^3\text{-atm.}}{\text{gm mole-}^\circ\text{K.}}$

T = $^\circ$K.

Y_{A_b} = mole fraction cumene in main gas stream, dimensionless

Y_{A_s} = mole fraction cumene on catalyst surface, dimensionless

Surface phenomena. The adsorption of cumene onto the catalyst surface, the reaction of cumene on the surface and the desorption of benzene from the catalyst surface are also handled together mathematically. Garver has shown that the following rate equation is consistent with a single site mechanism whereby propylene is not adsorbed and surface reaction is rate controlling.

$$(-r_{A1}) = \frac{C_L k_2 K_A \left[p_A - \frac{p_R p_S}{K} \right]}{1 + K_A p_A + K_R p_R} \qquad (2)$$

(r_{A1}) = reaction rate, $\frac{\text{gm moles A}}{\text{gm cat-sec.}}$

C_L = concentration of total active sites on catalyst surface, $\frac{\text{cm.}^2}{\text{gm cat.}}$

k_2 = forward reaction rate constant for surface reaction, $\frac{\text{gm moles}}{\text{cm.}^2\text{-sec.}}$

K_A = equilibrium adsorption constant for cumene, $\frac{1}{\text{atm.}}$

p_A = partial pressure of cumene, atm.

p_R = partial pressure of benzene, atm.

p_S = partial pressure of propylene, atm.

K_R = equilibrium adsorption constant for benzene, $\frac{1}{\text{atm.}}$

K = equilibrium constant for overall reaction, atm.

Effectiveness factor. The effect of pore diffusion

of reactants and products on the rate of reaction is expressed by applying a correction factor to the rate equation. This correction factor is known as ϵ, the effectiveness factor. The rate equation now reduces to the following expression:

$$(-r_{A1}) = \frac{\epsilon L k_2 K_A \left[p_A - \frac{p_R p_S}{K} \right]}{1 + K_A p_A + K_R p_R} \qquad (3)$$

In the case of irreversible reaction, K approaches infinity and the rate equation then becomes:

$$(-r_{A1}) = \frac{\epsilon L k_2 K_A p_A}{1 + K_A p_A + K_R p_R} \qquad (4)$$

The initial rate of reaction occurs when the partial pressure of cumene is equal to the total pressure and the partial pressures of benzene and propylene are zero.

$$r_o = \frac{\epsilon L k_2 K_A \pi}{1 + K_A \pi} \qquad (5)$$

r_{A1} = reaction rate, $\frac{\text{gm moles A}}{\text{gm cat-sec.}}$

r_o = initial reaction rate, $\frac{\text{gm moles A}}{\text{gm cat-sec.}}$

ϵ = effectiveness factor, dimensionless

L = total concentration of active sites, $\frac{\text{cm.}^2}{\text{gm cat.}}$

k_2 = forward reaction rate constant for surface reaction, $\frac{\text{gm-moles}}{\text{cm.}^2\text{-sec.}}$

K_A = equilibrium adsorption constant for cumene, $\frac{1}{\text{atm.}}$

K_R = equilibrium adsorption constant for benzene, $\frac{1}{\text{atm.}}$

K = equilibrium constant for overall reaction, atm.

p_A = partial pressure of cumene, atm.

p_R = partial pressure of benzene, atm.

p_S = partial pressure of propylene, atm.

π = total pressure, atm.

The effectiveness factor is defined as the ratio of the actual rate of reaction with pore diffusion present to the rate of reaction if the resistance caused by pore diffusion were absent. It is expressed by the following relationship wherein h_s is the Thiele Modulus:

$$\epsilon = \frac{3}{h_s}\left[\frac{1}{\tanh h_s} - \frac{1}{h_s}\right] \qquad (6)$$

$$h_s = r_p\left[\frac{k_s S_v}{D_e}\right]^{\frac{1}{2}} \qquad (7)$$

ϵ = effectiveness factor, dimensionless

h_s = Thiele Modulus, dimensionless

r_p = radius of catalyst particle, cm.

k_s = forward intrinsic rate constant for surface reaction, $\frac{\text{cm.}}{\text{sec.}}$

S_v = total surface of porous catalyst, $\frac{cm.^2}{cm.^3}$

D_e = effective pore diffusivity, $\frac{cm.^2}{sec.}$

Reaction Design Equation

The reaction design equation is obtained by substituting the rate equation into the plug flow reactor design equation.

$$\frac{W}{F_{A_o}} = \int_{X_{A_o}}^{X_{A_f}} \frac{dX_A}{(-r_{Al})} \qquad (8)$$

W = wt. catalyst, gms.

F_{A_o} = feed rate of cumene, $\frac{\text{gm moles A}}{\text{sec.}}$

X_{A_o} = initial conversion of cumene, dimensionless

X_{A_f} = final conversion of cumene, dimensionless

$(-r_{Al})$ = reaction rate, $\frac{\text{gm moles A}}{\text{gm cat-sec.}}$

Reaction design equation with external diffusion controlling. For bulk diffusion of cumene from the main gas stream to the surface of the catalyst, the integrated reactor design equation yields the following relationship for the mass transfer coefficient:

$$k_g = \frac{X_{A_b} RT}{(W/F_{A_o}) p_T a \ln\left[\frac{1+Y_{A_b}}{1+Y_{A_s}}\right]} \qquad (9)$$

After substituting the constants and employing the log mean mole fraction for the surface concentration of cumene, the equation reduces to the following:

$$k_g = \frac{6.26\ X_{A_f}\ T}{(W/F_{A_o})\ \ln\ (1+Y_{A_{LM}})} \qquad (10)$$

where,

k_g = mass transfer coefficient, $\frac{\text{cm.}}{\text{sec.}}$

X_{A_f} = final conversion of cumene, dimensionless

T = temperature, $^{o}K.$

W = wt. catalyst, gms.

F_{A_o} = initial cumene feed rate, $\frac{\text{gm moles}}{\text{sec.}}$

$Y_{A_{LM}}$ = log mean mole fraction of cumene in the bulk stream, dimensionless

R = gas constant, 82.06 $\frac{\text{cm.}^3\text{-atm.}}{\text{gm mole-}^{o}\text{K.}}$

p_T = total pressure, atm.

a = superficial surface area of catalyst, $\frac{\text{cm.}^2}{\text{gm}}$

Y_{A_b} = mole fraction cumene in bulk stream, dimensionless

Y_{A_s} = mole fraction cumene at catalyst surface, dimensionless

Reaction design equation with surface reaction controlling. For reversible reaction, the reaction design equation is as follows:

$$\frac{W}{F_{A_o}} = \gamma\left[\left[\frac{1}{2\delta} - \frac{1}{2\delta^3}\right]\ln\frac{(1+X_A\delta)}{(1-X_A\delta)} + \frac{X_A}{\delta^2}\right]$$

$$+ \beta\left[\frac{1}{2\delta^3}\ln\frac{(1+X_A\delta)}{(1-X_A\delta)} - \frac{1}{2\delta^2}\ln(1-\delta^2X_A^2) - \frac{X_A}{\delta^2}\right] \quad (11)$$

where,

$$\gamma = \frac{1}{\epsilon L k_2 k_A \pi} + \frac{1}{\epsilon L k_2} \quad (12)$$

$$\beta = \frac{2}{\epsilon L k_2 K_A \pi} + \frac{K_R}{\epsilon L k_2 K_A} \quad (13)$$

$$\delta = \left[1 + \frac{\pi}{K}\right]^{\frac{1}{2}} \quad (14)$$

For irreversible reaction, K approaches infinity, δ becomes unity and the design equation reduces to the following expression:

$$\frac{W}{F_{A_o}} = \gamma X_A + \beta\left[-\ln(1-X_A) - X_A\right] \quad (15)$$

W = wt. catalyst, gms.

F_{A_o} = feed rate of cumene, $\frac{\text{gm moles A}}{\text{sec.}}$

X_A = conversion of cumene, dimensionless

ϵ = effectiveness factor, dimensionless

L = total concentration of active sites, $\frac{\text{cm.}^2}{\text{gm cat.}}$

k_2 = forward reaction rate constant for surface reaction, $\frac{\text{gm moles}}{\text{cm.}^2\text{-sec.}}$

K_A = equilibrium adsorption constant for cumene, $\frac{1}{\text{atm.}}$

K_R = equilibrium adsorption constant for benzene, $\frac{1}{\text{atm.}}$

K = equilibrium constant for overall reaction, atm.

π = total pressure, atm.

Ultrasonic Engineering

Fundamental equations. As a sound wave travels through a gas, small volume elements of the gas containing millions of molecules alternately compress and expand in the direction of the propagation of the sound wave. The sine wave representations of the displacement, transverse velocity, and transverse acceleration are as follows:

$$y = Y \cos\left[\frac{2\pi}{\lambda}(x-Vt)\right] = Y \cos\left[2\pi f(t-\frac{x}{V})\right]; \quad y_{max} = Y \tag{16}$$

$$v = 2\pi f\, Y \sin 2\pi f(t-\tfrac{x}{V}); \quad v_{max} = 2\pi fY \tag{17}$$

$$a = 4\pi^2 f^2 Y \cos 2\pi f(t-\tfrac{x}{V}); \quad a_{max} = 4\pi^2 f^2 Y \tag{18}$$

y = displacement, cm.

Y = amplitude, cm.

λ = wavelength, $\frac{\text{cm.}}{\text{cycle}}$

$= VT = \frac{V}{f}$

T = period, $\frac{\text{sec.}}{\text{cycle}}$

V = velocity of propagation of wave form, $\frac{\text{cm.}}{\text{sec.}}$

f = frequency, $\frac{\text{cycles}}{\text{sec.}}$

$= \frac{1}{T}$

x = distance traversed by wave form, cm.

t = time, sec.

v = transverse velocity, $\frac{\text{cm.}}{\text{sec.}}$

a = transverse acceleration, $\frac{\text{cm.}}{\text{sec.}^2}$

Velocity of propagation. The velocity of propagation of a sound wave in a gas is a function on only the physical properties of the gas and not of the characteristics of the sound wave. This is illustrated in the following equations:

$$v = \left[\frac{1}{\rho_o k}\right]^{\frac{1}{2}} = \left[\frac{p\gamma}{\rho_o}\right]^{\frac{1}{2}} = \left[\frac{\gamma RT}{M}\right]^{\frac{1}{2}} \qquad (19)$$

V = velocity of propagation of wave form, $\frac{\text{cm.}}{\text{sec.}}$

ρ_o = original gas density, $\frac{\text{gms}}{\text{cm.}^2}$

k = compressibility, $\frac{\text{cm.}^2}{\text{dyne}} \frac{\text{cm.-sec.}^2}{\text{gm.}}$ (dyne = $\frac{\text{gm-cm.}}{\text{sec.}^2}$)

p = pressure, $\frac{\text{dynes}}{\text{cm.}^2}$, $\frac{\text{gm.}}{\text{cm-sec.}^2}$

$\gamma = \frac{C_p}{C_v}$, dimensionless

C_p = heat capacity of gas at constant pressure, $\frac{\text{cal}}{\text{gm-}^{o}\text{C.}}$

C_v = heat capacity of gas at constant volume, $\frac{\text{cal}}{\text{gm-}^{o}\text{C.}}$

$R = 8.31 \times 10^{7} \frac{\text{ergs}}{\text{mole-}^{o}\text{K.}} = 8.31 \times 10^{7} \frac{\text{dyne-cm.}}{\text{gm mole-}^{o}\text{K.}}$

$(\text{erg} = \text{dyne-cm.} = \frac{\text{gm-cm.}^{2}}{\text{sec.}^{2}})$

T = temperature of gas, ^{o}K.

M = molecular wt. of gas, $\frac{\text{gms.}}{\text{gm-mole}}$

Acoustic pressure. The acoustic pressure exerted by the sound wave as it traverses a gas is dependent upon the velocity of propagation and the intensity of the sound. The amplitude of the sound wave is a function of the acoustic pressure.

$$p_{max} = \left[2\rho_o IV\right]^{\frac{1}{2}} \qquad (20)$$

$$Y = \frac{p_{max}}{2\pi f \rho_o V}$$

p_{max} = maximum pressure caused by sound wave, $\frac{\text{dynes}}{\text{cm.}^{2}}$

ρ_o = original gas density, $\frac{\text{gms.}}{\text{cm.}^{3}}$

I = sound intensity, $\frac{\text{erg}}{\text{cm.}^{2}\text{-sec.}}$, $\frac{\text{dyne-cm.}}{\text{cm.}^{2}\text{-sec.}}$

$(10^{-7} \frac{\text{watt-sec.}}{\text{erg}})$

V = velocity of propagation, $\frac{\text{cm.}}{\text{sec.}}$

f = frequency, $\frac{1}{\text{sec.}}$

Y = amplitude, cm.

Conversion factor: $1 \frac{\text{gm-cm.}}{\text{dyne-sec.}^2}$

Typical values of wave characteristics. Values for the velocity of propagation, wavelength, acoustic pressure, amplitude, transverse velocity and acceleration were calculated for cumene at various frequencies and temperatures at the maximum power output and half power output of the equipment. A summary of these calculations is shown in Table 2.

As seen by the table, acoustic pressure as imposed by the sound wave should have little effect on the reaction rate because the pressure fluctuations above and below atmospheric are only a maximum of 1.62 psi at 650°F. and 1.50 at 1050°F. Furthermore, the acoustic pressure is lower at the higher frequency as a result of the mechanical characteristics of the equipment.

This research will, in fact, show that the dependency of reaction rate on power input alone for the range studied is negligible and that frequency alone and frequency together with power input are the important factors. Molecular acceleration, which is a function of both frequency and power, is very high in the ranges studied, as

TABLE 2

SUMMARY OF TYPICAL WAVE CHARACTERISTICS

T, ^{o}F.	650	650	650	650	1050	1050	1050	1050
f, $\frac{1}{\text{sec.}}$	26,000	26,000	39,000	39,000	26,000	26,000	39,000	39,000
I, $\frac{\text{watts}}{\text{cm.}^2}$	1.259	0.630	0.100	0.050	1.259	0.630	0.100	0.050
λ, cm.	0.806	0.806	0.537	0.537	0.935	0.935	0.623	0.623
V, $\frac{\text{cm.}}{\text{sec.}}$	20,945	20,945	20,945	20,945	24,298	24,298	24,298	24,298
Y, cm.	0.0138	0.0098	0.0026	0.0018	0.0149	0.0105	0.0028	0.0020
v_{max}, $\frac{\text{cm.}}{\text{sec.}}$	2,254	1,601	637	441	2,434	1,715	686	490
a_{max}, g	375,734	266,881	159,279	110,270	405,740	285,885	171,531	122,522
p_{max}, $\frac{\text{lb.}}{\text{in.}^2}$	1.62	1.15	0.46	0.32	1.50	1.06	0.42	0.30

indicated in the table. This molecular motion results in higher reaction rates by virtue of increased gas diffusion rates. It will be shown that the increased diffusion rate occurs both in the external diffusion zone and within the catalyst pores.

Detailed derivations of the ultrasonic relationships described in this chapter may be found in Appendix X.

CHAPTER III

EXPERIMENTAL EQUIPMENT

Flow Chart

Figure 1 is a schematic flow chart of the apparatus employed in this study. Valves and by-pass piping have been omitted from the drawing for the purpose of maintaining simplicity and clarity. Detailed specifications of all the equipment employed are described in Table 3.

The system consists of two feed tanks to which the cumene is charged, a feed rotameter for metering the feed to the reactor, the reactor and a heat exchanger to condense the cumene and benzene effluent. The small amount of propylene gas formed is vented to the atmosphere.

The apparatus is also equipped with a nitrogen source for pressurizing the feed tanks and blowing down the reactor prior to regeneration. A second rotameter is provided for metering regeneration air to the reactor.

Attached to the top of the reactor is the ultrasonic horn by which the catalyst bed is irradiated with ultrasonic energy.

Feed System

Cumene is charged to the feed tanks whereupon they

FIGURE 1

FLOW CHART
FOR EXPERIMENTAL REACTOR

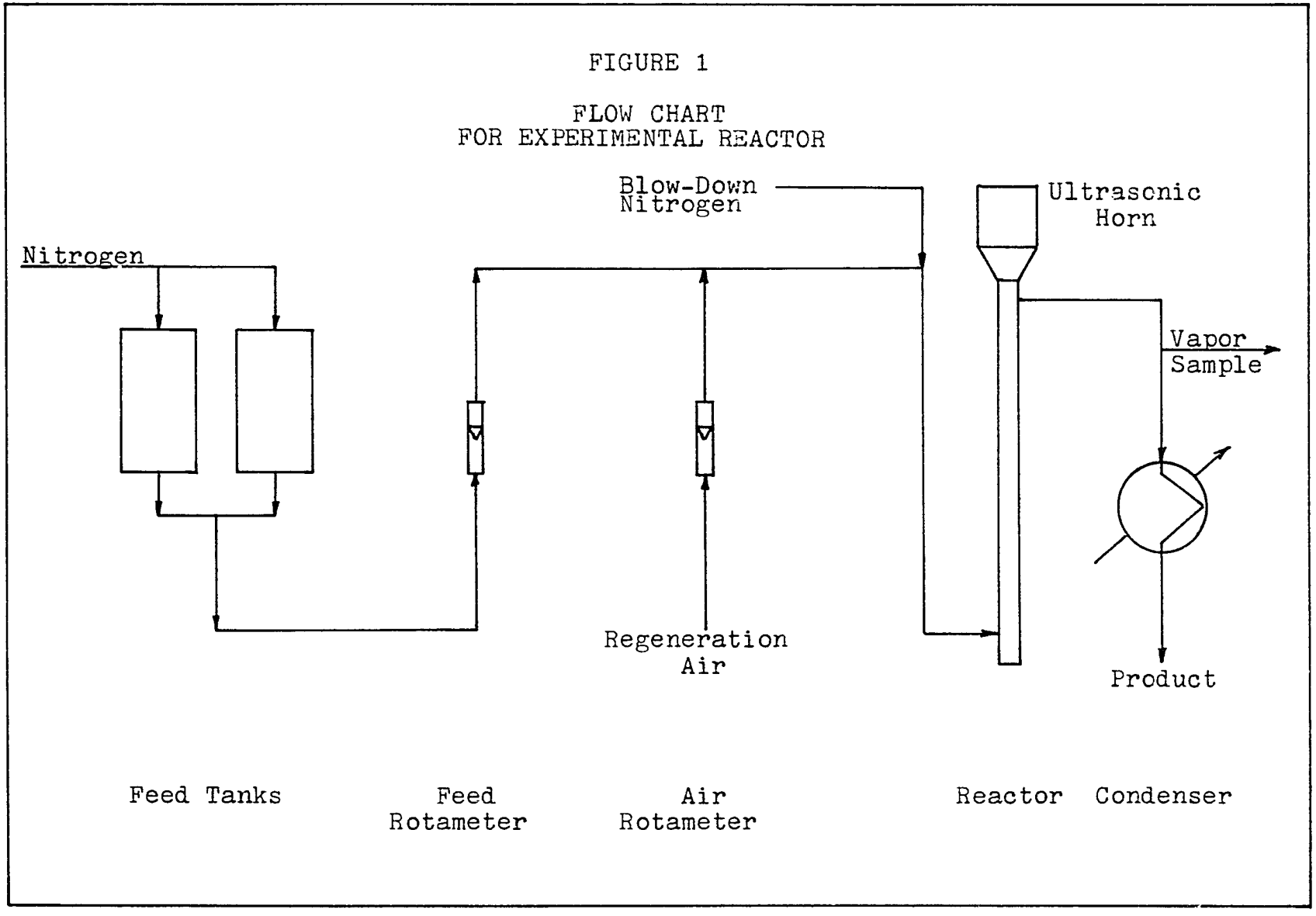

are pressured up to 10 psig with nitrogen. The nitrogen pressure is maintained constant by means of a gas pressure regulator so as to maintain a constant pressure drop across the feed rotameter needle valve. The feed rotameter is employed manually to control the cumene feed rate to the reactor; however, for measurement purposes, the difference in liquid level of the feed tanks for the duration of the run is employed for the average feed rate calculation.

Regeneration System

After each run, regeneration air is fed to the reactor through the air rotameter at a rate of approximately 0.1 scfm for a period of 24 hours to regenerate the catalyst by burning off the carbon deposits (see Appendix XIII).

Reactor

The reactor design is illustrated in Figures 2 and 3. It consists of a $\frac{1}{4}$ in. schedule 80 type 316 stainless steel pipe, $20\frac{1}{2}$ in. long, welded to a 2 in. O.D. stainless steel rod drilled to an I.D. of $^{25}/_{64}$ in. The $\frac{1}{4}$ in. pipe is encased in a 2 in. O.D. rod drilled to snugly fit the pipe. The casing provides the reactor with mass so as to stabilize the operating temperatures. The reactor is flanged at both ends and is equipped with a $\frac{1}{4}$ in. spud

FIGURE 2

REACTOR

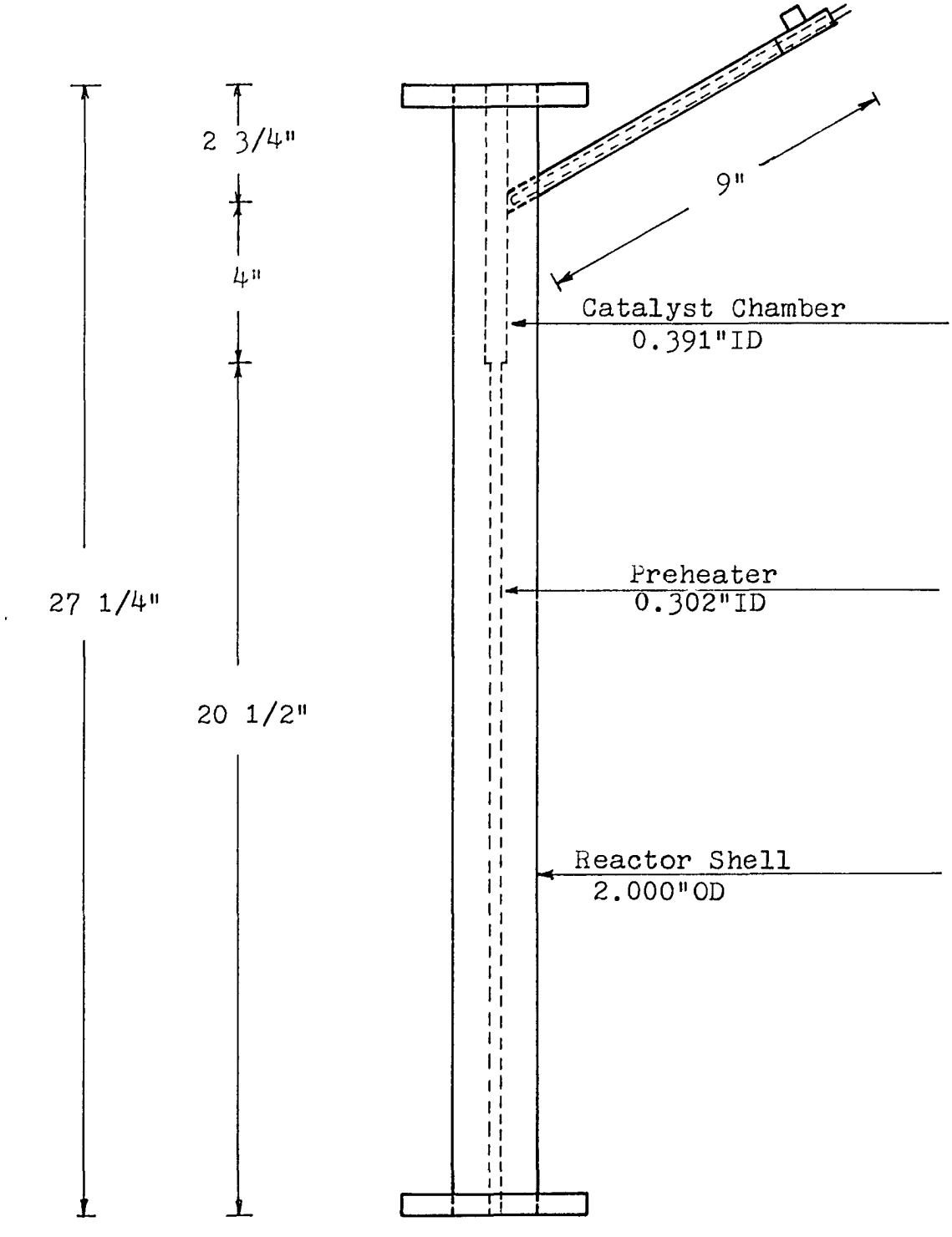

FIGURE 3

REACTOR THERMOCOUPLE LOCATION AND HEATING ZONES

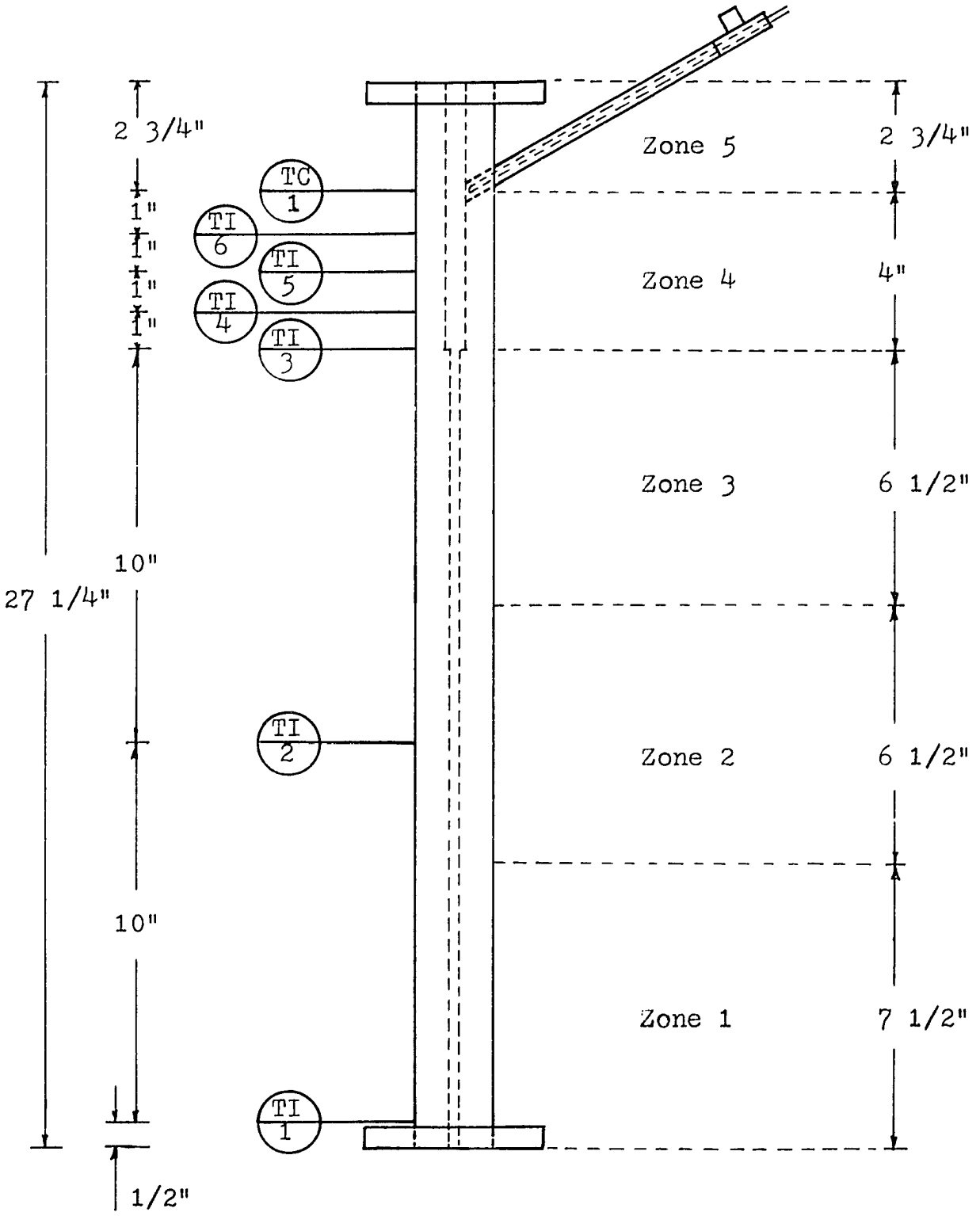

near the top for catalyst addition and product removal. Inserted within the spud is a 1/8 in. thermocouple well.

The ¼ in. x 20½ in. long pipe serves as the preheater section, and the upper 25/64 in. I.D. x 6 3/4 in. long cylinder is the catalyst chamber. The end of the thermocouple well inserted within the spud extends down into the catalyst chamber and is immersed in the catalyst bed. The catalyst is supported within the chamber by means of a fine mesh stainless steel screen.

The location of all seven thermocouples and five heating elements are illustrated in Figure 3. Six of the thermocouples, TI-1 through TI-6, are affixed to the outside of the reactor wall and connected to a temperature recorded. The seventh thermocouple, TC-1, is inserted in the thermowell and connected to a temperature controller.

The reactor is heated by five Nichrome V beaded wire heaters located as indicated in Figure 3. The power input to each heater is manually controlled by adjustment of five powerstats. The powerstats controlling the power input to heating zones 3 and 4 are automatically controlled by the temperature controller which continuously monitors the temperature at TC-1. Constant voltage is maintained to the control circuit by use of a constant

voltage transformer.

The entire reactor is insulated with approximately 4 in. of refractory rope and 2 in. of magnesia covered with an aluminum sheath.

Condenser

The reaction products, cumene, benzene and propylene, enter the condenser from the reactor at approximately 650-1050°F. whereupon they are cooled to approximately 75°F. The cumene and benzene are condensed and collected and the propylene, which remains in the vapor phase at this temperature, is vented to the atmosphere.

Ultrasonic Horn

The ultrasonic horn is 3 in. in diameter and is mounted directly atop the reactor by means of a specially fabricated 3 in. by 1 in. adapter flange. The horn is driven by a variable frequency ultrasonic generator with a variable output frequency of 10,000 to 50,000 cps.

The maximum operating temperature of the piezoelectric transducer which drives the horn is 300°C. (572°F.) and the minimum allowable operating temperature of the horn to prevent condensation of the highest boiler, cumene, is 153°C. (308°F.). Therefore, it is necessary to maintain the temperature of the ultrasonic horn at approximately 175°C. This is accomplished by recirculating

FIGURE 4

ULTRASONIC HORN

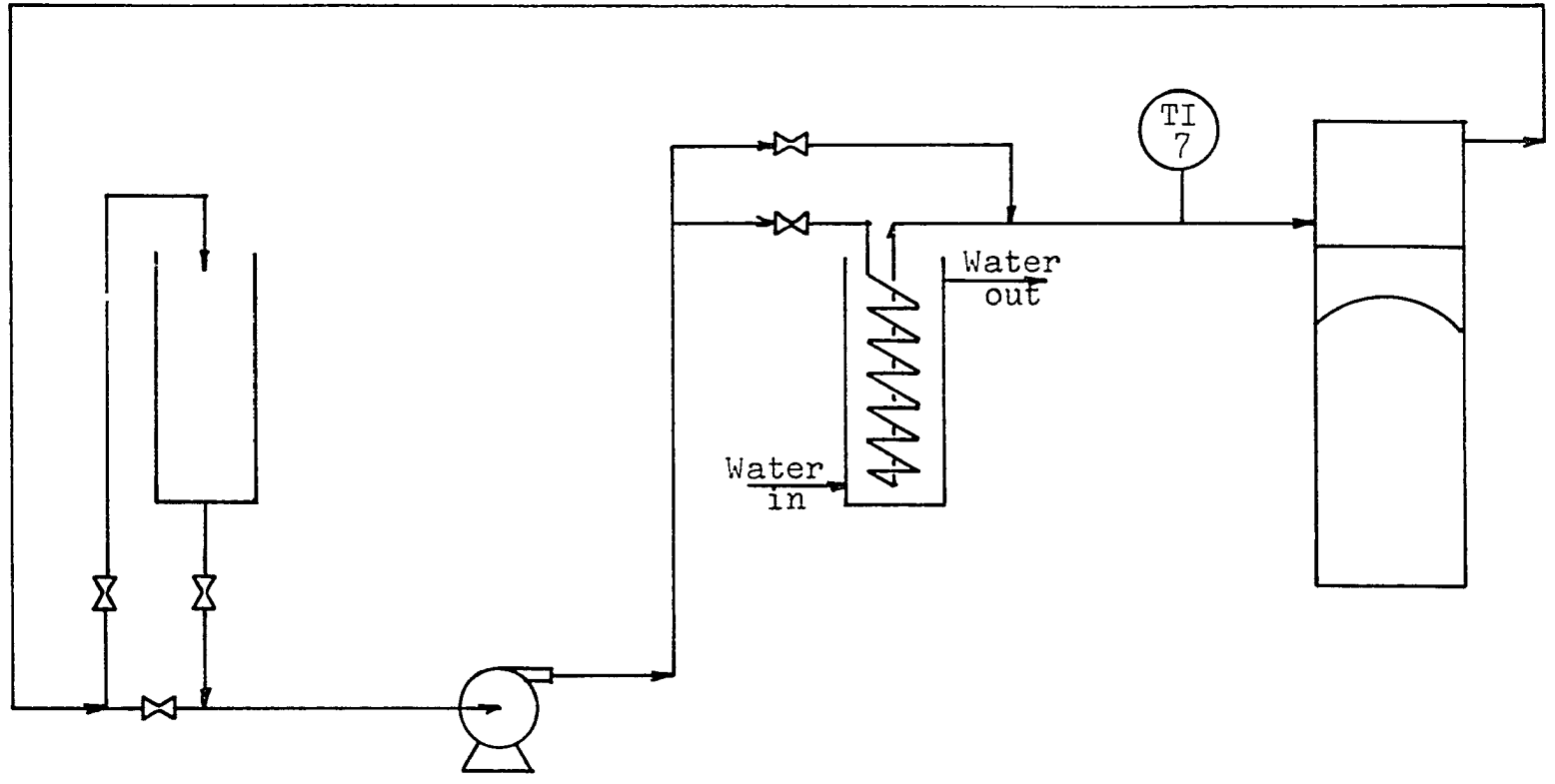

heated oil through the cooling chamber of the ultrasonic horn as illustrated in Figure 4.

The oil is recirculated through a water cooled heat exchanger to the ultrasonic horn cooling chamber and thence to an electrically heated surge pot by means of a 1 gpm centrifugal pump. By proper adjustment of the powerstat controlled electric heater and oil flow to the cooler, it is possible to maintain the recirculating oil at approximately 175°C.

Piping

All piping consists of ¼ in. stainless steel threaded pipe and fittings and ¼ in. copper tubing with compression type fittings. Teflon tape is employed on all threaded connections.

Analytical Instrumentation

The quality of the effluent product is analyzed by use of a gas-liquid chromatograph in conjunction with a single pen strip chart recorder. The chromatograph response was standardized daily by injecting and analyzing a known sample. The analytical system is designed to handle either gas samples taken from the reactor effluent prior to condensation or liquid samples from the condenser effluent. The analysis of the liquid samples proved to be almost identical to that of the gaseous sample. Comparative analyses and conversion calculations are shown in Appendix IX.

TABLE 3

EQUIPMENT SPECIFICATIONS

Feed Tank No. 1

Manufacturer	Corning Glass Co.
Material of construction	Pyrex conical pipe
Length	36 in.
Working pressure	50 psig, max.
Diameter	1 in.
Calibration	10.79 gms. cumene/in.

Feed Tank No. 2

Manufacturer	Corning Glass Co.
Material of construction	Pyrex conical pipe
Length	36 in.
Working pressure	50 psig, max.
Diameter	1½ in.
Calibration	24.66 gms. cumene/in.

Feed Rotameter

Manufacturer	Brooks Instrument Co.
Model No.	1357-8506
Meter size	2
Type	1357-01F1BAA
Serial no.	7010-48800
Tube no.	R-2-25-D
Scale	250 mm.
Wetted parts	Stainless steel
Packing	Teflon
O-rings	Kel-F
Valve needle taper no.	3
Orifice type	Small
Connections	¼ in. NPT
Float material	Sapphire

Maximum flow rate

Float Material	Gm./Hr. Cumene
Glass	355
Sapphire	640
Stainless steel	1,267
Carboloy	2,130
Tantalum	2,300

Calibration (Sapphire float): Figure 5

TABLE 3 (continued)

EQUIPMENT SPECIFICATIONS

Air Rotameter

Manufacturer	Fischer & Porter Co.
Tube no.	02-F-1/8-12-5/70
Type no.	TII-1077/1-2
Serial no.	TII-1077/1
Scale (direct calibration)	0-6 scfm hydrogen at $\frac{1}{2}$ psig and 75°F.

Reactor

Material of construction	Type 316 stainless steel
Overall length	$27\frac{1}{4}$ in.
Outside diameter	2.000 in.
Preheater	
Material of Construction	Type 316 stainless steel
Length	$20\frac{1}{2}$ in.
Outside diameter	2.000 in.
Inside diameter	0.302 in.
Catalyst Chamber	
Material of construction	Type 316 stainless steel
Length	4 in.
Outside diameter	2.000 in.
Inside diameter	0.391 in.

Temperature Recorder

Manufacturer	Westronics Inc.
Type	Strip chart
Range	0-1200°F.
No. of points	12
Model no.	MIIB/J/DV.5M
Serial no.	MIIB336

Temperature Controller

Manufacturer	Leeds & Northrup Co.
Type	Speedomax H
Volts/cycles	120/60
Catalog no.	200-901-010-0023-6-024-0
Serial no.	65-35480-1-1

TABLE 3 (continued)

EQUIPMENT SPECIFICATIONS

Temperature Controller (continued)

Range	0-2000°F.
Chart no.	620023
Chart speed	1 revolution/24 hrs.
Response time	5.0 seconds, full travel
Controller series	60

Heaters

Manufacturer	Cole-Parmer Instrument Co.
Type	Beaded Nichrome V wire
Catalog no.	3116-1
Length, each	12 ft.
Power, each	400 watts
Temperature	2000°F., max.

Powerstats

Manufacturer	Superior Electric Co.
Type	116
Phase	Single
Input	120 volts, 50/60 cps
Output	0-140 volts
Amps, max.	9
Kva, max.	1.3

Constant Voltage Transformer

Manufacturer	Sola Electric Co.
Catalog no.	20-13-150 D476
Type no.	CUN-1
Primary	95-130 volts, 60 cps, single phase
Secondary	118 volts, 4.24 amps

Refractory Rope

Manufacturer	Johns-Manville
Style no.	Thermo-Pac 2300
Temperature	2300°F., max.

TABLE 3 (continued)

EQUIPMENT SPECIFICATIONS

Condenser

Material of construction	Type 316 stainless steel
Type	Tube and shell
Length	36 in.
Shell side	1 in. sched. 40 pipe
Tube side	1-¼ in. sched. 40 pipe
Connections	¼ in. NPT
Coolant (shell side)	Water
Surface area	0.423 ft.^{2}

Ultrasonic Horn

Manufacturer	Macrosonics International
Material of construction	Type 316 stainless steel
Model no.	FH-15-0
Type	Oil cooled
Frequency range	10,000 cps to 100,000 cps
Acoustic energy	25 watts
Input	100 watts
Sound level	Above 166 db
Nominal impedence	400 ohms
Efficiency	25%
Length	18 in.
Diameter	3 in.
Weight	11 lb.
Operating temperature	300°C. max.
Serial no.	70-12

Ultrasonic Generator

Manufacturer	Macrosonics International
Model no.	150 LF
Volts/cycles	120/50-60
Amps/phase	4/single
Frequency range	10,000-50,000 cps (Figure 6)
Power output	20-80 watts
Output impedence	200-400 ohms
Weight	38 lb.
Serial no.	00405

TABLE 3 (continued)

EQUIPMENT SPECIFICATIONS

Heat Transfer Oil	
Manufacturer	Monsanto Chemical Co.
Type	Therminol FR-1
Operating temperature	700°F., max.
Thermometer, TI-7	
Manufacturer	Weston
Type	Stem and dial
Range	0-300°C.
Recirculation Pump	
Manufacturer	Eastern Engineering Co.
Material of construction	Carbon steel
Model	D11
Type	100
Horsepower	1/8
Rpm	3,450
Capacity	1 gpm
Oil Cooler	
Shell Side	
Material of construction	Type 316 stainless steel
Diameter	2 in. Sched. 40 pipe
Length	36 in.
Tube Side	
Material of construction	Copper
Diameter	¼ in.
Length	70 turns, 1 in. diameter
Heated Surge Pot	
Material of construction	Type 316 stainless steel
Diameter	2 in. sched. 40 pipe
Length	12 in.
Gas-Liquid Chromatograph	
Manufacturer	Varian Aerograph Co.
Model	A-90-P

TABLE 3 (continued)

EQUIPMENT SPECIFICATIONS

Gas-Liquid Chromatograph (continued)

Type	Manual temperature programmer
Part no.	90P3
Serial no.	343-026
Column	10% Carbowax, 20 mesh, on chrome-W

Strip Chart Recorder

Manufacturer	Minneapolis-Honeywell Regulator Co.
Type	Single pen strip chart recorder
Model no.	15307856-01-05-0-000-030-07136
Range	-0.05 to +1.05 mv
Chart no.	9283-NR
Volts/cycles	120/60
Serial no.	02003303008

Nitrogen

Manufacturer	Matheson Gas Products
Grade	Extra dry

Air

Manufacturer	Matheson Gas Products
Grade	Ultra zero
Hydrocarbons	0.1 ppm max.

Helium

Manufacturer	Matheson Gas Products
Grade	Zero
Hydrocarbons	2 ppm max.

FIGURE 5

FEED ROTAMETER CALIBRATION

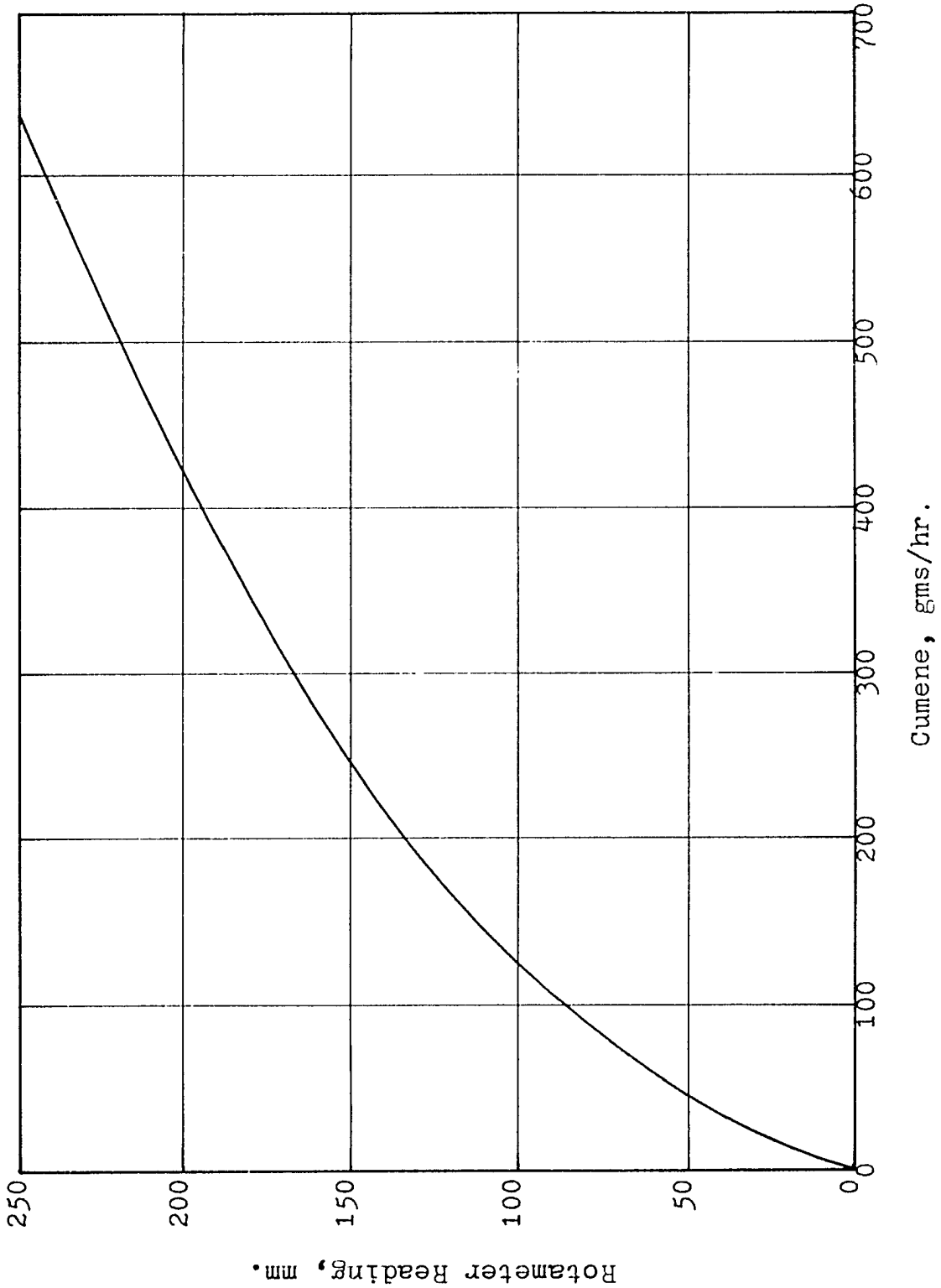

FIGURE 6

ULTRASONIC GENERATOR FREQUENCY CALIBRATION

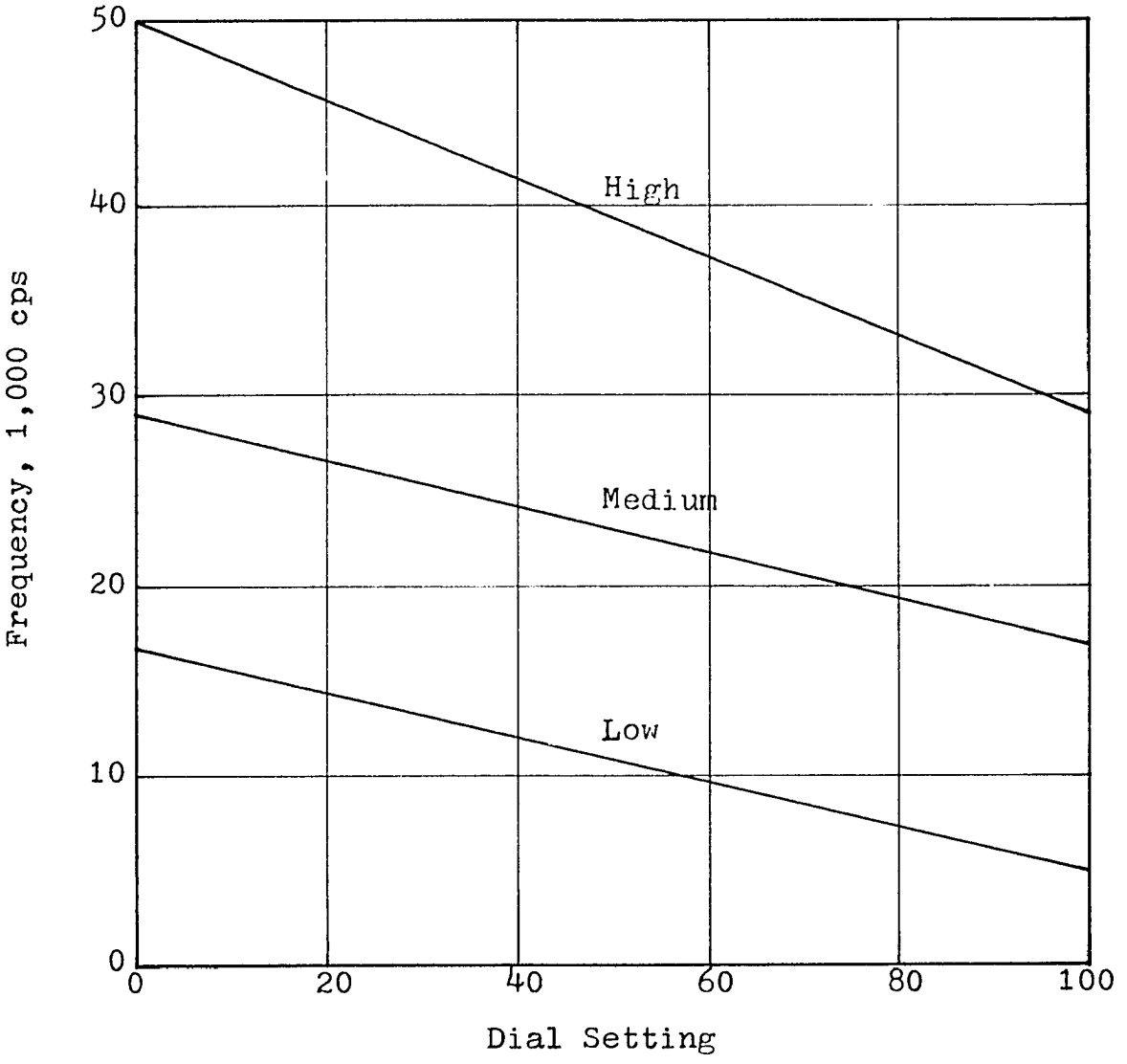

CHAPTER IV

EXPERIMENTAL PROCEDURE

Operating Conditions

The operating conditions studied in this investigation were temperatures of 650°F. to 1050°F., feed rates of 20 to 600 gms./hr., catalyst loadings of 0.958 to 5.748 gms., ultrasonic frequencies of 26,000 cps and 39,000 cps, and power outputs of 0.05 to 1.3 $\frac{\text{watts}}{\text{cm.}^2}$. The general procedure followed was to obtain the desired reactor temperature and then feed the cumene at a predetermined rate and catalyst loading. Each run was operated at two different ultrasonic frequencies and in the absence of ultrasound.

General Procedure

The reactor was purged with air at reaction temperature after each run for a period of approximately 24 hours to burn off any carbon deposit and regenerate the catalyst. Calculations indicate (Appendix XIII) that 10 minutes should be sufficient to burn off the carbon and visual inspection of the reactor after regeneration for 30 minutes indicated it to be free from carbon. Comparison of conversions in the absence of ultrasound between runs employing the same catalyst after many regenerations and nearly the same operating conditions also indicated complete reactivation. For example, comparing Run No. 14.83 with Run No.

22.135 shows conversions of 4.5% and 4.2% at feed rates of 593 gms./hr. and 622 gms./hr., respectively, all other conditions being identical. Similar checks are observed in many other runs, for example Run No. 33.23 and 36.53. The reactor was also purged with nitrogen after each run and after each air purge in order to avoid the safety hazard of hot cumene in the presence of air.

Each time the sonic frequency was changed during a run, the product collected during the first ten minutes was discarded and the product produced during the second ten minutes was blended and sampled as representative of those operating conditions. Previous work has shown that any decrease in catalyst activity during a run of this length of time could be neglected.

Temperature control. The temperature of the reactor was controlled by manually adjusting two voltage regulators which monitored the power input to the heating elements along the preheater section. The catalyst chamber temperature was controlled automatically by an on-off temperature controller connected in series with two additional voltage regulators which monitored the power input to the heating elements along the catalyst chamber. The temperature for this control point was sensed by a thermocouple located in the catalyst chamber itself (see Appendix XV). A fifth manually operated voltage regulator was employed to control a heating element located on the product discharge piping.

The heaters were never turned off so that the reactor was always at temperature equilibrium. When the reactor temperature was changed, approximately 24 hours was allowed for the catalyst bed to again reach temperature equilibrium.

Feed rate control. The cumene feed rate was controlled by pressurizing the feed tank to 10 psig with nitrogen and recording the tank level and time at the start and end of each run. The flow rate was controlled by the feed flow rotameter, but the rate used in any subsequent calculations was the rate obtained by difference of the calibrated feed tank level.

Application of ultrasound. Each run was operated first in the absence of ultrasound and then the ultrasonic generator was activated and frequencies of 26,000 cps and 39,000 cps were irradiated upon the catalyst bed. The order in which the higher and lower frequencies were employed was reversed many times throughout this study. Each run was operated in the absence of ultrasound after each of the frequency activated samples had been taken as a check for decrease in catalyst activity from the start to the end of the run. The analyses of the first and last sample, i.e., the samples taken in the absence of ultrasound were always essentially the same.

Sample analyses. In many instances, the gas stream was fed directly to the gas chromatograph for analysis as

a check against the liquid sample analysis. In all cases, both methods of analysis yielded essentially the same conversion calculation. The analysis of liquid samples was preferred, because the same sample was injected a minimum of three times into the gas chromatograph as a check of the analytical technique. The vapor sample, of course, could be injected only once.

The size of the gaseous sample was controlled by filling a small tubing coil with the reaction products and flushing the entire coil contents into the chromatograph with helium. Sample size of the liquid was controlled by use of a 10 microliter hyperdermic needle calibrated in 0.2 microliters. The analyses of known liquid samples were duplicated within 1%, indicating sample size control to be adequate.

Detailed Procedure

The details of the experimental procedure for a typical run are as follows:

1. Set the reactor air purge rate at 6.0 scfh employing the air flow rotameter.
2. Adjust the heater controls to obtain the desired reactor temperature.
3. Adjust the automatic temperature controller set point to the desired reactor temperature.
4. Allow approximately 24 hours for the reactor to equilibrate at the desired temperature.

5. Turn on the hot oil recirculation pump and adjust the heater control to maintain the oil at 155-160°C.
6. Turn off the air purge and purge the reactor with nitrogen for 20 minutes.
7. Shut down the nitrogen purge and pressurize the cumene feed tank to 10 psig with nitrogen.
8. Feed cumene to the reactor at the desired rate employing the feed flow rotameter to monitor that rate.
9. Record the feed tank level and time.
10. The first product will appear in 5 to 10 minutes. Discard the product obtained during the first 10 minutes and collect, blend and sample the product obtained during the second 10 minutes.
11. While maintaining all other operating conditions constant, activate the ultrasonic generator and adjust it to the desired frequency.
12. Discard the product obtained during the first 10 minutes and collect, blend and sample the product obtained during the second 10 minutes.
13. While maintaining all other operating conditions constant, readjust the ultrasonic generator to another frequency.
14. Discard the product obtained during the first 10 minutes and collect, blend and sample the product collected during the second 10 minutes.
15. While maintaining all other operating conditions constant, shut down the ultrasonic generator.

16. Discard the product obtained during the first 10 minutes and collect, blend and sample the product collected during the second 10 minutes.
17. Record the feed tank level and time.
18. Shut off the feed and purge the reactor with nitrogen for 20 minutes.
19. Shut down the power to the hot oil heater and shut down the recirculation pump.
20. Shut down the nitrogen purge and set the air purge rate at 6.0 scfh employing the air flow rotameter.
21. Air purge the reactor for 24 hours at the reaction temperature prior to starting the next run.
22. Thoroughly blend each of the four samples obtained in steps 10, 12, 14 and 16 to insure uniformity within each sample. Inject a portion of each of the samples three times into the gas chromatograph and calculate the conversion. If the calculated conversion of the samples obtained from steps 10 and 16 do not agree within 3%, discard the run. (This was never necessary.)

The data sheet employed for this study is shown in Figure 7. Copies of several actual completed data sheets are included in Appendix XIV.

FIGURE 7

DATA SHEET

Run No.		Reactor Diameter, cm.	
Date		Frequency, cps	
Catalyst, gms.		Power, watts	
Bed Height, cm.		Feed Tank Diameter, in.	

Time											
Tank Height, in.											
Rotameter, mm.											
Rota. Feed Rate, gms/hr.											
Tank Feed Rate, gms/hr.											
Heater No. 1											
Heater No. 2											
Heater No. 3											
Heater No. 4											
Hot Oil Heater											
TI-1, °F.											
TI-2, °F.											
TI-3, °F.											
TI-4, °F.											
TI-5, °F.											
TI-6, °F.											
TI-7, °F. (Hot Oil)											
TC-1, °F.											
Ultrasound											
W/F, gm cat-sec/gm mole											
Cumene, %											
Benzene, %											
Propylene, %											
Conversion, X											

CHAPTER V

EXPERIMENTAL RESULTS

Presentation of All Data

All the data collected (Appendix XIV) are presented herein as plots of conversion versus reciprocal space velocity. The best curve fit of the data was calculated for each temperature and frequency employed by the quadratic regression equation:

$$x = a + b\,(W/F) + C\,(W/F)^2 \qquad (21)$$

Since the external mass transfer rate is dependent upon feed rate, the equations of these curves are later employed to determine conversion at specific reciprocal space velocities for the calculation of mass transfer coefficients.

The three constants obtained for each condition are shown in Table 4. The plot of the curves showing all the data points are in Appendix XVI and the plots for each family of three curves for each frequency are shown for all the temperatures studied in Figures 8 through 16. The data points are omitted for clarity. It is noted that although several of the curves cross at low reciprocal space velocity, the actual data indicate higher conversions at higher frequencies in every case. This is because the shape of the quadratic curves near the origin often does not precisely fit the data points.

TABLE 4

QUADRATIC EQUATION CONSTANTS

Temp. °F.	cps x 10-3	Power	a	b x 10^6	C x 10^{11}
650	39	full	-0.000959	1.74	-0.91
650	26	full	-0.00605	1.76	-1.06
650	-	off	-0.00664	1.75	-1.10
700	39	full	0.0309	1.45	0.590
700	26	full	0.0253	0.923	0.790
700	-	off	0.0205	0.958	0.650
750	39	full	0.0231	7.55	-3.74
750	26	full	0.0051	6.66	-3.17
750	-	off	-0.0054	7.00	-3.70
800	39	full	0.0453	5.97	-2.32
800	26	full	0.0308	5.32	-1.93
800	-	off	0.0226	5.41	-2.09
850	39	full	0.0282	9.92	-5.87
850	26	full	0.0252	9.04	-5.76
850	-	off	0.0258	8.40	-5.60
850	39	half	0.0989	5.01	-2.00
850	26	half	0.0974	4.79	-2.03
850	-	off	0.0258	8.40	-5.60
900	39	full	0.0877	5.33	-1.86
900	26	full	0.0789	4.16	-1.13
900	-	off	0.0655	6.26	-3.15
950	39	full	0.0359	7.52	-1.75
950	26	full	0.0256	8.76	-4.30
950	-	off	0.0255	8.12	-4.42
1000	39	full	0.215	20.3	-39.5
1000	26	full	-0.0224	29.4	-75.2
1000	-	off	-0.0213	29.8	-81.5

Full power = 25 watts
Half power = 12.5 watts

FIGURE 8

CONVERSION vs. W/F

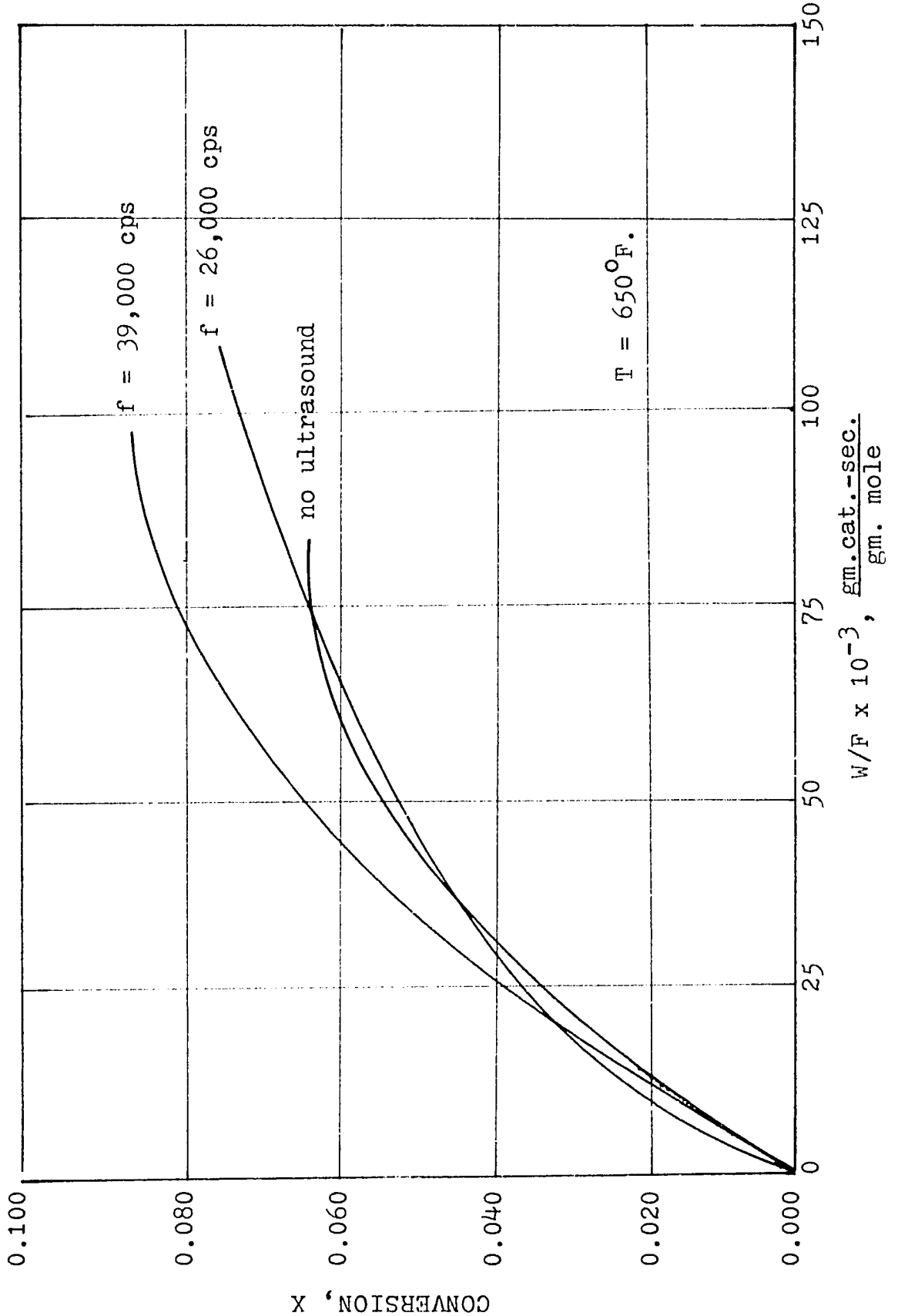

FIGURE 9

CONVERSION vs. W/F

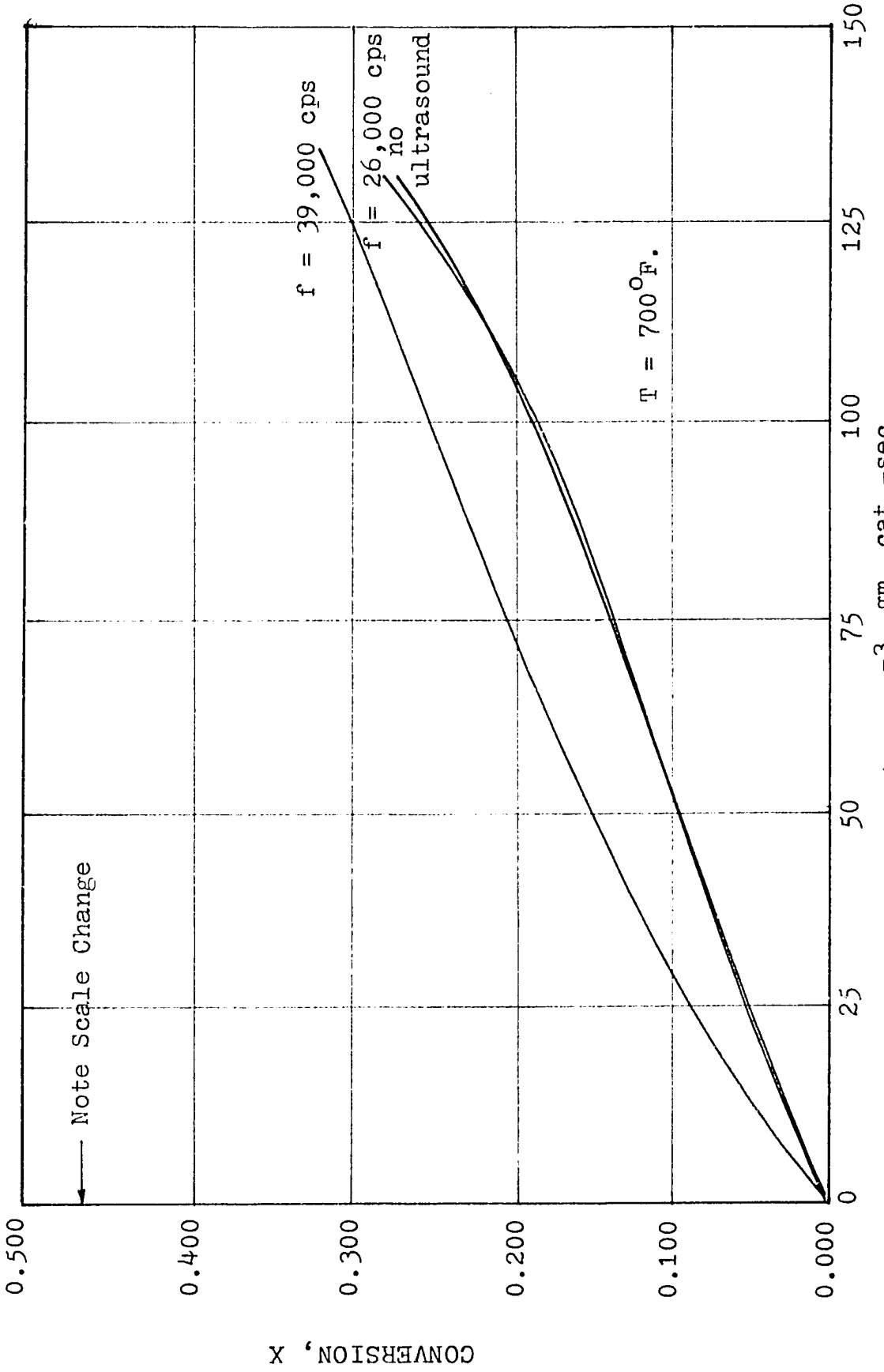

FIGURE 10

CONVERSION vs. W/F

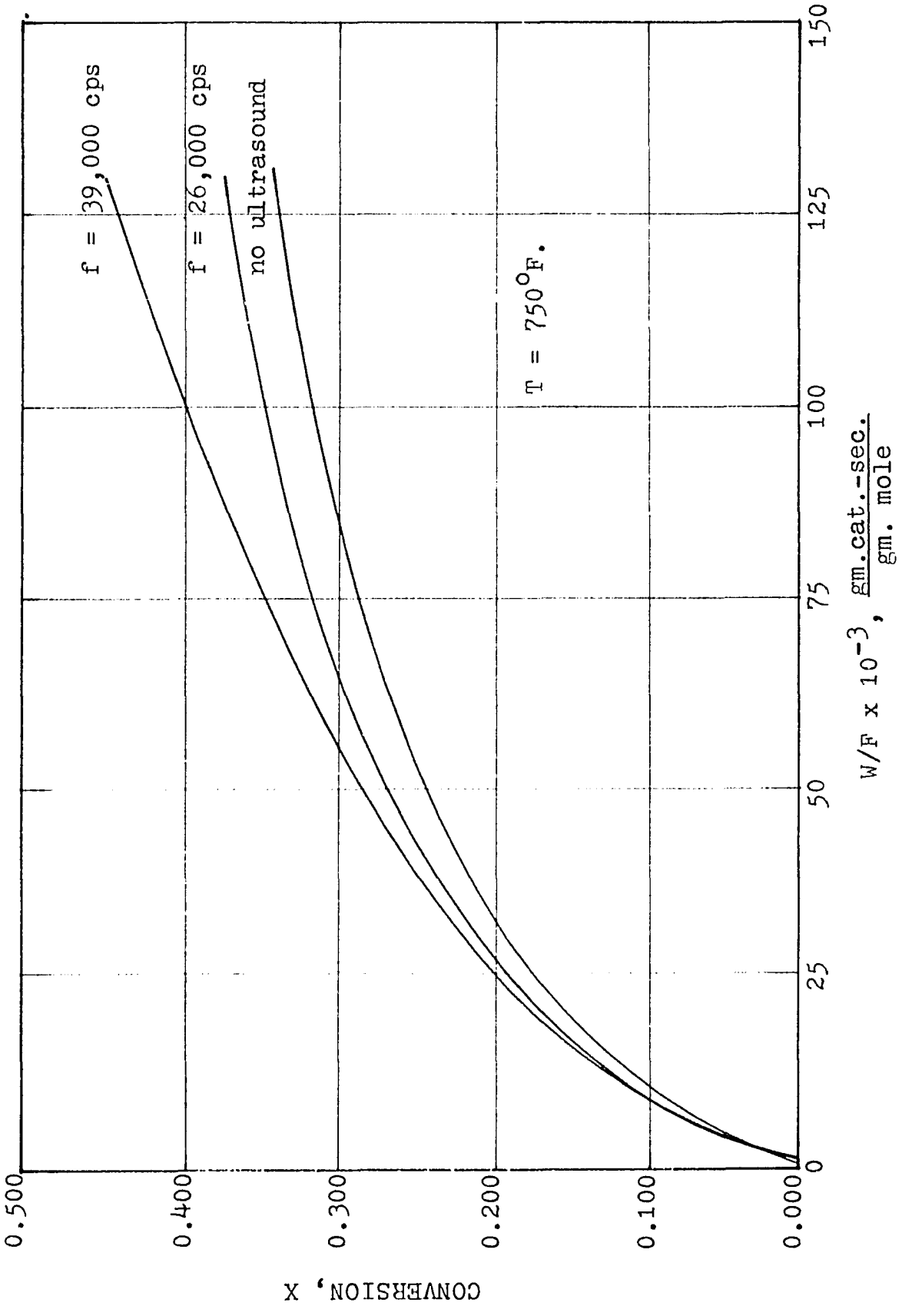

FIGURE 11

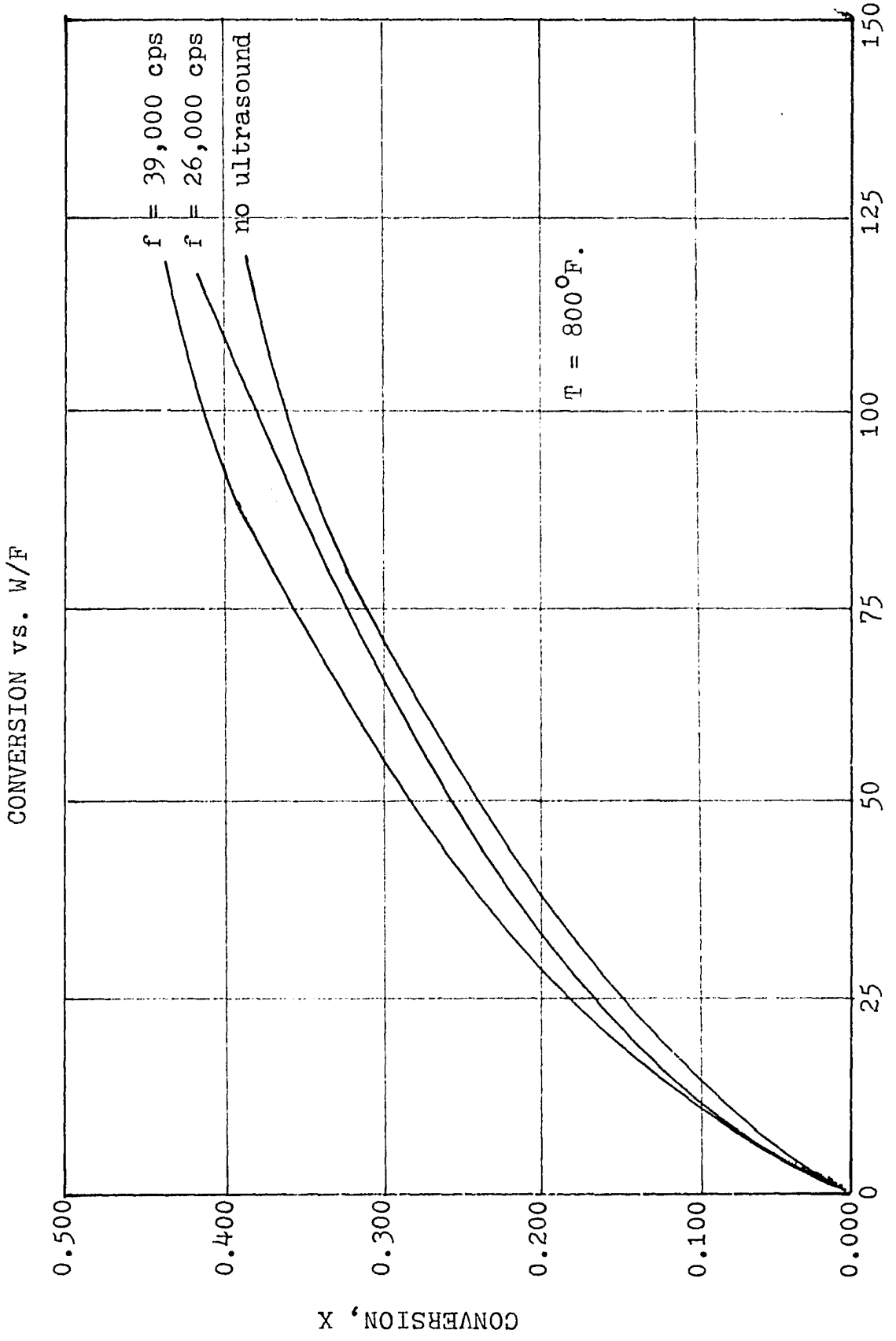

FIGURE 12

CONVERSION vs. W/F

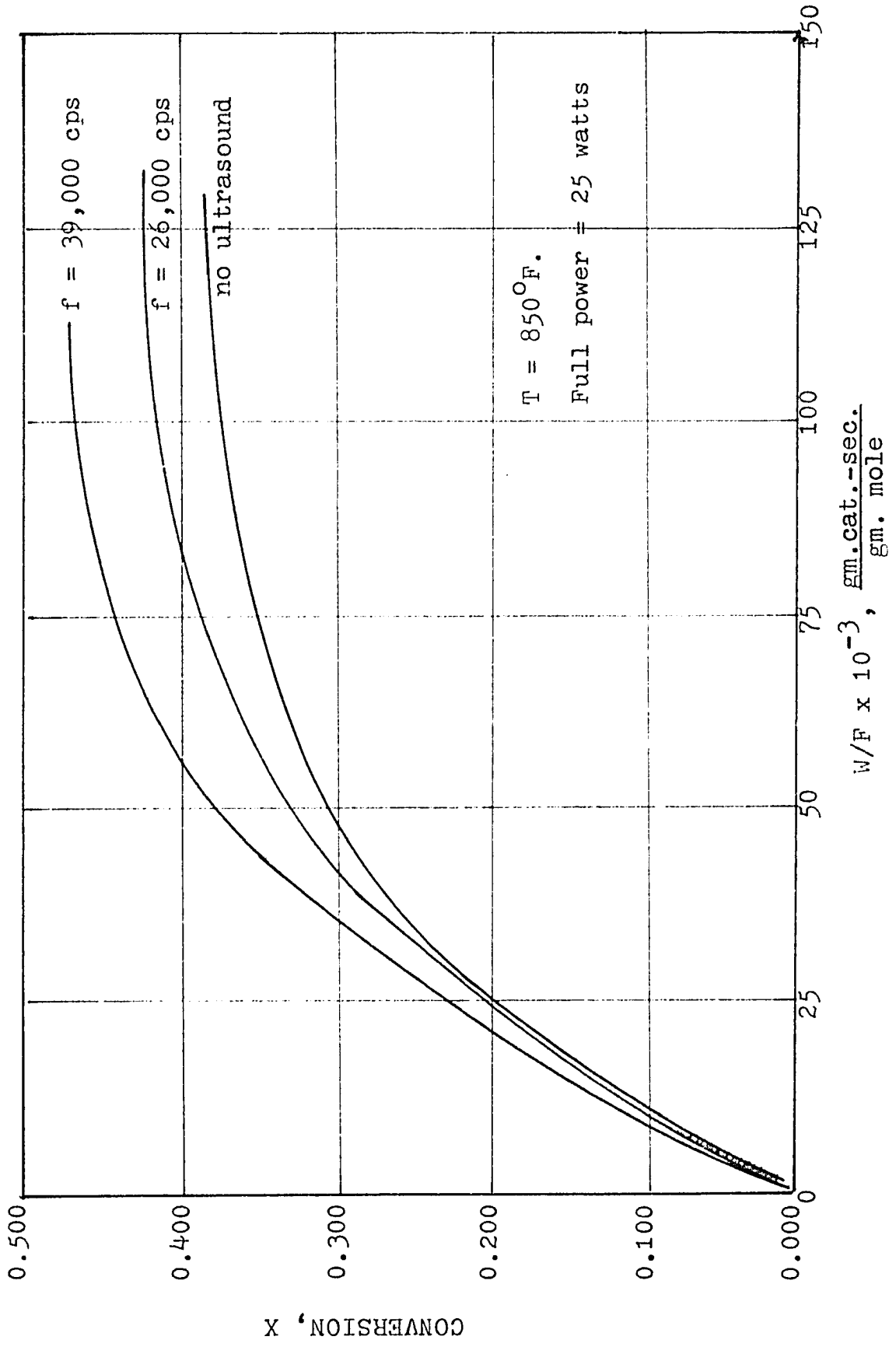

FIGURE 13

CONVERSION vs. W/F

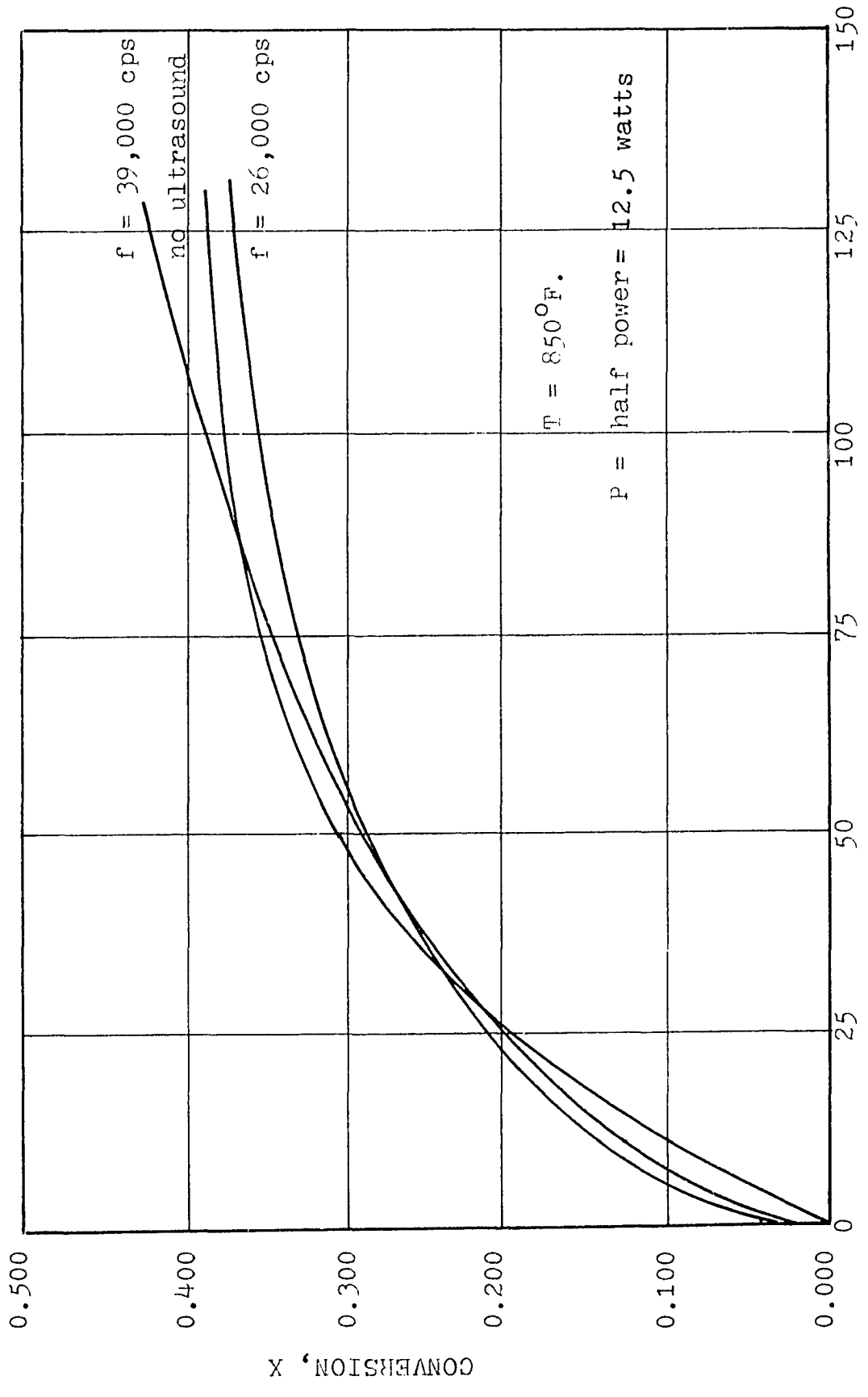

FIGURE 14

CONVERSION vs. W/F

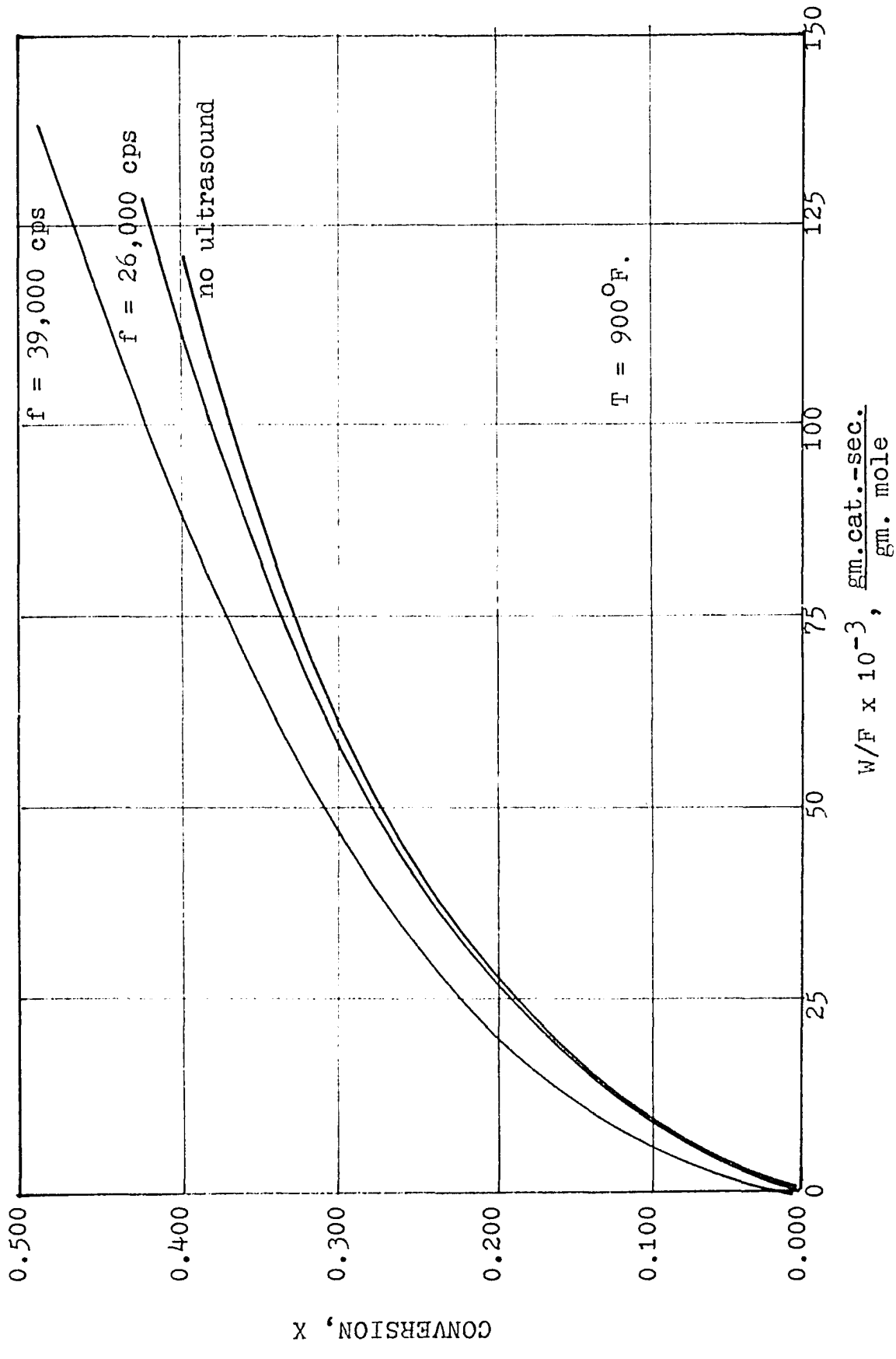

FIGURE 15

CONVERSION vs. W/F

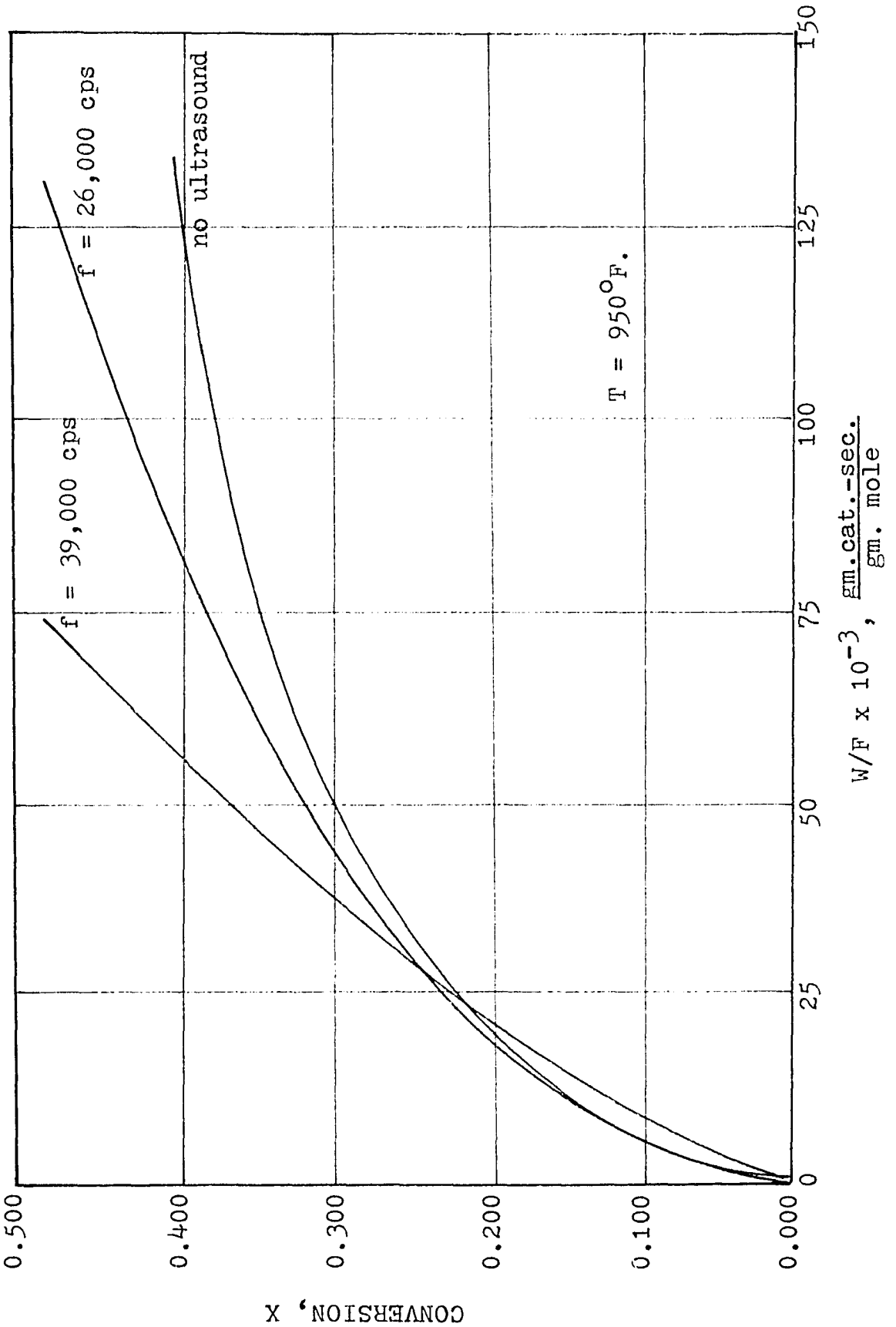

FIGURE 16

CONVERSION vs. W/F

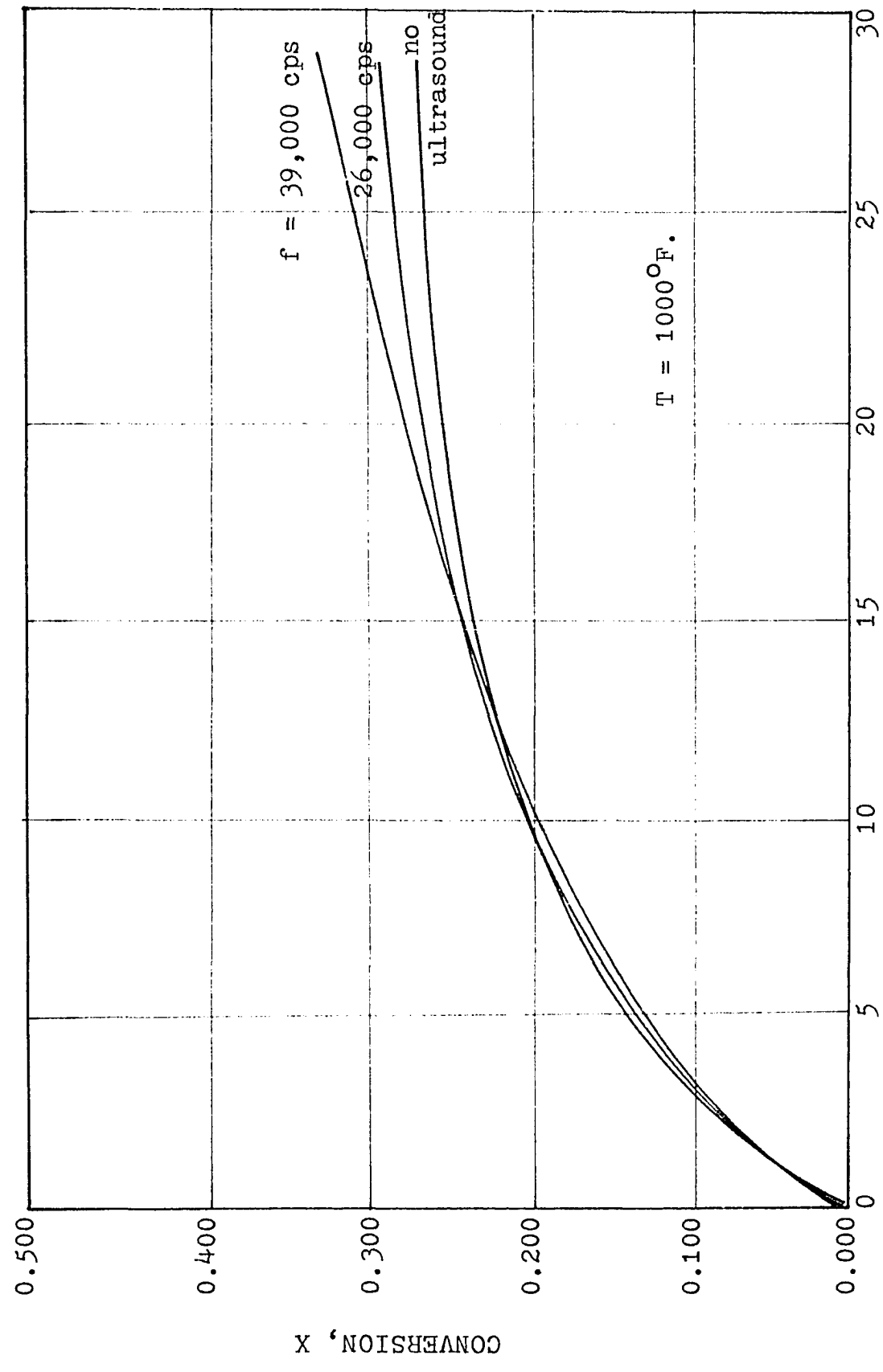

Conversions obtained at temperatures above 850°F. decreased slightly at higher temperatures at some feed rates indidicating partial coking of the reactor. Although some date were collected at 1050°F., coking of the reactor and catalyst at this temperature caused considerable mechanical difficulty with the apparatus. Therefore, attempts to study the effect of ultrasound at 1050°F. were abandoned.

The quadratic curves presented herein are employed for future calculation purposes only and should not be construed to represent a theoretical model of the reaction mechanism.

It will be shown that on the upper portion of the quadratic curves, at low feed rates, external bulk diffusion is the controlling factor for the reaction rate. On the lower portion of the curves, at high feed rates, the combined effect of surface reaction and internal pore diffusion control the rate of reaction.

Although the quadratic curves show a decrease in conversion at lower acoustical power inputs at low flow rates, it will be shown later that there is, in fact, negligible effect on either the mass transfer coefficient, k_g, or the kinetic rate constant, $\epsilon L k_2$.

External Diffusion Controlling

When external bulk diffusion controls the rate of reaction, the mass transfer coefficient, k_g, is the controlling factor. The mass transfer coefficient is calculated from the following equation derived in Chapter II and Appendix IV:

$$k_g = \frac{6.26\ X_{Af}\ T}{(W/F_{A_o}) \ln(1 + Y_{A_{LM}})} \qquad (22)$$

The mass transfer coefficient was calculated at three different feed rates corresponding to reciprocal space velocities of 20,000, 50,000 and 80,000 $\frac{\text{gm cat-sec.}}{\text{gm mole}}$. The results of these calculations are shown in Table 5.

Temperature effect. As is shown in the Appendix VI, the mass transfer coefficient is an exponential function of temperature. Therefore, a plot of the logarithm of the mass transfer coefficient versus temperature should yield a straight line. This, in fact, is the case as illustrated in Figures 17 through 22. The equations of the straight lines as obtained by the method of least squares are shown in Table 6. The calculation of the confidence intervals shown in Table 6 is demonstrated in Appendix XXII.

As shown in the graphs, the mass transfer coefficients calculated at 650°F. (616°K.) and 700°F. (644°K.) fall well below the theoretical curve. The reason for this phenomenon is because external bulk diffusion no longer controls the

TABLE 5

MASS TRANSFER COEFFICIENT

Temp. °F.	f cps x 10^{-3}	Power	W/FA_o = 20,000 gm cat-sec./gm mole		W/FA_o = 50,000 gm cat-sec./gm mole		W/FA_o = 80,000 gm cat-sec./gm mole	
			X_{A_f}	k_g, cm./sec.	X_{A_f}	k_g, cm./sec.	X_{A_f}	k_g, cm./sec.
650	39	Full	0.030	0.0085	0.063	0.0073	0.080	0.0059
650	26	Full	0.025	0.0071	0.056	0.0065	0.067	0.0049
650	-	Off	0.024	0.0068	0.053	0.0061	0.063	0.0046
700	39	Full	0.062	0.0180	0.118	0.0149	0.185	0.0154
700	26	Full	0.047	0.0141	0.091	0.0113	0.150	0.0122
700	-	Off	0.042	0.0126	0.085	0.0105	0.139	0.0112
750	39	Full	0.159	0.0541	0.307	0.0466	0.388	0.0392
750	26	Full	0.126	0.0419	0.259	0.0379	0.335	0.0325
750	-	Off	0.120	0.0397	0.252	0.0367	0.318	0.0304
800	39	Full	0.155	0.0548	0.286	0.0445	0.374	0.0389
800	26	Full	0.129	0.0448	0.249	0.0377	0.333	0.0336
800	-	Off	0.122	0.0421	0.241	0.0363	0.322	0.0322
850	39	Full	0.203	0.0772	0.378	0.0656	0.446	0.0511
850	26	Full	0.183	0.0686	0.333	0.0588	0.380	0.0413
850	-	Off	0.171	0.0635	0.306	0.0502	0.339	0.0357
850	39	Half	0.191	0.0720	0.299	0.0489	0.372	0.0402
850	26	Half	0.185	0.0694	0.286	0.0462	0.351	0.0373
850	-	Off	0.171	0.0635	0.269	0.0430	0.339	0.0357
900	39	Full	0.187	0.0730	0.308	0.0526	0.395	0.0451
900	26	Full	0.158	0.0604	0.259	0.0426	0.339	0.0370
900	-	Off	0.178	0.0690	0.300	0.0509	0.365	0.0407
950	39	Full	0.179	0.0720	0.368	0.0683	0.526	0.0696
950	26	Full	0.184	0.0743	0.356	0.0654	0.451	0.0559
950	-	Off	0.170	0.0680	0.321	0.0574	0.392	0.0463
1000	39	Full	0.270	0.1203	-	-	-	-
1000	26	Full	0.265	0.2277	-	-	-	-
1000	-	Off	0.249	0.1092	-	-	-	-

Note: Full power = 25 watts, half power = 12.5 watts

TABLE 6

CONSTANTS OF THE EQUATION OF MASS TRANSFER COEFFICIENTS

AS A FUNCTION OF TEMPERATURE

General Equation: $\log k_g = bT + a$

W/F_{A_o} gm cat-sec / gm mole	f x 10^{-3} cps	a	b	99% Confidence Interval		95% Confidence Interval		90% Confidence Interval		Approximate Confidence	
				a	b	a	b	a	b	a	b
80,000	-	-2.66	0.00169	0.05	0.00007	0.03	0.00004	0.02	0.00003	-	-
80,000	26	-2.75	0.00185	0.28	0.00038	0.15	0.00021	0.11	0.00015	75%	90%
80,000	39	-2.80	0.00203	0.31	0.00042	0.17	0.00023	0.12	0.00017	90%	97%
50,000	-	-2.74	0.00193	0.19	0.00026	0.10	0.00014	0.08	0.00011	-	-
50,000	26	-2.71	0.00190	0.39	0.00054	0.21	0.00029	0.16	0.00022	30%	25%
50,000	39	-2.32	0.00146	0.28	0.00043	0.15	0.00023	0.11	0.00017	97%	94%
20,000	-	-3.39	0.00294	0.05	0.00008	0.03	0.00005	0.02	0.00004	-	-
20,000	26	-3.36	0.00293	0.20	0.00024	0.12	0.00015	0.09	0.00011	52%	15%
20,000	39	-2.99	0.00253	0.31	0.00013	0.19	0.00008	0.14	0.00006	99%	99%

FIGURE 17

MASS TRANSFER COEFFICIENT vs. TEMPERATURE

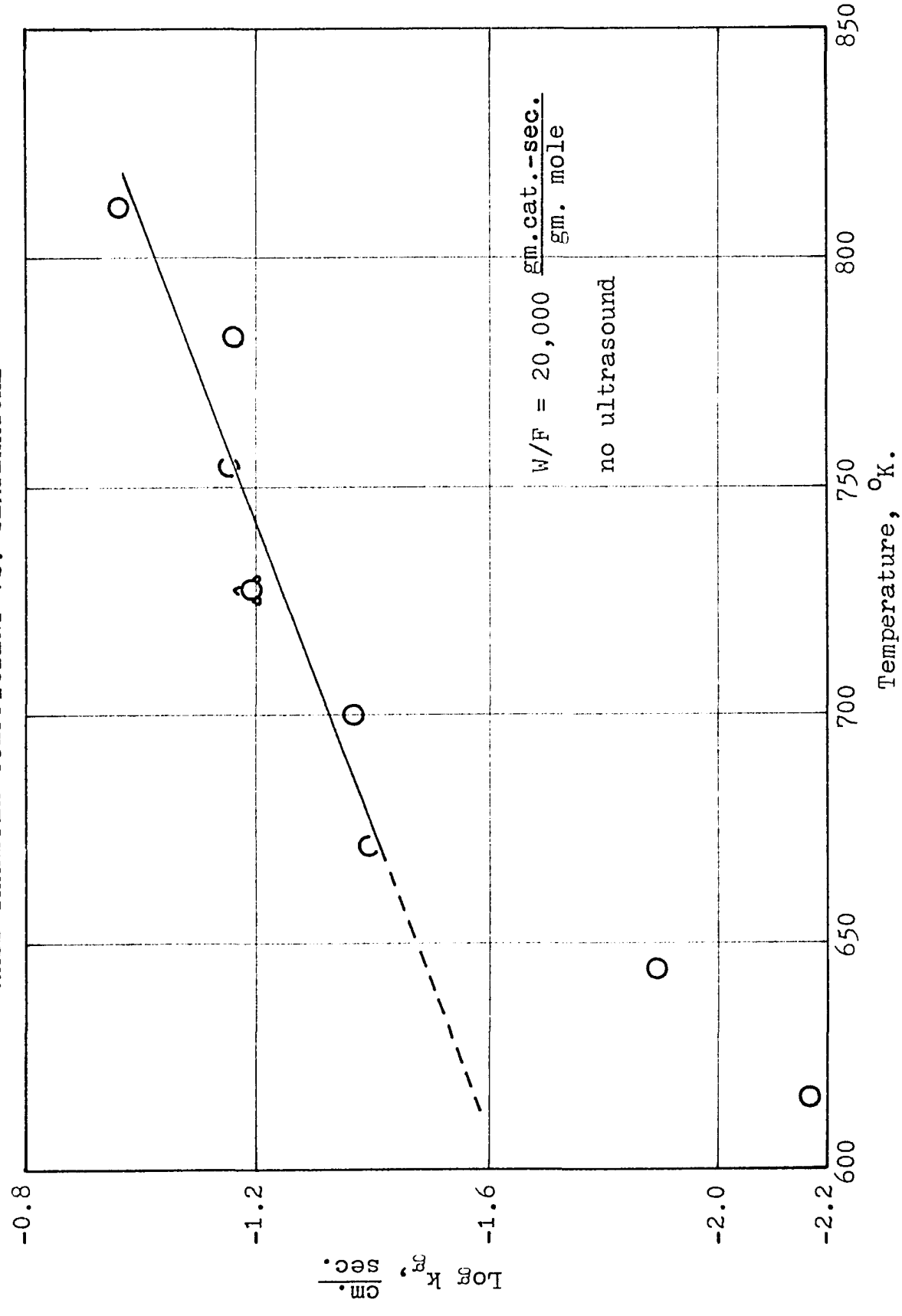

FIGURE 18

MASS TRANSFER COEFFICIENT vs. TEMPERATURE

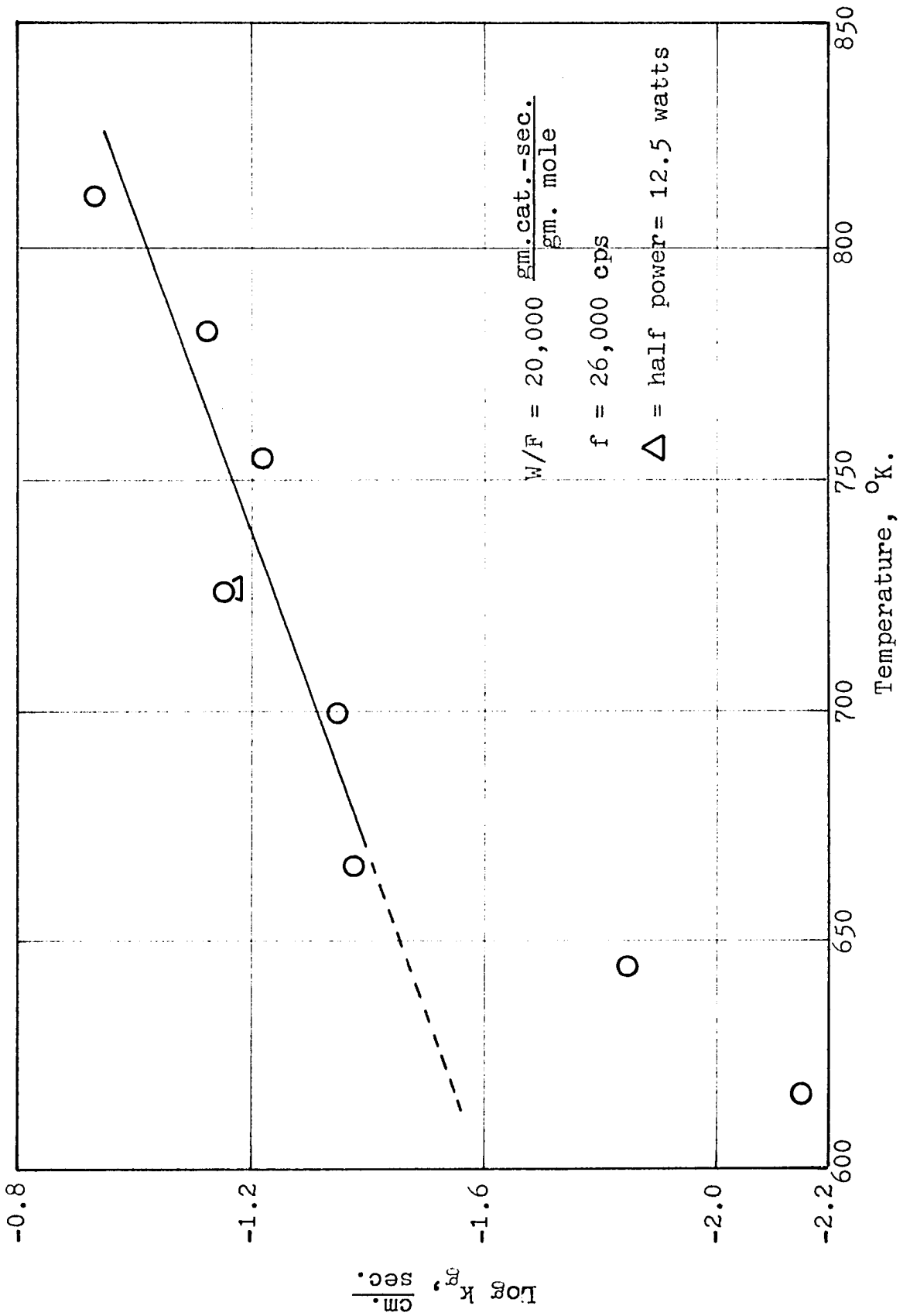

FIGURE 19

MASS TRANSFER COEFFICIENT vs. TEMPERATURE

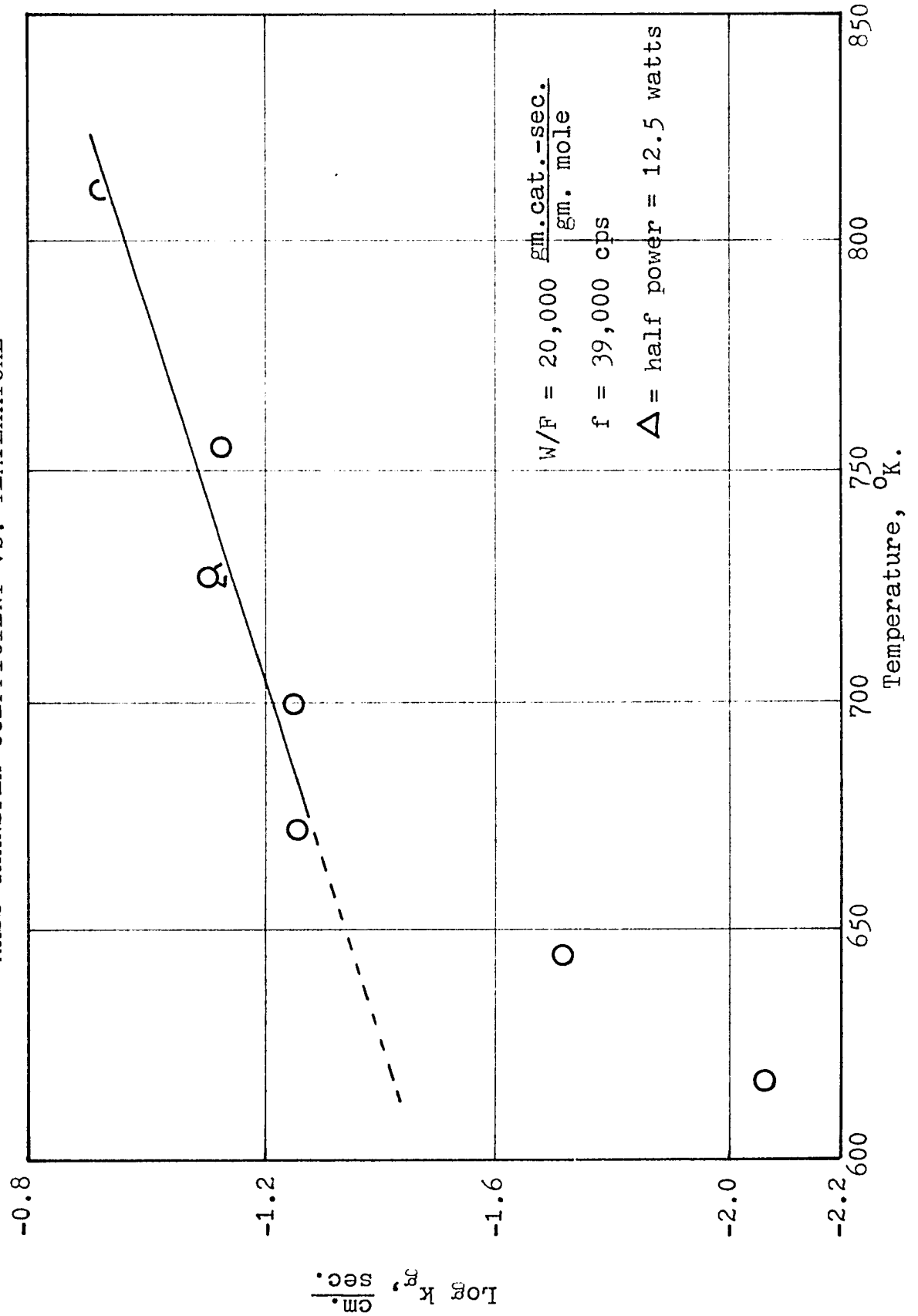

FIGURE 19A

MASS TRANSFER COEFFICIENT vs. TEMPERATURE

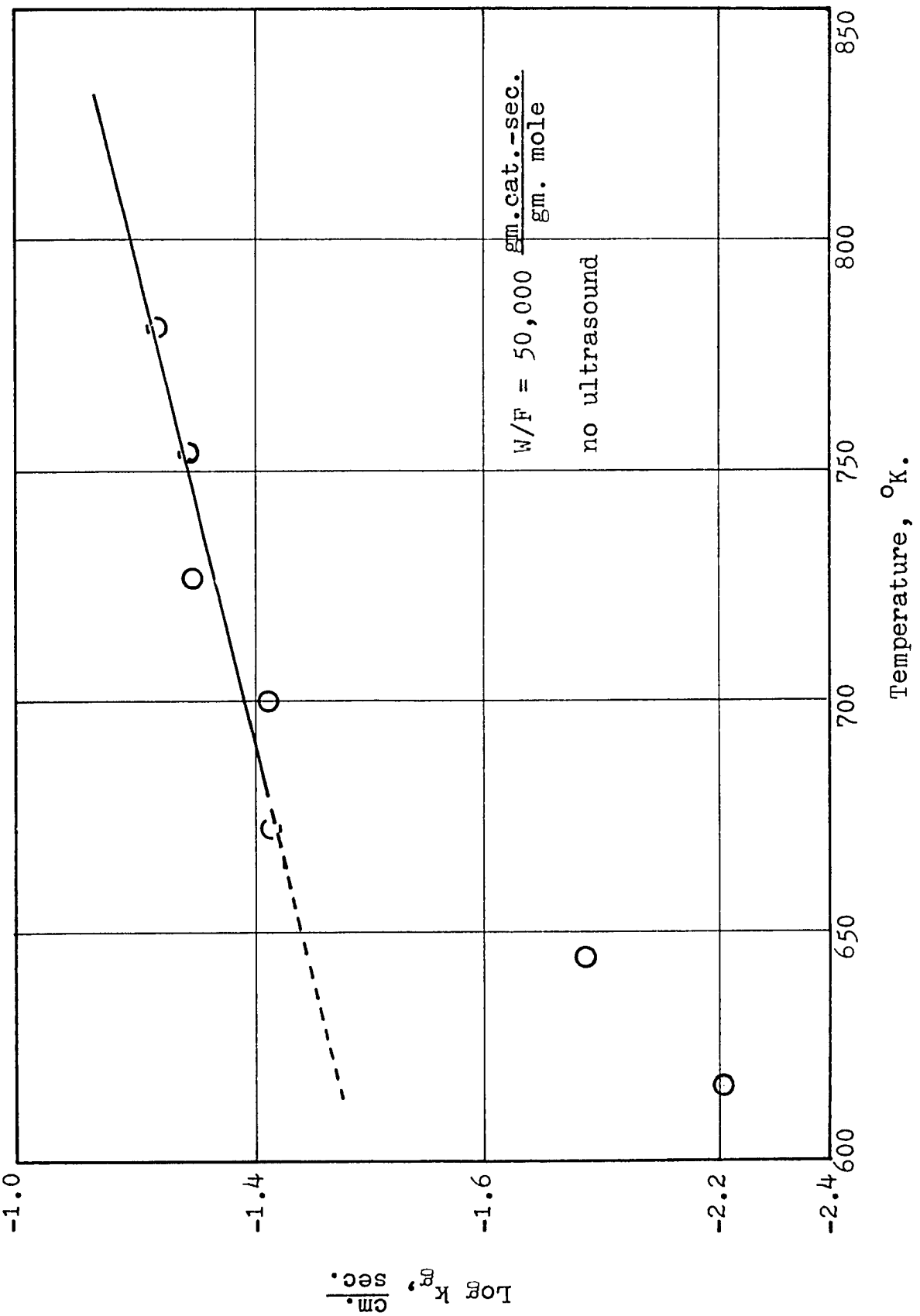

FIGURE 19B

MAS TRANSFER COEFFICIENT vs. TEMPERATURE

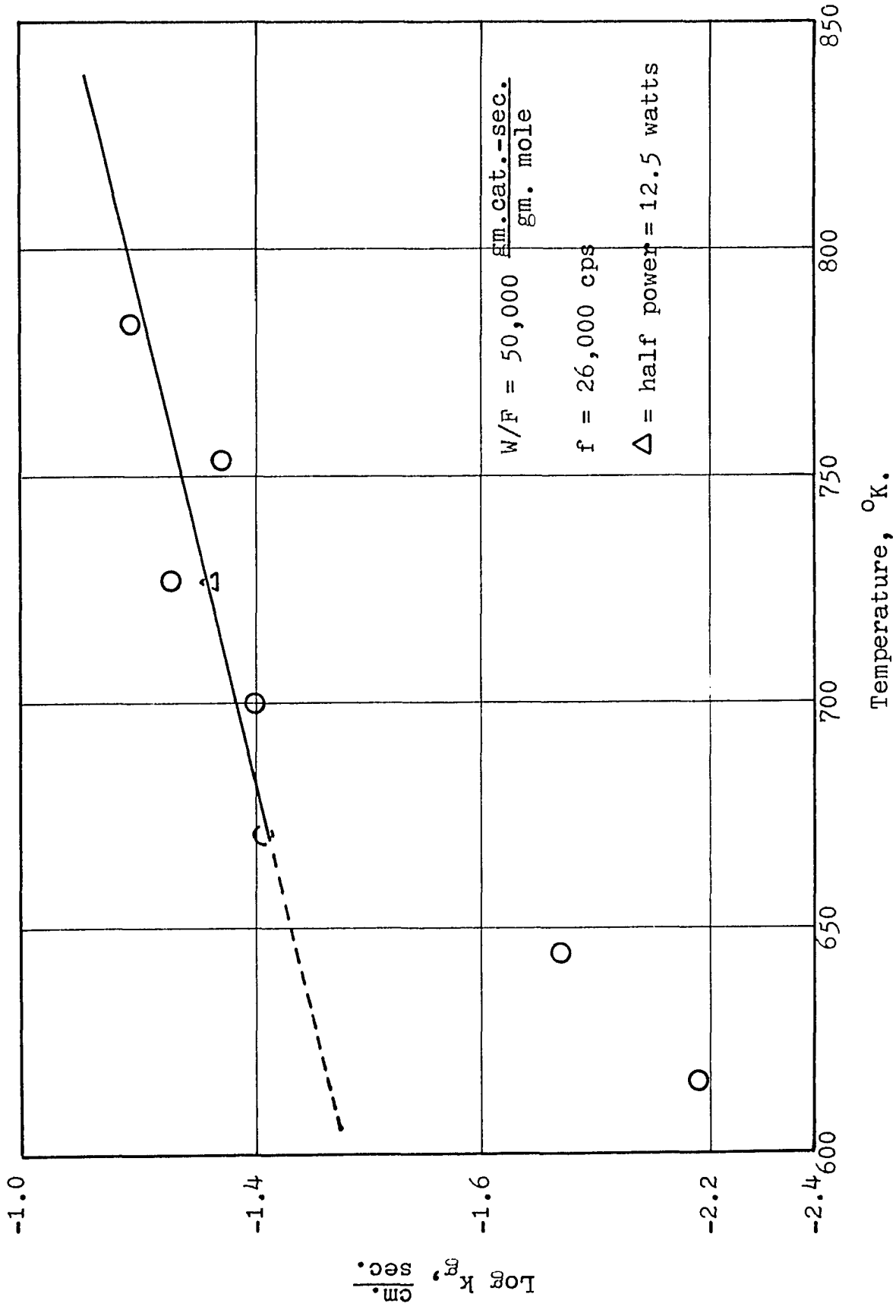

FIGURE 19C

MASS TRANSFER COEFFICIENT vs. TEMPERATURE

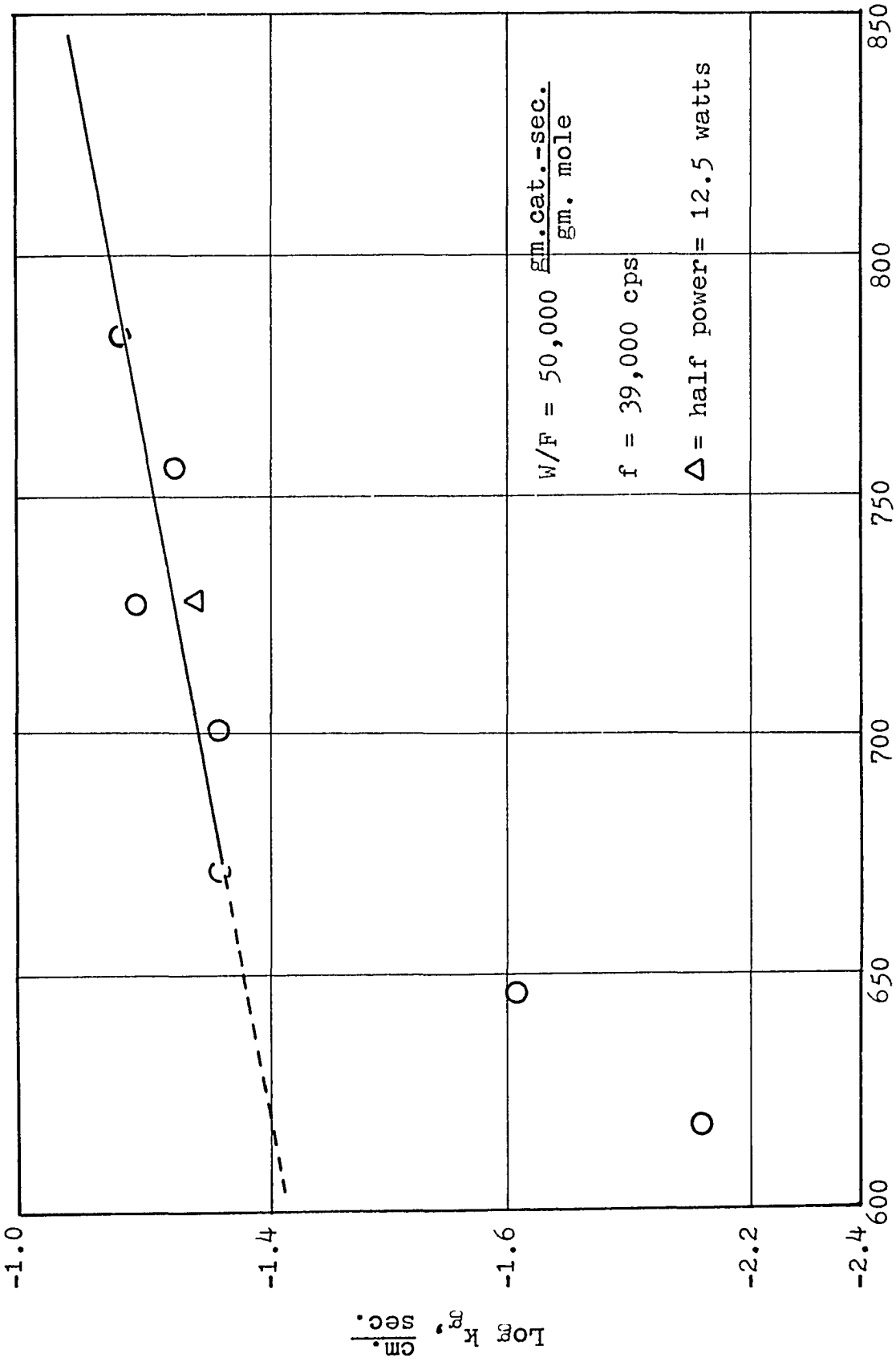

FIGURE 20

MASS TRANSFER COEFFICIENT vs. TEMPERATURE

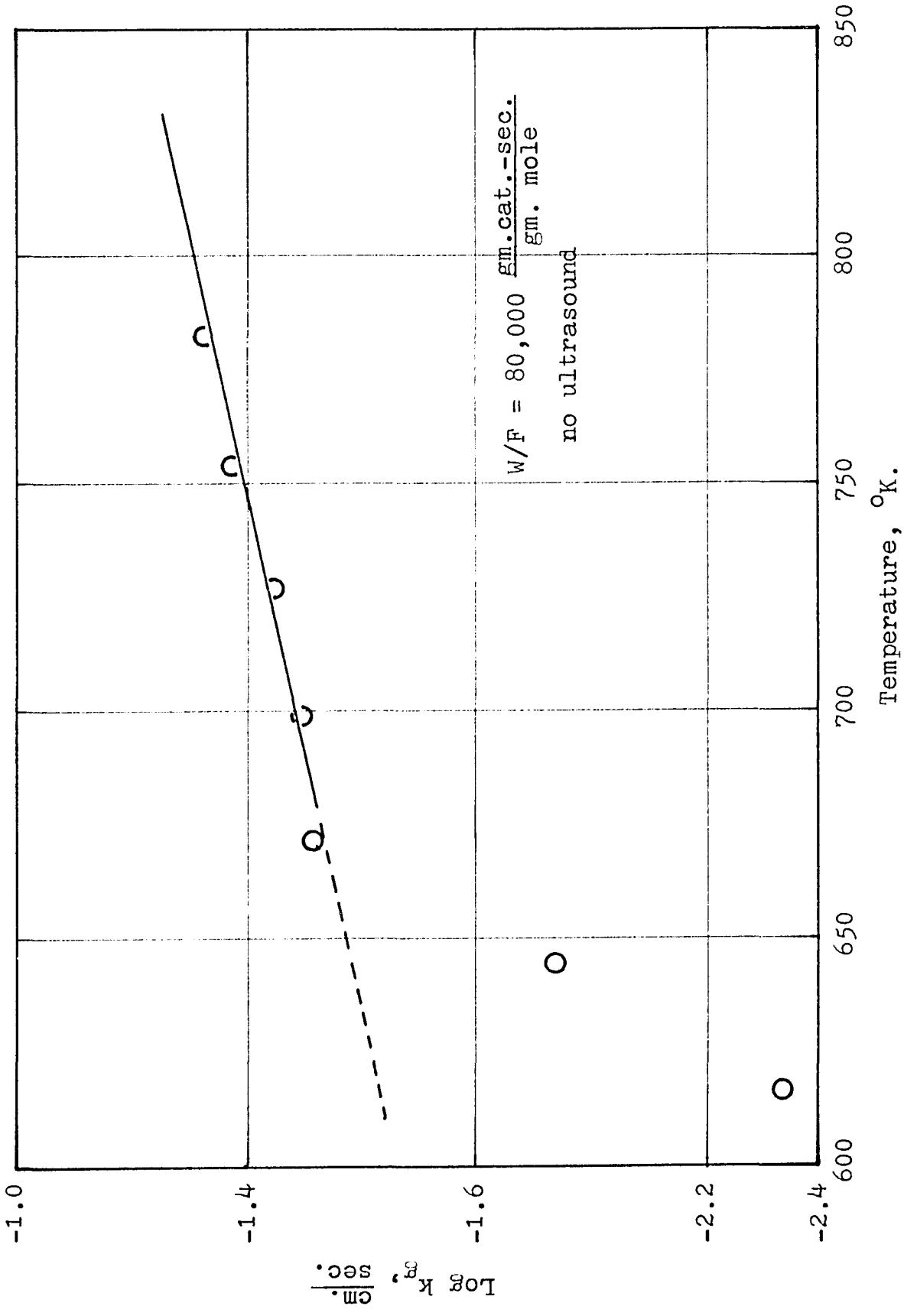

FIGURE 21

MASS TRANSFER COEFFICIENT vs. TEMPERATURE

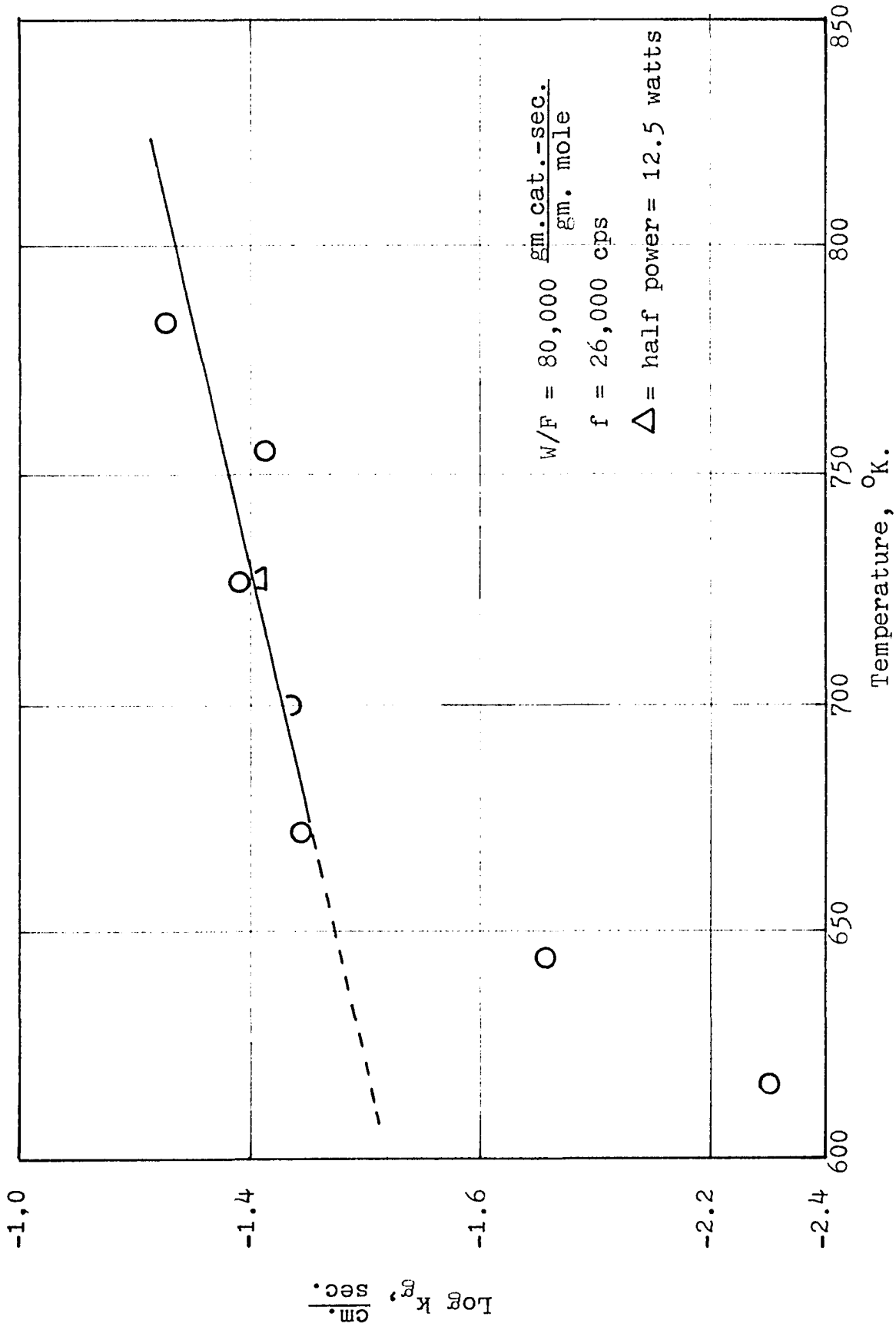

FIGURE 22

MASS TRANSFER COEFFICIENT vs. TEMPERATURE

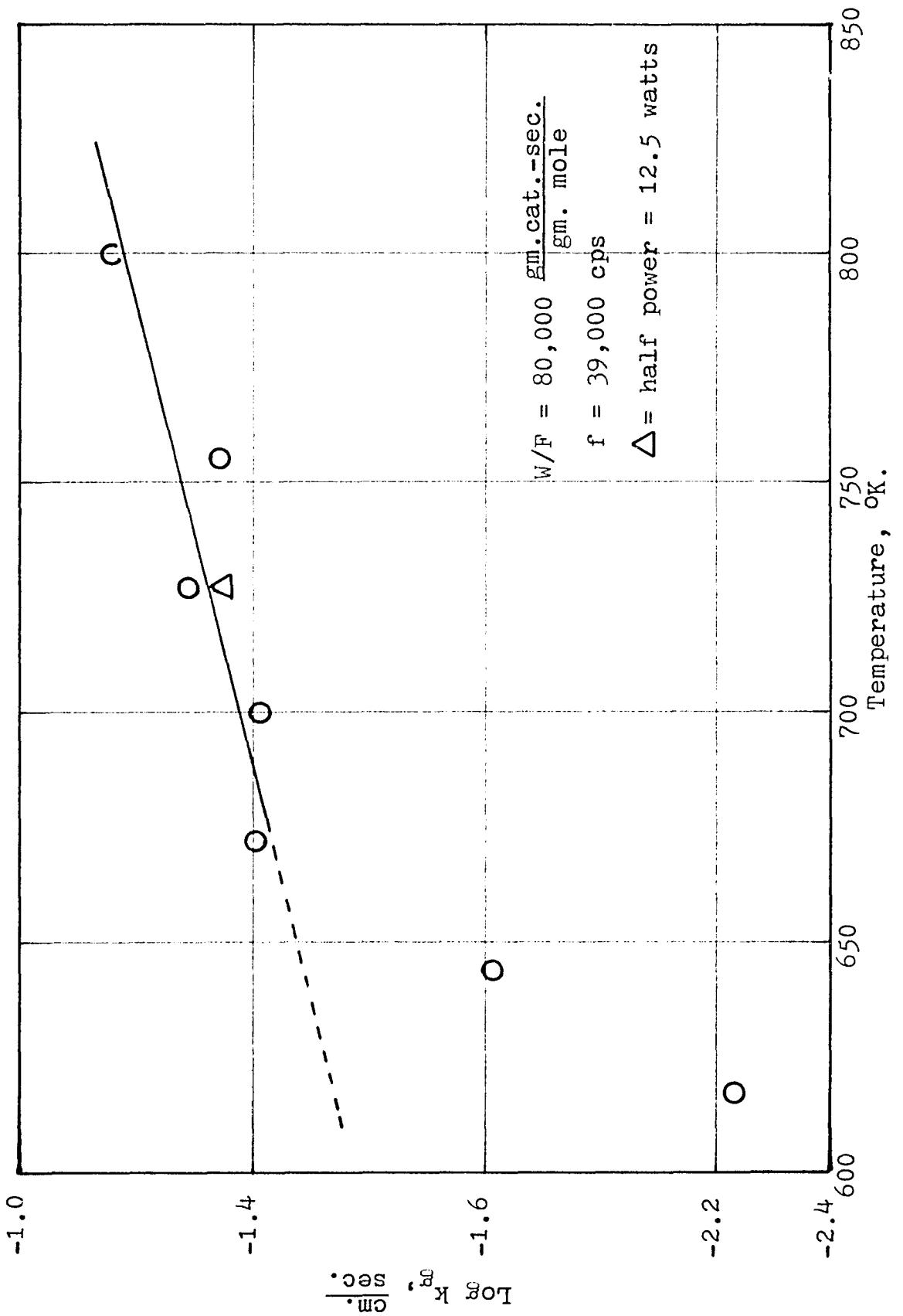

rate of reaction at these low temperatures. In fact, even at these low flow rates, surface reaction is so slow at 650°F. and 700°F. that it becomes the controlling factor in the overall reaction rate. At above 850°F. (727°K.) surface reaction rate is very rapid and external bulk diffusion controls the rate of reaction.

Ultrasonic effect. The family of three curves showing each frequency is plotted at the three feed rates in Figures 23, 23A and 24. In all cases, the mass transfer coefficient and hence the reaction rate is increased with the application of ultrasound. The mass transfer rate also increases at the higher frequencies. For example, at a reciprocal space velocity of 80,000 $\frac{\text{gm cat-sec.}}{\text{gm mole}}$ and a frequency of 39,000 cps, the mass transfer coefficient is increased by 37% at 1000°F. The increase of mass transfer rates at other conditions are shown in Table 7.

Since in this range of feed rate and temperature reaction rate is directly proportional to the mass transfer coefficient, the results illustrated in Table 7 also apply to reaction rate.

At high feed rates and low temperatures where surface reaction begins to control the rate of reaction, high frequency sound waves appear to have a much greater effect on the reaction rate than at higher temperatures where mass transport controls. This phenomenon is indicated in the

FIGURE 23

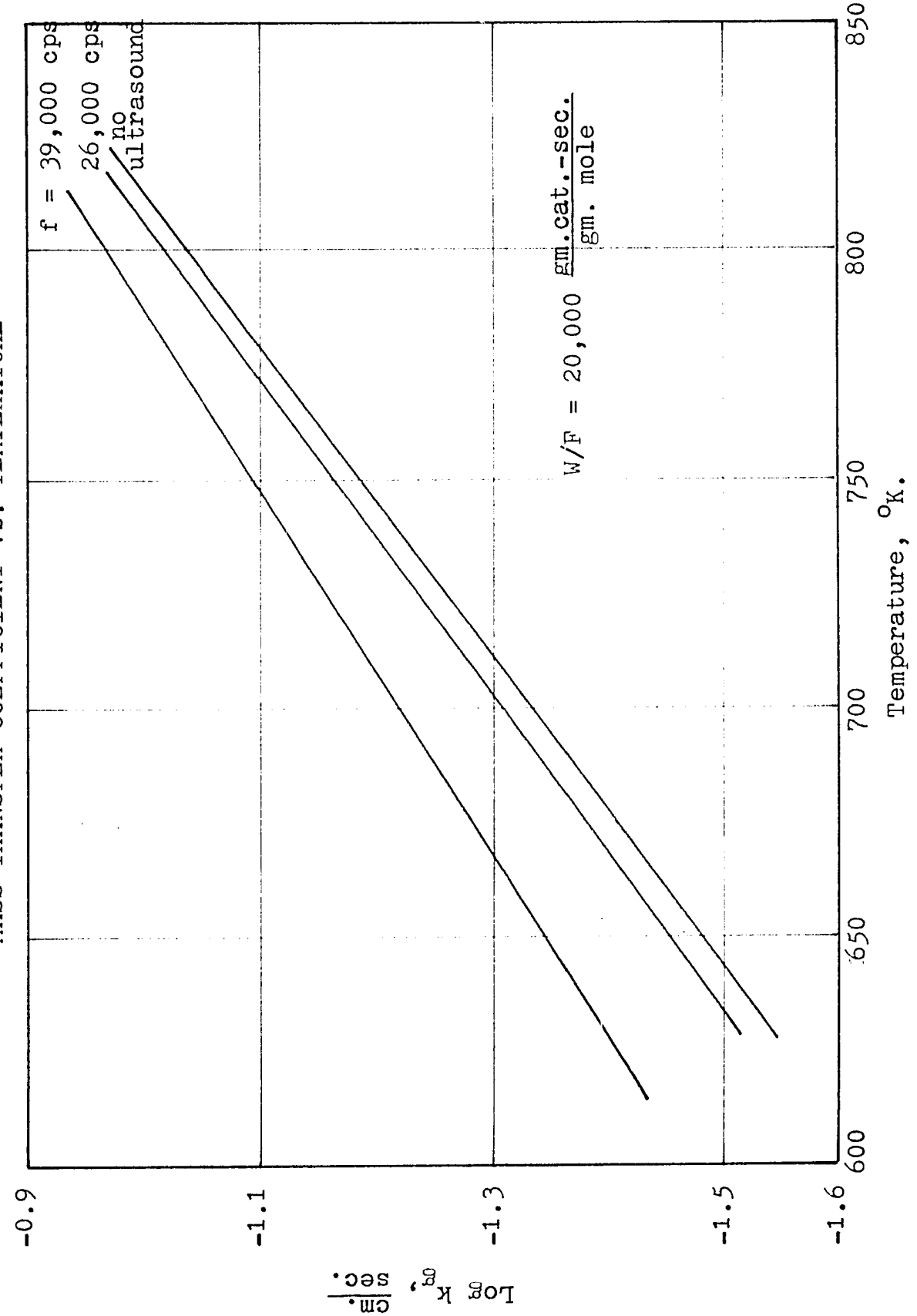

FIGURE 23A

MASS TRANSFER COEFFICIENT vs. TEMPERATURE

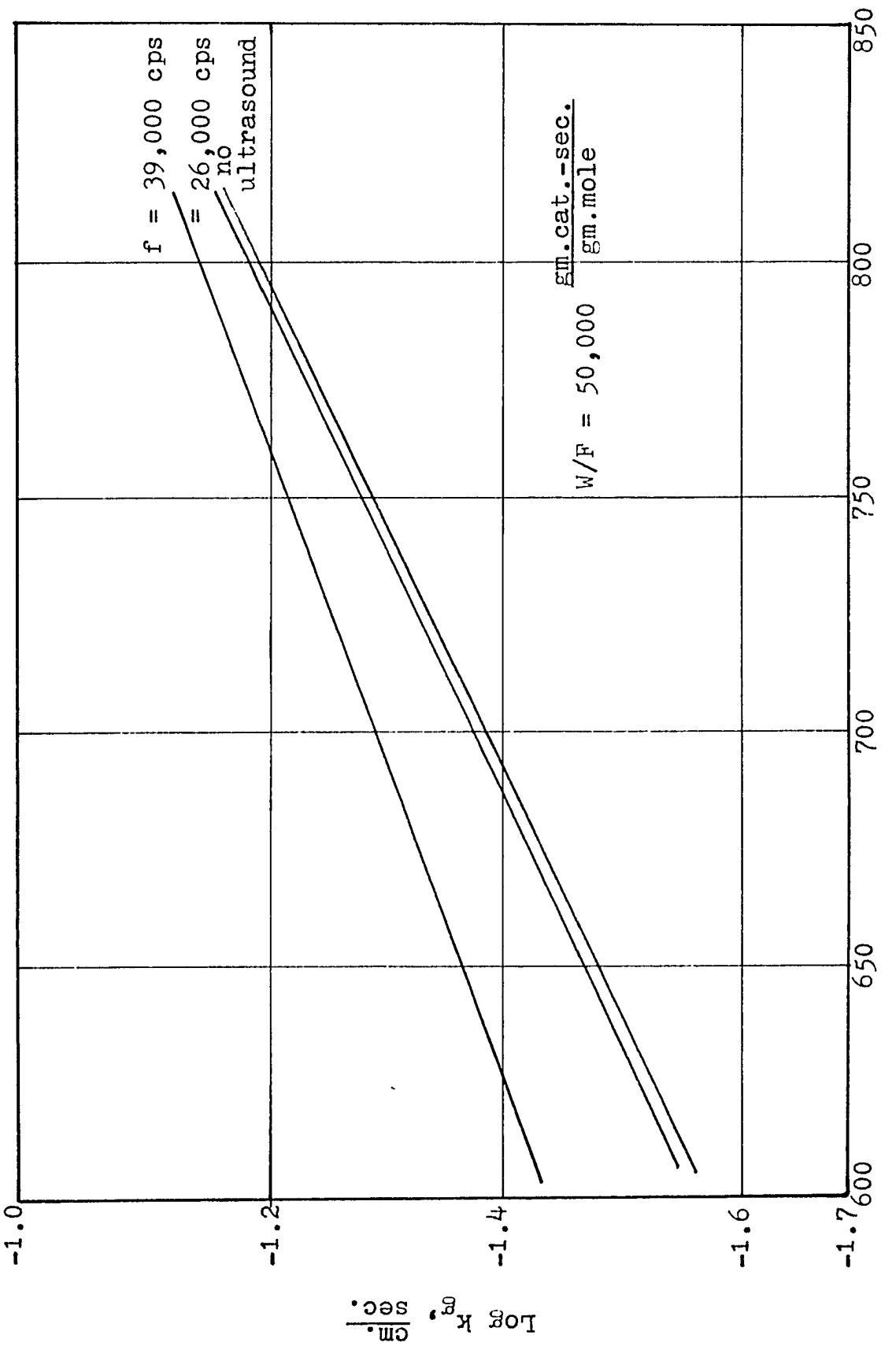

FIGURE 24

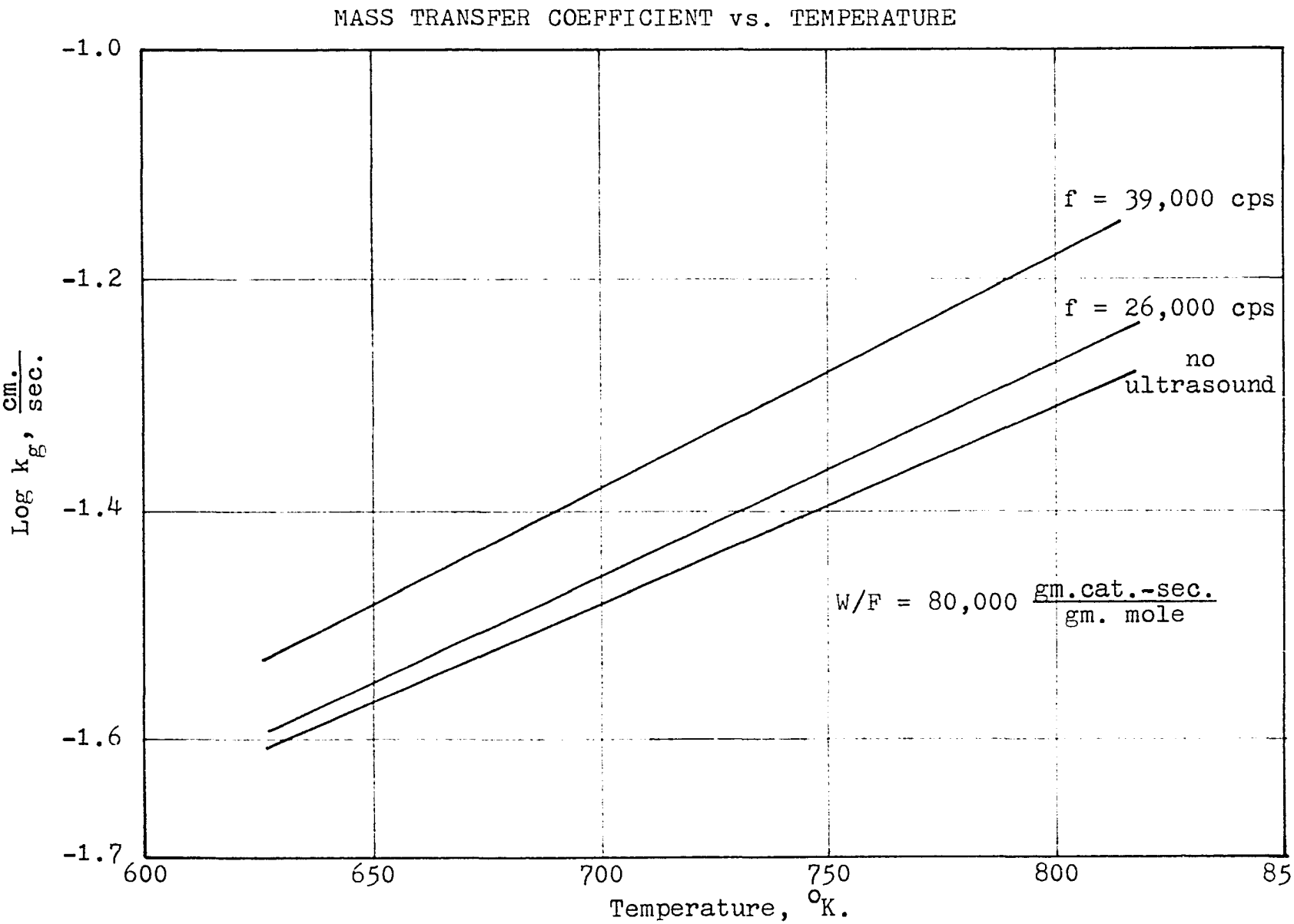

TABLE 7

INCREASE IN MASS TRANSFER COEFFICIENT AT SEVERAL FEED RATES, TEMPERATURES AND ULTRASONIC FREQUENCIES

W/F gm cat-sec. / gm mole	Temp., °F.	f, cps	Power	% Increase of k_g
80,000	650	26,000	Full	2.0
80,000	850	26,000	Full	6.2
80,000	850	26,000	Half	9.7
80,000	1000	26,000	Full	9.6
80,000	650	39,000	Full	2.2
80,000	850	39,000	Full	20.5
80,000	850	39,000	Half	18.2
80,000	1000	39,000	Full	36.7
50,000	650	26,000	Full	2.7
50,000	850	26,000	Full	1.9
50,000	850	26,000	Half	0.7
50,000	1000	26,000	Full	1.3
50,000	650	39,000	Full	35.0
50,000	850	39,000	Full	19.7
50,000	850	39,000	Half	13.7
50,000	1000	39,000	Full	9.5
20,000	650	26,000	Full	5.7
20,000	850	26,000	Full	5.4
20,000	850	26,000	Half	3.7
20,000	1000	26,000	Full	5.2
20,000	650	39,000	Full	40.4
20,000	850	39,000	Full	26.4
20,000	850	39,000	Half	28.8
20,000	1000	39,000	Full	16.8

Full power = 25 watts
Half power = 12.5 watts

data of Table 7 at reciprocal space velocities of 20,000 $\frac{\text{gm cat-sec.}}{\text{gm mole}}$ and frequencies of 39,000 cps. These data indicate that ultrasound has a greater influence upon pore diffusion and surface reaction rate than upon external mass transport.

The data points on the graphs represented by triangles are those obtained with the ultrasonic generator operating at half power. Since these points fall on the theoretical curve developed for full power within the 90% confidence interval, it is concluded that power input has no effect on the external mass transfer rate for the range of power input studied in this research.

Surface Reaction and Pore Diffusion Controlling

Reaction rate model. The reaction design equation for surface reaction controlling and propylene not adsorbed as derived in Chapter II is as follows:

$$\frac{W}{F_{A_o}} = \gamma\left[\left(\frac{1}{2\delta} - \frac{1}{2\delta^3}\right) \ln \frac{(1+X_A\delta)}{(1-X_A\delta)} + \frac{X_A}{\delta^2}\right] + \beta\left[\frac{1}{2\delta^3} \ln \frac{(1+X_A\delta)}{(1-X_A\delta)} - \frac{1}{2\delta^2} \ln (1-\delta^2 X_A^2) - \frac{X_A}{\delta^2}\right] \quad (23)$$

where,

$$\gamma = \frac{1}{\epsilon L k_2 K_A \Pi} + \frac{1}{\epsilon L k_2} \quad (24)$$

$$\mathcal{B} = \frac{2}{\epsilon Lk_2 K_A \pi} + \frac{K_R}{\epsilon Lk_2 K_A} \qquad (25)$$

$$\delta = \left[1 + \frac{\pi}{K}\right]^{\frac{1}{2}} \qquad (26)$$

The literature values of K, K_A and K_R are substituted into the surface reaction rate equation and the values of ϵLk_2 are calculated at each temperature as described in Appendix VIII. All the theoretical curves and the associated data points are also shown in Appendix VIII, and the data do, in fact, fit the theoretical model very well.

Ultrasonic effect. When surface reaction controls the rate of reaction, the application of ultrasound increased that rate by increasing the kinetic rate constant, ϵLk_2, which is directly proportional to the overall rate of reaction. The evaluation of the effectiveness factor based upon physical characteristics of the catalyst is shown in Appendix VI.

The graphs of conversion as a function of reciprocal space velocity as calculated by the reaction rate model are as illustrated in Figures 25 through 33. As illustrated by the graphs, the conversion is increased in the presence of ultrasound at every temperature studied. At temperatures above 900°F., the decrease in conversion at some flow rates again indicates possible coking of the reactor.

Table 8 shows the increase in the factor ϵLk_2 at several ultrasonic frequencies and temperatures.

FIGURE 25

CONVERSION vs. W/F

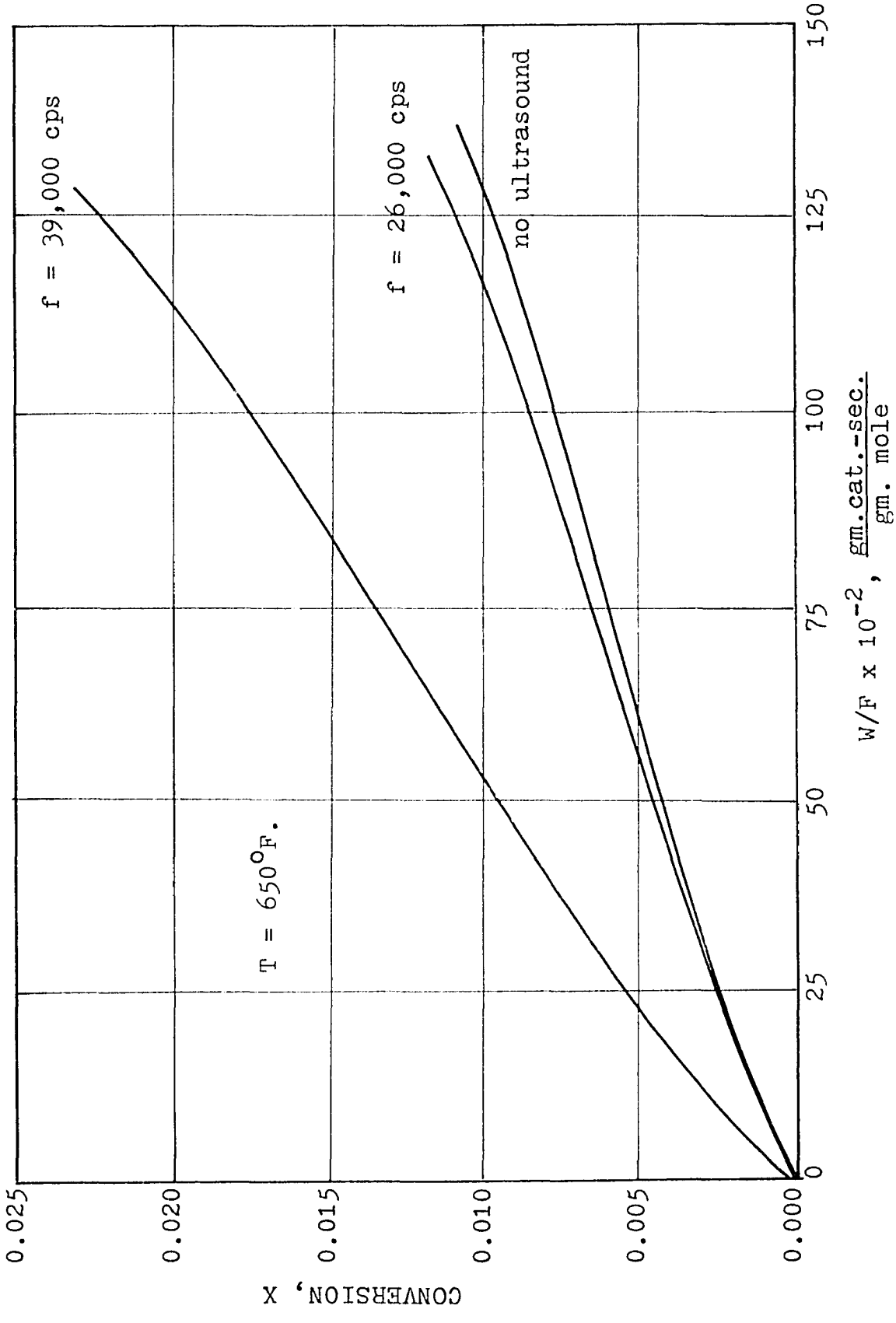

FIGURE 26

CONVERSION vs. W/F

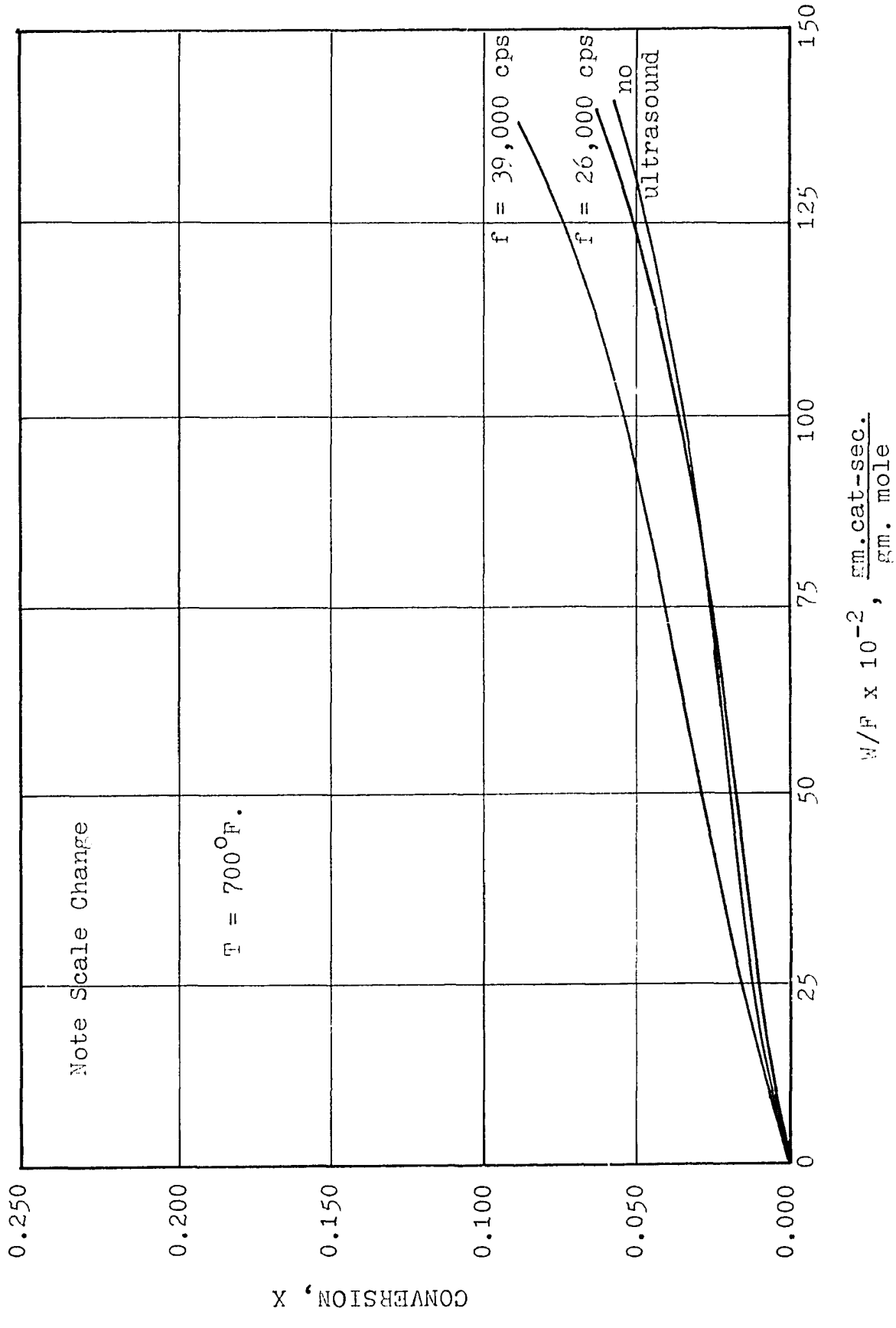

FIGURE 27

CONVERSION vs. W/F

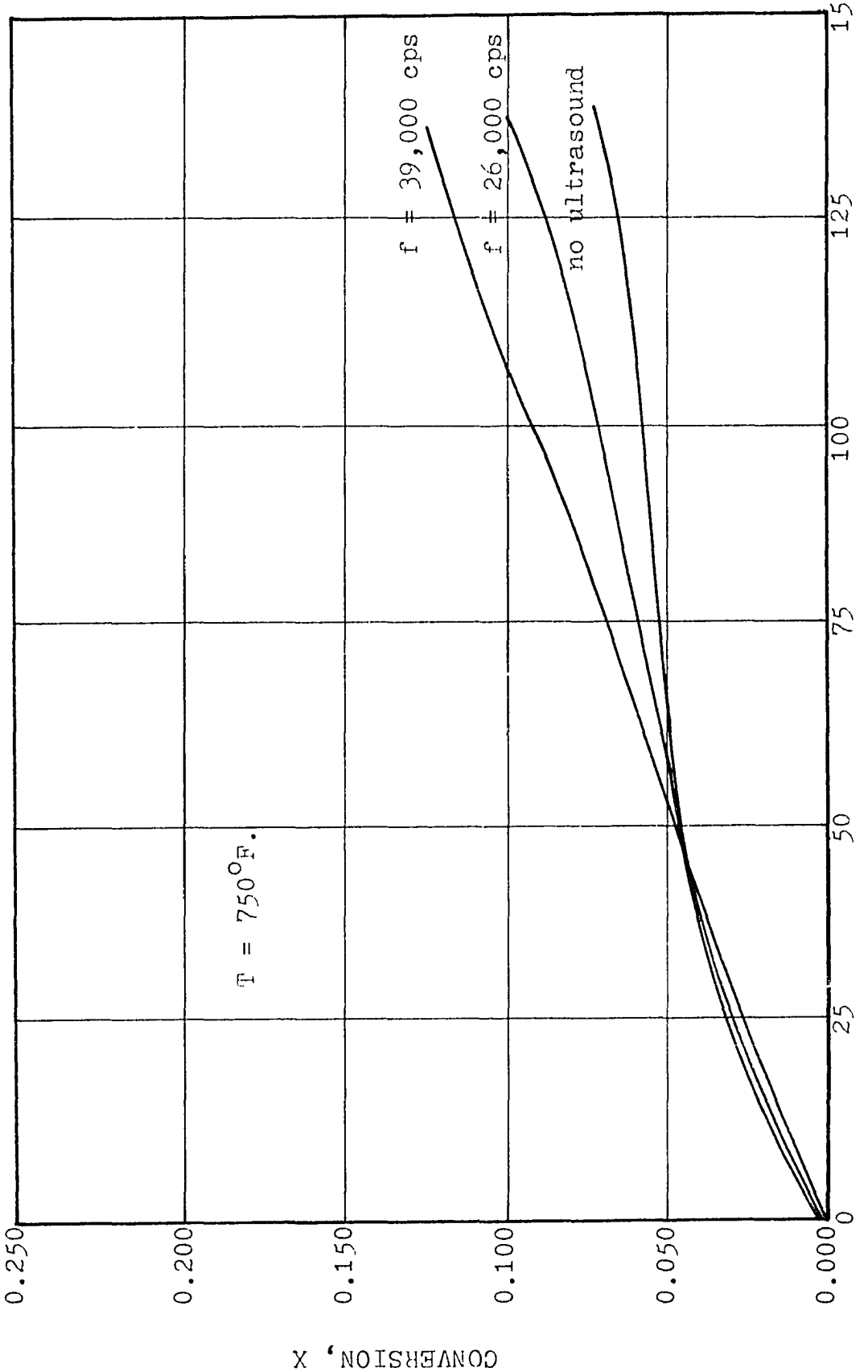

FIGURE 28

CONVERSION vs. W/F

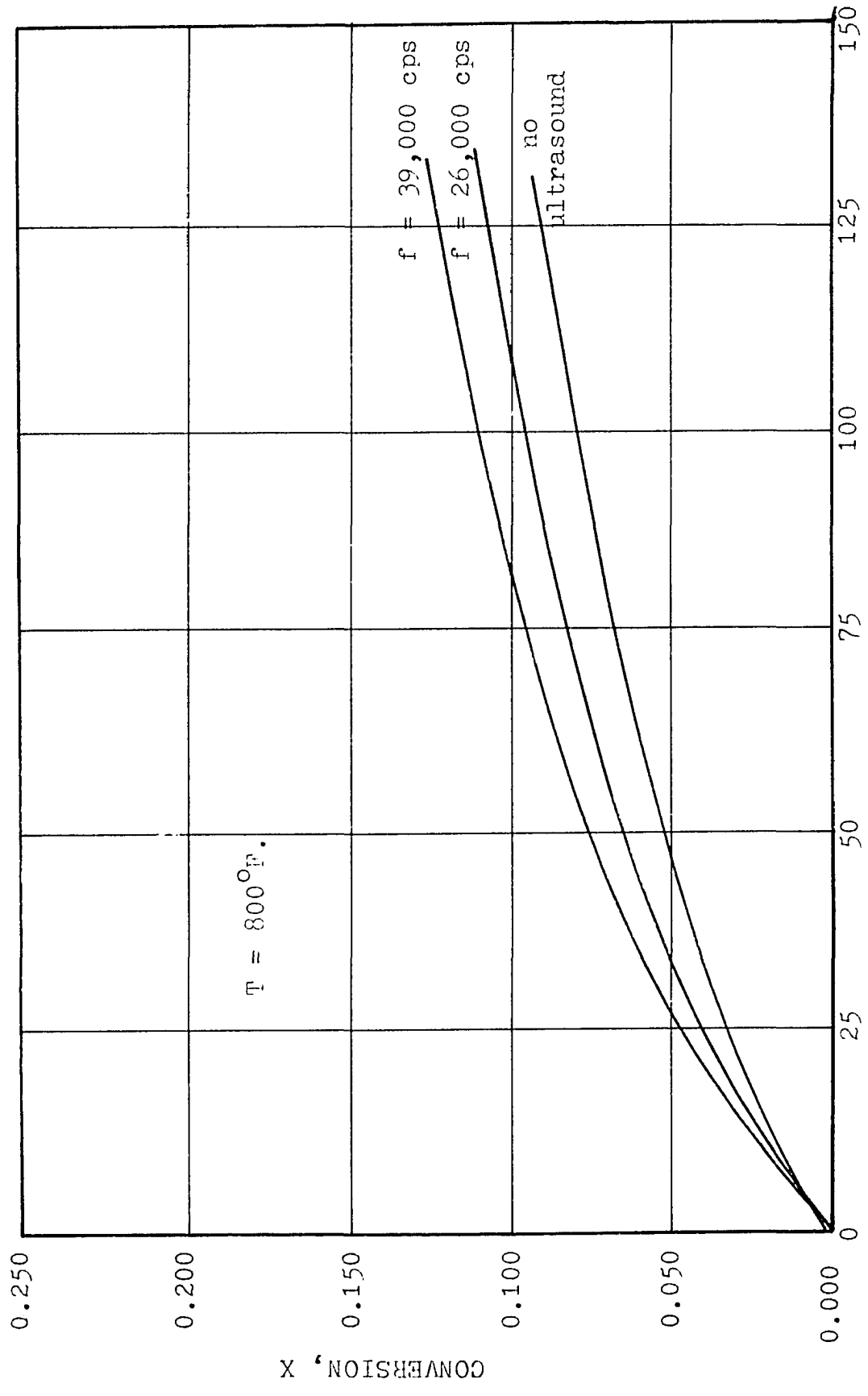

FIGURE 29

CONVERSION vs. W/F

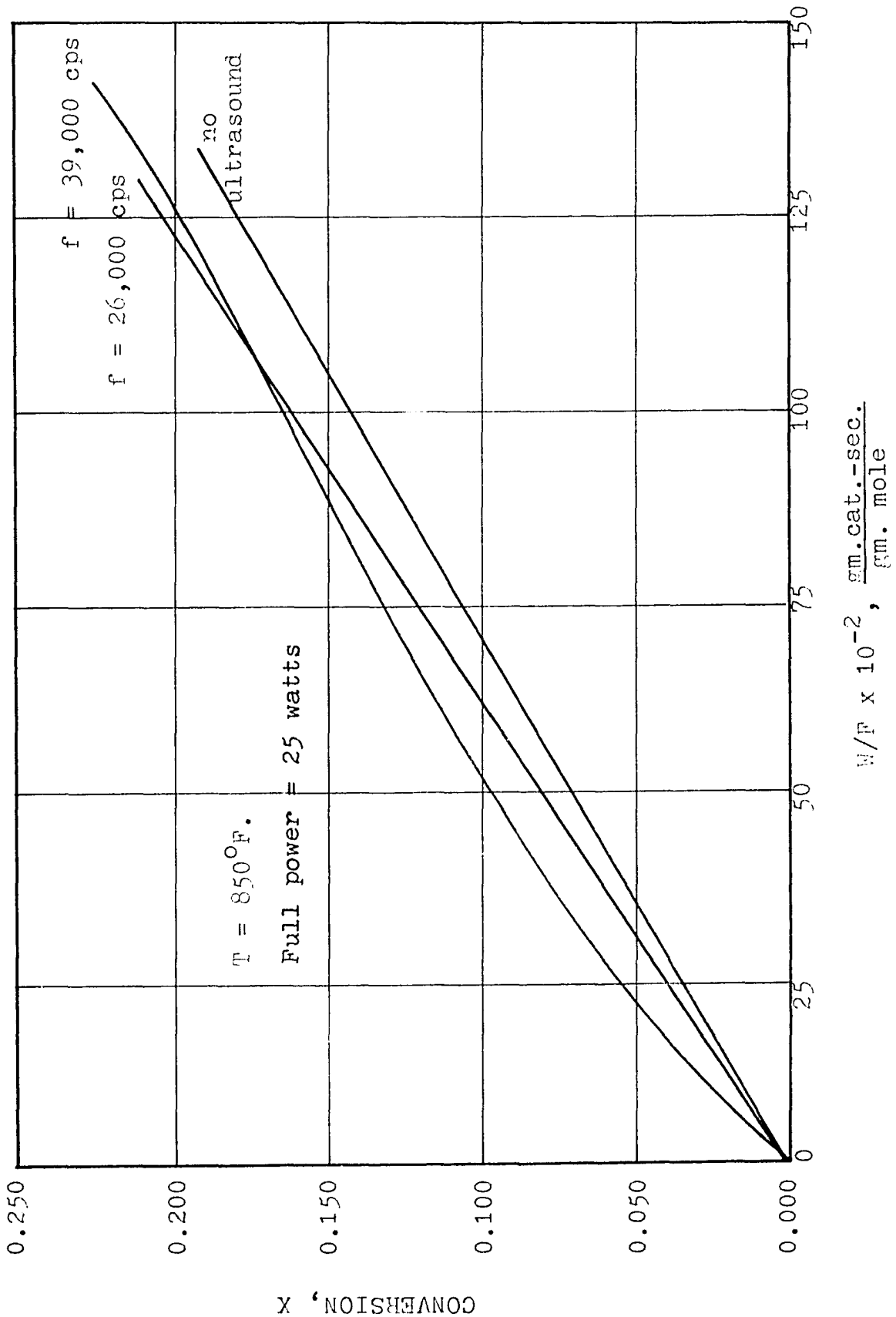

FIGURE 30

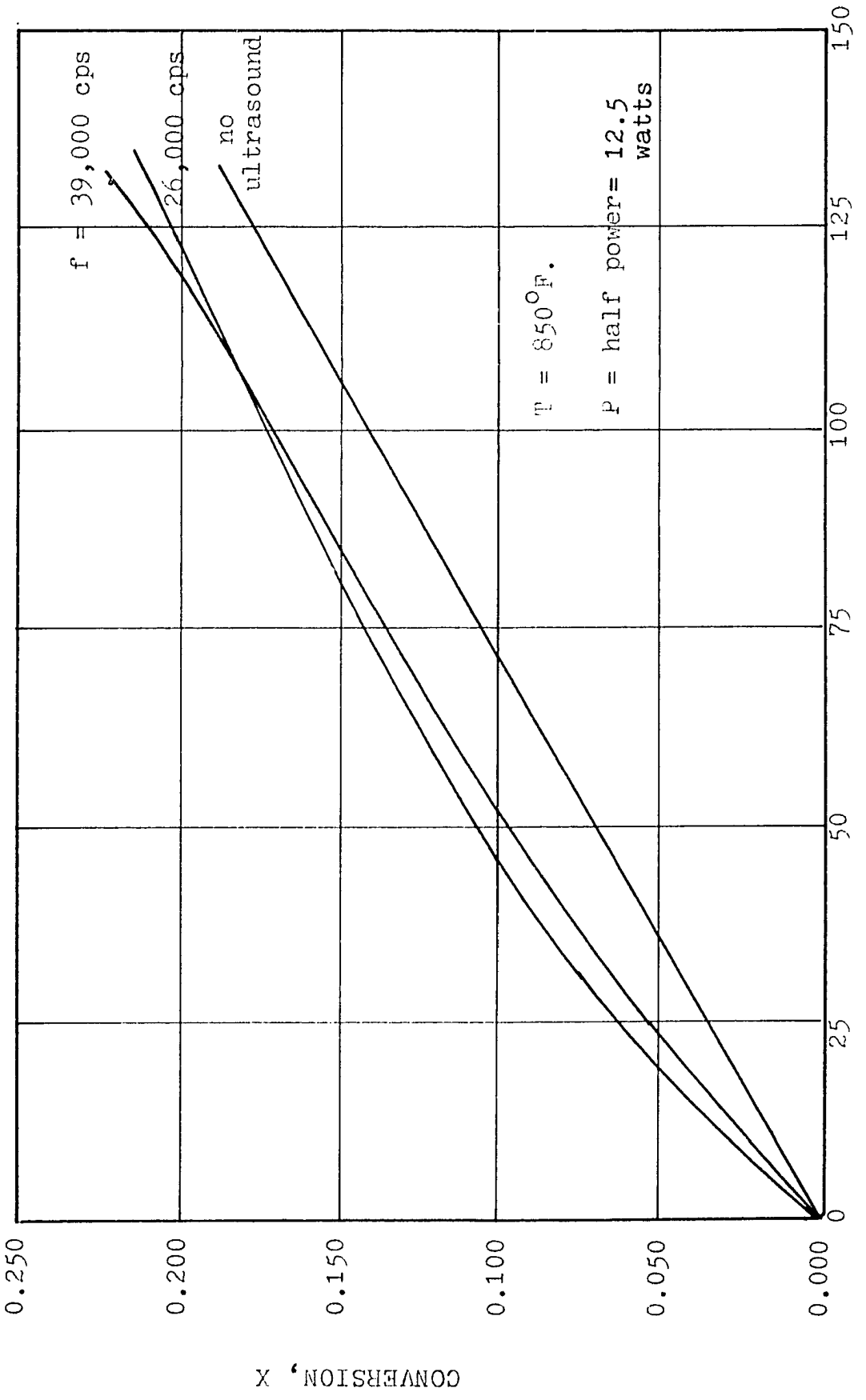

FIGURE 31

CONVERSION vs. W/F

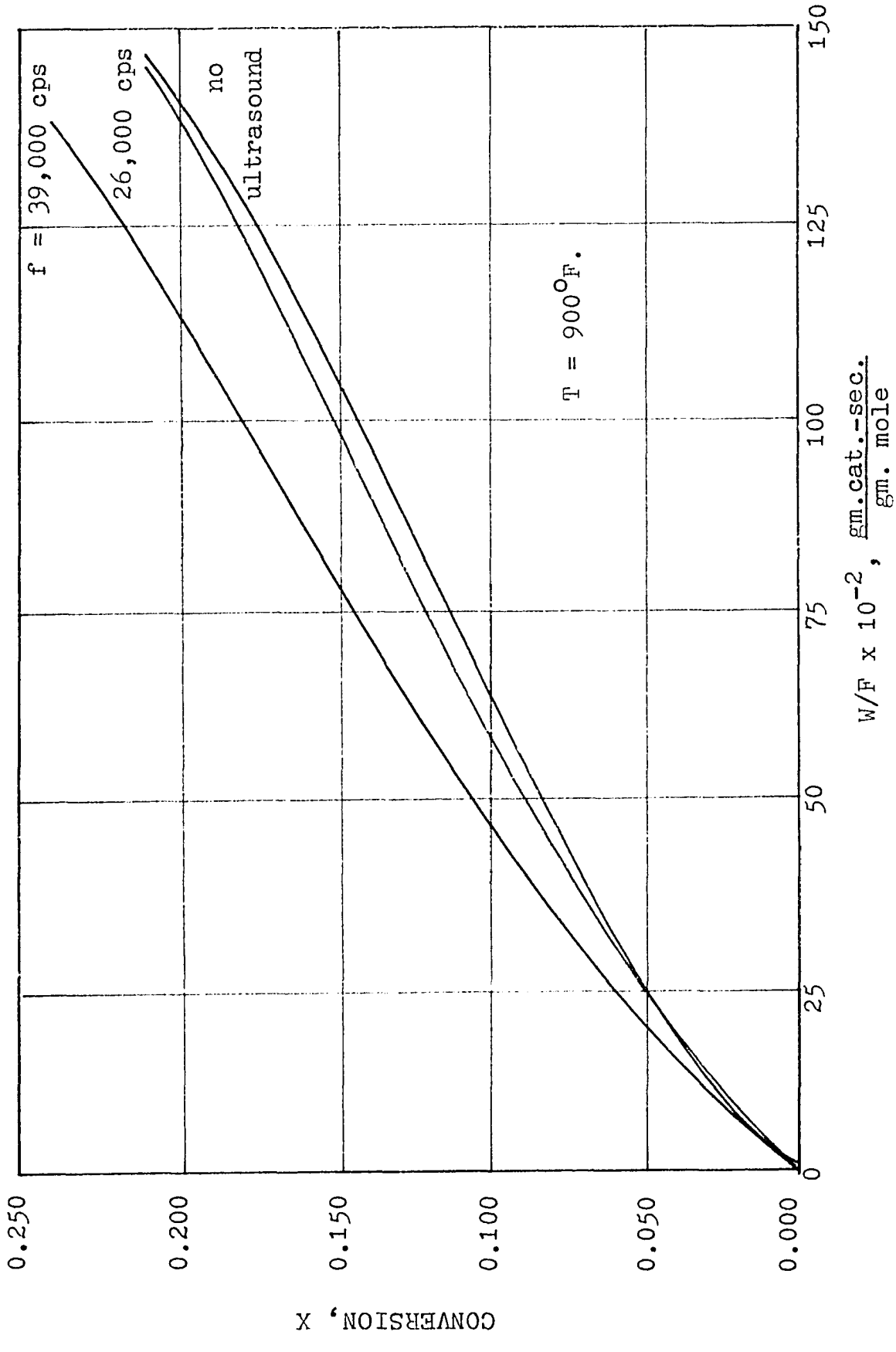

FIGURE 32

CONVERSION vs. W/F

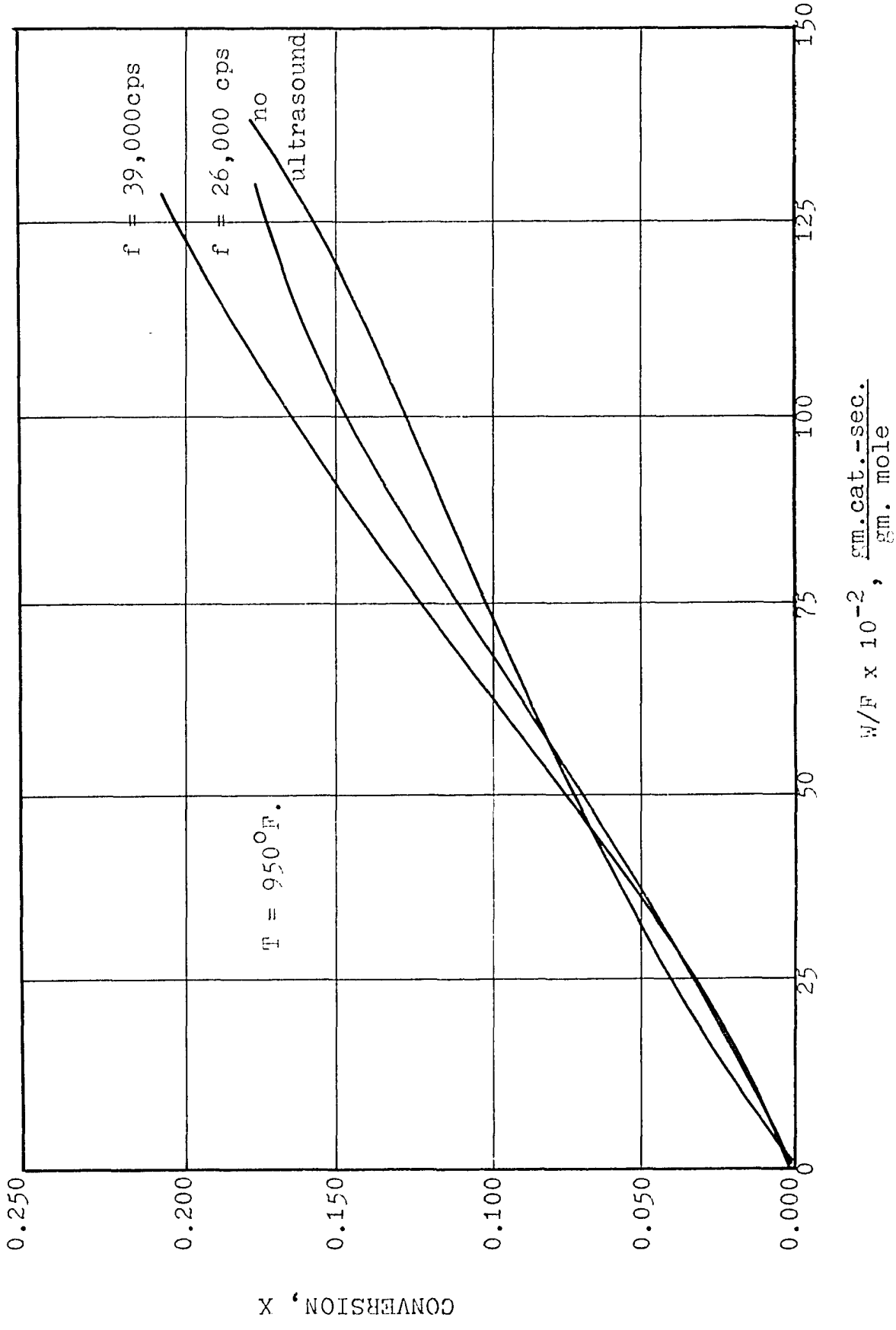

FIGURE 33

CONVERSION vs. W/F

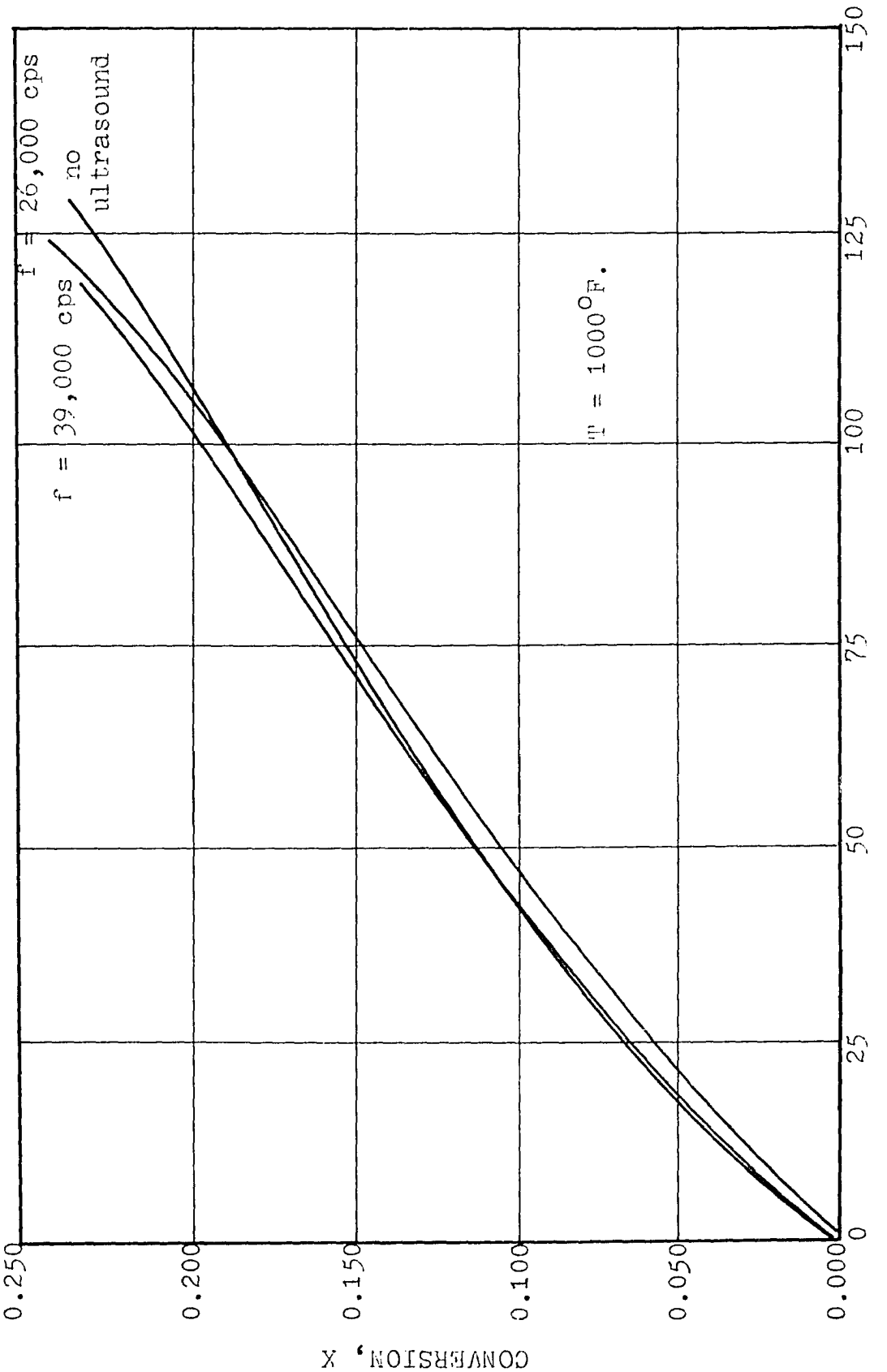

TABLE 8

INCREASE OF KINETIC RATE CONSTANT AT SEVERAL TEMPERATURES AND ULTRASONIC FREQUENCIES

	% Increase of $\epsilon_L k_2$	
T., °F.	26,000 cps	39,000 cps
650	36%	162%
750	20%	86%
850	9%	39%
900	4%	22%

TABLE 8A

CONSTANTS OF THE EQUATIONS OF KINETIC RATE CONSTANTS AS A FUNCTION OF TEMPERATURE

General Equation: $\log \epsilon L k_2 = b\left[\frac{1}{T}\right] + a$

Frequency, cps	No Ultrasound	26,000	39,000
a	-1.141	-1.637	-2.534
99% confidence interval	1.062	1.042	0.860
95% confidence interval	0.677	0.664	0.549
90% confidence interval	0.531	0.521	0.430
b	-4812	-4115	-2801
99% confidence interval	1343	1318	1088
95% confidence interval	857	840	694
90% confidence interval	671	659	544
Approximate confidence	-	65%	97%

For example, at 650°F. an ultrasonic frequency input of 39,000 cps increases the catalyst effectiveness factor by 162%.

Activation Energy

Arrhenius model. The activation energy, E, is calculated from the Arrhenius Law, employing the combined parameter, Lk_2, as the reaction rate constant.

$$\mathcal{E}Lk_2 = k_o e^{-\frac{E}{RT}} \qquad (27)$$

Figures 34 through 37 show the logarithm of the parameter $\mathcal{E}Lk_2$ plotted against reciprocal temperature. These plots yield a straight line, the equations for which, calculated by the method of least squares, are as follows and as shown in Table 8A.

$$\text{No ultrasound:} \quad \log \mathcal{E}Lk_2 = -4812 \frac{1}{T^{\circ}R.} - 1.141 \qquad (28)$$

$$\text{26,000 cps:} \quad \log \mathcal{E}Lk_2 = -4115 \frac{1}{T^{\circ}R.} - 1.637 \qquad (29)$$

$$\text{39,000 cps:} \quad \log \mathcal{E}Lk_2 = -2801 \frac{1}{T^{\circ}R.} - 2.534 \qquad (30)$$

These calculations, which are described fully in Appendix XVII, yield the values for the observed apparent activation energy as shown in Table 9.

The data in Table 9 indicate that both the observed apparent activation energy and the observed apparent frequency factor decrease as the ultrasonic frequency rises. However, an analysis based on the Thiele modulus would indicate that if ultrasound improves the effectiveness factor, then the apparent activation energy should rise and approach the real activation energy based on k_2 since $\mathcal{E}$ becomes closer to one.

To determine the real effect of ultrasound on and k_2, it is suggested that further studies with small particle sizes be made ($\mathcal{E} \sim 1$) to separate these effects.

FIGURE 34

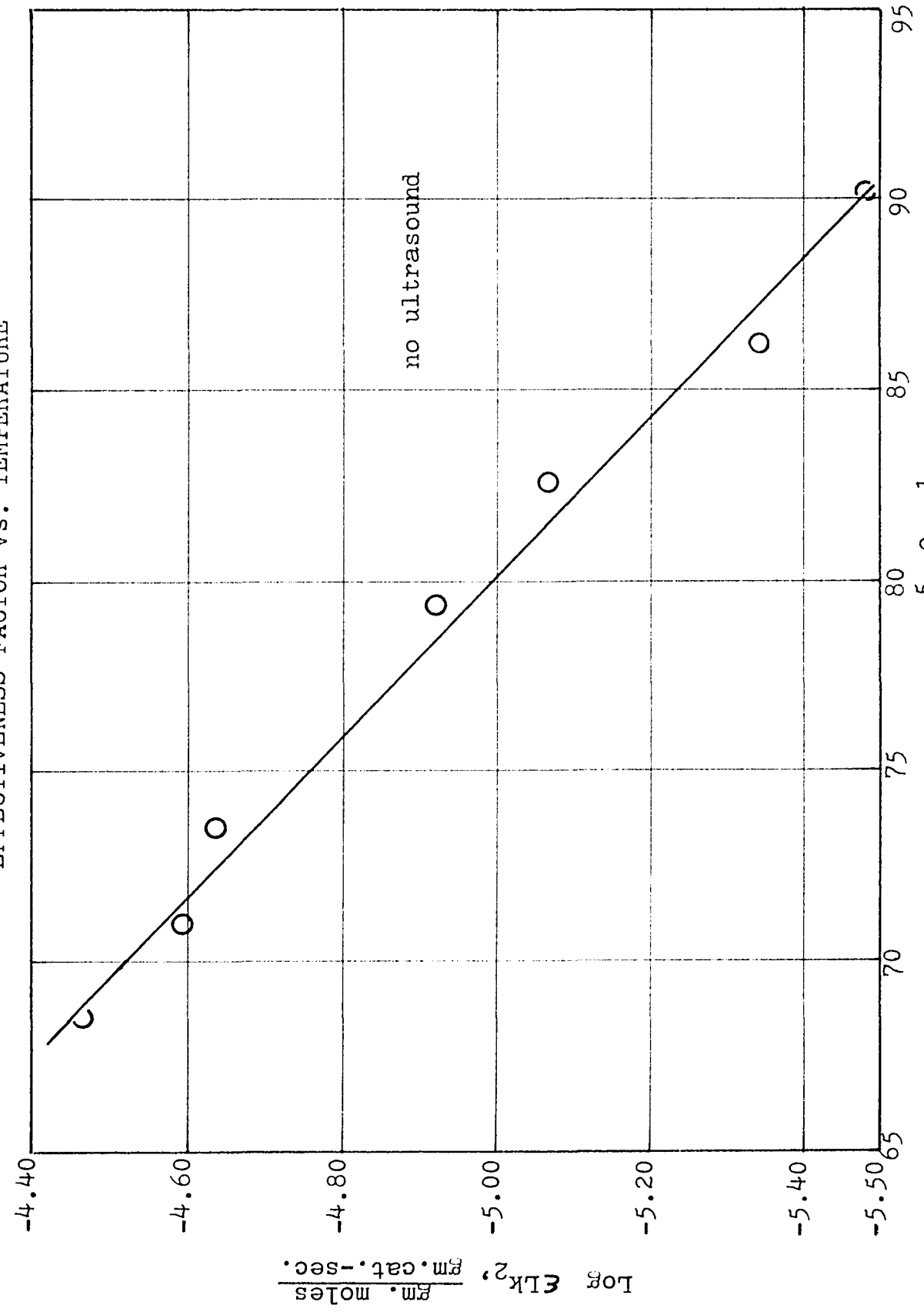

FIGURE 35

EFFECTIVENESS FACTOR vs. TEMPERATURE

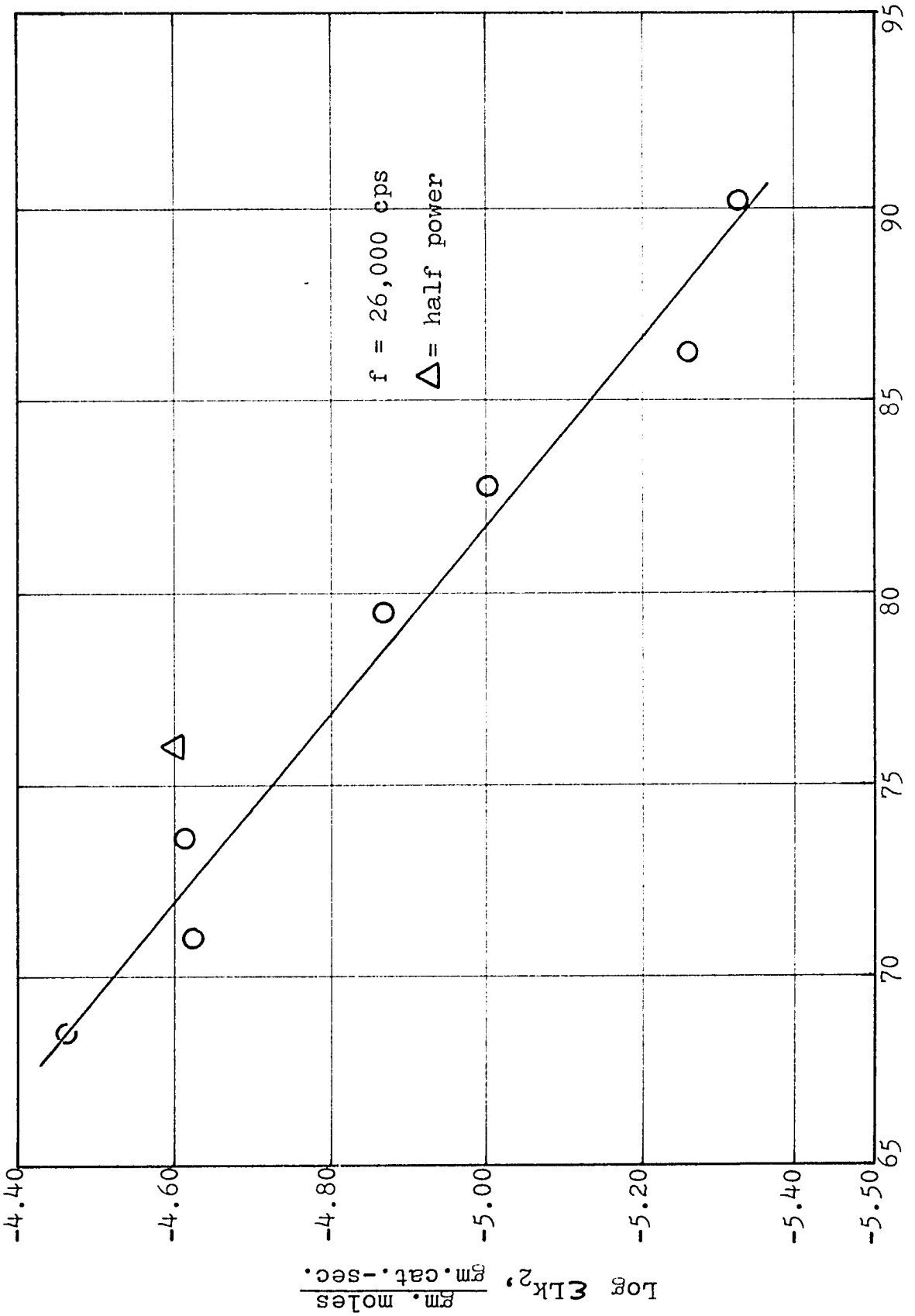

FIGURE 36

EFFECTIVENESS FACTOR vs. TEMPERATURE

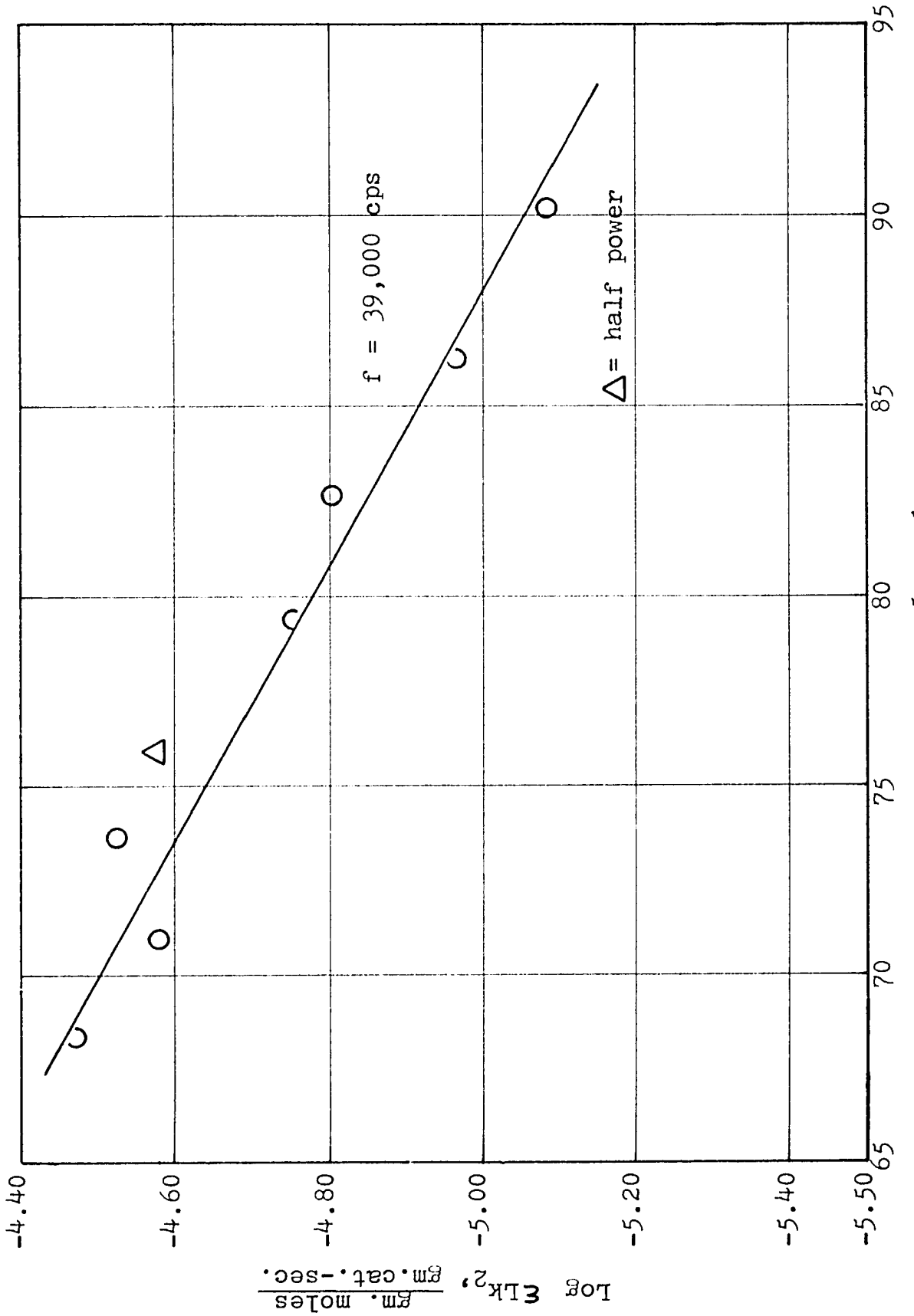

FIGURE 37

EFFECTIVENESS FACTOR vs. TEMPERATURE

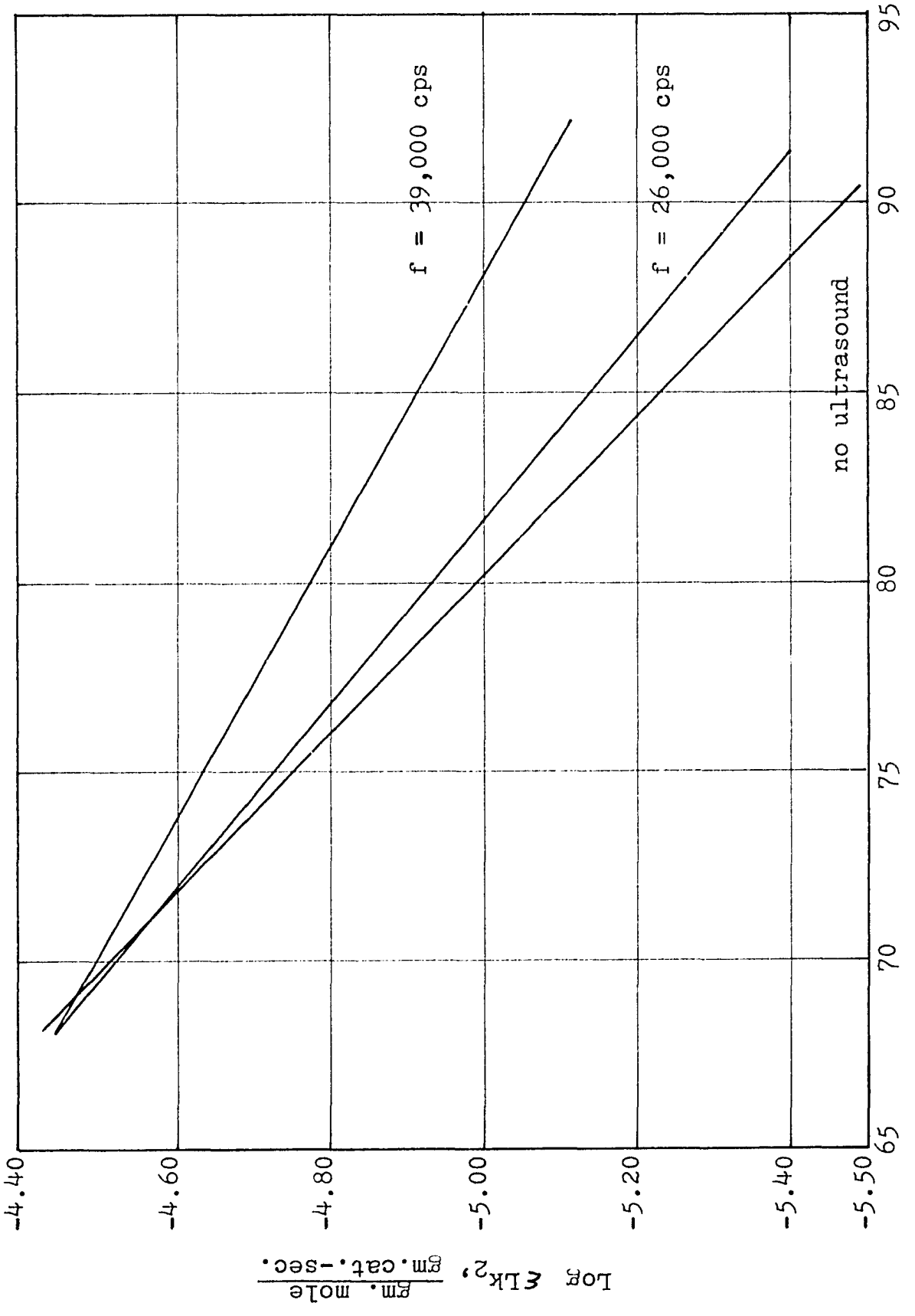

TABLE 9

ACTIVATION ENERGY AND CHARACTERIZATION FACTOR

Frequency f cps	Activation Energy, E kcal / gm mole	Character. Factor, k_o gm moles / gm cat-sec.	Investigator
No Ultrasound	11.0	-	Eberly [101]
No Ultrasound	34.0	-	Bezre[5]
No Ultrasound	27.0	-	Spozhakina[76]
No Ultrasound	18.0	-	Romanovskii[102]
No Ultrasound	3.0	-	Panchenkov[50]
No Ultrasound	13.2	0.0021	Rase[64]
No Ultrasound	5.4	0.0700	Garver[22]
No Ultrasound	12.1	0.0723	Lintner
26,000	10.4	0.0231	Lintner
39,000	7.1	0.0029	Lintner

Table 9 also illustrates the values of activation energy and characterization factor obtained by several other investigators. Considering the wide range of values obtained by other observers, the value calculated by these data appear to be reasonable. It is interesting to note that the total ultrasonic power input to the reactor ranged between 4.3 and 103.4 $\frac{\text{kcal}}{\text{gm mole}}$ which bracketed the activation energy.

Ultrasonic effect. As shown in Figure 37, the value of the effectiveness factor parameter, ϵLk_2, increases with increasing frequency. At low values of reciprocal temperature or high values of temperature, the values of ϵLk_2 become equal at all frequencies because surface reaction rate no longer controls. At high temperatures, surface reaction rate is very rapid and bulk diffusion from the main gas stream to the surface of the catalyst controls the overall rate of reaction.

The values of ϵLk_2 obtained at half the power output of the equipment are plotted as triangles on the graphs for frequencies of 26,000 cps and 39,000 cps. The plots indicate that this decrease in power input has negligible effect on the value of ϵLk_2.

Summary of Results

In general, all the data lead to identical conclusions. Ultrasound increases the rate of reaction ahd the reaction

rate increases with increasing frequency. Power input has negligible effect on the rate of reaction for the range studied.

Throughout the range of feed rates and temperatures studied, external bulk diffusion controls at low feed rates and high temperatures and conversely, surface reaction controls or pore diffusion at high feed rates and low temperatures. These phenomena are illustrated in Figure 38.

It should be noted that when the dimensions of ϵLk_2 are transposed from $\frac{\text{gm moles}}{\text{gm cat-sec.}}$ to $\frac{\text{cm.}}{\text{sec.}}$, as shown in Appendix XVIII, it can be plotted as a function of temperature as illustrated in Figure 38. In this figure, ϵLk_2 is described as the intrinsic reaction rate constant, k_s. The scale of the abscissa has been altered to correspond to k_g, the mass transfer coefficient scale. This alteration is necessary because the ϵLk_2 term is not a function of k_2, the forward rate constant, alone, but also of ϵ and L, the catalyst effectiveness factor and the concentration of active sites on the catalyst surface.

Acoustic Streaming

This research shows for the first time that the application of ultrasonic vibrations to a solid catalyzed gas reaction results in an increased reaction rate with increasing frequency as a result of increased diffusion rates. The diffusion rate is increased both externally from the

FIGURE 38

RATE CONSTANTS vs. TEMPERATURE

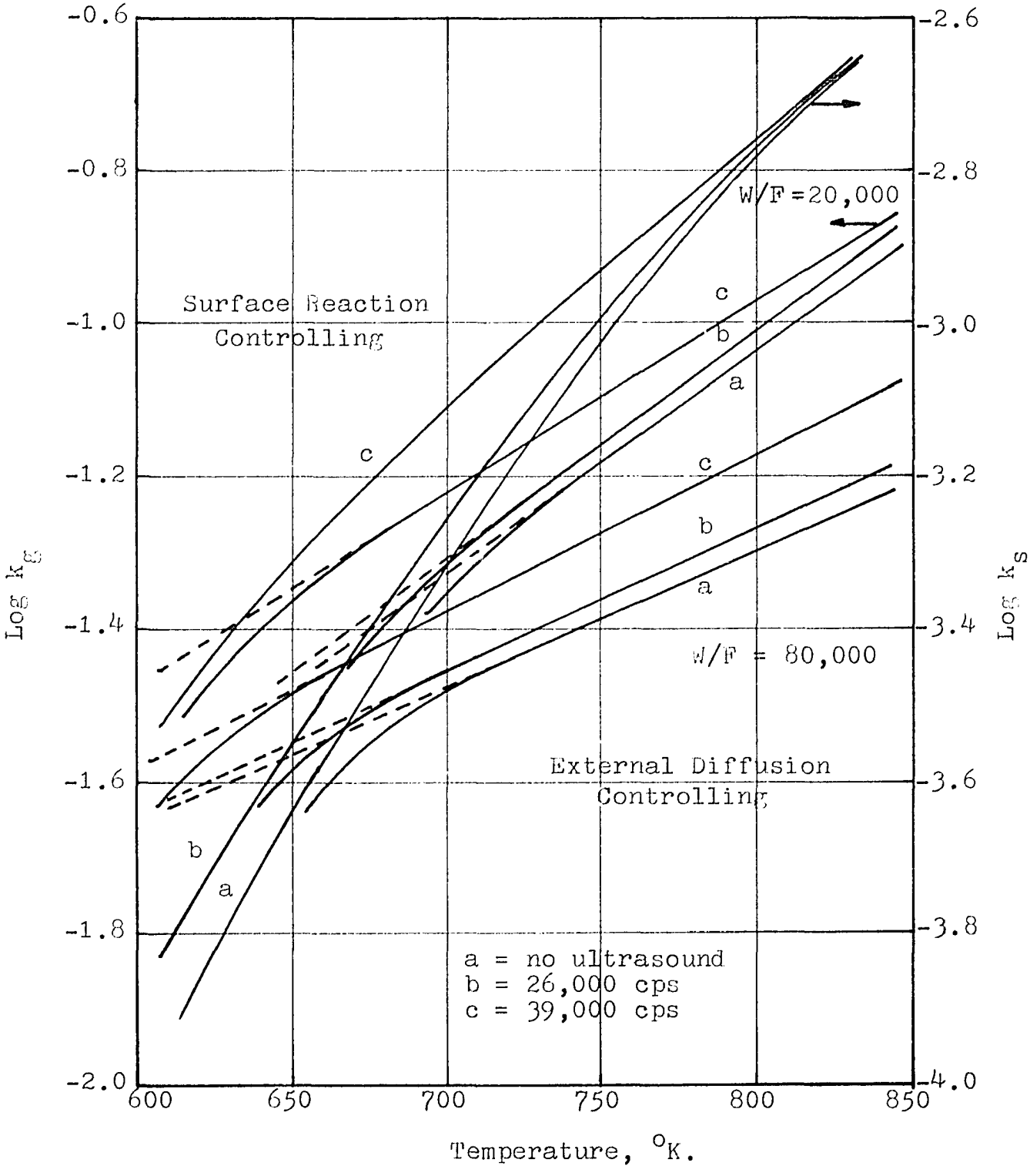

bulk gas stream to the catalyst surface and internally within the catalyst pore.

Fogler and Lund[20] have independently offered a mathematical explanation for this phenomena which they have identified as acoustic streaming. Their mathematical model states that within a duct, through which there is a concentration gradient, mass transfer occurs by molecular diffusion alone. However, when ultrasound is applied to the duct, small vortex cells are set up in which the gas moves circularly similar to eddy currents. This forced convection within each cell coupled with diffusion between cells results in a faster transport rate within the duct than with diffusion alone.

If one assumes the duct to be a tubular reactor shell or the pore of a catalyst, this model explains the results and conclusions of this research.

Thermal Effects

The application of acoustic energy to a catalyst bed may cause "hot spots" within the bed and thereby result in localized accelerated reaction rates. This thermal effect alone or together with increased diffusion rates may explain the increase in reaction rate observed in this research.

CHAPTER VI

CONCLUSIONS

The effect of ultrasonic vibrations on heterogeneous catalysis may be summarized as follows:

1. All the data collected at all temperatures and frequencies yield quadratic curves when plotted as conversion versus reciprocal space velocity.
2. In the area where external bulk diffusion controls the rate of reaction, the logarithm of the mass transfer coefficient is a linear function of temperature at all ultrasonic frequencies. The mass transfer coefficient and, therefore, the rate of reaction increases with increasing ultrasonic frequency.
3. In the area where surface reaction and internal pore diffusion control the rate of reaction, the data fit the reaction rate model previously derived by Garver at all frequencies and temperatures.
4. The kinetic rate constant, ϵLk_2, increases with increasing frequency.
5. The activation energy calculated from these data decrease with increasing frequency.
6. Power input appears to affect the rate of reaction in the plots of conversion versus reciprocal space

velocity at low feed rates. However, in the logarithmic plots of mass transfer coefficient and kinetic rate constant versus temperature, the effect of power is not statistically significant for the range studied.

7. The increases of mass transfer coefficients and kinetic rate constants obtained at a frequency of 39,000 cps are statistically significant within confidence intervals of 90%. The results obtained at 26,000 cps lie within confidence limits of 50 to 60%, but the raw data lead this author to believe that the lower frequency also increases the rate of reaction.

CHAPTER VII

RECOMMENDATIONS

This research demonstrates for the first time the quantitative effect of ultrasonic vibrations on the rate of a solid catalyzed gas reaction. It further demonstrates that this reaction rate is increased in the reactant feed flow range where external bulk diffusion controls and in the range where internal pore diffusion is the controlling factor. Increasing ultrasonic frequency results in faster reaction rates, and power input in the range studied has negligible effect. These phenomena have never previously been quantitatively demonstrated.

It is this author's hope that this research will influence other investigators to continue studies of the effect of ultrasonic vibrations on heterogeneous catalyzed reactions. The areas recommended for further study are as follows:

1. Employ the use of powdered catalyst (Appendix XII) to obtain an absolute value for the forward reaction rate constant, k_2. The absolute values of the effectiveness factor, ϵ, could then be calculated at various operating conditions employing standard catalyst. It would then be possible to determine the effect of ultrasound on each parameter alone.

2. Study frequencies up to 10^{11} cps and power inputs to 120 $\frac{\text{watts}}{\text{cm.}}$ to expand the range of this study. It is now possible to obtain these conditions with modern ultrasonic equipment, but this equipment is, of course, considerably more expensive.
3. Study the effect of ultrasonic vibrations on systems other than the cumene cracking reaction and silica-alumina catalyst.
4. Investigate the possible thermal effects on the datalyst due to the application of ultrasonic energy.

APPENDIX I

PHYSICAL PROPERTIES OF CUMENE, BENZENE AND PROPYLENE

PHYSICAL PROPERTIES OF CUMENE, BENZENE AND PROPYLENE

The overall chemical reaction and some of the physical properties of the reactants and products, both published and calculated, are as follows:

Reaction

$$C_6H_5-CH-(CH_3)_2 \longrightarrow C_6H_6 + CH_3-CH=CH_2$$

$$A \longrightarrow R + S$$

Cumene ⟶ Benzene and Propylene

Physical Properties

	Cumene	Benzene	Propylene
M, $\frac{gms}{gm\ mole}$	120.19	78.11	42.08
SpG	0.862	0.879	-
MP, $^oC.$	-96.9	5.4	-185
BP, $^oC.$	152.5	80.1	-48
C_P at 650°F., $\frac{cal}{gm-^oC.}$	0.588	0.541	0.624
C_P at 1050°F., $\frac{cal}{gm-^oC.}$	0.736	0.682	0.756
C_V at 650°F., $\frac{cal}{gm-^oC.}$	0.571	0.515	0.576
C_V at 1050°F., $\frac{cal}{gm-^oC.}$	0.719	0.656	0.708
T_C, $^oK.$	636.0	562.6	365.0
V_b, $\frac{cm^3}{gm\ mole}$	162.6	96.0	66.6
P_C, atm.	32.2	48.6	45.5
V_C, $\frac{cm^3}{gm\ mole}$	357	260	181
σ, Å	6.43	5.27	4.678

	Cumene	Benzene	Propylene
ε_A/K, °K.	490	440	298.9
μ_C, $\frac{gms}{cm\text{-}sec.}$	315×10^{-6}	312×10^{-6}	233×10^{-6}
σ_{AR}, σ_{AS}, Å	-	5.85	5.554
ε_{AR}/K, ε_{AS}/K, °K.	-	464	383
$KT_{650}/\varepsilon_{AR}$, $KT_{650}/\varepsilon_{AS}$, °K.	-	1.328	1.608
$KT_{1050}/\varepsilon_{AR}$, $KT_{1050}/\varepsilon_{AS}$, °K.	-	1.808	2.190
$[\Omega_{AR}]$ 650, $[\Omega_{AS}]$ 650	-	1.262	1.165
$[\Omega_{AR}]$ 1050, $[\Omega_{AS}]$ 1050	-	1.114	1.043
$[D_{AB}]$ 650, $[D_{AR}]$ 650, $[D_{AS}]$ 650, $\frac{cm.^2}{sec.}$	0.1141	0.0956	0.1416
$[D_{AB}]$ 1050, $[D_{AR}]$ 1050, $[D_{AS}]$ 1050, $\frac{cm.^2}{sec.}$	0.2044	0.1722	0.2513

Calculation of Critical Temperature of Cumene by the Method of Eduljee [56]

$$T_C = \frac{100T_b}{\sum \Delta_T} \qquad (31)$$

T_b = normal boiling point = 152.5°C. = 425.5°K.

Edujlee's contributions:

$$\sum \Delta_T = 9\Delta_{TC} + 12\Delta_{T_{TH}} + 3\Delta_{TC=C} + \Delta_{TRing} + \Delta_{TP}$$

Δ_T = Eduljee atomic contribution by carbon

= -55.32

ΔT_{TH} = Eduljee atomic contribution by hydrogen

= +28.52

$\Delta_{TC=C}$ = Eduljee structural contribution by carbon-carbon double bond

= +56.61

Δ_{TRing} = Edujlee structural contribution by benzene ring

= +53.52

Δ_{TP} = Eduljee position contribution by two branches on the second carbon atom

= -1.42

$\sum \Delta_T = 9(-55.32) + 12(28.52) + 3(56.61) + 53.52 - 1.42$

= 66.29

$$T_C = \frac{100(525.5)}{66.29} = 642^{\circ}K.$$

Calculation of Critical Temperature of Cumene by the Method of Nokay [56]

$$\log T_C = 1.2806 + 0.2985 \log S + 0.62164 \log T_b \qquad (32)$$

S = specific gravity of liquid = 0.862 $\frac{gms}{cm.^3}$

T_b = normal boiling point = 152.5°C. = 766.9°R.

$$\log T_C = 1.2806 + 0.2985 \log(0.862) + 0.62164 \log(766.9)$$
$$= 1.2806 + 0.2985(-0.06449) + 0.62164(2.88474)$$
$$= 1.2806 - 0.01925 + 1.79327 = 3.05462$$
$$T_C = 1134^{\circ}R. = 674^{\circ}F. = 357^{\circ}C. = 630^{\circ}K.$$

Calculation of the Molar Volume of Cumene at the Normal Boiling Temperature by the Method of Kopps [56]

$$V_b = 9V_{bC} + 12V_{bH} + V_{bRing} \qquad (33)$$

V_{bC} = Kopps' additive atomic volume for carbon
= 14.8

V_{bH} = Kopps' additive atomic volume for hydrogen
= 3.7

V_{bRing} = Kopps' additive atomic volume for benzene
= -15.0

$$V_b = 9(14.8) + 12(3.7) - 15.0$$
$$= 162.6 \frac{cm.^3}{gm\text{-}mole}$$

Calculation of the Critical Pressure of Cumene by the Method of Eduljee

$$P_C = \left(\frac{10^4 M}{\sum \Delta_P}\right)^2 \qquad (34)$$

M = molecular weight = 120.19 $\frac{gms}{gm\text{-}mole}$

Eduljee's contributions:

$$\sum \Delta_P = 9\Delta_{PC} + 12\Delta_{PH} + \Delta_{PRing} + \Delta_{PP}$$

Δ_{PC} = Eduljee atomic contribution by carbon

= -9.35

Δ_{PH} = Eduljee atomic contribution by hydrogen

= +16.20

Δ_{PRing} = Eduljee structural contribution by benzene ring

= +84.5

Δ_{PP} = Eduljee position contribution by one branch on second carbon atom

= -1.6

$$\sum \Delta_P = 9(-935) + 12(16.20) + 84.5 - 1.6 = 193.15$$

$$P_C = \frac{120.19 \times 10^4}{(193.15)^2} = 32.2 \text{ atm.}$$

Calculation of the Critical Volume of Cumene by the Method of Herzog

$$V_C = \frac{21.75\ T_C}{P_C} \qquad (35)$$

P_C = 32.2 atm.

T_C = 636.0°K.

$$V_C = \frac{21.75(636.0)}{32.2} = 430 \frac{\text{cm.}^3}{\text{gm-mole}}$$

Calculation of the Critical Volume of Cumene by the Method of Benson

$$V_C = V_b(0.422 \log P_C + 1.981) \tag{36}$$

$$V_b = 162.6 \frac{cm.^3}{gm\text{-}mole}$$

$$P_C = 32.2 \text{ atm.}$$

$$V_C = 162.6\left[0.422 \log (32.2) + 1.981\right]$$

$$= 162.6\ (2.195)$$

$$= 357 \frac{cm.^3}{gm\text{-}mole}$$

Calculation of Lennard-Jones Parameters for Cumene

$$\sigma_A = 1.18V_b^{2/3} = 1.18(162.6)^{2/3} = (1.18)(5.45)$$

$$= 6.43 \text{ Å} \tag{37}$$

$$\frac{\varepsilon_A}{K} = \frac{T_C}{1.30} = \frac{636.0}{1.30} = 490^{\circ}K$$

Calculation of the Molar Volume of Benzene at the Normal Boiling Temperature by the Method of Kopps

$$V_b = 6V_{bC} + 6V_{bH} + V_{bRing} \tag{38}$$

V_{bC} = Kopps' additive atomic volume for carbon

= 14.8

V_{bH} = Kopps' additive atomic volume for hydrogen

= 3.7

V_{bRing} = Kopps' additive atomic volume for benzene ring

= -15.0

$$V_b = 6(14.8) + 6(3.7) - 15.0 = 96.0 \frac{cm.^3}{gm\text{-}mole}$$

Calculation of the Molar Volume of Propylene at the Normal Boiling Temperature by the Method of Kopps

$$V_b = 3V_{bC} + 6V_{bH} \qquad (39)$$

V_{bC} = Kopps' additive atomic volume for carbon

V_{bH} = Kopps' additive atomic volume for hydrogen

= 3.7

$$V_b = 3(14.8) + 6(3.7) = 66.6 \frac{cm.^3}{gm\text{-}mole}$$

Calculation of the Critical Viscosity of Cumene by the Method of Uyehara and Watson

$$\mu_C = \frac{61.6\ M^{1/2} T_C^{1/2}}{V_C^{2/3}} \qquad (40)$$

$M = 120.19 \frac{gms}{gm\text{-}mole}$

$T_C = 636.0^{\circ}K.$

$V_C = 357 \frac{cm.^3}{gm\text{-}mole}$

$$\mu_C = \frac{(61.6)(120.19)^{1/2}(636.0)^{1/2}}{(357)^{2/3}} = 338 \text{ micropoise}$$

$$= 338 \times 10^{-6} \frac{gm}{cm\text{-}sec.}$$

or, alternatively

$$\mu_C = \frac{7.70\ M^{1/2} P_C^{2/3}}{T_C^{1/6}}$$

$P_C = 32.2$ atm.

$$\mu_C = \frac{(7.70)(120.19)^{1/2}(32.2)^{2/3}}{(636.0)^{1/6}} = 292 \text{ micropoise}$$

$$= 292 \times 10^{-6} \frac{\text{gm}}{\text{cm-sec.}}$$

Calculation of the Combined Lennard-Jones Parameters for Cumene, Benzene and Propylene

$$\sigma_{AR} = \frac{\sigma_A + \sigma_R}{2} = \frac{6.43 + 5.27}{2} = 5.85 \text{ Å} \quad (41)$$

$$\sigma_{AS} = \frac{\sigma_A + \sigma_S}{2} \quad \frac{6.43 + 4.678}{2} = 5.554 \text{ Å} \quad (42)$$

$$\frac{\varepsilon_{AR}}{K} = \left[\left(\frac{\varepsilon_A}{K}\right)\left(\frac{\varepsilon_R}{K}\right)\right]^{\frac{1}{2}} = \left[(490)(440)\right]^{\frac{1}{2}} = 646^{\circ}\text{K.} \quad (43)$$

$$\frac{\varepsilon_{AS}}{K} = \left[\left(\frac{\varepsilon_A}{K}\right)\left(\frac{\varepsilon_S}{K}\right)\right]^{\frac{1}{2}} = \left[(490)(298.9)\right]^{\frac{1}{2}} = 383^{\circ}\text{K.} \quad (44)$$

$$\frac{KT_1}{\varepsilon_{AR}} = \frac{616^{\circ}\text{K.}}{464^{\circ}\text{K.}} = 1.328; \left[\Omega_{AR}\right] 650 = 1.262$$

$$\frac{KT_2}{\varepsilon_{AR}} = \frac{839^{\circ}\text{K.}}{464^{\circ}\text{K.}} = 1.808; \left[\Omega_{AR}\right] 1050 = 1.114$$

$$\frac{KT_1}{\varepsilon_{AS}} = \frac{616^{\circ}\text{K.}}{383^{\circ}\text{K.}} = 1.608; \left[\Omega_{AS}\right] 650 = 1.165$$

$$\frac{KT_2}{\varepsilon_{AS}} = \frac{839^{\circ}\text{K.}}{383^{\circ}\text{K.}} = 2.190; \left[\Omega_{AS}\right] 1050 = 1.043$$

Calculate the Diffusivity of Cumene in Benzene at 650°F.

$$D_{AR} = \frac{0.0018583\left[T^3\left(\frac{1}{M_A} + \frac{1}{M_R}\right)\right]^{\frac{1}{2}}}{p_T \nabla^2_{AR} \Omega_{AR}} \qquad (45)$$

$$= \frac{0.0018583\left[(616)^3\left(\frac{1}{120.19} + \frac{1}{78.11}\right)\right]^{\frac{1}{2}}}{(1.0)(5.85)^2(1.262)}$$

$$\left[D_{AR}\right]_{650} = 0.0956 \ \frac{cm.^2}{sec.}$$

Calculate the Diffusivity of Cumene in Benzene at 1050°F.

$$D_{AR} = \frac{0.0018583\left[T^3\left(\frac{1}{M_A} + \frac{1}{M_R}\right)\right]^{\frac{1}{2}}}{p_T \nabla^2_{AR} \Omega_{AR}} \qquad (45)$$

$$= \frac{0.0018583\left[(839)^3\left(\frac{1}{120.19} + \frac{1}{78.11}\right)\right]^{\frac{1}{2}}}{(1.0)(5.85)^2(1.114)}$$

$$\left[D_{AR}\right]_{1050} = 0.1722 \ \frac{cm.^2}{sec.}$$

Calculate the Diffusivity of Cumene in Propylene at 650°F.

$$D_{AS} = \frac{0.0018583\left[T^3\left(\frac{1}{M_A} + \frac{1}{M_S}\right)\right]^{\frac{1}{2}}}{p_T \nabla^2_{AS} \Omega_{AS}} \qquad (46)$$

$$= \frac{0.0018583\left[(616)^3\left(\frac{1}{120.19} + \frac{1}{42.08}\right)\right]^{\frac{1}{2}}}{(1.0)(5.554)^2(1.165)}$$

$$\left[D_{AS}\right]_{650} = 0.1416 \ \frac{cm.^2}{sec.}$$

Calculate the Diffusivity of Cumene in Propylene at 1050°F.

$$D_{AS} = \frac{0.0018583\left[T^3\left(\frac{1}{M_A} + \frac{1}{M_S}\right)\right]^{\frac{1}{2}}}{p_T \nabla_{AS}^2 \Omega_{AS}} \qquad (46)$$

$$= \frac{0.0018583\left[(839)^3\left(\frac{1}{120.19} + \frac{1}{42.08}\right)\right]^{\frac{1}{2}}}{(1.0)(5.554)^2(1.043)}$$

$$\left[D_{AS}\right]_{1050} = 0.2513 \ \frac{cm.^2}{sec.}$$

Calculate the Diffusivity of Cumene in Benzene and Propylene

$$D_{AB} = \frac{(1 - Y_A)}{\frac{Y_R}{D_{AR}} + \frac{Y_S}{D_{AS}}} \qquad (47)$$

$$Y_A + Y_R + Y_S = 1$$

$$Y_R = Y_S$$

$$Y_A + 2Y_R = 1$$

$$Y_R = \frac{1 - Y_A}{2} = Y_S$$

$$D_{AB} = \frac{1 - Y_A}{\frac{1-Y_A}{2D_{AR}} + \frac{1-Y_A}{2D_{AS}}} = \frac{2}{\frac{1}{D_{AR}} + \frac{1}{D_{AS}}}$$

At 650°F.

$$\left[D_{AB}\right]_{650} = \frac{2}{\frac{1}{D_{AR\ 650}} + \frac{1}{D_{AR\ 650}}} = \frac{2}{\frac{1}{0.0956} + \frac{1}{0.1416}}$$

$$= 0.1141 \ \frac{cm.^2}{sec.}$$

At 1050°F.

$$\left[D_{AB}\right]_{1050} = \frac{2}{\frac{1}{D_{AR\ 1050}} + \frac{1}{D_{AS\ 1050}}} = \frac{2}{\frac{1}{0.1722} + \frac{1}{0.2513}}$$

$$= 0.2044 \frac{cm.^2}{sec.}$$

Calculation of the Heat Capacity of Cumene by the Method of Hougan, Watson and Ragatz[29]

U.O.P. characterization factor.

$$K = \frac{(T_B)^{1/3}}{G} \tag{48}$$

T_B = boiling point at 1 atm. = 767°R.

G = specific gravity at 60°F. = 0.862

$$K = \frac{(767)^{1/3}}{0.862} = 10.62$$

Empirical equation.

$$C_P = (0.0450K-0.233) + (0.440 + 0.0177K) \times 10^{-3}t - 0.1530 \times 10^{-6}t^2 \tag{49}$$

At t = 650°F.

$$C_P = (0.0450)(10.62)-0.233 + 0.440+(0.0177)(10.62)\ (650 \times 10^{-3}) - (0.1530)(650)^2 \times 10^{-6}$$

$$C_P = 0.588 \frac{cal}{gm-°C.}$$

$$C_V = C_P - \frac{2.0 \frac{cal}{gm\ mole\text{-}^oC.}}{120.19 \frac{gms}{gm\text{-}mole}} = 0.571 \frac{cal}{gm\text{-}^oC.} \qquad (50)$$

At $t = 1050^oF.$

$$C_P = (0.0450)(10.62)-0.233 + 0.440+(0.0177)(10.62)\ (1050 \times 10^{-3}) - (01530)(1050)^2 \times 10^{-6}$$

$$C_P = 0.736 \frac{cal}{gm\text{-}^oC.}$$

$$C_V = C_P - \frac{2.0 \frac{cal}{gm\ mole\text{-}^oC.}}{120.19 \frac{gms}{gm\text{-}mole}} = 0.719 \frac{cal}{gm\text{-}^oC.} \qquad (50)$$

Calculation of the Heat Capacity of Benzene by the Method of Hougan, Watson and Ragatz[29]

U.O.P. characterization factor.

$$K = \frac{(T_B)}{G} \qquad (48)$$

T_B = boiling point at 1 atm. = $636^oR.$

G = specific gravity at $60^oF.$ = 0.879

$$K = \frac{(636)}{0.879} = 9.78$$

Empirical equation.

$$C_P = (0.0450K-0.233) + (0.440+0.0177K) \times 10^{-3}t - 0.1530 \times 10^{-6}t^2 \qquad (49)$$

At $t = 650^oF.$

$$C_P = (0.0450)(9.78)-0.233 + 0.440+(0.0177)(9.78)\ (650 \times 10^{-3}) - (0.1530)(650)^2 \times 10^{-6}$$

$$C_P = 0.541 \frac{cal}{gm-^oC.}$$

$$C_V = C_P - \frac{2.0 \frac{cal}{gm\text{-}mole\text{-}^oC.}}{78.11 \frac{gms}{gm\text{-}mole}} = 0.515 \frac{cal}{gm-^oC.} \qquad (50)$$

At $t = 1050^oF.$

$$C_P = (0.0450)(9.78)-0.233 + 0.440+(0.0177)(9.78)\ (1050 \times 10^{-3}) - (0.1530)(1050)^2 \times 10^{-6}$$

$$C_P = 0.682 \frac{cal}{gm-^oC.}$$

$$C_V = C_P - \frac{2.0 \frac{cal}{gm\ mole\text{-}^oC.}}{78.11 \frac{gms}{gm\text{-}mole}} = 0.656 \frac{cal}{gm-^oC.} \qquad (50)$$

Calculation of the Heat Capacity of Propylene by the Method of Hougan, Watson and Ragatz[29]

Empirical equation.

$$C_P = 1.97 + (27.69 \times 10^{-3})T - (5.25 \times 10^{-6})T^2 \quad (51)$$

At $T = 650^{\circ}F. = 1110^{\circ}R.$

$$C_P = 1.97 + (27.69 \times 10^{-3})(1110) - (5.25 \times 10^{-6})(1110)^2$$

$$C_P = \frac{26.237 \ \frac{cal}{gm\ mole\text{-}^{\circ}C.}}{42.08 \ \frac{gms}{gm\text{-}mole}} = 0.624 \ \frac{cal}{gm\text{-}^{\circ}C.}$$

$$C_V = C_P - \frac{2.0 \ \frac{cal}{gm\ mole\text{-}^{\circ}C.}}{42.08 \ \frac{gms}{gm\text{-}mole}} = 0.576 \ \frac{cal}{gm\text{-}^{\circ}C.} \quad (52)$$

At $T = 1050^{\circ}F. = 1510^{\circ}R.$

$$C_P = 1.97 + (27.69 \times 10^{-3})(1510) - (5.25 \times 10^{-6})(1510)^2$$

$$C_P = \frac{31.811 \ \frac{cal}{gm\ mole\text{-}^{\circ}C.}}{42.08 \ \frac{gms}{gm\text{-}mole}} = 0.756 \ \frac{cal}{gm\text{-}^{\circ}C.}$$

$$C_V = C_P - \frac{2.0 \ \frac{cal}{gm\ mole\text{-}^{\circ}C.}}{42.08 \ \frac{gms}{gm\text{-}mole}} = 0.708 \ \frac{cal}{gm\text{-}^{\circ}C.} \quad (52)$$

APPENDIX II

PHYSICAL PROPERTIES OF SILICA-ALUMINA CATALYST

PHYSICAL PROPERTIES OF SILICA-ALUMINA CATALYST

The catalyst employed in this study was TCC (Thermofor Catalytic Cracking) Silica-Alumina Cracking Catalyst, supplied by the Mobil Chemical Company, Paulsboro Catalyst Plant, Paulsboro, New Jersey. The catalyst is designated as "Durabead 1" by Mobil.

The physical properties and Tyler screen data for the catalyst are as follows:

Loose bulk density	$0.74 \frac{gms}{cm.^3}$
Packed bulk density	$\rho_B = 0.82 \frac{gms}{cm.^3}$
Particle density	$\rho_P = 1.28 \frac{gms}{cm.^3}$
True solid density	$\rho_t = 2.32 \frac{gms}{cm.^3}$
Average diameter	$d_P = 0.358$ cm.
Surface area	$S_g = 250 \times 10^4 \frac{cm.^2}{gm}$
Average pore diameter	$d = 72 \times 10^{-8}$ cm.
Effective pore diffusivity	$D_e = 0.015 \frac{cm.^2}{sec.}$
Pore volume	$V_g = 0.35 \frac{cm.^3}{gm}$
Internal void fraction	$\Theta = 0.448$
External void fraction	$\varepsilon = 0.32$
Superficial surface area	$a = 13.1 \frac{cm.^2}{gm}$
Equivalent pore radius	$r_e = 2.8 \times 10^{-7}$ cm.
Tortuosity factor	$\tau = 5.6$

Radius of catalyst pellet	$r_P = 0.179$ cm.
Total surface of porous catalyst	$S_V = 320 \times 10^4 \frac{\text{cm.}^2}{\text{cm.}^3}$

Tyler Screen Analysis	Wt. %
On 4 mesh	2.5
On 5 mesh	27.0
On 6 mesh	43.4
On 7 mesh	22.2
On 8 mesh	3.9
On 10 mesh	0.6
Through 10 mesh	0.3
	99.9

Calculation of Superficial Area of Catalyst Surface, a

$$\text{Catalyst Area/Pellet} = 4\pi r_P^2 \frac{\text{cm.}^2}{\text{Pellet}} \tag{53}$$

$$\text{Catalyst Wt./Pellet} = \left[\frac{4}{3}\pi r_P^3 \frac{\text{cm.}^3}{\text{Pellet}}\right] \left[\rho_P \frac{\text{gms. Pellet}}{\text{cm.}^3 \text{ Pellet}}\right] \tag{54}$$

$$= \frac{4}{3}\pi r_P^3 \rho_P \frac{\text{gms}}{\text{Pellet}}$$

$$a = \frac{(4\pi r_P^2 \frac{\text{cm.}^2}{\text{Pellet}})}{(\frac{4}{3}\pi r_P^3 \rho_P \frac{\text{gms}}{\text{Pellet}})} = \frac{3}{r_P \rho_P} \frac{\text{cm.}^2 \text{ catalyst}}{\text{gm. catalyst}} \tag{55}$$

$r_P = 0.179$ cm.

$\rho_P = 1.28 \frac{\text{gms}}{\text{cm.}^3}$

$$a = \frac{3}{(0.179 \text{ cm.})(1.28 \frac{\text{gms}}{\text{cm.}^3})} = 13.10 \frac{\text{cm.}^2 \text{ catalyst}}{\text{gm. catalyst}}$$

APPENDIX III

CONTINUOUS REACTION MODEL

CONTINUOUS REACTION MODEL

In solid-catalyzed gas-phase reactions, it is assumed that the reaction takes place at the gas-solid interface. The interface lies on the external surface of the catalyst and on the internal surfaces within the catalyst pore. The overall rate of reaction depends upon the availability of these surfaces.

For the continuous reaction model, it is assumed that the reaction mechanism consists of seven distinct processes. That process, or combination of processes, which are significantly slower than the others, control the rate of reaction. The seven processes involved in the catalytic cracking of cumene are described below and illustrated in Figure 39.

Gas Film Diffusion of Reactants

Reactant cumene (A) diffuses from the main gas stream to the external surface of the catalyst.

Pore Diffusion of Reactants

Reactant cumene (A) diffuses from the external surface of the catalyst (mouth of the catalyst pore) into the catalyst pore).

Adsorption of Reactants

Reactant cumene (A) is adsorbed onto the surface of

the catalyst.

Surface Reaction

Adsorbed cumene (A) reacts to form adsorbed benzene (R) and propylene (S) which is not adsorbed. This single site reaction mechanism was shown in previous work by Garver to be the actual mechanism occurring.

In the dual site reaction mechanism, both products are adsorbed.

Desorption of Products

Adsorbed product benzene (R) is desorbed from the catalyst surface.

Pore Diffusion of Products

Products benzene (R) and propylene (S) diffuse from the catalyst pore to the external surface of the catalyst (mouth of the catalyst pore).

Gas Film Diffusion of Products

Products benzene (R) and propylene (S) diffuse from the external surface of the catalyst into the main gas stream.

FIGURE 39

CONTINUOUS REACTION MODEL

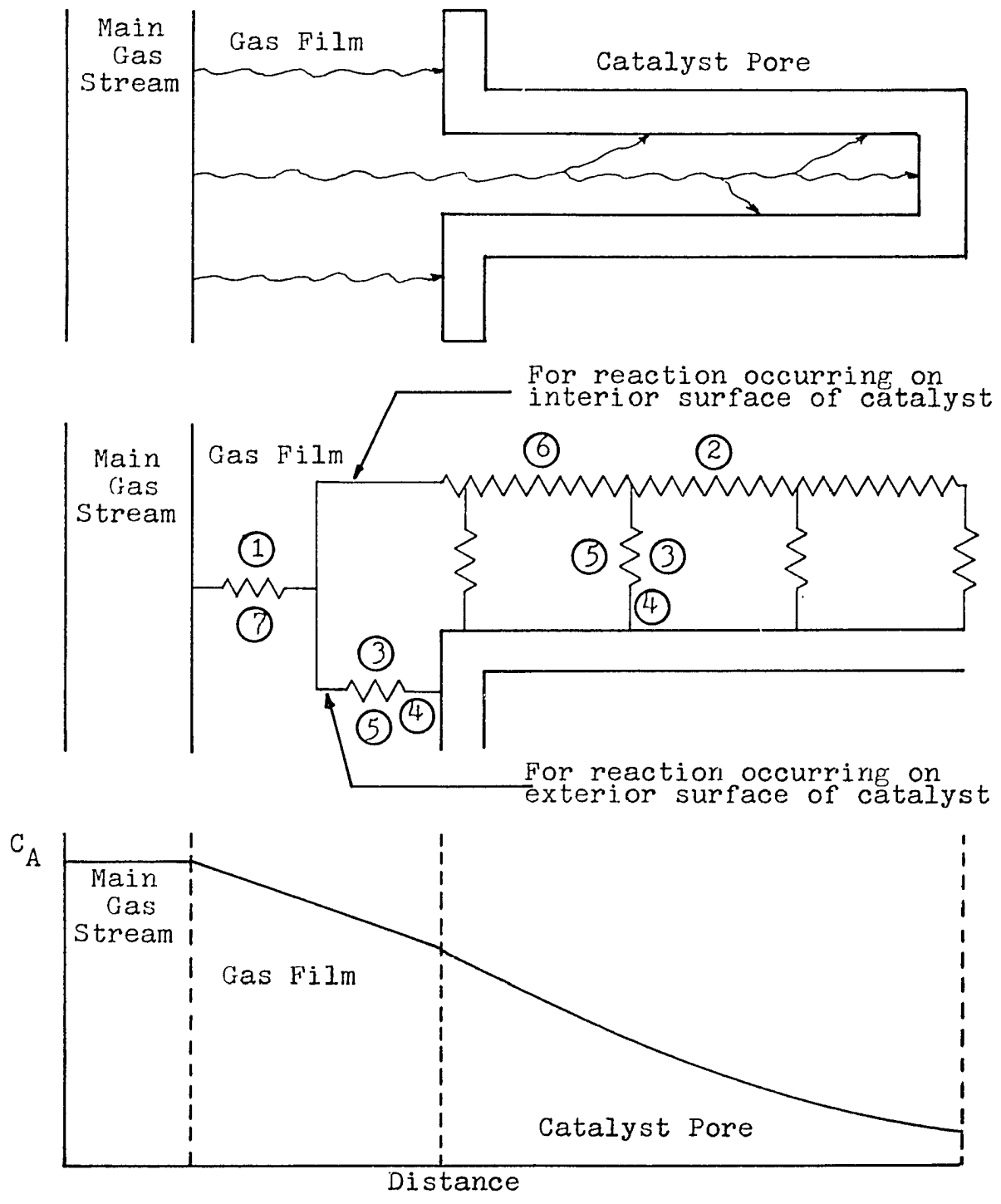

APPENDIX IV

GAS FILM DIFFUSION

GAS FILM DIFFUSION

The gas film diffusion of cumene (A), benzene (R) and propylene (S), which is process one and seven of the reaction mechanism, can be handled mathematically as a simple diffusion process. Reactant A (cumene) diffuses from the main gas stream to the catalyst surface and products R and S (benzene and propylene) diffuse from the catalyst surface into the main gas stream. These phenomena are illustrated in Figure 40.

The diffusion rate is calculated as follows:

Material Balance on A

Input - Output + Generation = Accumulation

Input = rate of mass transfer of A into differential element across rectangular surface at z

$$= (A_z \text{cm}^2)\left(N_{A_z} \frac{\text{gm-moles}}{\text{cm}^2\text{-sec.}}\right) = LWN_{A_z} \frac{\text{gm-moles}}{\text{sec.}} \quad (56)$$

Output = rate of mass transfer of A out of differential element across rectangular surface at z + dz

$$= (A_z \text{cm}^2)\left[N_{A_z} + \frac{d}{dz}(N_{A_z})dz \ \frac{\text{gm-moles}}{\text{cm}^2\text{-sec.}}\right]$$

$$= LW\left[N_{A_z} + \frac{dN_{A_z}}{dz}dz\right]\frac{\text{gm-moles}}{\text{sec.}} \quad (57)$$

Generation = rate of formation of A within differential element between z and z + dz

FIGURE 40

GAS FILM DIFFUSION OF A, R, AND S

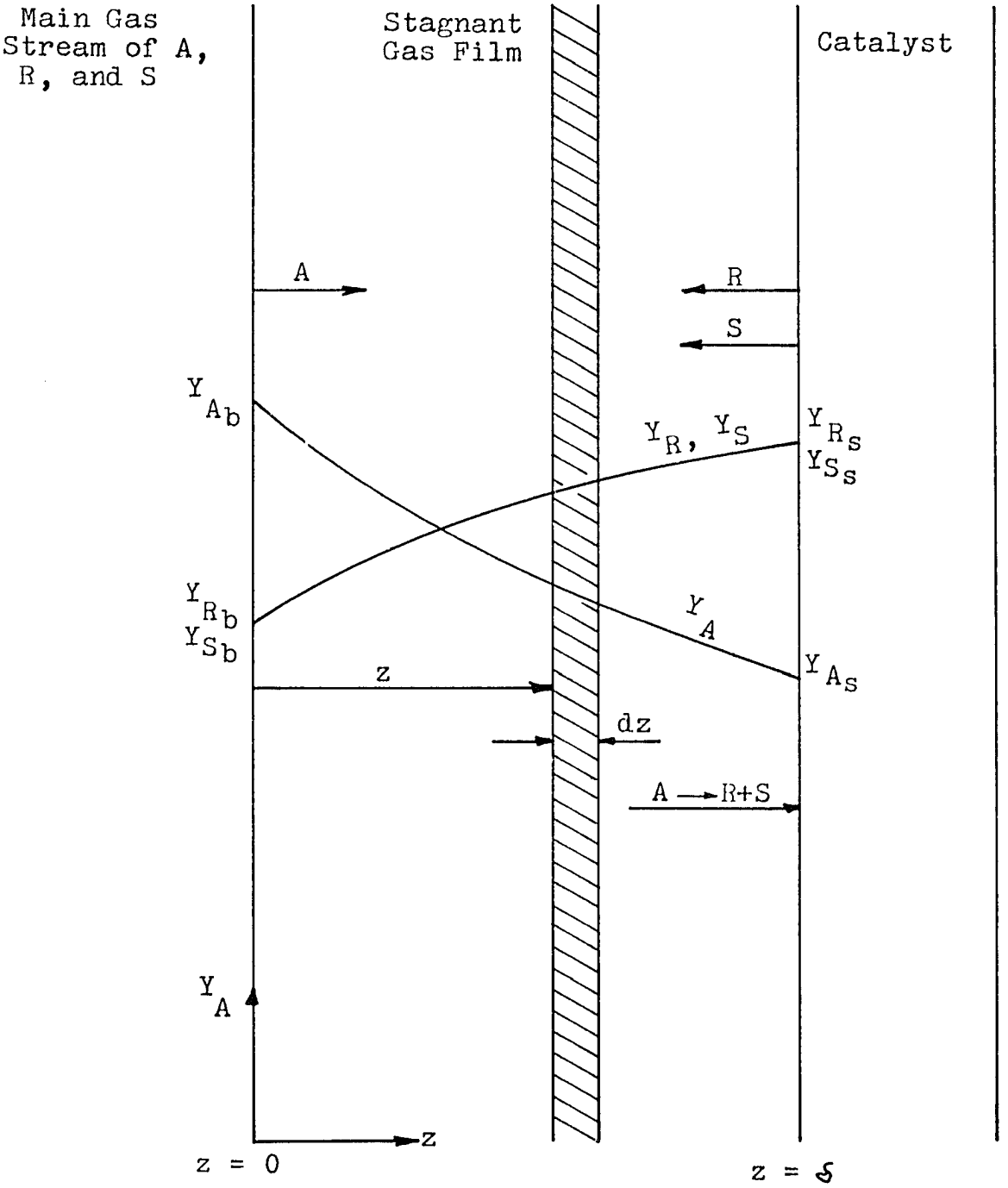

= nil (reaction takes place at catalyst surface only, not within differential element) (58)

Accumulation = rate of accumulation of A within differential element between z and z+dz

= nil (steady state) (59)

Substituting,

$$LWN_{A_z} - LWN_{A_z} - LW\frac{dN_{A_z}}{dz}\,dz = 0$$

$$- LW\frac{dN_{A_z}}{dz}dz = 0$$

$$- \frac{dN_{A_z}}{dz} = 0 \qquad (60)$$

Define Fick's Law for System

$$N_{A_z} = cD_{AB}\frac{\partial x_A}{\partial z} + Y_A(N_{A_z} + N_{B_z}) \qquad (61)$$

From the stoichiometry of the reaction, A ⟶ R + S, one mole of A yields one mole of R plus one mole of S; therefore, A diffuses at half the combined rate of R + S, and

$$N_{A_z} = -\tfrac{1}{2}N_{B_z}$$

$$N_{B_z} = -2N_{A_z}$$

$$N_{A_z} = -cD_{AB}\frac{\partial Y_A}{\partial z} + Y_A(N_{A_z} - 2N_{A_z})$$

$$= -cD_{AB}\frac{\partial Y_A}{\partial z} - Y_A N_{A_z}$$

$$N_{A_z}(1 + Y_A) = -cD_{AB}\frac{\partial Y_A}{\partial z}$$

$$N_{A_z} = -\frac{cD_{AB}}{(1+Y_A)}\frac{\partial Y_A}{\partial z}$$

$$N_{A_z} = -\frac{cD_{AB}}{(1+Y_A)}\frac{dY_A}{dz}$$

Substituting,

$$-\frac{dN_{A_z}}{dz} = -\frac{d}{dz}\left[-\frac{cD_{AB}}{(1+Y_A)}\frac{dY_A}{dz}\right] = 0$$

$$\frac{d}{dz}\left[\frac{cD_{AB}}{(1+Y_A)}\frac{dY_A}{dz}\right] = 0 \qquad (62)$$

Integrating,

$$\int\frac{d}{dz}\left[\frac{cD_{AB}}{(1+Y_A)}\frac{dY_A}{dz}\right] = c_1$$

$$\frac{cD_{AB}}{(1+Y_A)}\frac{dY_A}{dz} = c_1$$

Since cD_{AB} is constant at constant pressure and temperature,

$$cD_{AB}\int\frac{dY_A}{(1+Y_A)} = c_1\int dz$$

$$cD_{AB}\ln(1+Y_A) = c_1 z + c_2$$

Boundary Conditions

At $z = 0$, $Y_A = Y_{A_b}$

At $z = \delta$, $Y_A = Y_{A_s}$

$$cD_{AB}\ln(1+Y_{A_b}) = c_2$$

$$cD_{AB}\ln(1+Y_{A_s}) = c_1\delta + c_2$$

$$= c_1\delta + cD_{AB}\ln(1+Y_{A_b})$$

$$c_1 = \frac{cD_{AB}\ln(1+Y_{A_s})}{\delta} - \frac{cD_{AB}\ln(1+Y_{A_b})}{\delta}$$

$$= \frac{cD_{AB}}{\delta}\ln\left[\frac{(1+Y_{A_s})}{(1+Y_{A_b})}\right]$$

$$cD_{AB}\ln(1+Y_A) = \frac{cD_{AB}}{\delta}\ln\left[\frac{(1+Y_{A_s})}{(1+Y_{A_b})}\right] z + cD_{AB}\ln(1+Y_{A_b})$$

$$\ln\frac{(1+Y_A)}{(1+Y_{A_b})} = \frac{z}{\delta}\ln\frac{(1+Y_{A_s})}{(1+Y_{A_b})}$$

$$\frac{(1+Y_A)}{(1+Y_{A_b})} = \frac{(1+Y_{A_s})^{\frac{z}{\delta}}}{(1+Y_{A_b})^{\frac{z}{\delta}}}$$

$$(1+Y_A) = \frac{(1+Y_{A_b})}{(1+Y_{A_b})^{\frac{z}{\delta}}}(1+Y_{A_s})^{\frac{z}{\delta}}$$

$$(1+Y_A) = (1+Y_{A_s})^{\frac{z}{\delta}}(1+Y_{A_b})^{1-\frac{z}{\delta}} \qquad (63)$$

Calculate Molar Flow Through Film

$$\frac{(dN_A \text{ gm-moles})}{(dt \text{ sec.})} = (A_z \text{cm}^2)\left(N_{A_z}\frac{\text{gm-moles}}{\text{cm}^2\text{-sec.}}\right) = \text{constant} \qquad (64)$$

$$N_{A_z} = \frac{-cD_{AB}}{(1+Y_A)}\frac{dY_A}{dz}$$

$$\frac{dN_A}{dt} = \frac{-A_z c D_{AB}}{(1+Y_A)} \frac{dY_A}{dz}$$

Integrating,

$$\frac{dN_A}{dt} \int_0^{\delta} dz = -A_z c D_{AB} \int_{x_{A_b}}^{x_{A_s}} \frac{dY_A}{(1+x_A)}$$

$$dN_A\ (\delta) = -A_z c D_{AB} \ln\left[\frac{(1+Y_{A_s})}{(1+Y_{A_b})}\right]$$

$$\frac{1}{A_z} \frac{dN_A}{dt} = \frac{c D_{AB}}{\delta} \ln\left[\frac{1+Y_{A_s}}{1+Y_{A_b}}\right]$$

Let $A_z = S_{EX}$, external surface area of catalyst, cm^2.

Let $\frac{D_{AB}}{\delta} = k_g$, mass transfer coefficient, $\frac{cm}{sec.}$

Let $c = \frac{p_T}{RT}$

Let a = superficial area of catalyst surface, $\frac{cm^2}{gm.}$

$$r_A = \frac{a}{S_{EX}} \frac{dN_A}{dt} = c k_g a \ln\left[\frac{1+Y_{A_b}}{1+Y_{A_s}}\right] = \frac{p_T k_g a}{RT} \ln\left[\frac{1+Y_{A_b}}{1+Y_{A_s}}\right] \qquad (65)$$

Where r_A = gm moles A diffusing toward the catalyst surface per second per gm. catalyst.

APPENDIX V

SURFACE PHENOMENA

SURFACE PHENOMENA

The adsorption of cumene (A) onto the catalyst surface, the reaction of cumene on the catalyst surface, and the desorption of benzene (R) from the catalyst surface, which are processes three, four and five of the reaction mechanism, are handled together mathematically. The following reaction mechanisms are possible:

Single Site Mechanism (Propylene Not Adsorbed)

1. Reactant molecule A (cumene) is adsorbed onto the catalyst surface.

$$A + 1 \rightleftharpoons A \cdot 1$$

2. Adsorbed reactant A (cumene) reacts to form adsorbed product R (benzene) and unadsorbed product S (propylene).

$$A \cdot 1 \rightleftharpoons R \cdot 1 + S$$

3. Adsorbed product R (benzene) is desorbed from the catalyst surface.

$$R \cdot 1 \rightleftharpoons R + 1$$

Single Site Mechanism (Benzene Not Adsorbed)

1. Reactant molecule A (cumene) is adsorbed onto the catalyst surface.

$$A + 1 \rightleftharpoons A \cdot 1$$

2. Adsorbed reactant A (cumene) reacts to form adsorbed product S (propylene) and unadsorbed product R (benzene).

$$A \cdot 1 \rightleftharpoons R + S \cdot 1$$

3. Adsorbed product S (propylene) is desorbed from the catalyst surface.

$$S \cdot 1 \rightleftharpoons S + 1$$

Dual Site Mechanism (Both Benzene and Propylene Are Adsorbed)

1. Reactant molecule A (cumene) is adsorbed onto the catalyst surface.

$$A + 1 \rightleftharpoons A \cdot 1$$

2. Adsorbed reactant A (cumene) reacts to form adsorbed product R (benzene) and adsorbed product S (propylene).

$$A \cdot 1 + 1 \rightleftharpoons R \cdot 1 + S \cdot 1$$

3. Adsorbed product R (benzene) is desorbed from the catalyst surface.

$$R \cdot 1 \rightleftharpoons R + 1$$

4. Adsorbed product S (propylene) is desorbed from the catalyst surface.

$$S \cdot 1 \rightleftharpoons S + 1$$

Garver has shown that at the conditions of his study (1.0 atm., 850-1050°F.) the actual reaction mechanism is

the single site mechanism with propylene not adsorbed and with the surface reaction controlling. The reaction rate expression for this mechanism is derived as follows:

Reactions

1. $A + 1 \underset{k'_1}{\overset{k_1}{\rightleftharpoons}} A\cdot 1$ (adsorption of A)

2. $A\cdot 1 \underset{k'_2}{\overset{k_2}{\rightleftharpoons}} R\cdot 1 + S$ (surface reaction; S not adsorbed)

3. $R\cdot 1 \underset{k'_3}{\overset{k_3}{\rightleftharpoons}} R + 1$ (desorption of R)

4. $A \underset{k'}{\overset{k}{\rightleftharpoons}} R + S$ (overall reaction)

Rate equations are now written for each of the reaction steps. Since surface reaction controls and is therefore the slowest step, it is assumed that the adsorption and desorption steps reach equilibrium.

Rate Equations

1. $(-r_A) = k_1 p_A C_1 - k'_1 C_{A1}$ (66)

(adsorption of A; at equilibrium)

2. $(-r_{A1}) = k_2 C_{A1} - k'_2 p_S C_{R1}$ (67)

(surface reaction and S not adsorbed; controlling)

3. $(-r_{R1}) = k_3 C_{R1} - k'_3 p_R C_1$ (68)

(desorption of R; at equilibrium)

$$K_3 = \frac{1}{K_R} = \frac{k_3}{k'_3} = \frac{p_R C_1}{C_{R1}}$$

4. $(-r_A) = kp_A - k' p_R p_S$ (overall reaction) (69)

$$K = \frac{k}{k'} = \frac{p_R p_S}{p_A}$$

Calculation of $(-r_{A1})$ in Terms of C_1

$$(-r_{A1}) = k_2 C_{A1} - k'_2 p_S C_{R1} \quad (70)$$

$$C_{A1} = K_A p_A C_1$$

$$C_{R1} = K_R p_R C_1$$

$$k'_2 = \frac{k_2}{K_2} = \frac{k_2 K_A}{K K_R}$$

$$\frac{K_A K_2}{K_R} = \frac{C_{A1}}{p_A C_1} \cdot \frac{p_S C_{R1}}{C_{a1}} \cdot \frac{p_R C_1}{C_{R1}} = \frac{p_R p_S}{p_A} = K$$

$$K_2 = \frac{K K_R}{K_A}$$

$$(-r_{A1}) = k_2 K_A p_A C_1 - \frac{k_2 K_A p_S K_R p_R C_1}{K K_R}$$

$$= k_2 K_A C_1 \left[p_A - \frac{p_R p_S}{K} \right]$$

Definition of C_1

$$C_1 = C_L - C_{A1} - C_{R1} - C_{S1} \tag{71}$$

$$C_{A1} = K_A p_A C_1$$

$$C_{R1} = k_R p_R C_1$$

$$C_{S1} = 0 \text{ (S not adsorbed)}$$

$$C_1 = C_L - K_A p_A C_1 - K_R p_R C_1$$

$$C_1 = \frac{C_L}{1 + K_A p_A + K_R p_R}$$

Substitute C_1 into Rate Equation

$$(-r_{A1}) = \frac{C_L k_2 K_A \left[p_A - \frac{p_R p_S}{K} \right]}{1 + K_A p_A + K_R p_R} \tag{72}$$

For irreversible reaction, k is very large and k' is very small and K approaches infinity. The above then reduces to the following expression:

$$(-r_{A1}) = \frac{C_L k_2 K_A p_A}{1 + K_A p_A + K_R p_R} \tag{73}$$

The initial rate of reaction, r_o, occurs when the partial pressure of A is equal to the total pressure, π, and the partial pressures of R and S are equal to zero.

$$(-r_{A1}) = \frac{C_L k_2 K_A \left[p_A - \frac{p_R p_S}{K} \right]}{1 + K_A p_A + K_R p_R} \tag{74}$$

$$(-r_{A1}) = r_o$$

$$p_A = \pi$$

$$p_R = p_S = 0$$

$$r_o = \frac{C_L k_2 K_A \pi}{1 + K_A \pi} \qquad (74)$$

APPENDIX VI

PORE DIFFUSION

PORE DIFFUSION

The effect of pore diffusion (processes two and six of the reaction mechanism) on the rate of reaction is expressed by applying a correction factor to the rate equation. The term C_L, total concentration of available active sites, is replaced by the product of the terms L, the total concentration of active sites, and ϵ, the ratio of the actual reaction rate to the theoretical reaction rate if the resistance to pore diffusion were absent. ϵ is known as the catalyst effectiveness factor.

The effectiveness factor of spherical catalysts with arbitrarily shaped pores is derived as follows:

Rate Equation

$$-(r_A) = \frac{\epsilon L k_2 K_A \left[p_A - \frac{p_R p_S}{K} \right]}{1 + K_A p_A + K_R p_R} = k p_A - k' p_R p_S$$

$$= k_S S_g C_A - k'_S S_g C_R C_S \qquad (75)$$

Flow Chart

A cross section of the catalyst particle is shown in Figure 41. The concentration of cumene on the surface of the particle is CA_s and the radius of the particle is r_p.

FIGURE 41

CROSS SECTION OF CATALYST PARTICLE
SHOWING DIFFERENTIAL ELEMENT

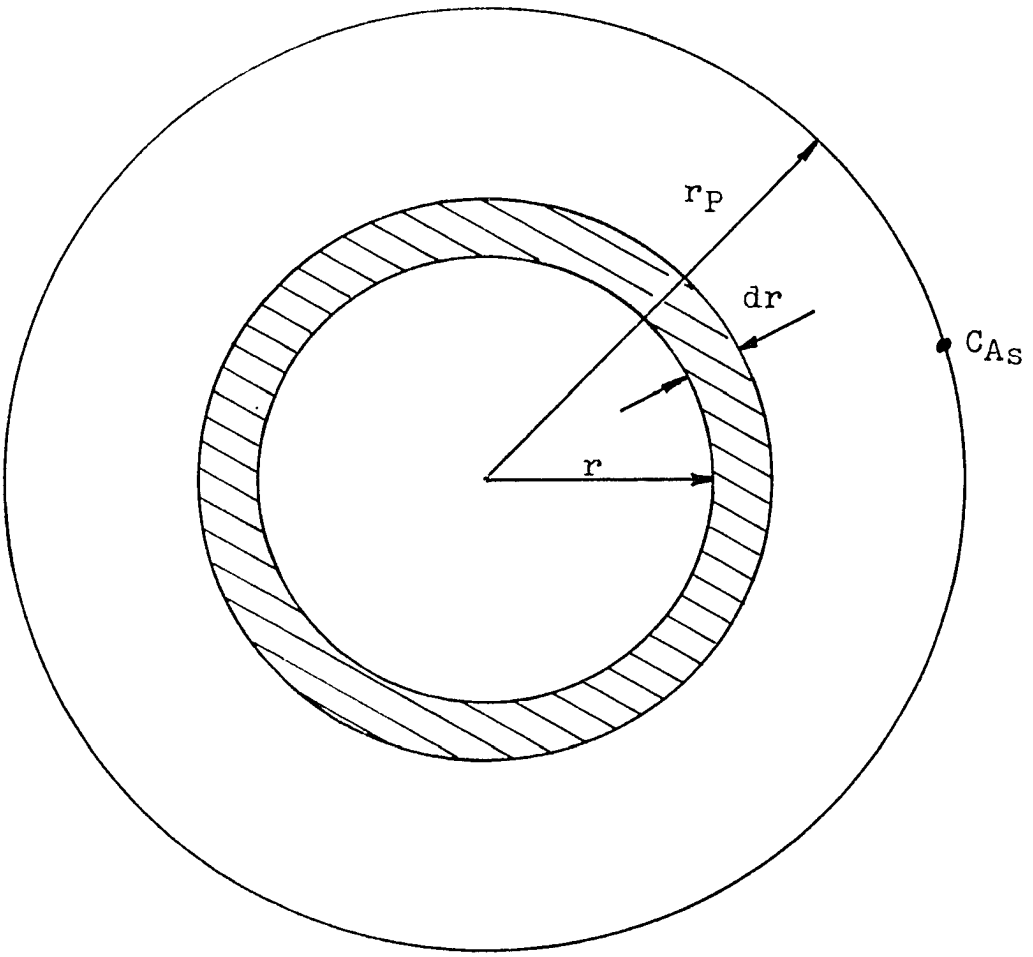

Material Balance on Differential Element, dr.

Input - Output + Generation = Accumulation

Input

$$(4\pi r^2 cm^2)(D_e \frac{cm^2}{sec.})\left[-\frac{dC_A}{dr}\frac{\frac{moles}{cm^3}}{cm}\right]$$

$$= -4\pi r^2 D_e \frac{dC_A}{dr}\frac{gm\ moles}{sec.} \qquad (76)$$

Output

$$(4\pi(r+dr)^2 cm^2)(D_e \frac{cm^2}{sec.})\left[-\frac{dC_A}{dr} - \frac{d}{dr}\left(\frac{dC_A}{dr}\right)dr\ \frac{\frac{moles}{cm^3}}{cm}\right]$$

$$= -4\pi(r^2+2rdr+dr^2)D_e\left[\frac{dC_A}{dr} + \frac{d^2C_A}{dr^2}dr\right]\frac{gm\ moles}{sec.} \qquad (77)$$

Generation

$$(r_A \frac{gm\ moles}{gm\ cat\text{-}sec.})(dW_C\ gms\ cat.) = r_A dW_C \frac{gm\ moles}{sec.} \qquad (78)$$

$$= (r_A \frac{gm\ moles}{gm\ cat\text{-}sec.})(4\pi r^2 dr cm^3)(\rho_P \frac{gm\ cat.}{cm^3})$$

$$= (r_A)(4\pi\rho_P r^2 dr)\frac{gm\ moles}{sec.}$$

Accumulation = 0 (steady state) (79)

Material Balance

$$-4\pi r^2 D_e \frac{dC_A}{dr} + 4\pi r^2 D_e \frac{dC_A}{dr} + 4\pi r^2 D_e \frac{d^2C_A}{dr^2} dr$$

$$+8\pi r dr D_e \frac{dC_A}{dr} + 8\pi r dr D_e \frac{d^2C_A}{dr^2} dr$$

$$+(r_A)(4\pi\rho_P r^2 dr) = 0$$

$$4\pi r^2 D_e \frac{d^2C_A}{dr^2} dr + 8\pi r dr D_e \frac{dC_A}{dr} + (r_A)(4\pi\rho_P r^2 dr) = 0$$

$$\frac{d^2C_A}{dr^2} + \frac{2}{r}\frac{dC_A}{dr} + \frac{\rho_P}{D_e}(r_A) = 0 \qquad (80)$$

Calculation of Rate Equation

$$(-r_A) = k_S S_g C_A - k'_S S_g C_R C_S \qquad (81)$$

Assume irreversible reaction

$k_S >> k'_S$

$$(-r_A) = k_S S_g C_A$$

Substitute Rate Equation Into Material Balance

$$\frac{d^2C_A}{dr^2} + \frac{2}{r}\frac{dC_A}{dr} - \frac{\rho_P k_S S_g C_A}{D_e} = 0 \qquad (82)$$

Integrate

Change of Variable

Let $x = C_A r$

$$dx = C_A dr + r dC_A \qquad r dC_A = dx - C_A dr$$

$$\frac{dC_A}{dr} = \frac{1}{r}\frac{dx}{dr} - \frac{C_A}{r} = \frac{1}{r}\frac{dx}{dr} - \frac{x}{r^2}$$

$$\frac{d^2C_A}{dr} = \left[\frac{dx}{dr}\right]\left[-\frac{1}{r^2}\right] + \frac{1}{r}\frac{d^2x}{dr^2} + \frac{x(2)}{r^3} - \frac{1}{r^2}\frac{dx}{dr}$$

$$= \frac{1}{r}\frac{d\,x}{dr^2} - \frac{2}{r^2}\frac{dx}{dr} + \frac{2x}{r^3}$$

Substitute

$$\frac{1}{r}\frac{d^2x}{dr^2} - \frac{2}{r^2}\frac{dx}{dr} + \frac{2x}{r^3} + \frac{2}{r^2}\frac{dx}{dr} - \frac{2x}{r^3} - \frac{\rho_p k_S S_g x}{D_e r} = 0$$

$$\frac{d^2x}{dr^2} - \left[\frac{k_S \rho_P S_g}{D_e}\right] x = 0$$

General Solution

$$x = M_1 e^{mr} + M_2 e^{-mr} = C_A r$$

$$m = \frac{-b \pm \sqrt{b^2-4ac}}{2a} = \frac{0 \pm \sqrt{o + \frac{4k_S \rho_P S_g}{D_e}}}{2} = \left[\frac{k_S \rho_P S_g}{D_e}\right]^{\frac{1}{2}}$$

$$C_A = \frac{1}{r}\left[M_1 e^{mr} + M_2 e^{-mr}\right] \qquad (83)$$

Boundary Conditions

At $r = 0$, $\frac{dC_A}{dr} = 0$

At $r = r_P$, $C_A = C_{A_s}$

$$\frac{dC_A}{dr} = \left[\frac{1}{r} mM_1 e^{mr} - mM_2 e^{-mr}\right] - \frac{1}{r^2}\left[M_1 e^{mr} + M_2 e^{-mr}\right]$$

$$r^2 \frac{dC_A}{dr} = \left[r\, mM_1 e^{mr} - mM_2 e^{-mr}\right] - \left[M_1 e^{mr} + M_2 e^{-mr}\right]$$

$$0 = 0 - M_1 - M_2$$

$$M_1 = -M_2$$

$$C_{A_S} = \frac{1}{r_P}\left[M_1 e^{mr_P} + M_2 e^{-mr_P}\right]$$

$$C_{A_S} r_P = M_1 e^{mr_P} - M_1 e^{-mr_P}$$

$$M_1 = \frac{C_{A_S} r_P}{e^{mr_P} - e^{-mr_P}}$$

$$M_2 = \frac{-C_{A_S} r_P}{e^{mr_P} - e^{-mr_P}}$$

Back Substitute

$$C_A = \frac{1}{r}\left[\frac{C_S r_P e^{mr}}{e^{mr_P} - e^{mr_P}} - \frac{C_S r_P e^{-mr}}{e^{mr_P} - e^{-mr_P}}\right]$$

$$= \frac{C_{A_S} r_P}{r}\left[\frac{e^{mr} - e^{-mr}}{e^{-mr_P} - e^{-mr_P}}\right] = \frac{C_{A_S} r_P}{r}\left[\frac{\sinh mr}{\sinh mr_P}\right]$$

$$C_A = \frac{C_{A_S} r_P}{r}\left[\frac{\sinh mr}{\sinh mr_P}\right] \qquad (84)$$

$$m = \left[\frac{k_S \rho_P S_g}{D_e}\right]^{\frac{1}{2}} = \left[\frac{k_S S_V}{D_e}\right]^{\frac{1}{2}}$$

Calculation of Actual Reaction Rate

Actual reaction rate = Rate of diffusion into catalyst pellet

$$-R_P = (4\pi r_P^2 \text{ cm}^2)(D_e \frac{\text{cm}^2}{\text{sec}}) \left[- \frac{dC_A}{dr} \frac{\frac{\text{gm moles}}{\text{cm}^3}}{\text{cm}} \right]_{r = r_P} \quad (85)$$

$$= -4\pi r_P^2 D_e \left[\frac{dC_A}{dr}\right]_{r = r_P} \frac{\text{gm moles}}{\text{sec.}}$$

$$\frac{dC_A}{dr} = \frac{d}{dr}\left[\frac{C_{A_s} r_P \sinh mr}{r \sinh mr_P}\right] = \frac{C_{A_s} r_P}{\sinh mr_P} \frac{d}{dr}\left[\frac{\sinh mr}{r}\right]$$

$$= \frac{C_{A_s} r_P}{\sinh mr_P}\left[\frac{rm \cosh mr - \sinh mr}{r^2}\right]$$

$$= \frac{C_{A_s} r_P}{\sinh mr_P}\left[\frac{m \cosh mr}{r} - \frac{\sinh mr}{r^2}\right]$$

$$\left[\frac{dC_A}{dr}\right]_{r=r_P} = \frac{C_{A_s} r_P}{\sinh mr_P}\left[\frac{m \cosh mr_P}{r_P} - \frac{\sinh mr_P}{r^2_P}\right]$$

$$= \frac{C_{A_s}}{r_P}\left[\frac{mr_P}{\tanh mr_P} - 1\right]$$

$$R_P = 4\pi r_P^2 D_e \frac{C_{A_S}}{r_P}\left[\frac{mr_P}{\tanh mr_P} - 1\right]$$

$$= 4\pi r_P^2 D_e C_{A_S} mr_P \left[\frac{1}{\tanh mr_P} - \frac{1}{mr_P}\right]$$

$$= 4\pi r_P^2 D_e C_{A_S} \left[\frac{k_S S_V}{D_e}\right]^{\frac{1}{2}} \left[\frac{1}{\tanh (\frac{k_S S_V}{D_e})^{\frac{1}{2}} r_P} - \frac{1}{(\frac{k_S S_V}{D_e})^{\frac{1}{2}} r_P}\right]$$

$$\text{Let } h_S = mr_P = r_P \left[\frac{k_S S_V}{D_e}\right]^{\frac{1}{2}} \quad \text{(Thiele Modulus)}$$

$$R_P = 4h_S \pi r_P D_e C_{A_s} \left[\frac{1}{\tanh h_S} - \frac{1}{h_S}\right] \tag{86}$$

Calculation of Maximum Reaction Rate

$$R_{max} = \left(\frac{4}{3}\pi r_P^3 cm^3\right)\left(k_S \frac{cm}{sec}\right)\left(S_V \frac{cm^2}{cm^3}\right)\left(C_{A_s} \frac{gm\ moles}{cm^3}\right)$$

$$= \frac{4\pi r_P^3 k_S S_V C_{A_s}}{3} \frac{gm\ moles}{sec.} \tag{87}$$

Definition of Effectiveness Factor

ϵ = effectiveness factor

$$= \frac{\text{actual rate of reaction with pore diffusion present}}{\text{rate of reaction if resistance of pore diffusion were absent}}$$

$$= \frac{R_P}{R_{max}}$$

$$= \frac{4h_S \pi r_P D_e C_{A_s}}{\frac{4}{3}\pi r_P^3 k_S S_V C_{A_s}} \left[\frac{1}{\tanh h_S} - \frac{1}{h_S}\right]$$

$$= \frac{3h_S D_e}{r_P^2 k_S S_V} \left[\frac{1}{\tanh h_S} - \frac{1}{h_S}\right]$$

$$= \frac{3r_P k_S^{\frac{1}{2}} S_V^{\frac{1}{2}} D_e}{D_e^{\frac{1}{2}} r_P^2 k_S S_V} \left[\frac{1}{\tanh h_S} - \frac{1}{h_S}\right]$$

$$= \frac{3}{\frac{r p k_S^{\frac{1}{2}} S_V^{\frac{1}{2}}}{D_e^{\frac{1}{2}}}} \left[\frac{1}{\tanh h_S} - \frac{1}{h_S} \right]$$

$$\epsilon = \frac{3}{h_S} \left[\frac{1}{\tanh h_S} - \frac{1}{h_S} \right] \qquad (88)$$

Calculation of Effective Diffusivity, D_e

Definition of Effective Diffusivity

$$D_e = \frac{D_S \theta}{\tau} \qquad (89)$$

D_e = effective diffusivity, $\frac{cm^2}{sec.}$

θ = fraction voids in catalyst particle

τ = tortuosity factor

D_S = combined diffusivity, $\frac{cm^2}{sec.}$

$$= \frac{1}{D_{AB}} + \frac{1}{D_K}$$

D_{AB} = diffusivity of A in A + R + S, $\frac{cm^2}{sec.}$

D_K = Knudsen diffusivity, $\frac{cm^2}{sec.}$

Molecular Diffusivity of A in A + R + S

As previously calculated, the molecular diffusivity of A in A + R + S, D_{AB}, are as follows:

$$\left[D_{AB}\right]_{650^\circ F.} = 0.1141 \ \frac{cm^2}{sec.}$$

$$\left[D_{AB}\right]_{1050^\circ F.} = 0.2044 \ \frac{cm^2}{sec.}$$

Satterfield[70] has shown that in the temperature range of 200°K. to 5000°K., D_{AB} is well represented by a power function of temperature, that exponent being 1.82. The relationship between molecular diffusivity and temperature then becomes as follows:

$$D_{AB} = -0.00633 + 0.1008 + 10^{-5}T^{1.82}$$

Where T is in °K. the values for D_{AB} at several temperatures are as follows:

T, °F.	T, °K.	D_{AB}, $\frac{cm.^2}{sec.}$
650	616	0.1141
700	644	0.1242
750	672	0.1347
800	700	0.1456
850	728	0.1568
900	756	0.1684
950	783	0.1799
1000	811	0.1922
1050	839	0.2044

Calculation of Knudsen Diffusivity

$$D_K = \frac{4\bar{r}_e}{3}\left[\frac{2R_gT}{M}\right]^{\frac{1}{2}} \qquad (90)$$

$$R_g = \frac{(82.06 \frac{cm^3\text{-atm}}{gm\ mole\ ^oK})(14.7 \frac{lb.}{in^2 atm})(454 \frac{gms}{lb.})(980 \frac{cm}{sec^2})}{(2.54 \frac{cm}{in})\ (2.54 \frac{cm}{in})}$$

$$= 8.32 \times 10^7 \frac{gm\text{-}cm^2}{gm\ mole\text{-}^oK\text{-}sec^2}$$

$$M = 120.19 \frac{gms}{gm\ mole}$$

$$r_e = \frac{2V_g}{S_g}$$

V_g = pore volume/gm. catalyst, $\frac{cm^3}{gm}$

$$S_g = 250 \times 10^4 \frac{cm^2}{gm}$$

$$r_e = \frac{(2)(0.350 \frac{cm^3}{gm})}{(250 \times 10^4 \frac{cm^2}{gm})} = 2.80 \times 10^{-7}\ cm.$$

$$D_K = \frac{(4)(280 \times 10^{-7} cm)}{3}\left[\frac{2(8.32 \times 10^7 \frac{gm\text{-}cm^2}{gm\ mole\text{-}^oK\text{-}sec^2})}{(120.19 \frac{gms}{gm\ mole})}\right]^{\frac{1}{2}} (T^oK)^{\frac{1}{2}}$$

$$D_K = 2.478 \times 10^{-4}\ T^{\frac{1}{2}} \frac{cm^2}{sec}$$

The values for D_K at several temperatures are as follows:

T, $^oF.$	T, $^oK.$	$(T^oK)^{\frac{1}{2}}$	D_K, $\frac{cm^2}{sec.}$
650	616	24.82	0.00615
700	644	25.38	0.00629
750	672	25.92	0.00647
800	700	26.46	0.00656
850	728	26.98	0.00669

T, °F.	T, °K.	$(T^{\circ}K.)^{\frac{1}{2}}$	D_K, $\frac{cm^2}{sec.}$
900	756	27.50	0.00681
950	783	27.98	0.00693
1000	811	28.48	0.00706
1050	839	28.97	0.00718

Calculation of Combined Diffusivity

$$\frac{1}{D_S} = \frac{1}{D_{AB}} + \frac{1}{D_K} \tag{91}$$

$$\left[\frac{1}{D_S}\right]_{650} = \frac{1}{0.1141} + \frac{1}{0.00615} = 171.4$$

$$\left[D_S\right]_{650} = 0.00584 \ \frac{cm^2}{sec.}$$

Similarly,

T, °F.	D_S, $\frac{cm^2}{sec.}$
650	0.00584
700	0.00599
750	0.00613
800	0.00628
850	0.00642
900	0.00655
950	0.00667
1000	0.00681
1050	0.00694

Calculation of Effective Diffusivity

$$D_e = \frac{D_s \theta}{\tau} = \frac{D_s(0.448)}{5.6} = 0.080\ D_s \qquad (92)$$

T, °F.	D_s, $\frac{cm^2}{sec.}$
650	0.000467
700	0.000479
750	0.000490
800	0.000502
850	0.000514
900	0.000524
950	0.000534
1000	0.000545
1050	0.000555

Calculation of Thiele Modulus, h_S

Definition of Thiele Modulus

$$h_S = r_P \left[\frac{k_S S_V}{D_e}\right]^{\frac{1}{2}} \qquad (93)$$

r_P = radius of catalyst particle = 0.179 cm.

S_V = total surface area of porous catalyst

$= 320 \times 10^4\ \frac{cm^2}{cm^3}$

k_S = forward intrinsic rate constant for surface reaction, $\frac{cm.}{sec.}$

Calculation of k_S

Initial Rate of Reaction

$$r_o = \frac{\epsilon L k_2 K_A \pi}{1 + K_A \pi} \tag{94}$$

Pseudo First Order Reaction (Appendix XI)

$$r_o = k_S S_g C_{A_o} \tag{95}$$

Calculate k_S

$$k_S = \frac{\epsilon L k_2 K_A \pi}{(1 + K_A \pi) S_g C_{A_o}} \tag{96}$$

k_A = equilibrium adsorption constant for cumene, $\frac{1}{\text{atm.}}$

π = 1 atm.

$S_g = 250 \times 10^4 \frac{\text{cm}^2}{\text{gm}}$

C_{A_o} = initial cumene concentration, $\frac{\text{gm moles}}{\text{cm}^3}$

$\log \epsilon L k_2 = -4812 \frac{1}{T^oR} - 1.141$ (no ultrasound)

Calculation of h_S

$$h_S = r_P S_V^{\frac{1}{2}} \left[\frac{k_S}{D_e}\right]^{\frac{1}{2}} = (0.179)(320 \times 10^4)^{\frac{1}{2}} \left[\frac{k_S}{D_e}\right]^{\frac{1}{2}}$$

$$= 320 \left[\frac{k_S}{D_e}\right]^{\frac{1}{2}}$$

Calculation of Effectiveness Factor, ϵ

$$\epsilon = \frac{3}{h_S}\left[\frac{1}{\tanh h_S} - \frac{1}{h_S}\right]$$

Summary of Calculations (No Ultrasound)

T $^{o}F.$	$\epsilon lk_2 \times 10^5$ $\frac{gm\ moles}{gm\ cat\text{-}sec.}$	$k_S \times 10^7$ $\frac{cm.}{sec.}$	h_S	ϵ
650	0.334	0.499	3.31	0.63
700	0.514	0.789	4.11	0.55
750	0.762	1.200	5.01	0.48
800	1.099	1.778	5.01	0.48
850	1.534	2.541	7.12	0.36
900	2.126	3.605	8.39	0.32
950	2.794	4.849	9.64	0.28
1000	3.657	6.486	11.04	0.25
1050	4.702	8.526	12.54	0.22

At frequency inputs of 26,000 cps and 39,000 cps the rate constant ϵlk_2 increases as shown previously because the effectiveness factor, ϵ, or surface reaction rate constant, k_2, increases. When the effectiveness factor increases, the Thiele Modulus, h_S, must decrease, requiring the effective diffusivity, D_e, to increase. The effect of ultrasound, therefore, may be to increase the diffusion rate of cumene in the catalyst pores.

APPENDIX VII

REACTION DESIGN EQUATION

REACTION DESIGN EQUATION

The reaction design equation is derived by substituting the rate equation for the single site mechanism, S (propylene) not adsorbed, with surface reaction controlling into the plug flow reactor design equation. The derivation is as follows:

Derivation of Design Equation for Plug Flow Reactor

Flow Chart (Figure 42)

Material Balance

Input - Output + Generation = Accumulation

Input

$$F_A \frac{\text{gm moles A}}{\text{sec.}}$$

Output

$$(F_A + dF_A) \frac{\text{gm moles A}}{\text{sec.}}$$

Generation

$$(+r_A \frac{\text{gm moles A}}{\text{gm cat-sec.}})(dW \text{ gm cat.}) = (+r_A)dW \frac{\text{gm moles A}}{\text{sec.}}$$

Accumulation = 0 (steady state)

Material Balance

$$F_A - F_A - dF_A = r_A dW = 0$$

$$-dF_A = (-r_A)dW$$

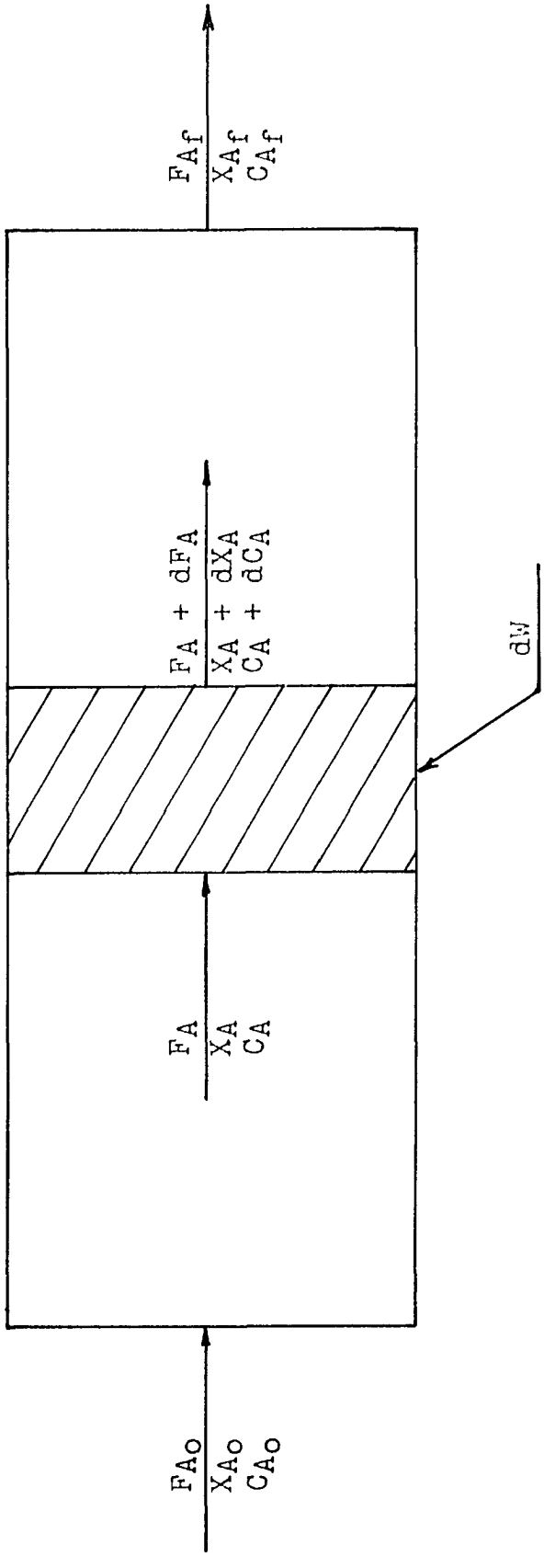

FIGURE 42

CROSS SECTION OF PLUG FLOW REACTOR SHOWING DIFFERENTIAL ELEMENT

$$F_A = F_{A_o} - X_A F_{A_o}$$

$$dF_A = -F_{A_o} dX_A$$

$$F_{A_o} dX_A = (-r_A) dW$$

$$\frac{dW}{F_{A_o}} = \frac{dX_A}{(-r_A)}$$

Integrate

$$\int_0^W \frac{dW}{F_{A_o}} = \int_{X_{A_o}}^{X_{A_f}} \frac{dX_A}{(-r_A)}$$

$$\frac{W}{F_{A_o}} = \int_{X_{A_o}}^{X_{A_f}} \frac{dX_A}{(-r_A)} \qquad (97)$$

Calculation of Reaction Design Equation, Surface Reactions Controlling

Rate Equation for Single Site Mechanism, S (Propylene) Not Adsorbed, and Surface Reaction Controlling

$$(-r_A) = \frac{\epsilon L k_2 K_A \left[p_A - \frac{p_R p_S}{K} \right]}{1 + K_A p_A + K_R p_R} \qquad (98)$$

Substitute Rate Equation Into Plug Flow Reactor Design Equation

$$\frac{W}{F_{A_o}} = \int_{X_{A_o}}^{X_{A_f}} \frac{dX_A}{\frac{\epsilon L k_2 K_A \left[p_A - \frac{p_R p_S}{K}\right]}{1 + K_A p_A + K_R p_R}}$$

Solve for Partial Pressures in Terms of Conversion and Total Pressure

Material Balance

	Inlet	Reactor	Outlet
A	$N_{A_o}=N_{A_o}$	$N_A=N_{A_o}-X_A N_{A_o}$	$N_{A_f}=N_{A_o}-X_{A_f} N_{A_o}$
R	$N_{R_o}=N_{R_o}$	$N_R=N_{R_o}+X_A N_{A_o}$	$N_R=N_{R_o}+X_{A_f} N_{A_o}$
S	$N_{S_o}=N_{S_o}$	$N_S=N_{S_o}+X_A N_{A_o}$	$N_S=N_{S_o}+X_{A_f} N_{A_o}$
Total	$N_{A_o}+N_{R_o}+N_{S_o}$	$N_{A_o}+N_{R_o}+N_{S_o}+X_A N_{A_o}$	$N_{A_o}+N_{R_o}+N_{S_o}+X_{A_f} N_{A_o}$

$$p_A = \frac{N_A \Pi}{N_T} = \frac{(N_{A_o}-X_A N_{A_o})\Pi}{(N_{A_o}+N_{R_o}+N_{S_o}+X_A N_{A_o})}$$

$$p_R = \frac{N_R \Pi}{N_T} = \frac{(N_{R_o}+X_A N_{A_o})\Pi}{(N_{A_o}+N_{R_o}+N_{S_o}+X_A N_{A_o})}$$

$$p_S = \frac{N_S \Pi}{N_T} = \frac{(N_{S_o}+X_A N_{A_o})\Pi}{(N_{A_o}+N_{R_o}+N_{S_o}+X_A N_{A_o})}$$

However, $N_{R_o} = N_{S_o} = 0$

$$p_A = \frac{N_{A_o}(1 - X_A)\Pi}{N_{A_o}(1 + X_A)} = \frac{(1 - X_A)\Pi}{(1 + X_A)}$$

$$p_R = \frac{X_A N_{A_o}\Pi}{N_{A_o}(1 + X_A)} = \frac{X_A\Pi}{(1 + X_A)}$$

$$p_S = \frac{X_A N_{A_o}\Pi}{N_{A_o}(1 + X_A)} = \frac{X_A\Pi}{(1 + X_A)}$$

Substitute for Partial Pressures in Rate Equation

$$(-r_A) = \frac{\epsilon L k_2 K_A\left[p_A - \frac{p_R p_S}{K}\right]}{1 + K_A p_A + K_R p_R}$$

$$= \frac{\epsilon L k_2 K_A\left[\frac{(1-X_A)\Pi}{(1+X_A)} - \frac{X_A^2\Pi^2}{(1+X_A)^2 K}\right]}{1 + \frac{K_A(1-X_A)\Pi}{(1+X_A)} + \frac{K_A X_A\Pi}{(1+X_A)}}$$

$$\frac{1}{(-r_A)} = \frac{1 + \frac{K_A(1-X_A)\Pi}{(1+X_A)} + \frac{K_R X_A\Pi}{(1+X_A)}}{\epsilon L k_2 K_A\left[\frac{(1-X_A)\Pi}{(1+X_A)} - \frac{X_A^2\Pi^2}{(1+X_A)^2 K}\right]}$$

$$\frac{1}{(-r_A)} = \frac{(1 + K_A\Pi)}{\epsilon L k_2 K_A\Pi\left[1 - (1+\frac{\Pi}{K})X^2\right]}$$

$$+ \frac{(2 + K_R\Pi)X_A}{\epsilon L k_2 K_A\Pi\left[1 - (1+\frac{\Pi}{K})X_A^2\right]}$$

$$+ \frac{(1 - K_A\Pi + K_R\Pi)X^2}{\epsilon L k_2 K_A\Pi\left[1 - (1+\frac{\Pi}{K})X_A^2\right]}$$

$$\frac{(1 + K_A\Pi)}{\epsilon Lk_2 K_A \Pi\left[1 - (1+\frac{\Pi}{K})X_A{}^2\right]}$$

$$= \left[\frac{1}{\epsilon Lk_2 K_A \Pi} + \frac{K_A \Pi}{\epsilon Lk_2 K_A \Pi}\right]\left[\frac{1}{1 - (1+\frac{\Pi}{K})X_A{}^2}\right]$$

$$= \gamma\left[\frac{1}{1 - \delta^2 X_A{}^2}\right] = \frac{\gamma}{1 - \delta^2 X_A{}^2}$$

$$\gamma = \frac{1}{\epsilon Lk_2 K_A \Pi} + \frac{1}{\epsilon Lk_2}$$

$$\delta = \left[1 + \frac{\Pi}{K}\right]^{\frac{1}{2}}$$

$$\frac{(2 + K_R\Pi)X_A}{\epsilon Lk_2 K_A \Pi\left[1 - (1+\frac{\Pi}{K})X^2\right]}$$

$$= \left[\frac{2}{\epsilon Lk_2 K_A \Pi} + \frac{K_R \Pi}{\epsilon Lk_2 K_A \Pi}\right]\left[\frac{X_A}{1 - (1+\frac{\Pi}{K})X_A{}^2}\right]$$

$$= \beta\left[\frac{X_A}{1 - \delta^2 X_A{}^2}\right] = \frac{\beta X_A}{1 - \delta^2 X_A{}^2}$$

$$\beta = \frac{2}{\epsilon Lk_2 K_A \Pi} + \frac{K_R}{\epsilon Lk_2 K_A}$$

$$\delta = \left[1 + \frac{\Pi}{K}\right]^{\frac{1}{2}}$$

$$\frac{(1 - K_A\Pi + K_R\Pi)X_A^2}{\epsilon Lk_2K_A\Pi\left[1 - (1+\frac{\Pi}{K})X_A^2\right]}$$

$$= \left[\frac{1}{\epsilon Lk_2K_A\Pi} - \frac{K_A\Pi}{\epsilon Lk_2K_A\Pi} + \frac{K_R\Pi}{\epsilon Lk_2K_A\Pi}\right]\left[\frac{X_A^2}{1 - (1+\frac{\Pi}{K})X_A^2}\right]$$

$$= \left[\frac{1}{\epsilon Lk_2K_A\Pi} - \frac{1}{\epsilon Lk_2} + \frac{K_R}{\epsilon Lk_2K_A}\right]\left[\frac{X_A^2}{1 - (1+\frac{\Pi}{K})X_A^2}\right]$$

$$= \left[\beta - \gamma\right]\left[\frac{X_A^2}{1 - \delta^2X_A^2}\right] = \left[\frac{(\beta - \gamma)X_A^2}{1 - \delta^2X_A^2}\right]$$

$$\beta - \gamma = \frac{2}{\epsilon Lk_2K_A\Pi} + \frac{K_R}{\epsilon Lk_2K_A} - \frac{1}{\epsilon Lk_2K_A\Pi} - \frac{1}{\epsilon Lk_2}$$

$$= \frac{1}{\epsilon Lk_2K_A\Pi} - \frac{1}{\epsilon Lk_2} + \frac{K_R}{\epsilon Lk_2K_A}$$

$$\delta = \left[1 + \frac{\Pi}{K}\right]^{\frac{1}{2}}$$

$$\frac{1}{(-r_A)} = \frac{\gamma}{1 - \delta^2X_A^2} + \frac{\beta X_A}{1 - \delta^2X_A^2} + \frac{(\beta - \gamma)X_A^2}{1 - \delta^2X_A^2}$$

Substitute Rate Equation into Plug Flow Reactor Design Equation and Integrate

$$\frac{W}{F_{A_O}} = \int_{X_{A_O}}^{X_{A_f}} \frac{\gamma dX_A}{1 - \delta^2X_A^2} + \int_{X_{A_O}}^{X_{A_f}} \frac{\beta X_A dX_A}{1 - \delta^2X_A^2} + \int_{X_{A_O}}^{X_{A_f}} \frac{(\beta - \gamma)X_A^2 dX_A}{1 - \delta^2X_A^2}$$

$$\gamma \int_{X_{A_o}=o}^{X_{A_f}=X_A} \frac{dX_A}{-\delta^2 X_A^2+1} = \frac{\gamma}{2\delta} \ln\left[\frac{1+X_A\delta}{1-X_A\delta}\right]_o^{X_A} = \frac{\gamma}{2\delta} \ln \frac{1+X_A\delta}{1-X_A\delta}$$

$$\beta \int_{X_{A_o}=o}^{X_{A_f}=X_A} \frac{X_A dX_A}{-\delta^2 X_A+1} = \frac{\beta}{-2\delta^2} \ln\left[-\delta^2 X_A^2+1\right]_o^{X_A} = \frac{-\beta}{2\delta^2} \ln\left(-\delta^2 X_A^2+1\right)$$

$$(\beta-\gamma) \int_{X_{A_o}=o}^{X_{A_f}=X_A} \frac{X_A^2 dX_A^2}{-\delta^2 X_A^2+1} = \frac{(\beta-\gamma)X_A}{-\delta^2} - \frac{(\beta-\gamma)}{-\delta^2} \int_o^{X_A} \frac{dX_A}{-\delta^2 X_A^2+1}$$

$$= \frac{-(\beta-\gamma)X_A}{\delta^2} + \frac{(\beta-\gamma)}{\delta^2}\left[\frac{1}{2\delta} \ln \frac{(1+X_A\delta)}{(1-X_A\delta)}\right]$$

$$\frac{W}{F_{A_o}} = \frac{\gamma}{2\delta} \ln \frac{(1+X_A\delta)}{(1-X_A\delta)} - \frac{\beta}{2\delta^2} \ln\left(-\delta^2 X_A^2+1\right) - \frac{(\beta-\gamma)}{\delta^2} X_A$$

$$+ \frac{(\beta-\gamma)}{\delta^2}\left[\frac{1}{2\delta} \ln \frac{(1+X_A\delta)}{(1-X_A\delta)}\right]$$

$$\frac{W}{F_{A_o}} = \gamma\left[\left(\frac{1}{2\delta} - \frac{1}{2\delta^3}\right) \ln \frac{(1+X_A\delta)}{(1-X_A\delta)} + \frac{X_A}{\delta^2}\right]$$

$$+\beta\left[\frac{1}{2\delta^3} \ln \frac{(1+X_A\delta)}{(1-X_A\delta)} - \frac{1}{2\delta^2} \ln(1-\delta^2 X^2) - \frac{X_A}{\delta^2}\right] \quad (99)$$

$$\gamma = \frac{1}{\epsilon L k_2 K_A \Pi} + \frac{1}{\epsilon L k_2}$$

$$\beta = \frac{2}{\epsilon L k_2 K_A \Pi} + \frac{K_R}{\epsilon L k_2 K_A}$$

$$\delta = \left[1 + \frac{\Pi}{K}\right]^{\frac{1}{2}}$$

Calculation of Reaction Design Equation, External Diffusion Controlling

Rate Equation for External Diffusion Controlling

$$r_A = \frac{p_T k_g a}{RT} \ln \frac{1+Y_{A_b}}{1+Y_{A_s}} \quad (100)$$

Substitute Rate Equation into Plug Flow Reactor Equation

$$\frac{W}{F_{A_o}} = \int_{X_{A_o}}^{X_{A_f}} \frac{dX_A}{\frac{p_T k_g a}{RT} \ln \frac{1+Y_{A_b}}{1+Y_{A_s}}}$$

$$= \frac{X_{A_f} RT}{p_T k_g a \ln \frac{1+Y_{A_b}}{1+Y_{A_s}}}$$

Calculate Mass Transfer Coefficient, k_g

$$k_g = \frac{X_{A_f} RT}{(W/F_{A_o}) p_T a \ln \frac{1+Y_{A_b}}{1+Y_{A_s}}} \qquad (101)$$

Y_{A_s} = 0 (mole fraction cumene at catalyst surface)

$R = 82.03 \frac{cm^3\text{-atm.}}{gm\ mole\text{-}^oK.}$

$T = {}^oK.$

$F_{A_o} = \frac{gm\ moles\ cumene\ feed}{sec.}$

W = gms. catalyst

p_T = 1.0 atm.

$a = 13.1 \frac{cm^2}{gm.}$

$k_g = \frac{cm.}{sec.}$

X_{A_f} = conversion

$Y_{A_b} = \frac{Y_{A_i} - Y_{A_o}}{\ln \frac{Y_{A_i}}{Y_{A_o}}} = Y_{A_{LM}}$ (mole fraction cumene in bulk gas stream)

Y_{A_i} = 1.0 (mole fraction cumene at reactor inlet)

$Y_{A_o} = \frac{1 - X_{A_f}}{1 + X_{A_f}}$ (mole fraction cumene at reactor outlet)

$$k_g = \frac{6.261832\ X_{A_f} T}{(W/F_{A_o}) \ln(1+Y_{A_{LM}})}$$

APPENDIX VIII

EVALUATION OF REACTION RATE CONSTANTS

EVALUATION OF REACTION RATE CONSTANTS

As previously derived, the reaction design equation for the catalytic cracking of cumene in a continuous plug flow reactor is as follows:

$$\frac{W}{F_{A_o}} = \gamma\left[\left(\frac{1}{2\delta} - \frac{1}{2\delta^3}\right)\ln\frac{(1+X_A\delta)}{(1-X_A\delta)} + \frac{X_A}{\delta^2}\right]$$

$$+\beta\left[\frac{1}{2\delta^3}\ln\frac{(1+X_A\delta)}{(1-X_A\delta)} - \frac{1}{2\delta^2}\ln(1-\delta^2X_A^2) - \frac{X_A}{\delta^2}\right] \qquad (99)$$

Where,

$$\gamma = \frac{1}{\epsilon Lk_2K_A\Pi} + \frac{1}{\epsilon Lk_2}$$

$$\beta = \frac{2}{\epsilon Lk_2K_A\Pi} + \frac{K_R}{\epsilon Lk_2K_A}$$

$$\delta = \left[1 + \frac{\Pi}{K}\right]^{\frac{1}{2}}$$

Garver [22] experimentally determined the reaction rate constants at atmospheric pressure to be as follows:

	850°F.	950°F.	1050°F.
K, atm.	2.05	6.22	15.96
ϵLk_2, $\frac{\text{gm moles}}{\text{gm cat-sec.}}$	1.777×10^{-5}	2.165×10^{-5}	2.917×10^{-5}
K_A, $\frac{1}{\text{atm.}}$	2.24	2.13	1.90
K_R, $\frac{1}{\text{atm.}}$	2.45	1.86	1.47
γ, $\frac{\text{gm cat-sec.}}{\text{gm mole}}$	81,300	67,800	52,250

	850°F.	950°F.	1050°F.
β, $\frac{\text{gm cat-sec.}}{\text{gm mole}}$	111,500	83,600	62,500
δ, dimensionless	1.224	1.070	1.031

The above constants were obtained as follows:

Equilibrium Constant, K

Garver calculated the thermodynamic equilibrium constant for the dealkylation of cumene from the logarithms of the equilibrium constants of formation for cumene, benzene and propylene. The values for the equilibrium constants of formation were obtained from Circular C461 of the National Bureau of Standards.

The equation expressing the equilibrium constant as a function of temperature is as follows:

$$\log K = -8{,}927\left[\frac{1}{T}\right] + 7.126,$$

where K is in atmospheres and T is in Rankine.

Adsorption Constant for Cumene, K_A, and Combined Effectiveness Factor and Forward Reaction Rate Constant for Surface Reaction, ϵLk_2

Plot W/F_{A_o} vs. X_A at varying F_{A_o} and total pressure, π, and constant temperature, T, as shown in Figure 43.

FIGURE 43

PLOT OF X_A VS. $\frac{W}{F_{A_o}}$ AT CONSTANT TEMPERATURE

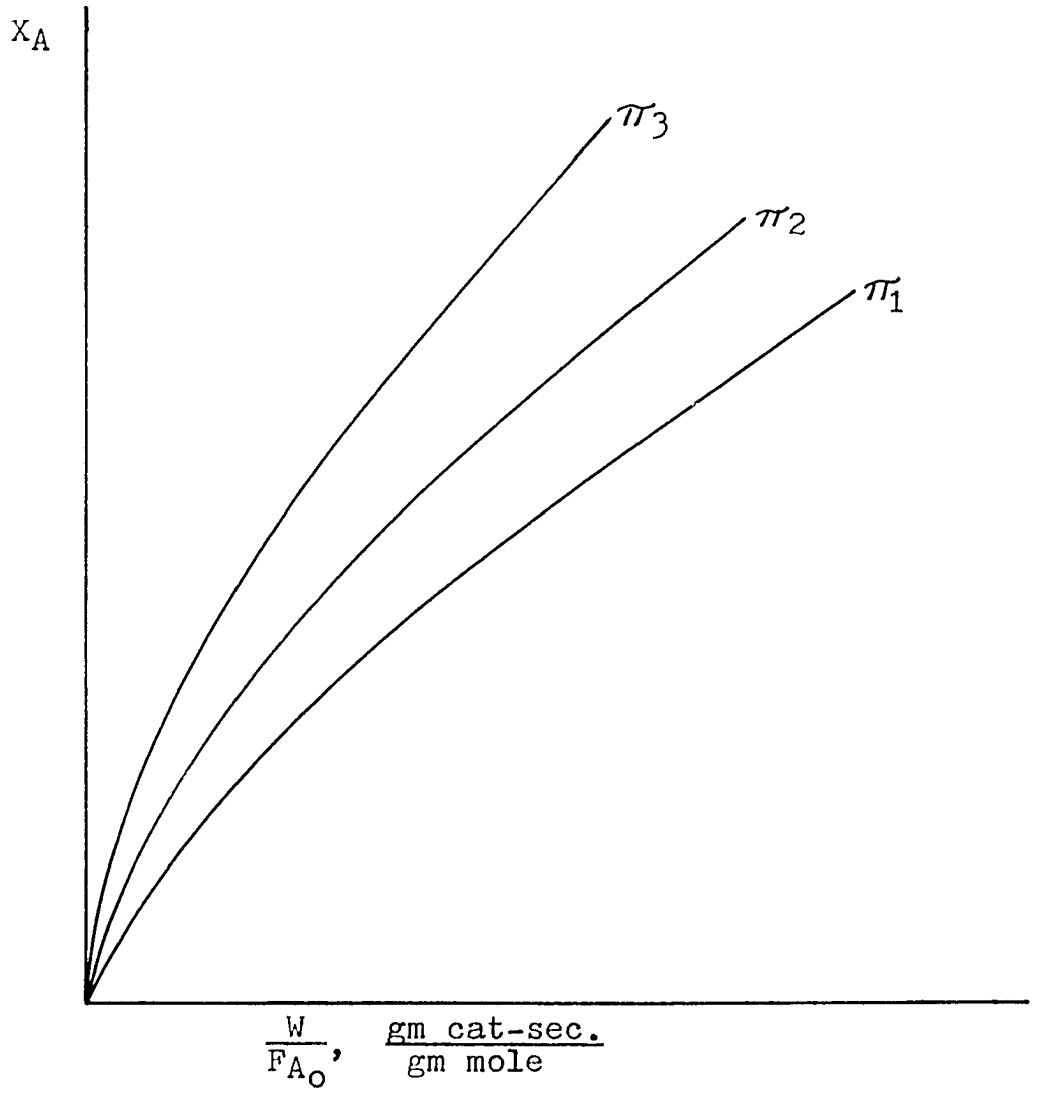

Rearrange the plug flow reactor design equation.

$$\frac{W}{F_{A_o}} = \int_{X_{A_o}}^{X_{A_f}} \frac{dX_A}{(-r_A)}$$

$$d\left(\frac{W}{F_{A_o}}\right) = \frac{dX_A}{(-r_A)}$$

$$(-r_A) = \frac{dX_A}{d\left(\frac{W}{F_{A_o}}\right)}$$

Plot the slope, $dX_A/d(\frac{W}{F_{A_o}})$ vs. X_A at π_1, π_2 and π_3. and extrapolate back to $X_A = 0$ to find initial rate, r_o, as shown in Figure 44.

Rearrange the initial rate equation.

$$r_o = \frac{\epsilon Lk_2 K_A \pi}{1+K_A \pi}$$

$$\frac{r_o}{\pi} = \frac{\epsilon Lk_2 K_A}{1+K_A \pi}$$

$$\frac{\pi}{r_o} = \frac{1}{\epsilon Lk_2 K_A} + \frac{\pi}{\epsilon Lk_2}$$

Plot $\frac{\pi}{r_o}$ vs. π as shown in Figure 45.

Calculate ϵLk_2 and K_A from the slope and intercept.

Repeat at 850°F., 950°F. and 1050°F.

FIGURE 44

PLOT OF REACTION RATE VS. CONVERSION AT CONSTANT TEMPERATURE

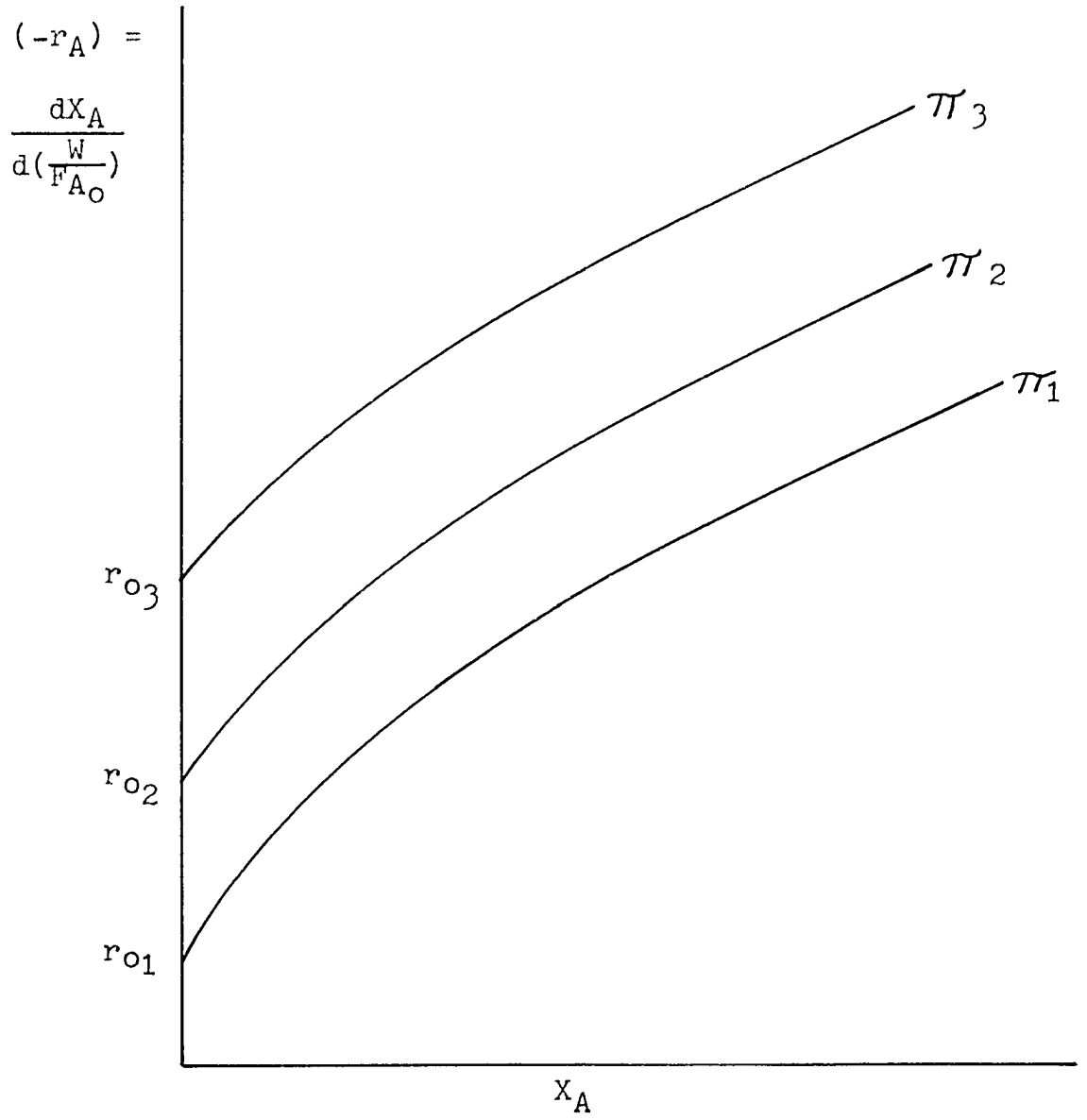

FIGURE 45

PLOT OF $\frac{\pi}{r_o}$ VS. π

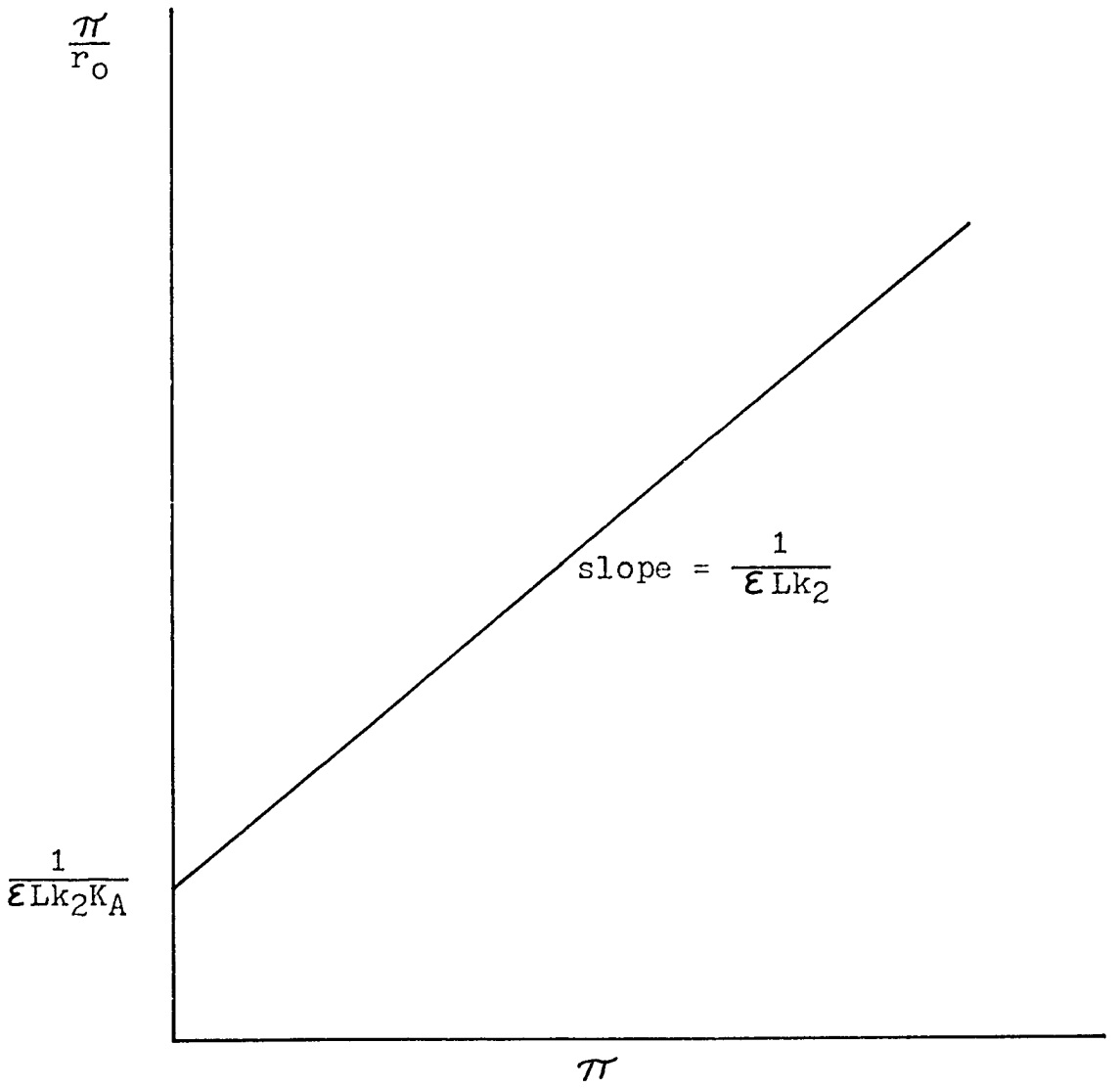

Adsorption Constant for Benzene, K_B

Assume Irreversible Reaction

Reaction Design Equation

$$\frac{W}{FA_o} = \gamma\left[\left(\frac{1}{2\delta} - \frac{1}{2\delta^3}\right)\ln\frac{(1+X_A\delta)}{(1-x_A\delta)} + \frac{X_A}{\delta^2}\right]$$

$$+\beta\left[\frac{1}{2\delta^3}\ln\frac{(1+X_A\delta)}{(1-X_A\delta)} - \frac{1}{2\delta^2}\ln(1-\delta^2X^2) - \frac{X_A}{\delta^2}\right] \quad (99)$$

For irreversible reaction

$$K = \frac{k}{k'} = >> 1$$

$$= \left[1 + \frac{\pi}{K}\right]^{\frac{1}{2}} = \left[1 + 0\right]^{\frac{1}{2}} = 1$$

Back substitute

$$\frac{W}{F_{A_o}} = \gamma\left[\left(\frac{1}{1} - \frac{1}{1}\right)\ln\frac{(1+X_A)}{(1-X_A)} + \frac{X_A}{1}\right]$$

$$+\beta\left[\frac{1}{2}\ln\frac{(1+X_A)}{(1-X_A)} - \frac{1}{2}\ln(1-X_A^2) - \frac{X_A}{1}\right]$$

$$= \gamma X_A + \beta\left[\frac{1}{2}\ln\frac{(1+X_A)}{(1-X_A)(1-X_A^2)} - X_A\right]$$

$$= \gamma X_A + \beta\left[\frac{1}{2}\ln\frac{1}{(1-X_A)^2} - X_A\right]$$

$$\frac{W}{F_{A_o}} = \gamma X_A + \beta\left[-\ln(1-X_A) - X_A\right] \quad (102)$$

Rearrange the irreversible rate equation:

$$\frac{W}{FA_o} - \gamma X_A = \beta\left[-\ln(1-X_A) - X_A\right]$$

Calculate γ at 850°F., 950°F. and 1050°F., and π_1, π_2, and π_3.

$$\gamma = \frac{1}{\epsilon Lk_2 K_A \pi} + \frac{1}{\epsilon Lk_2}$$

Plot $\left[\frac{W}{FA_o} - X_A\right]$ vs. $\left[-\ln(1-X_A) - X_A\right]$ at 850°F., 950°F. and 1050°F., and at π_1, π_2 and π_3 as shown in Figure 46.

Calculate K_R from slope of straight line.

Reaction Design Equation Constants γ, β, and δ

Since K, ϵLk_2, K_A and K_R are now known, γ, β and δ can be calculated at 850°F., 950°F. and 1050°F., and π_1, π_2 and π_3.

Summary of Results

Garver's investigation led to the following values for K, K_A and K_R:

$$\log K = -8927\left[\frac{1}{T^oR}\right] + 7.126 \qquad (103)$$

FIGURE 46

PLOT OF $\left[\frac{W}{FA_o} - \gamma X_A\right]$ VS. $\left[-\ln(1-X_A)-X_A\right]$

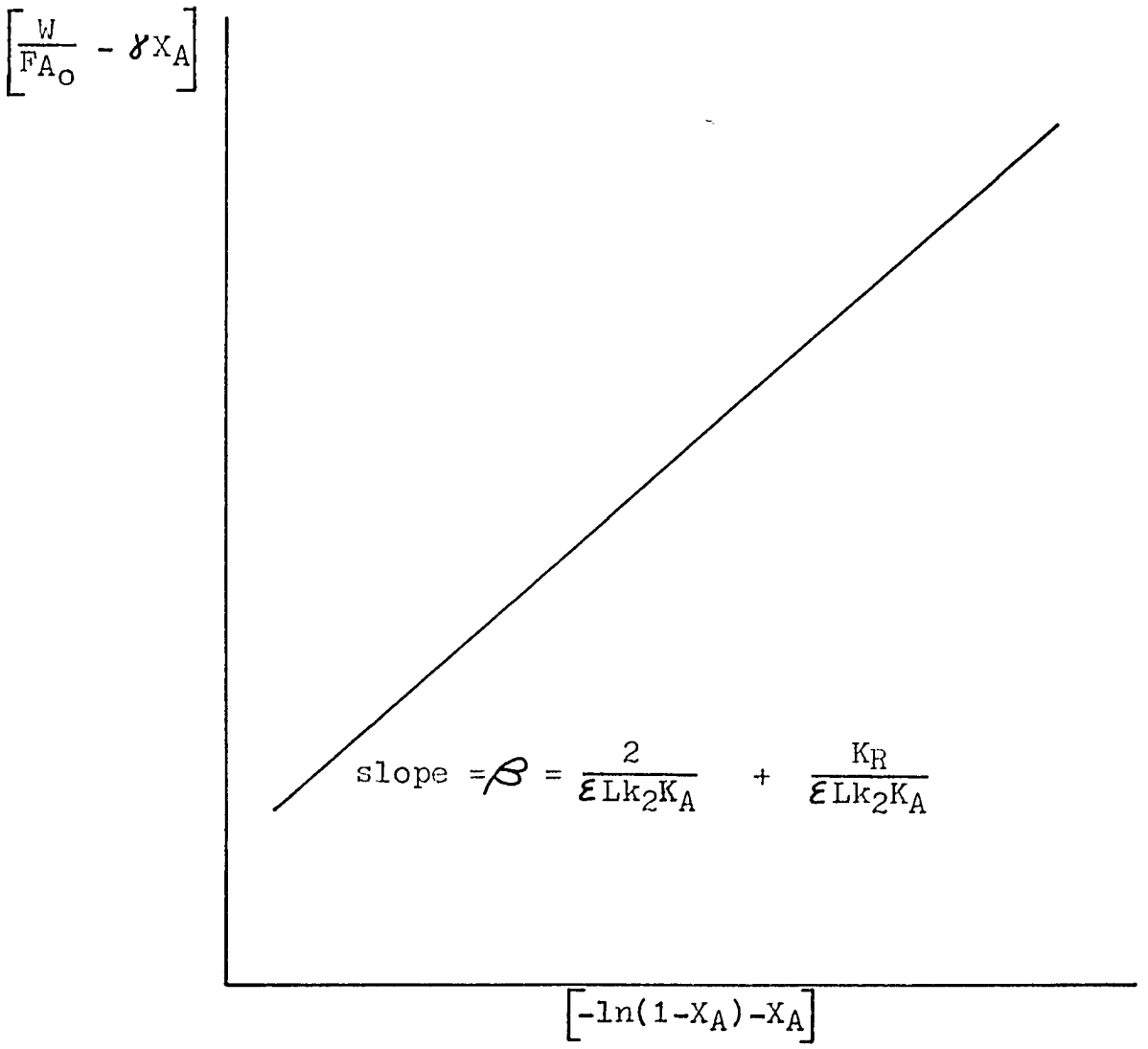

$$\log K_A = 700\left[\frac{1}{T^{\circ}R}\right] - 0.179 \qquad (104)$$

$$\log K_R = 2195\left[\frac{1}{T^{\circ}R}\right] - 1.286 \qquad (105)$$

Evaluation of Reaction Rate Constants

For this research, π = 1 atm. and ϵLk_2 is handled as a single constant. The rate equation then contains four parameters; ϵLk_2, K_A, K_R and K. The values of the parameters K, K_A and K_R obtained by Garver and extrapolated to 650°F. are shown in Figure 47.

These literature values of three of the four parameters were substituted into the surface reaction rate equation, and the fourth parameter, ϵLk_2, was computer calculated by curve fitting the data by use of Marquardt's non-linear square fit program.

Table 10 shows the literature values of K, K_A and K_R for each of the temperatures studied along with the calculated values of ϵLk_2 at 26,000 cps, 39,000 cps and in the absence of ultrasound.

The graphs of conversion as a function of reciprocal space velocity illustrating all the data points and the calculated theoretical curves are illustrated in Figures 48 through 73. Considerable scattering of the data is apparent at 650°F. because of the low conversions obtained at that temperature and the accompanying analytical errors.

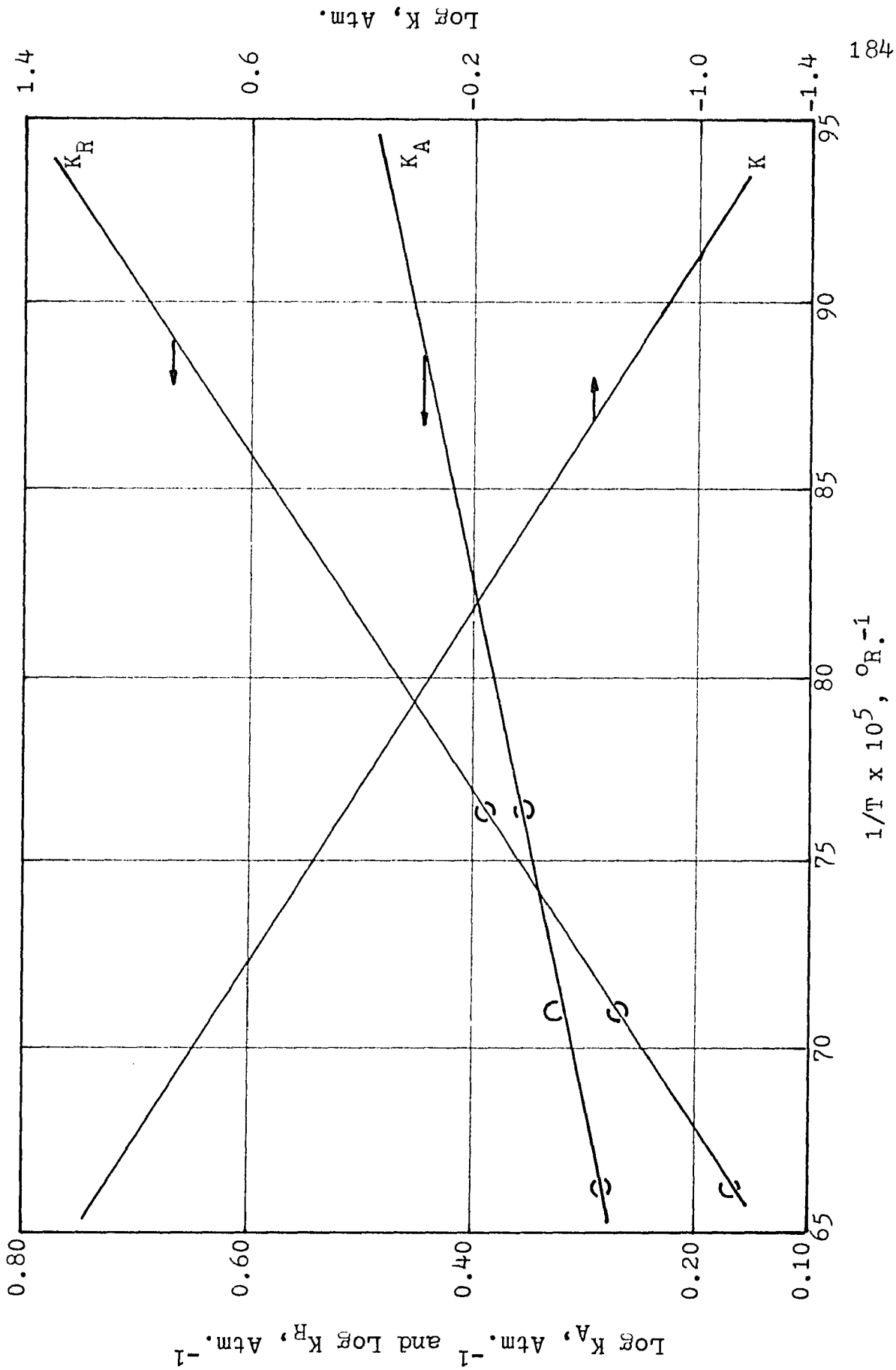

FIGURE 47

REACTION CONSTANTS vs. TEMPERATURE

TABLE 10

SUMMARY OF VALUES OF REACTION RATE CONSTANTS

T °F.	Power	K Atm.	K_A $\frac{1}{Atm.}$	K_R $\frac{1}{Atm.}$	$\epsilon Lk_2 \times 10^5$, $\frac{gm\ moles}{gm\ cat\text{-}sec.}$		
					No Ultrasound	26,000 cps	39,000 cps
650	full	0.121	2.830	4.908	0.317	0.479	0.813
700	full	0.270	2.657	4.032	0.449	0.523	1.082
750	full	0.561	2.510	3.368	0.875	1.009	1.591
800	full	1.100	2.381	2.854	1.219	1.385	1.794
850	full	2.050	1.267	2.448	2.489	2.830	2.904
850	half	2.050	2.267	2.448	2.489	2.509	2.704
900	full	3.654	2.167	2.124	2.499	2.470	3.054
950	full	6.235	2.078	1.863	2.341	2.403	2.614
1000	full	10.27	1.998	1.647	3.470	3.470	3.360

FIGURE 48

CONVERSION vs. W/F

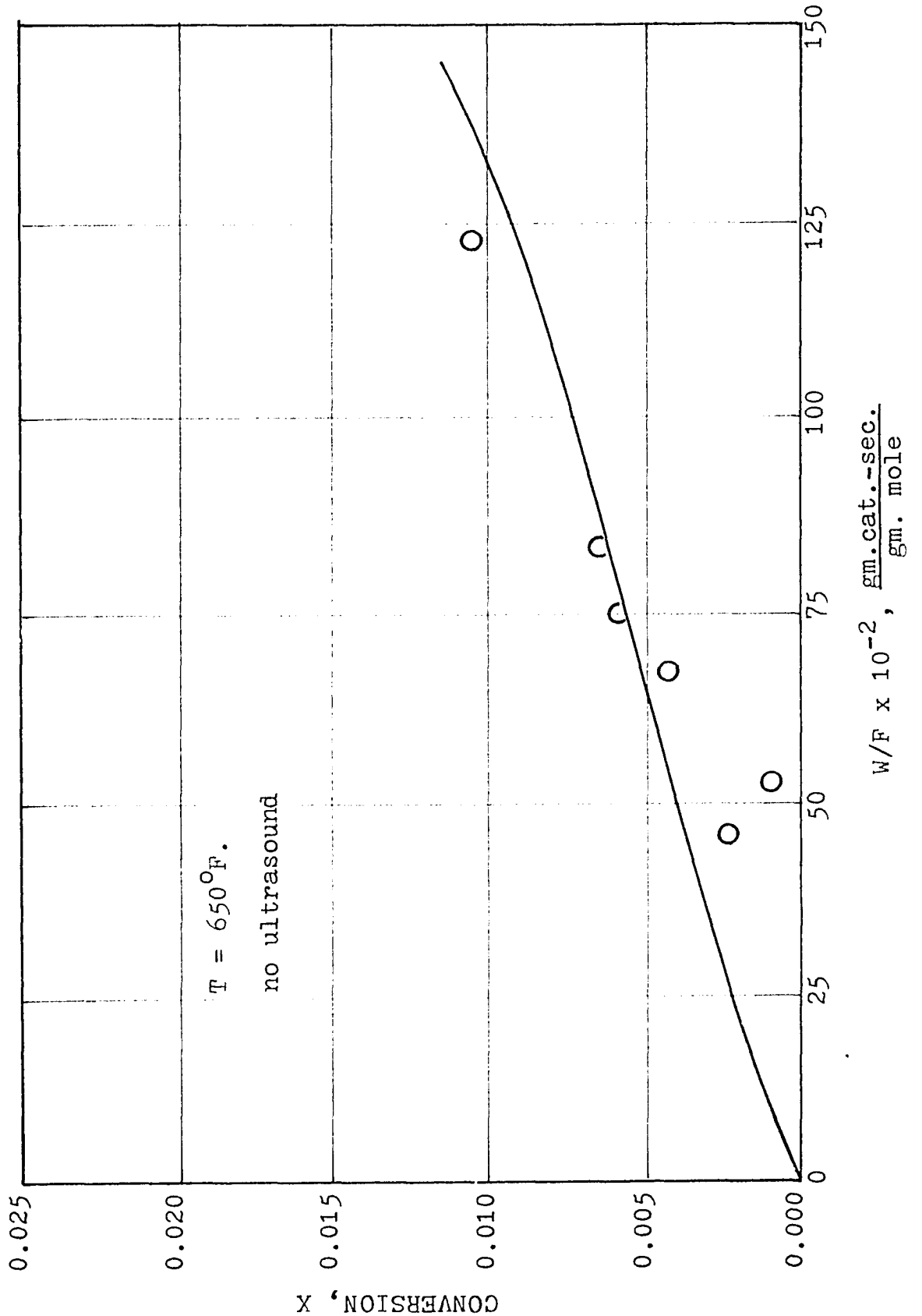

FIGURE 49

CONVERSION vs. W/F

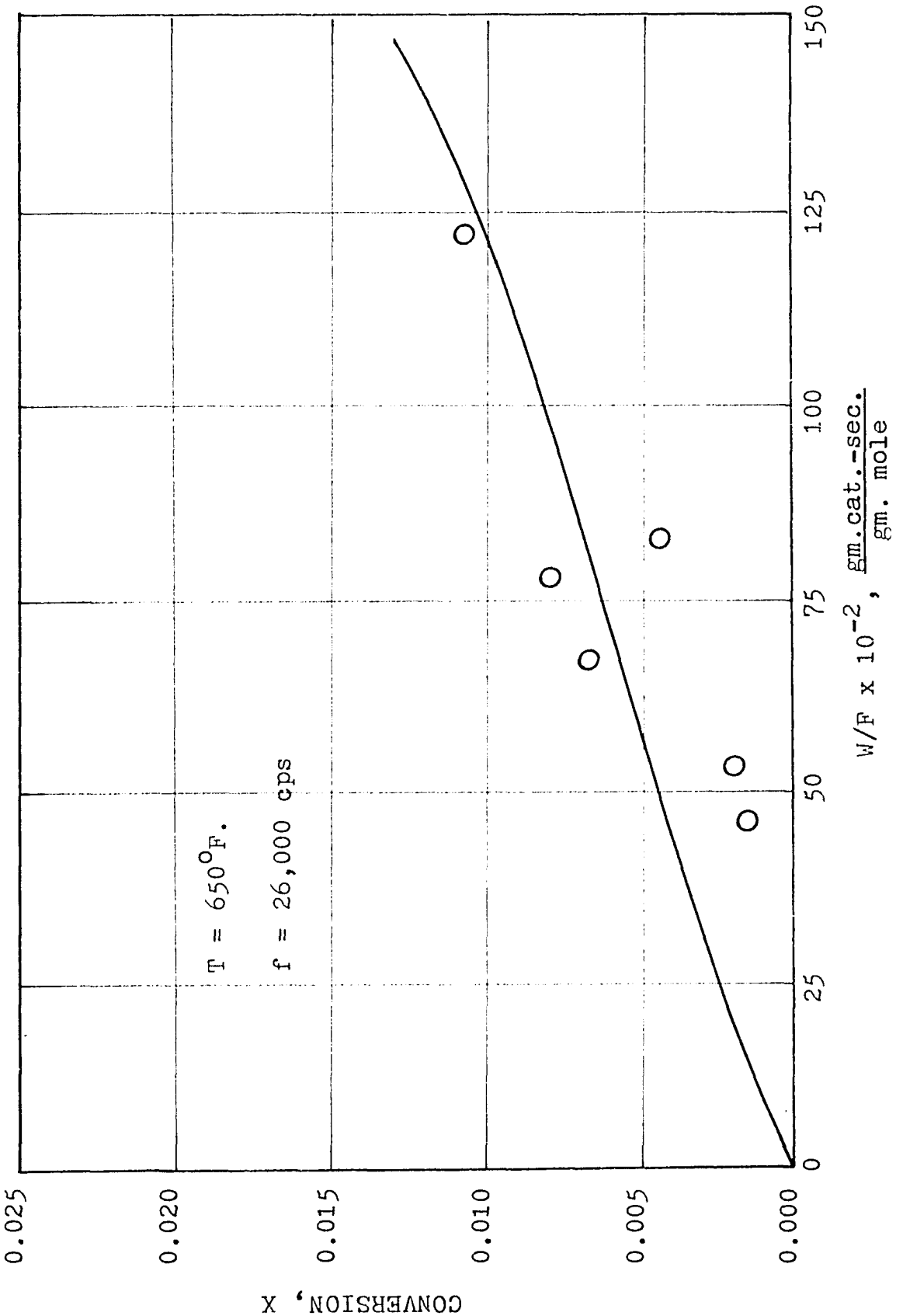

FIGURE 50

CONVERSION vs. W/F

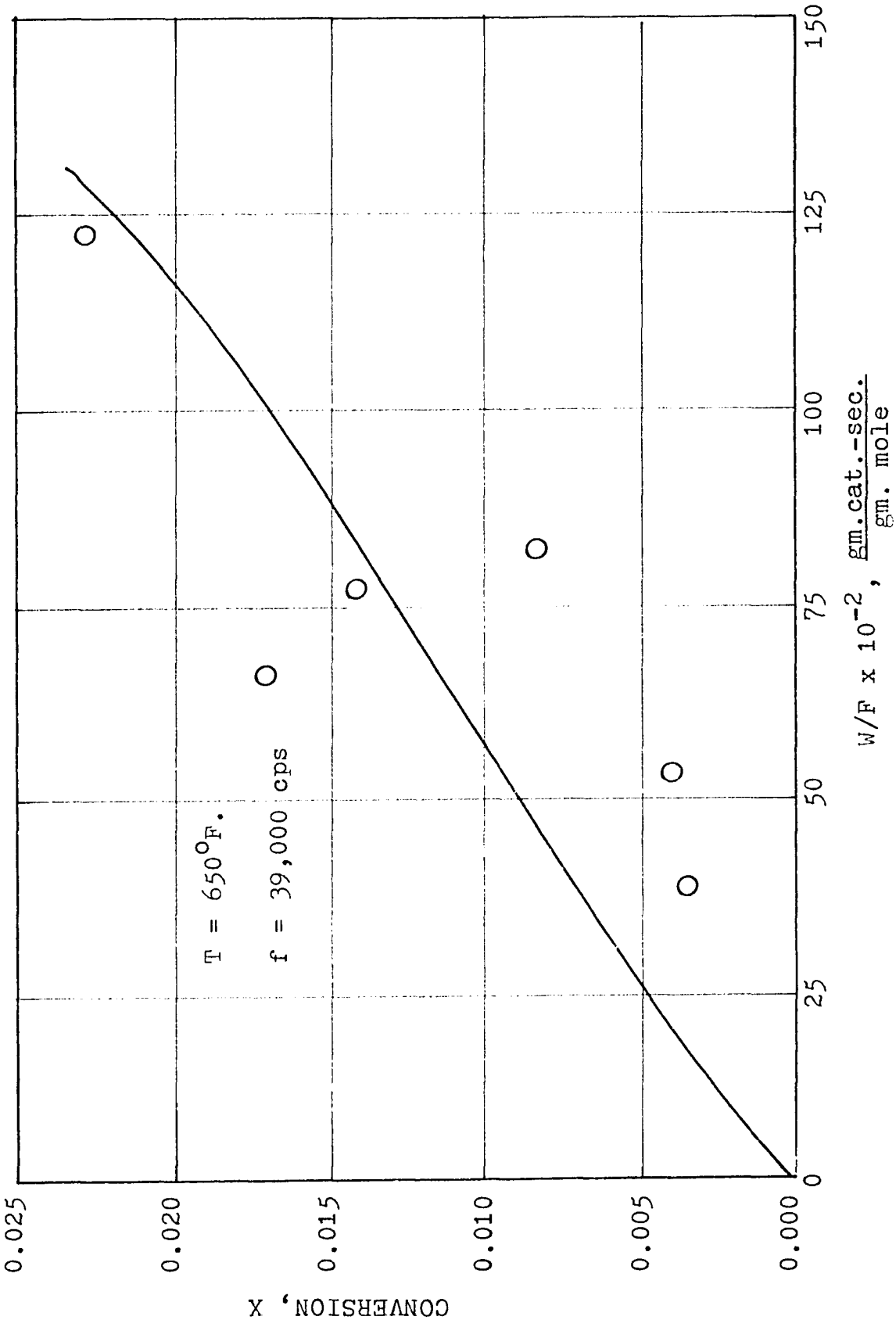

FIGURE 51

CONVERSION vs. W/F

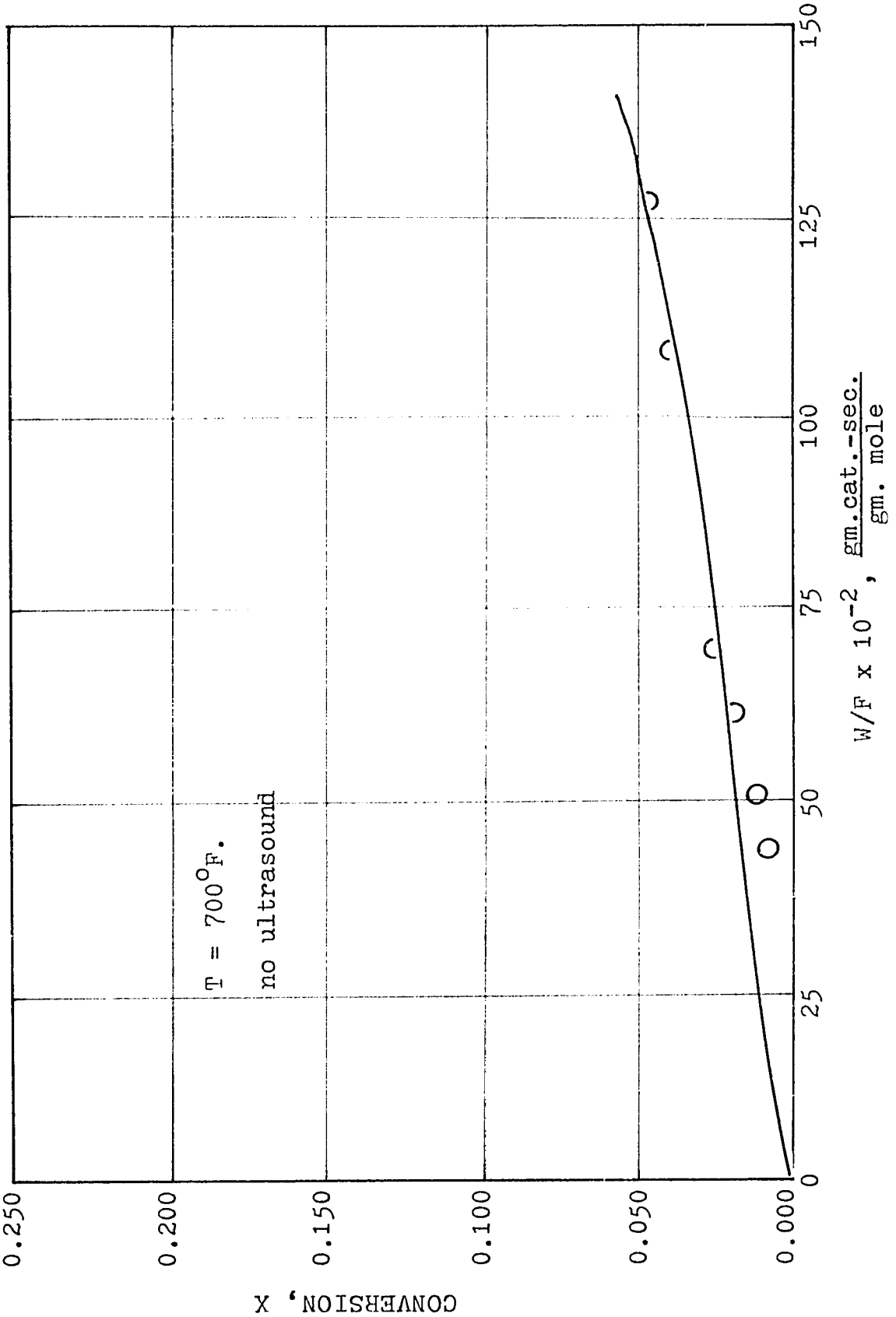

FIGURE 52

CONVERSION vs. W/F

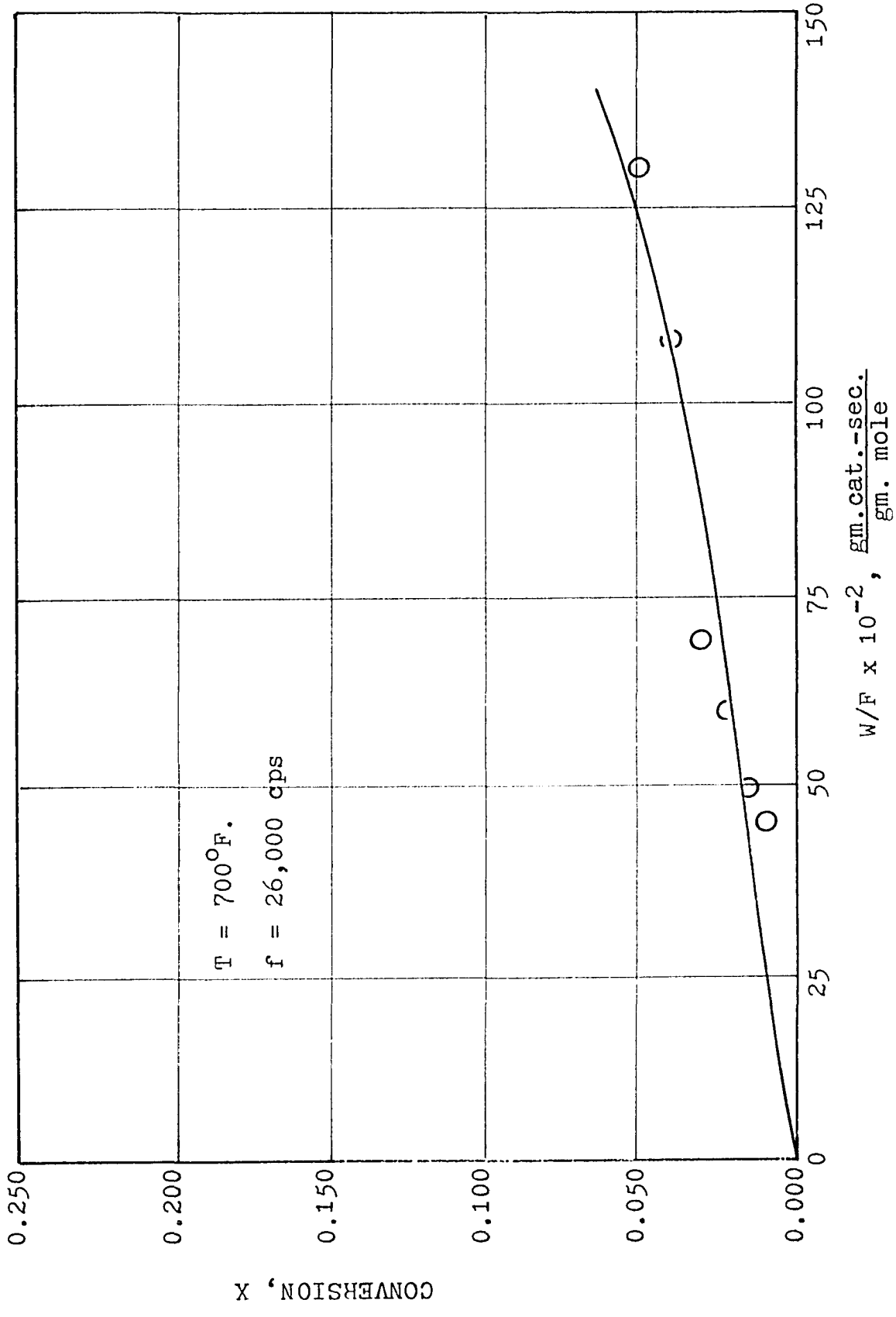

FIGURE 53

CONVERSION vs. W/F

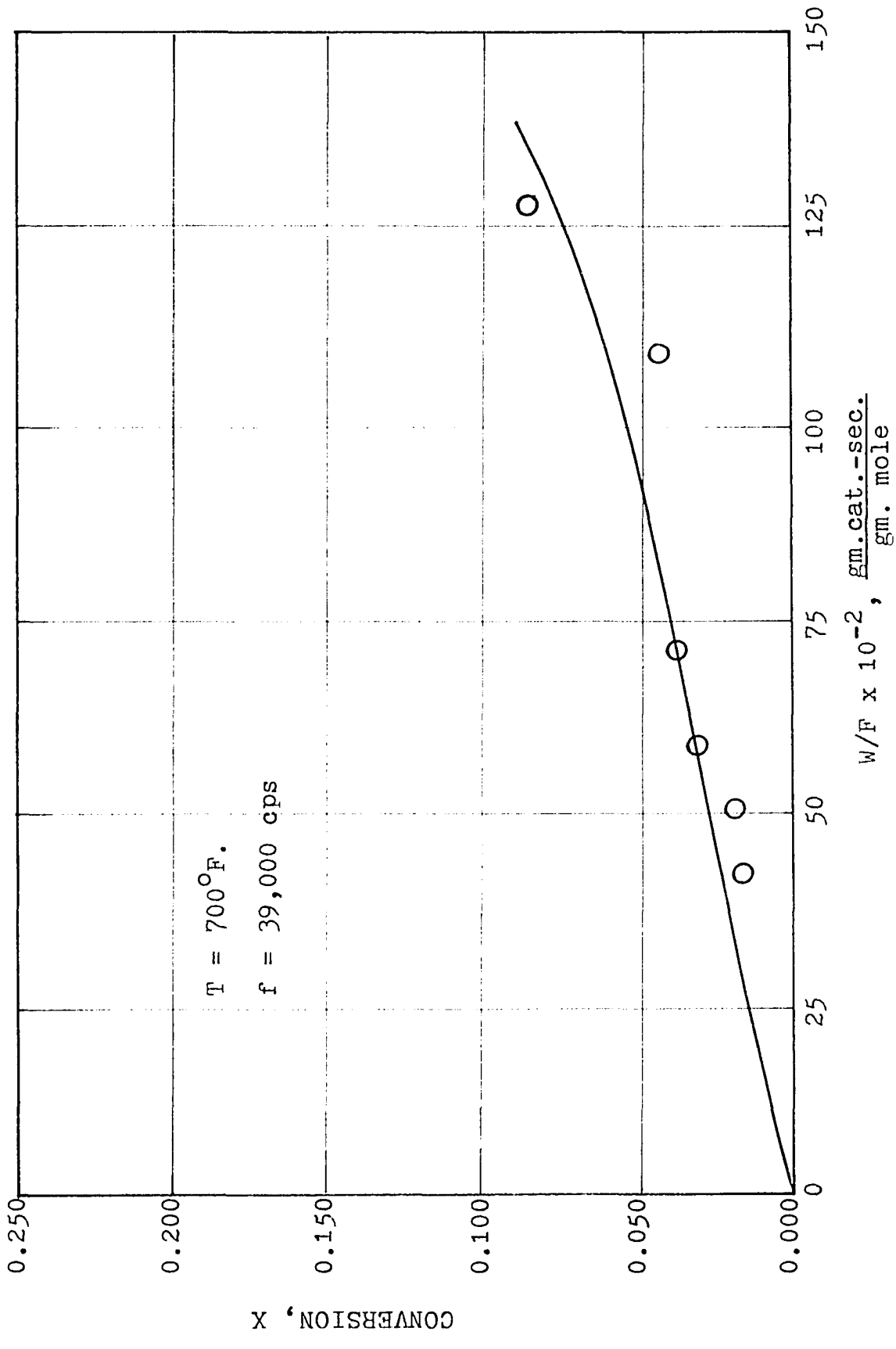

FIGURE 54

CONVERSION vs. W/F

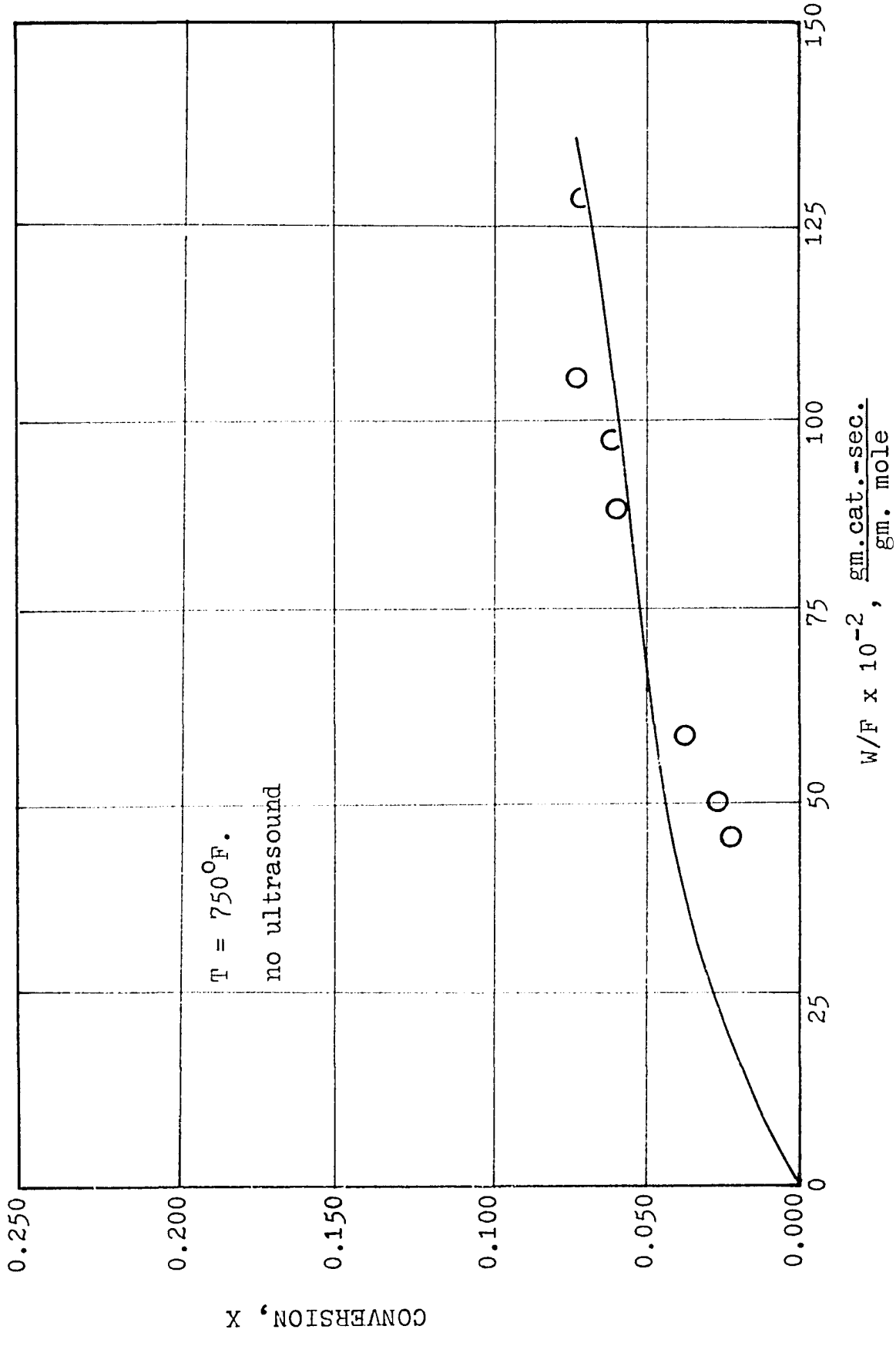

FIGURE 55

CONVERSION vs. W/F

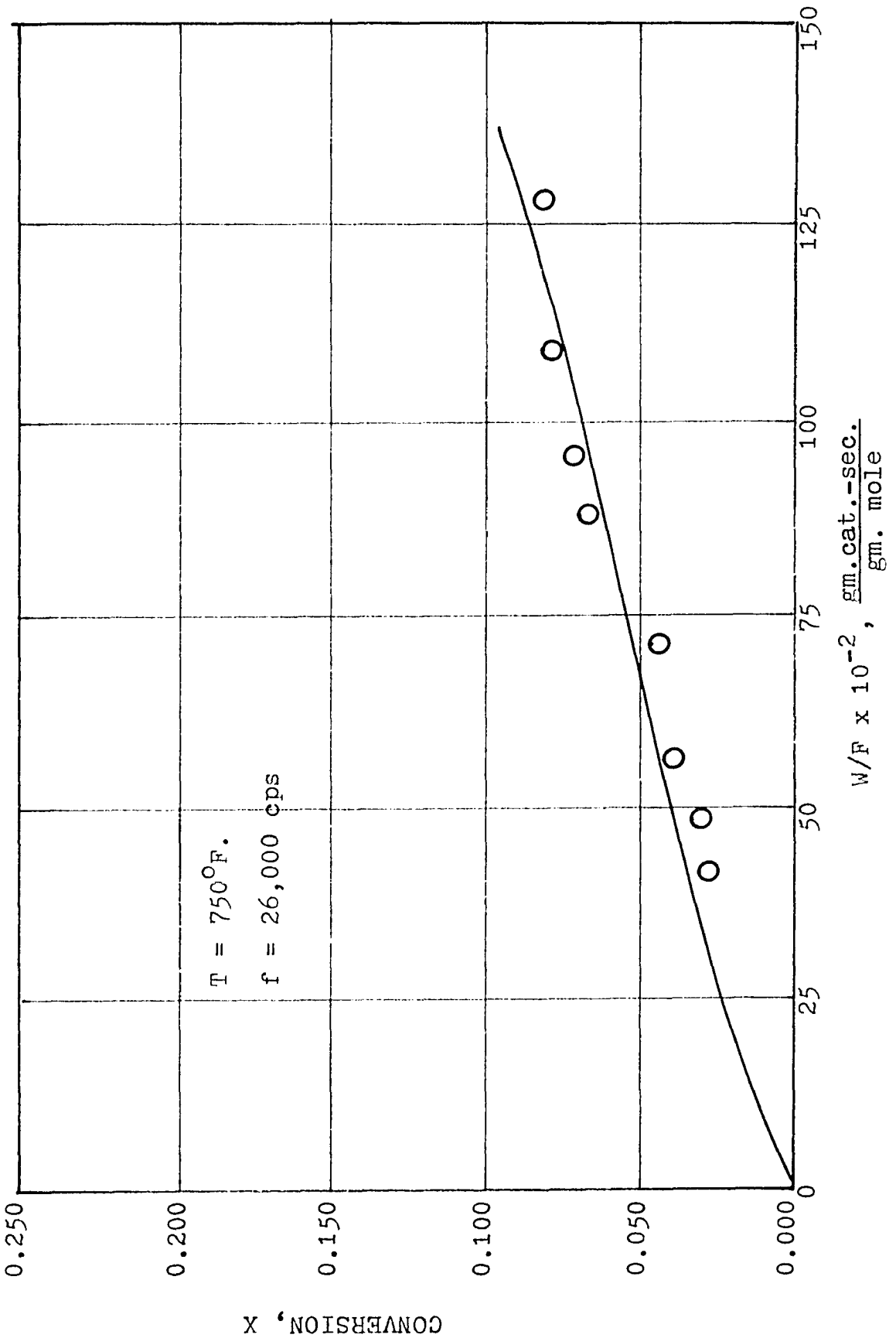

FIGURE 56
CONVERSION vs. W/F

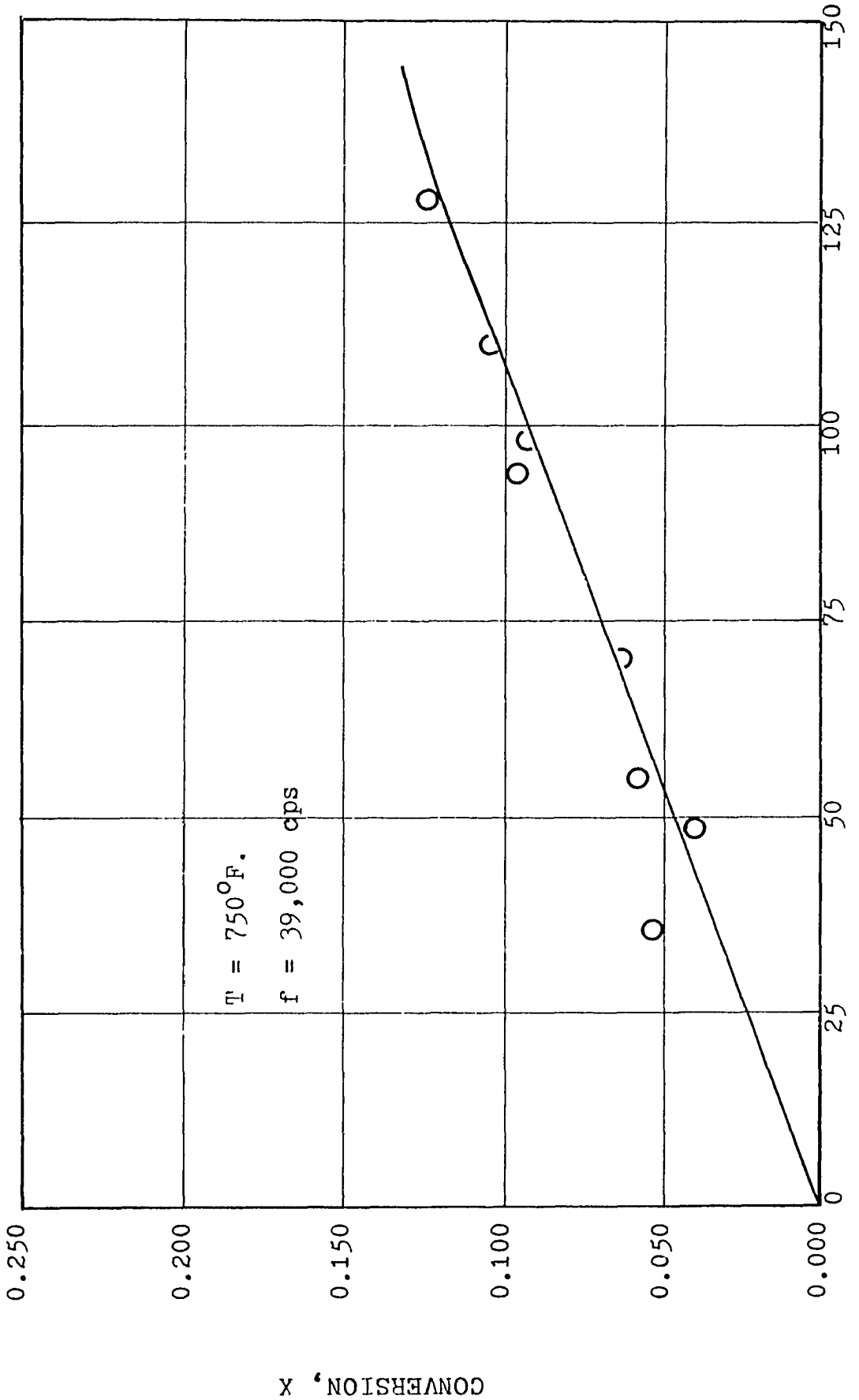

FIGURE 57

CONVERSION vs. W/F

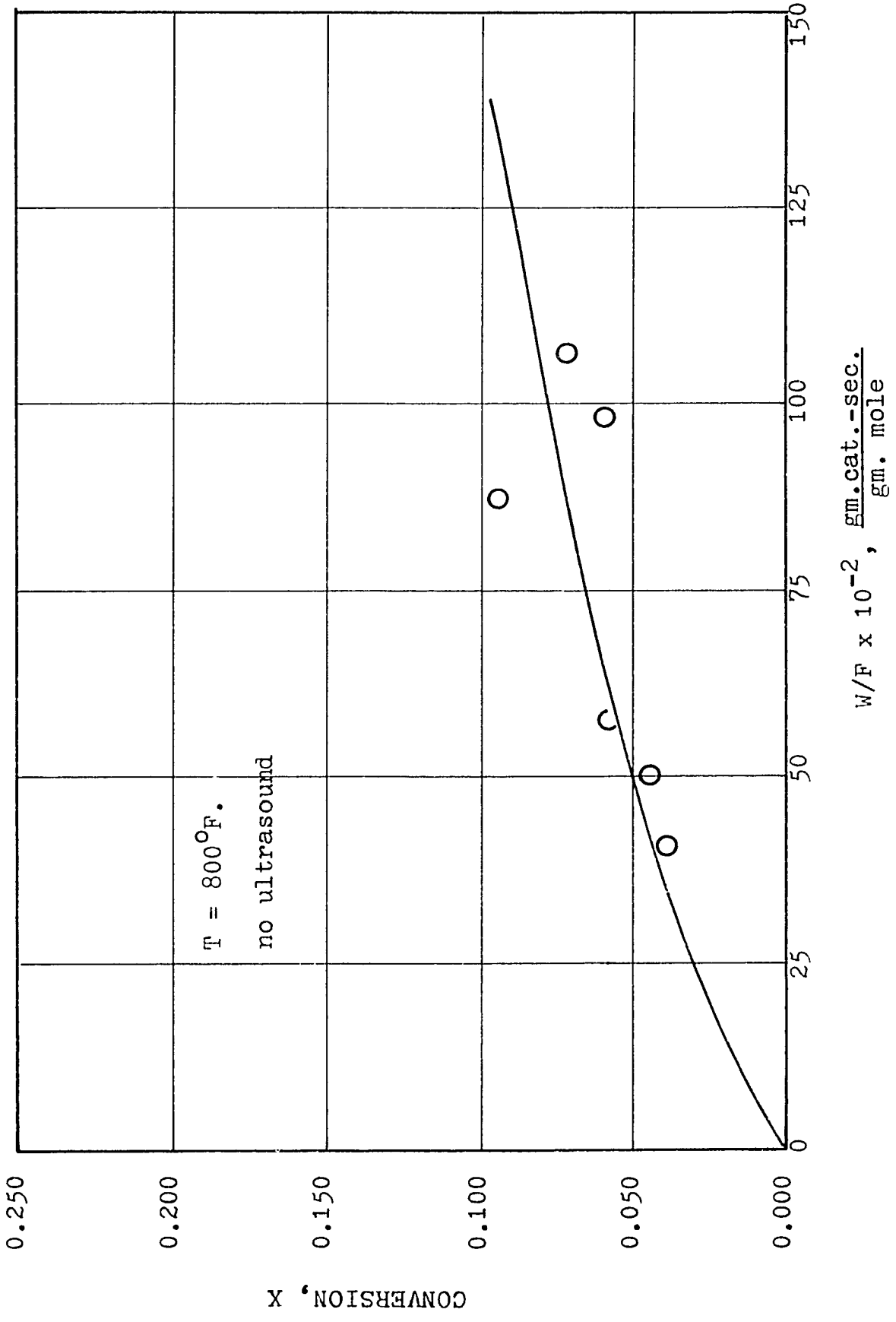

FIGURE 58

CONVERSION vs. W/F

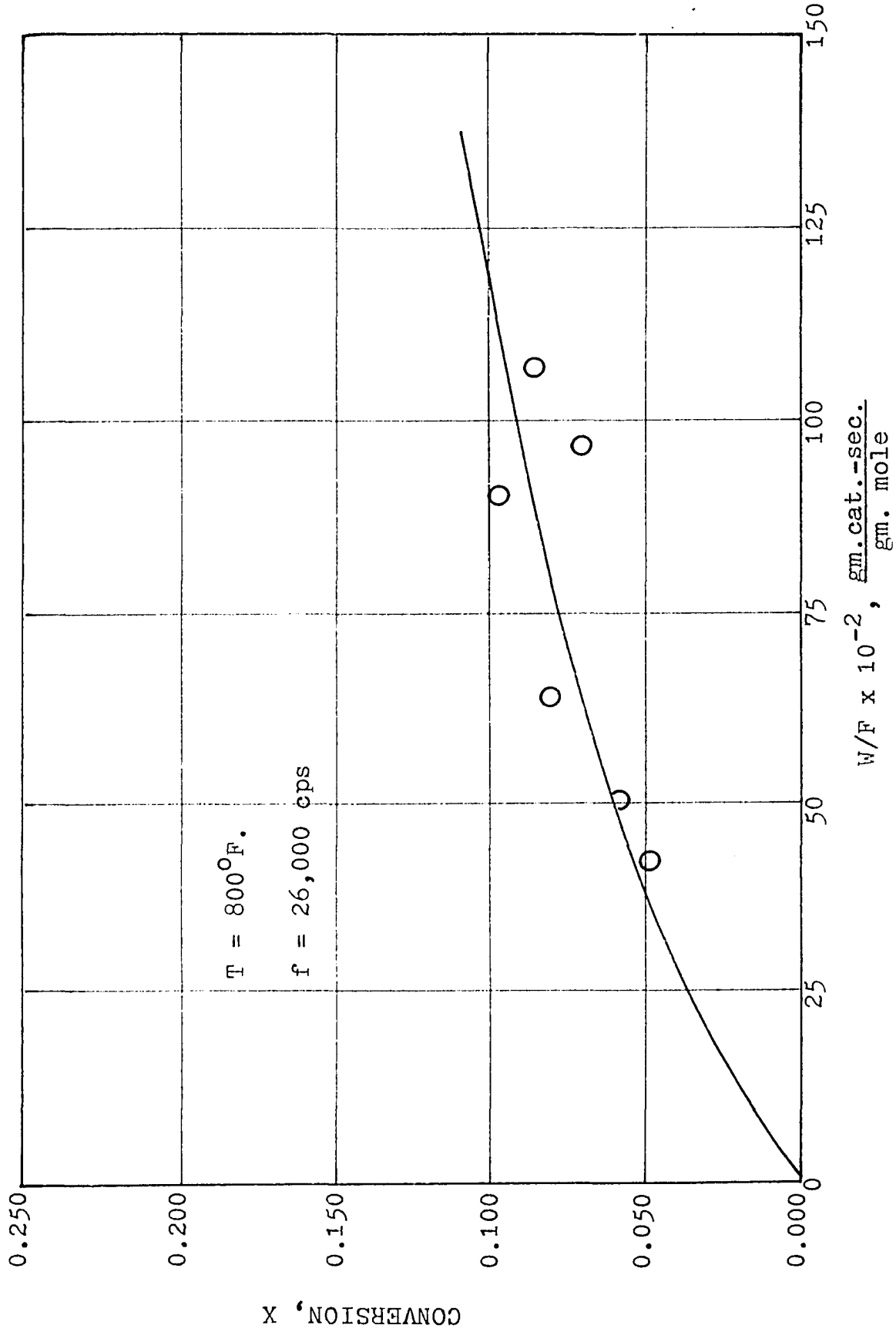

FIGURE 59

CONVERSION vs. W/F

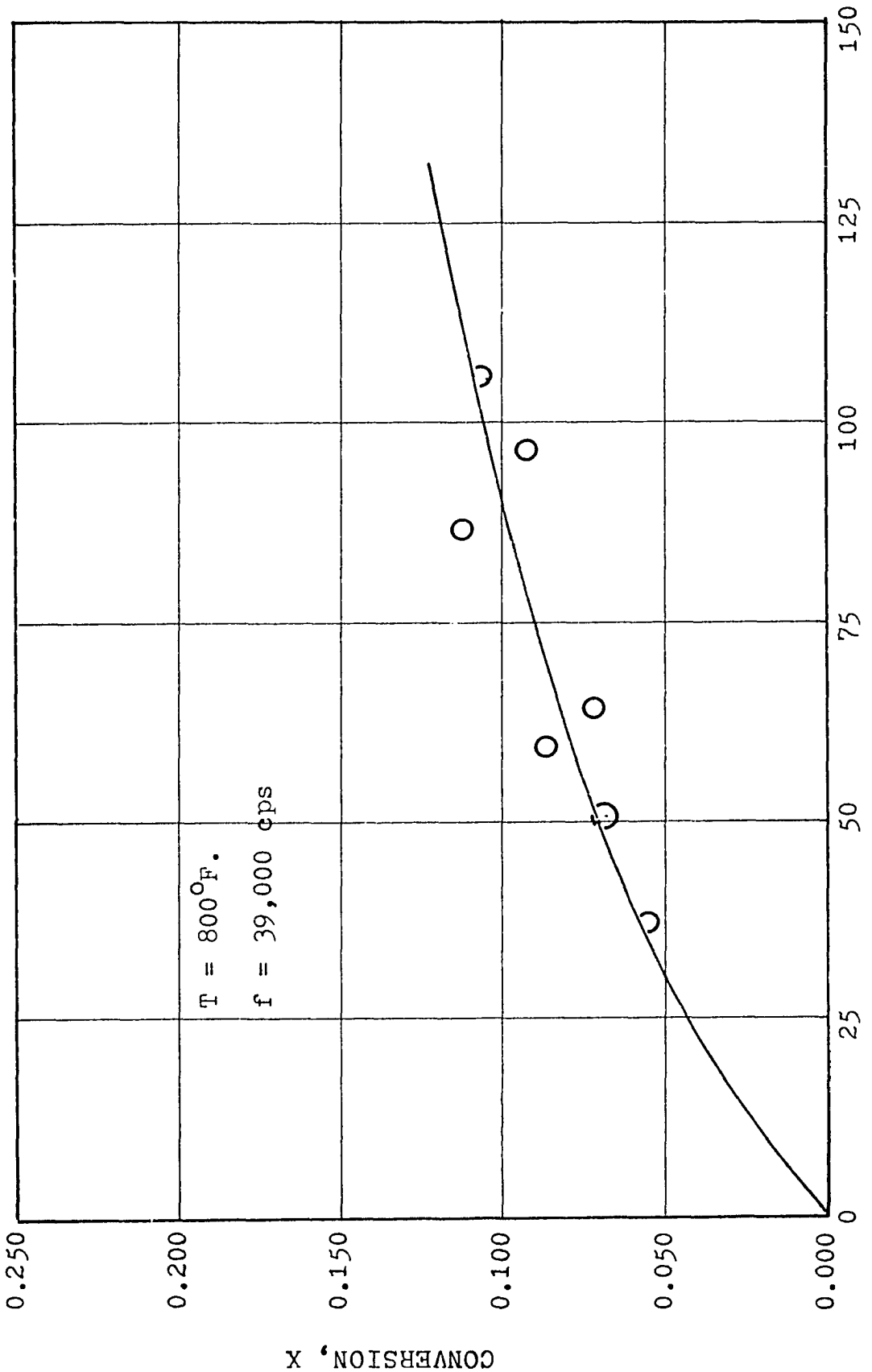

FIGURE 60

CONVERSION vs. W/F

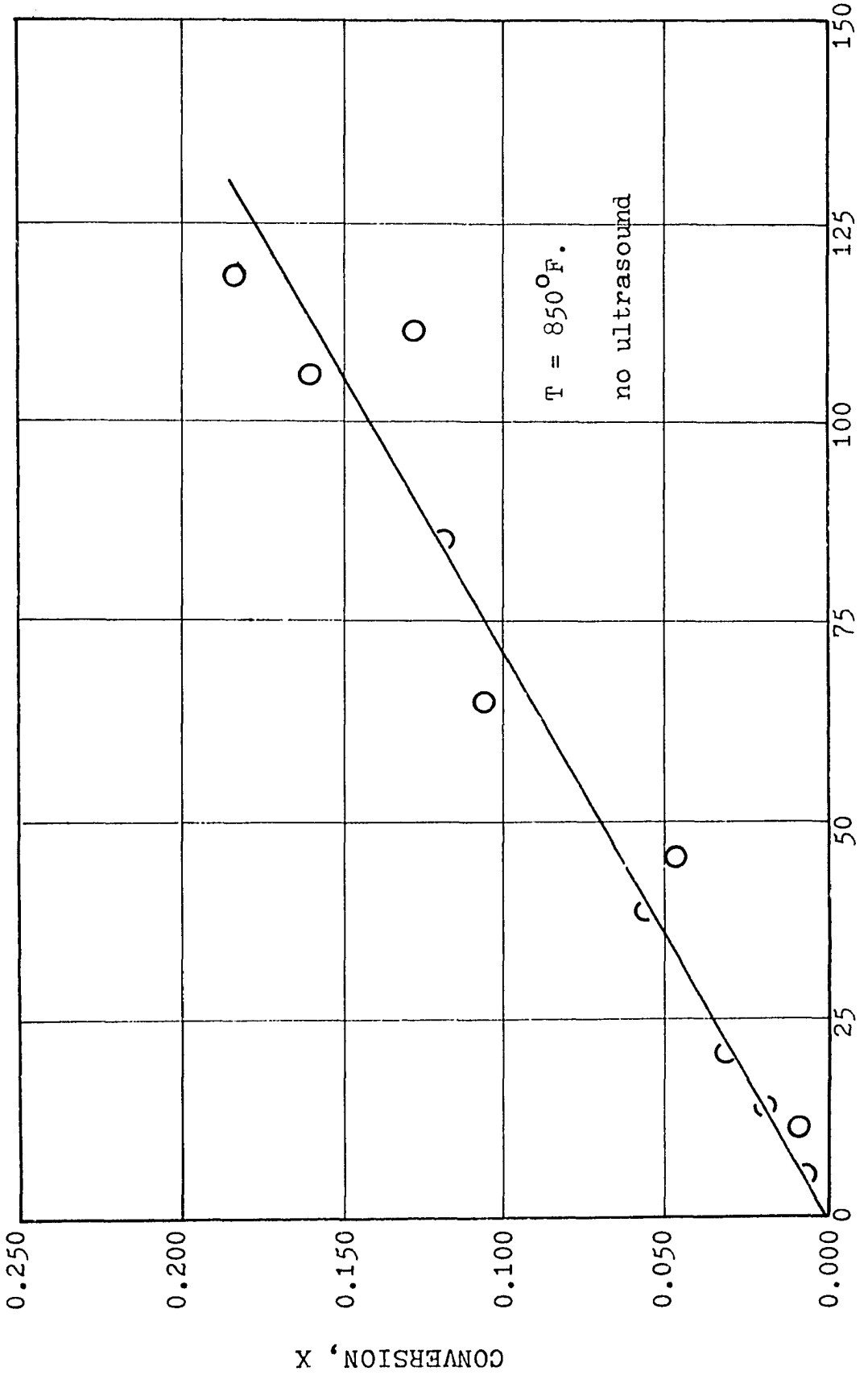

FIGURE 61

CONVERSION vs. W/F

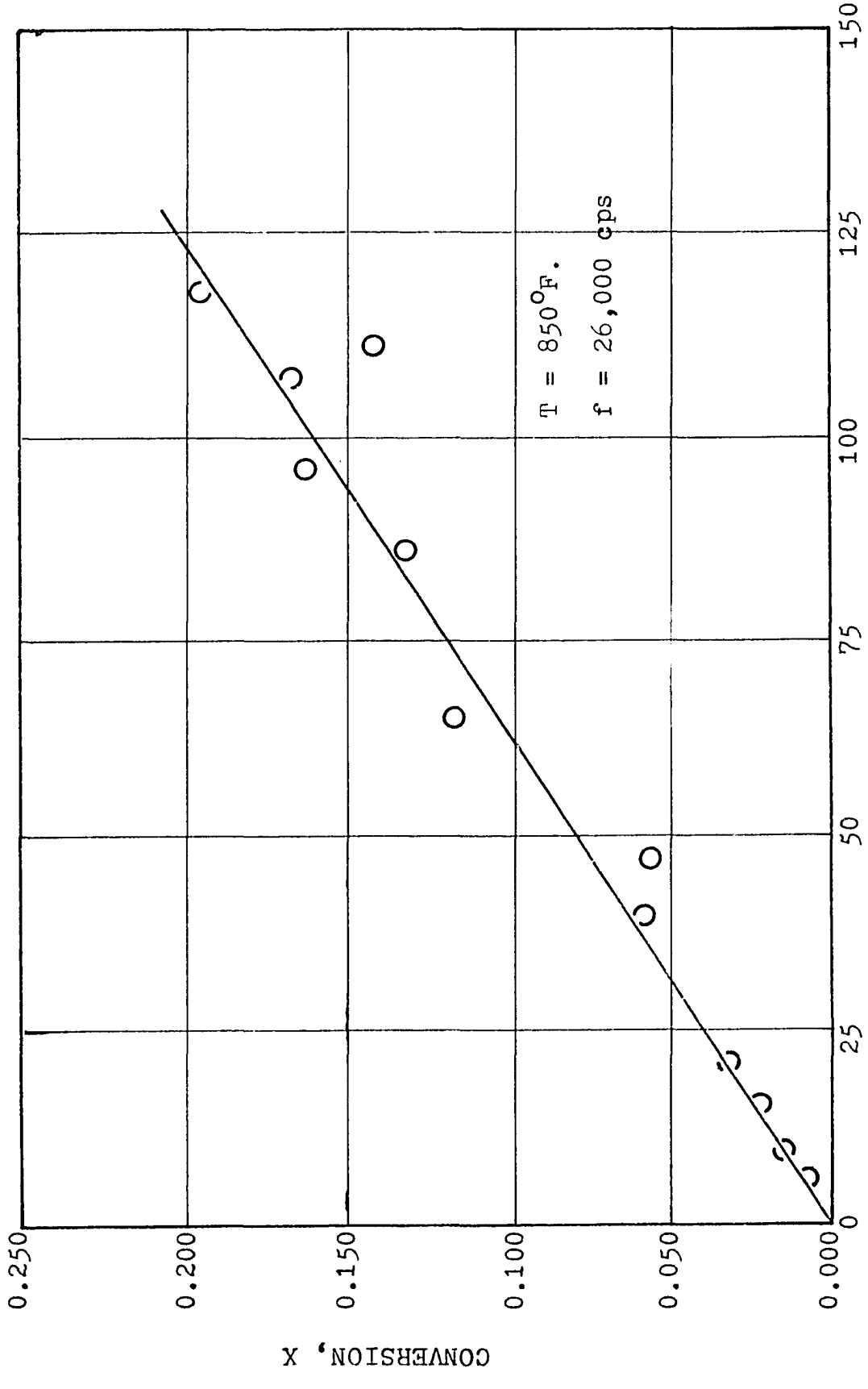

FIGURE 62

CONVERSION vs. W/F

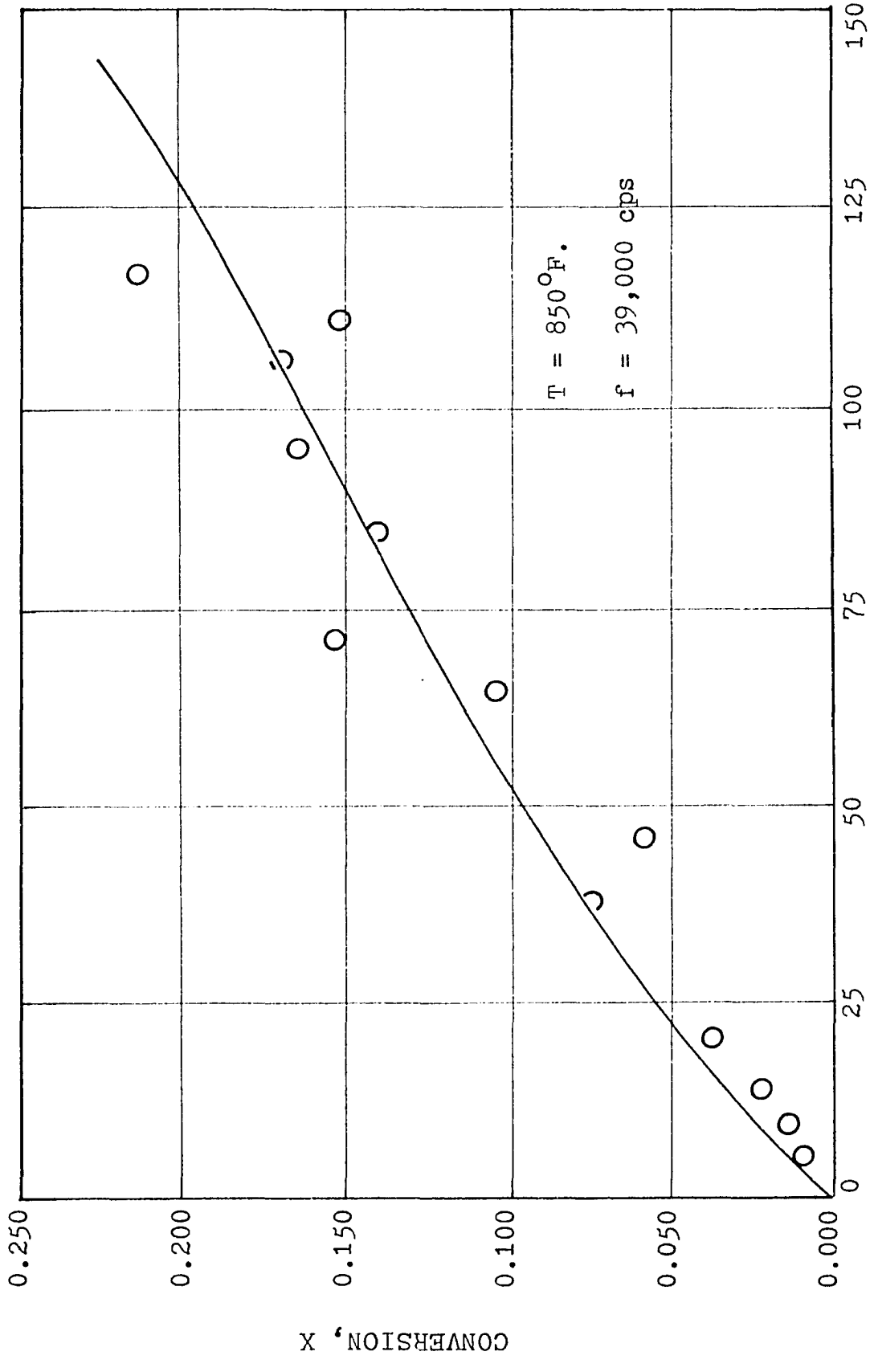

FIGURE 63

CONVERSION vs. W/F

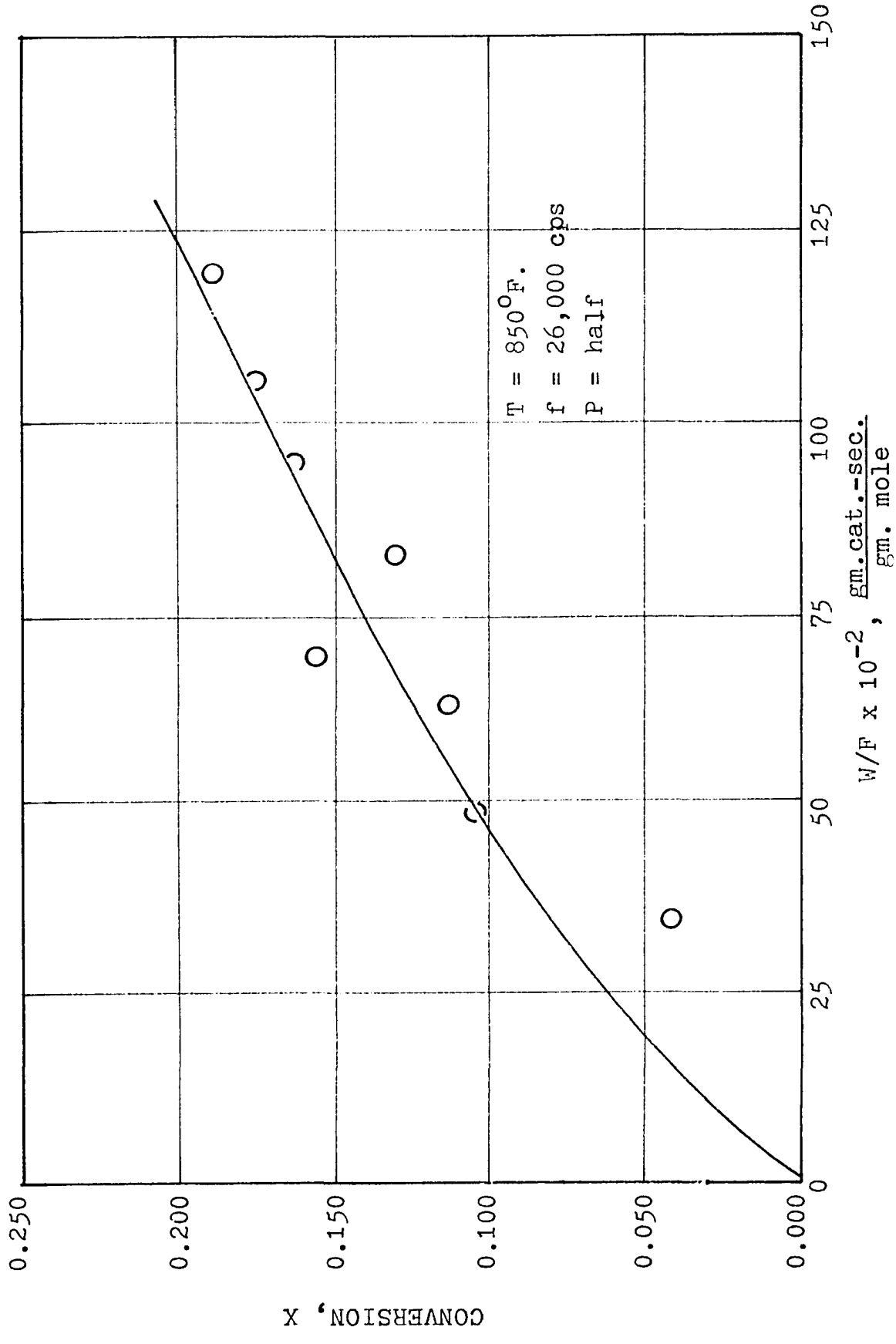

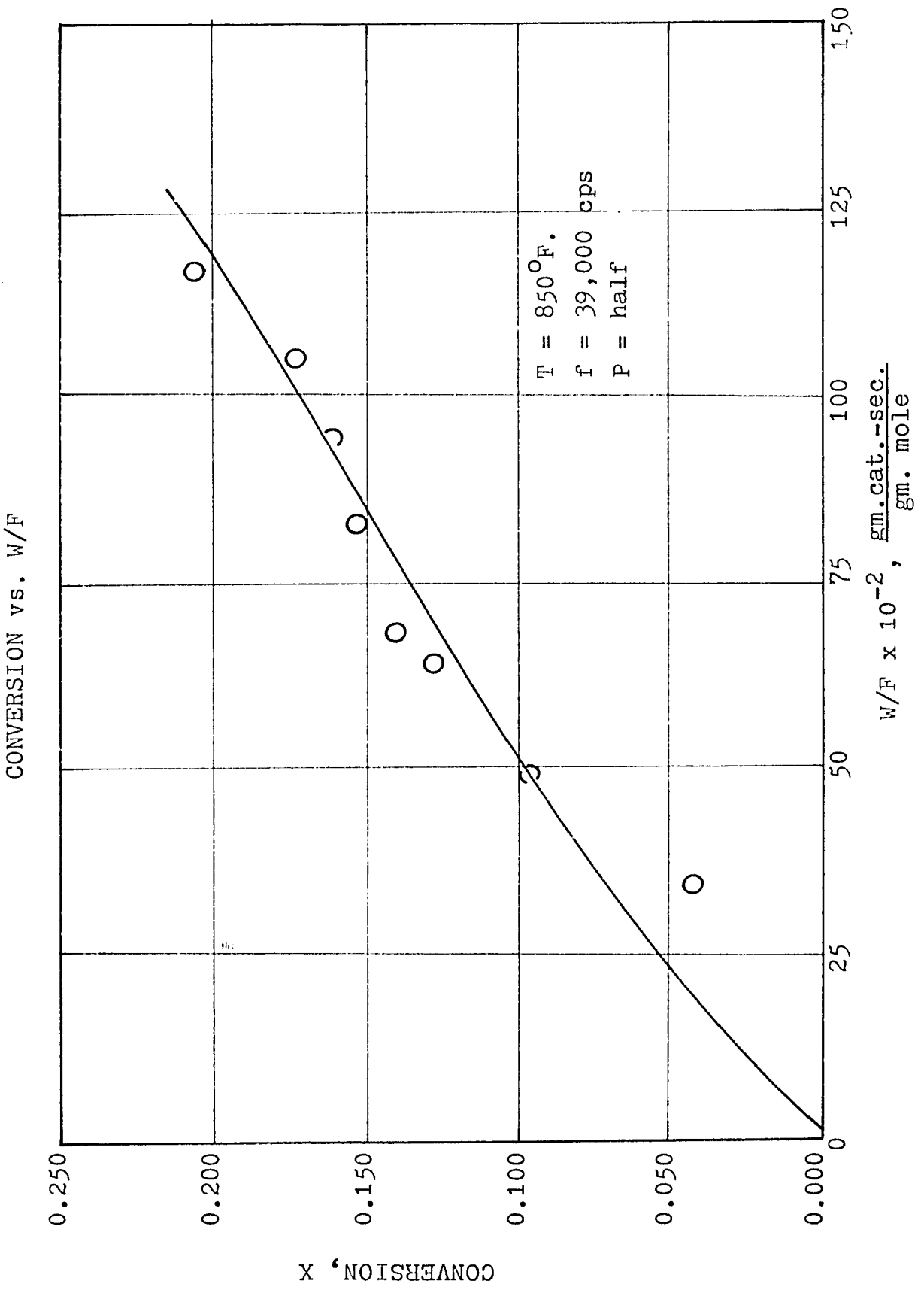

FIGURE 64

FIGURE 65

CONVERSION vs. W/F

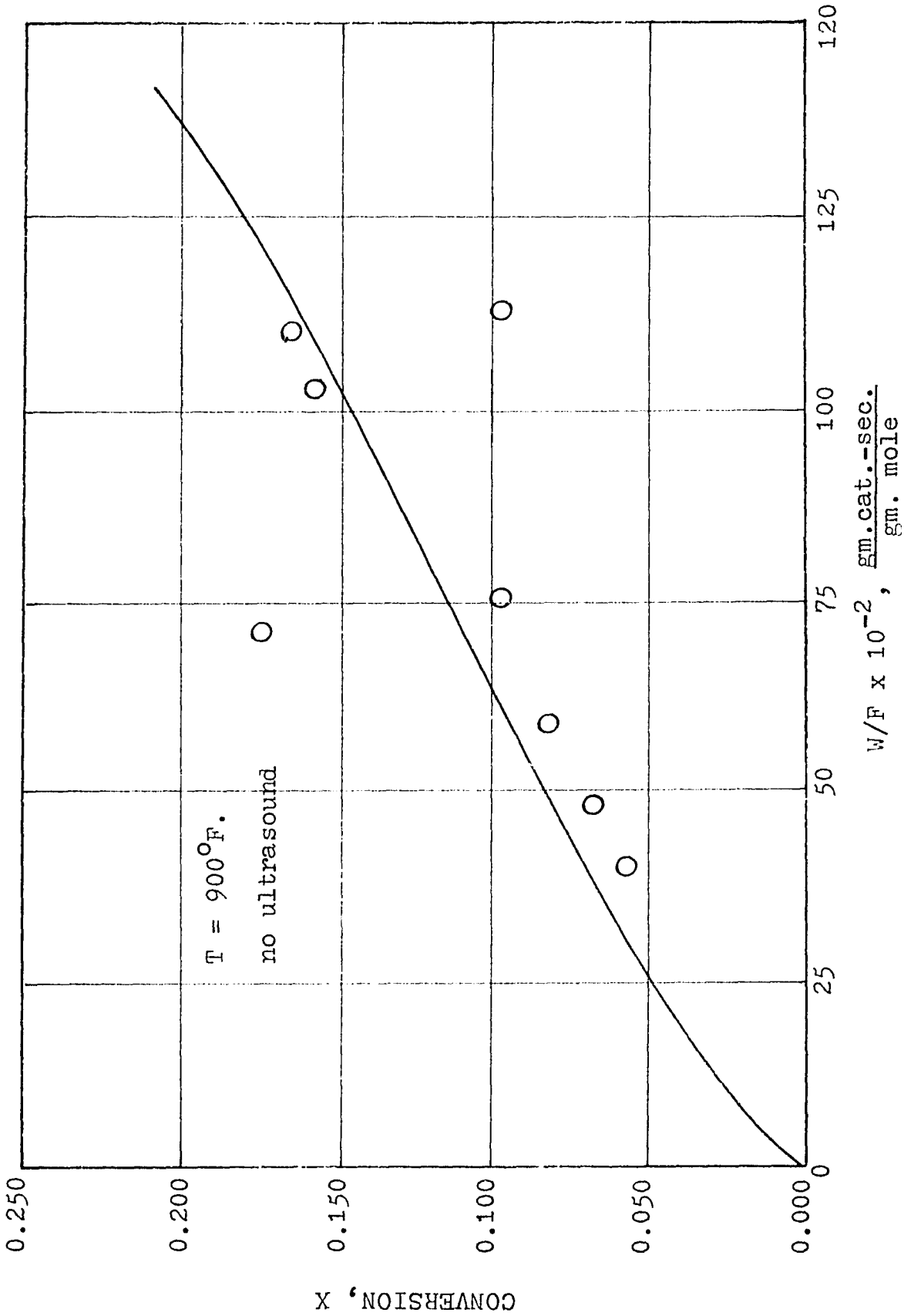

FIGURE 66

CONVERSION vs. W/F

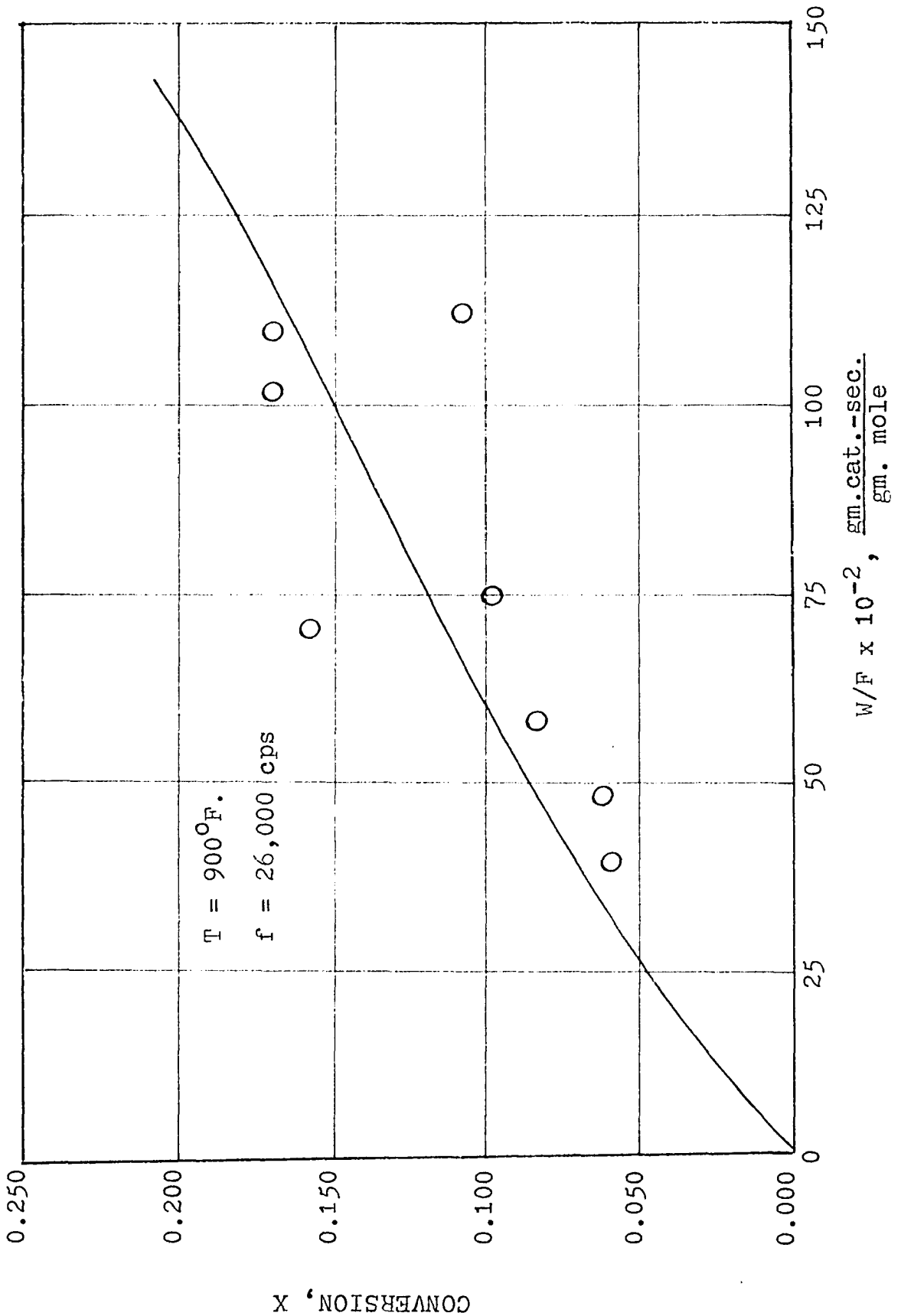

FIGURE 67

CONVERSION vs. W/F

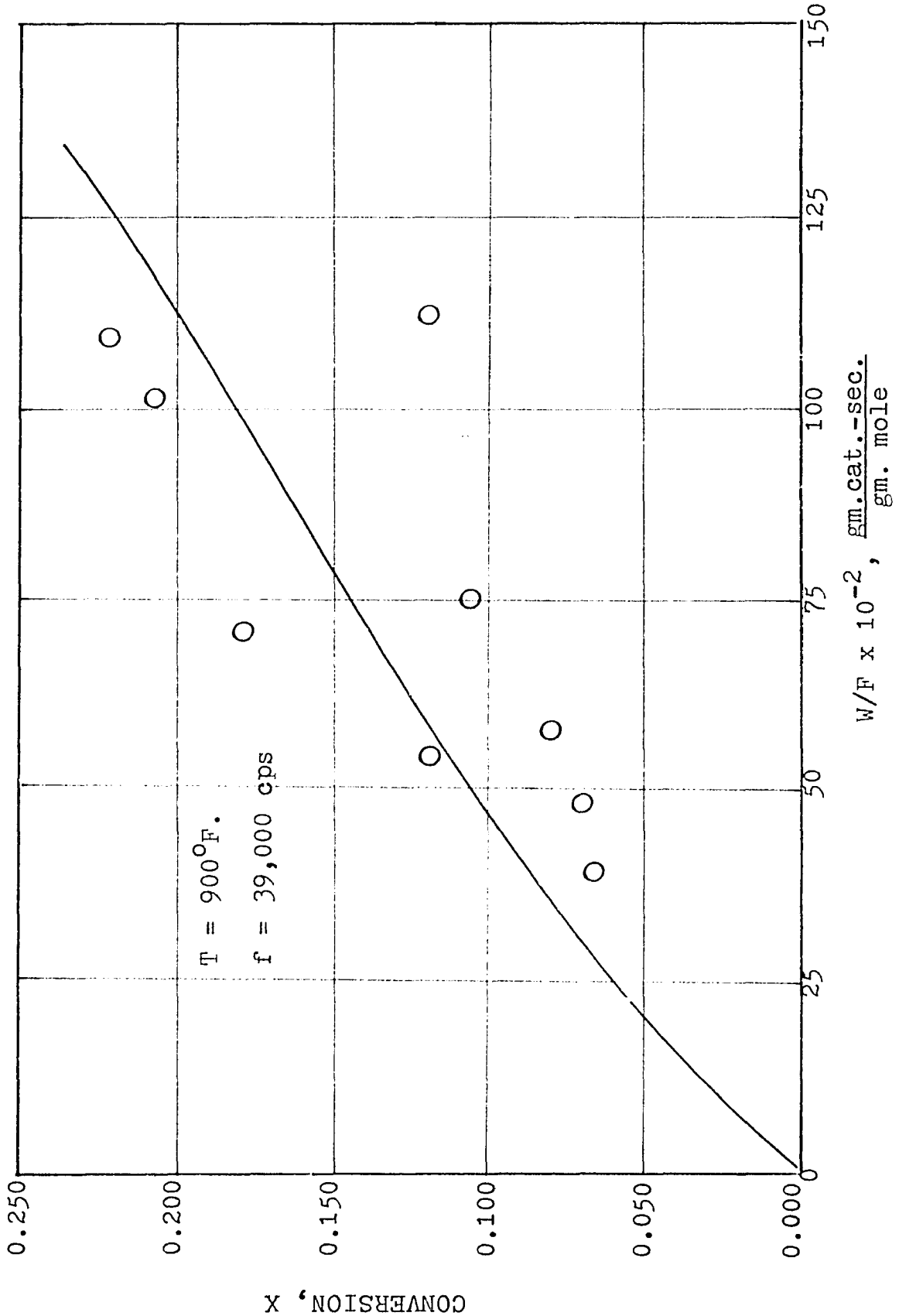

FIGURE 68

CONVERSION vs. W/F

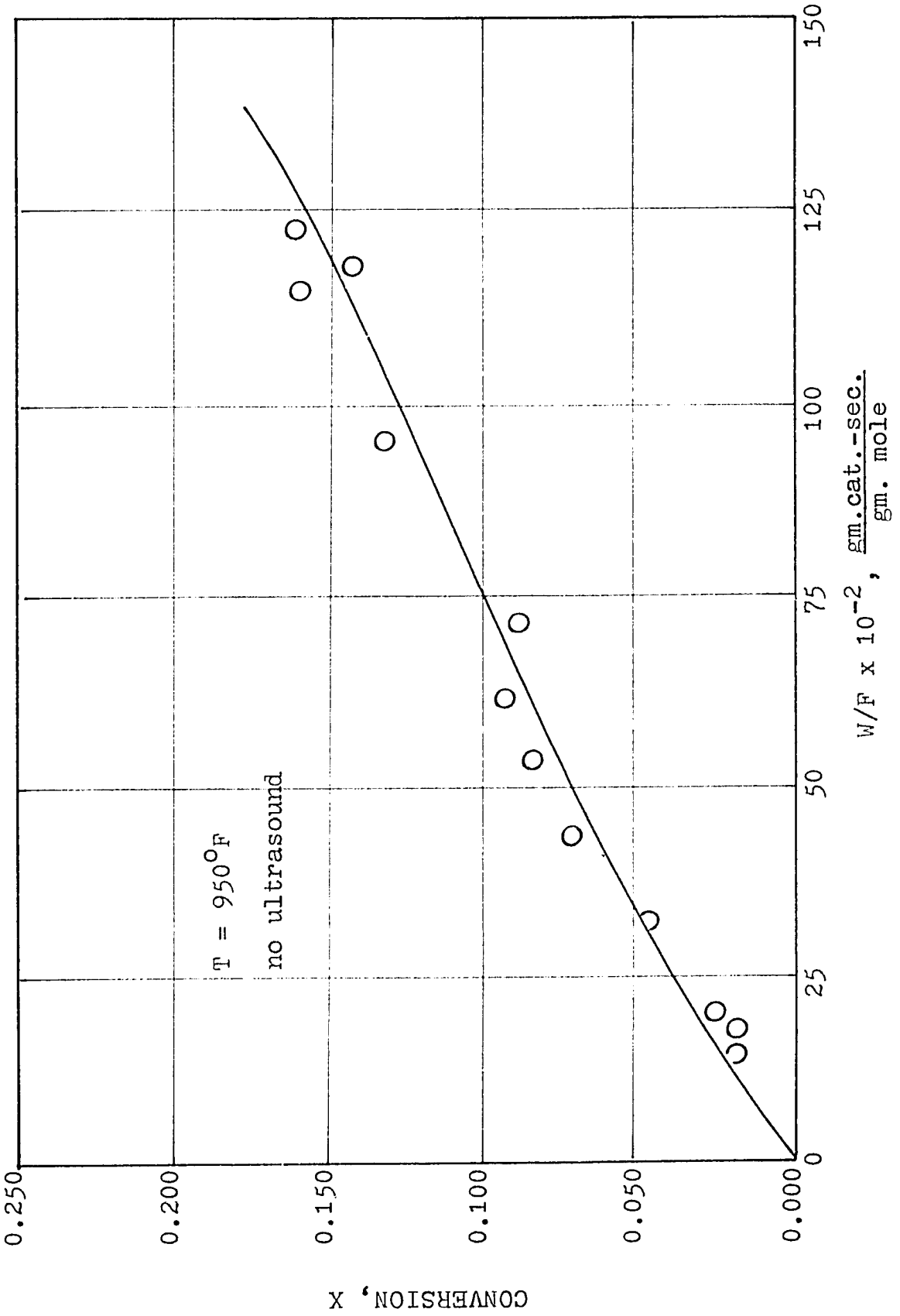

FIGURE 69

CONVERSION vs. W/F

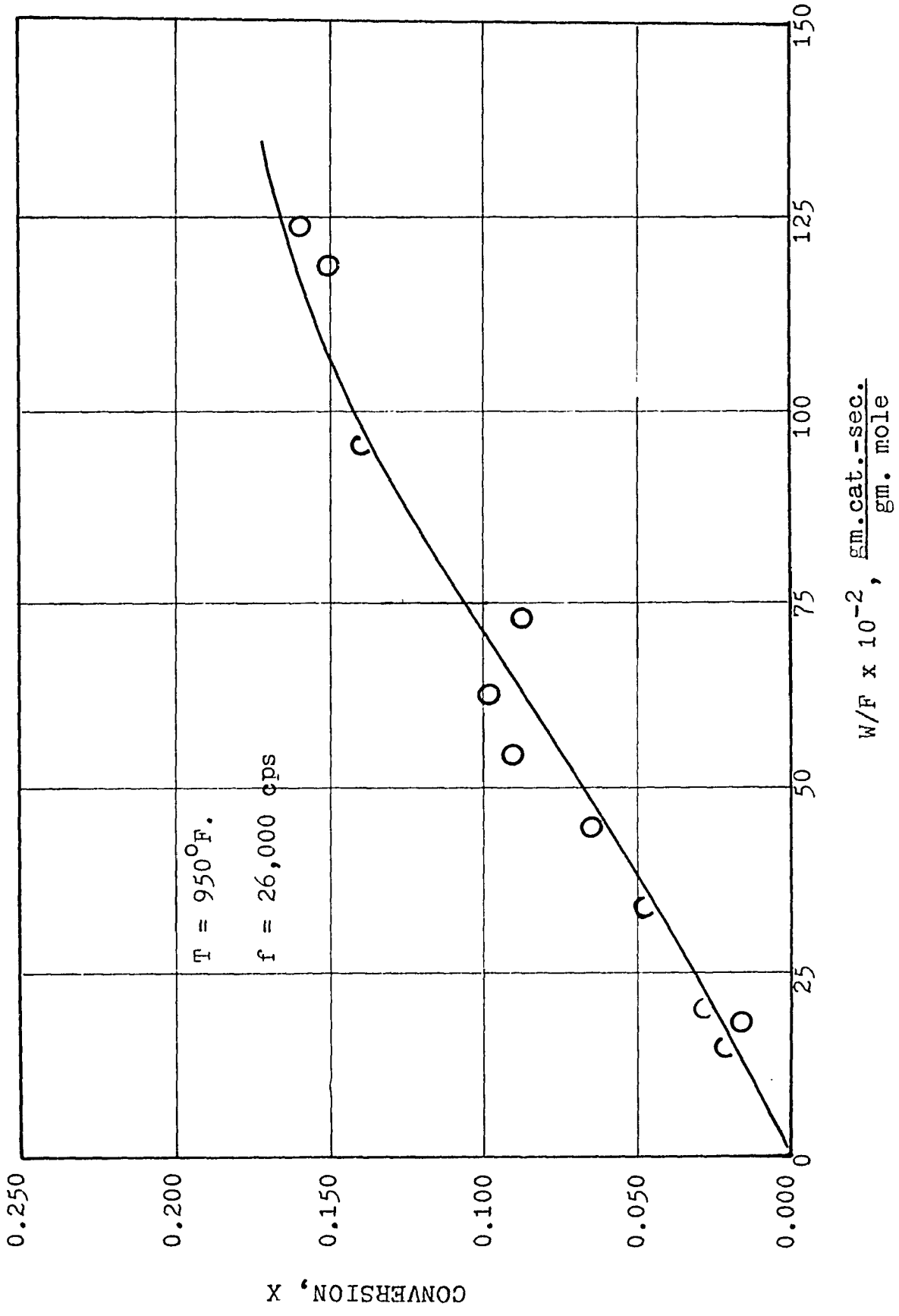

FIGURE 70

CONVERSION vs. W/F

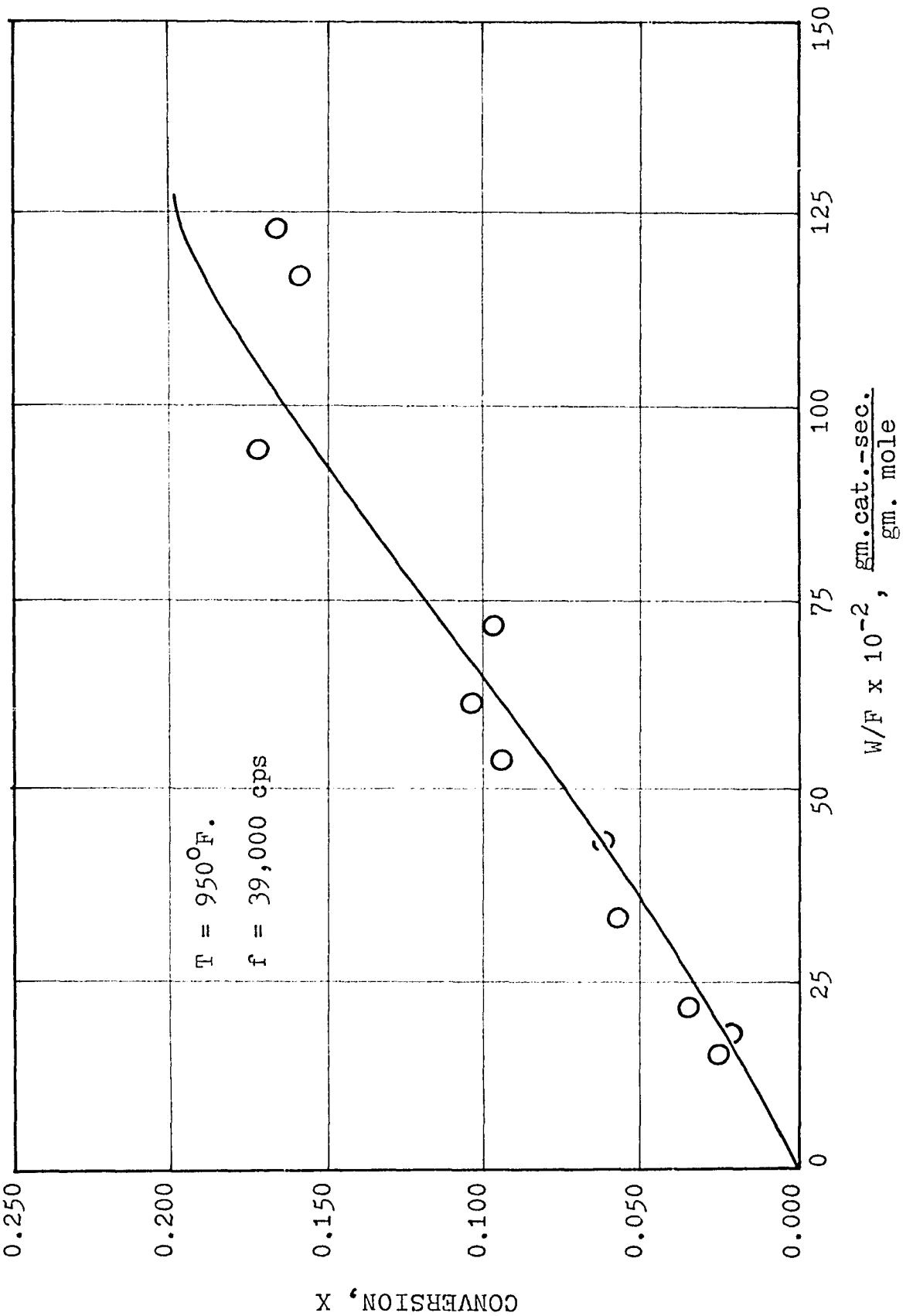

FIGURE 71

CONVERSION vs. W/F

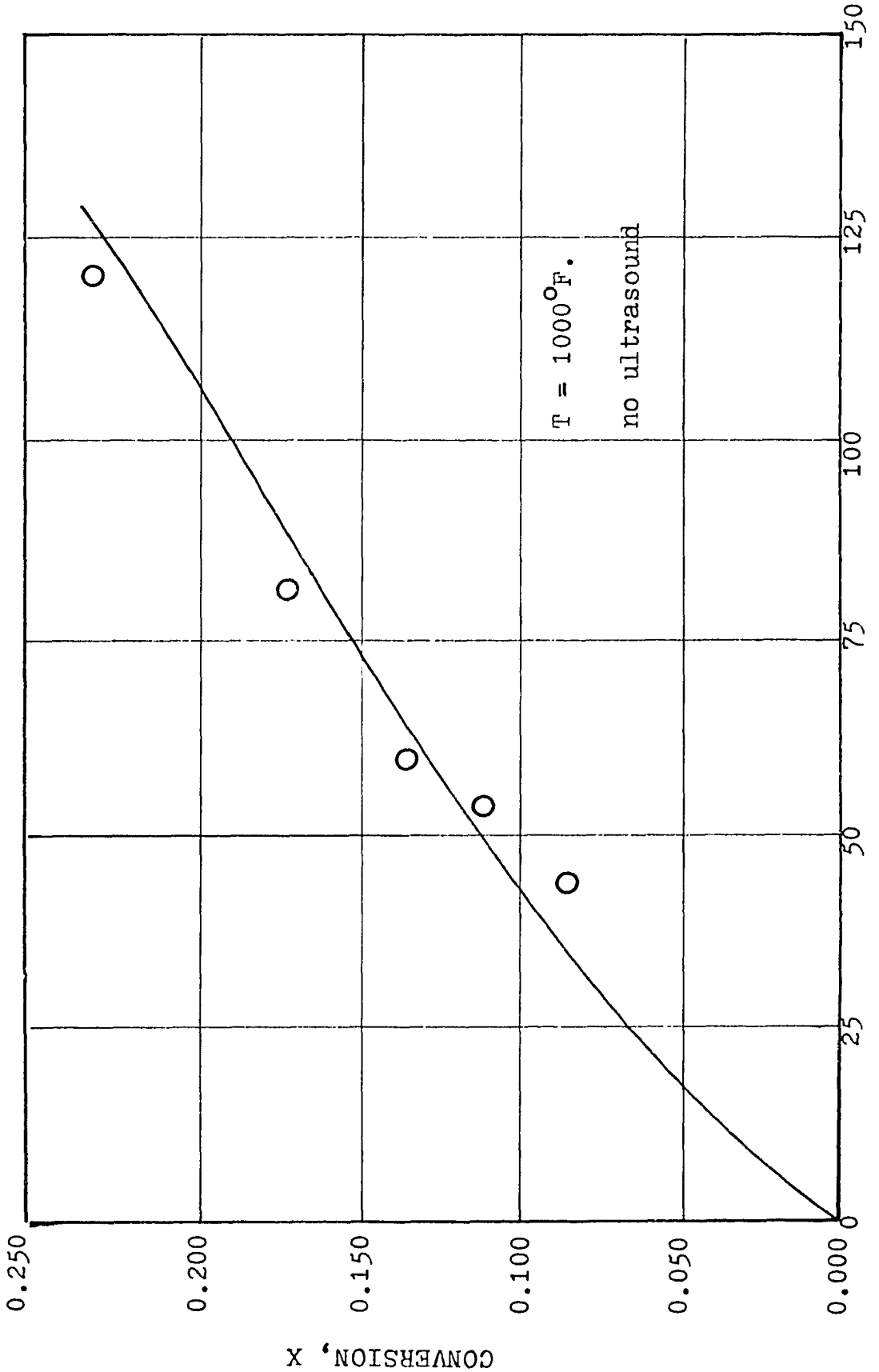

FIGURE 72

CONVERSION vs. W/F

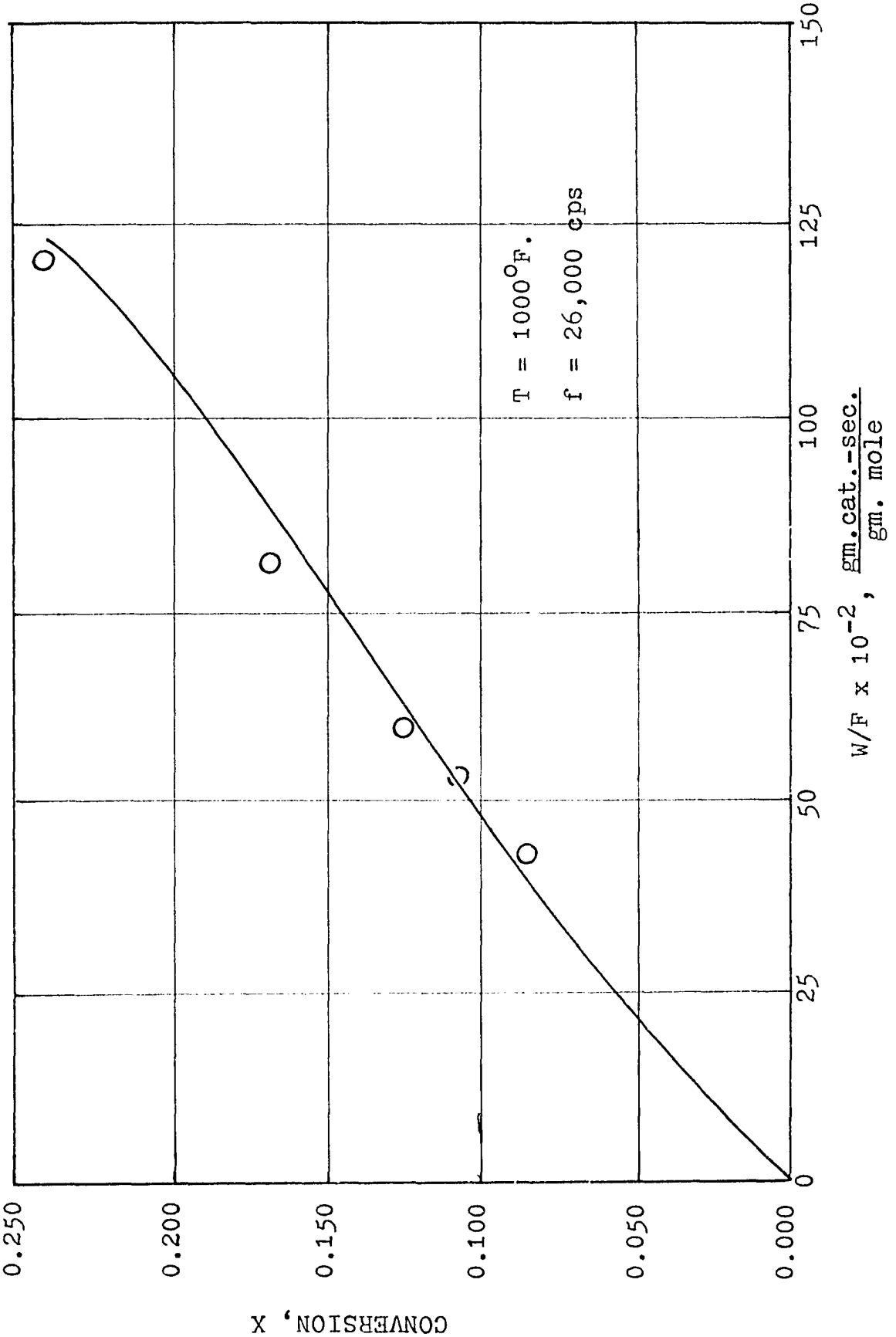

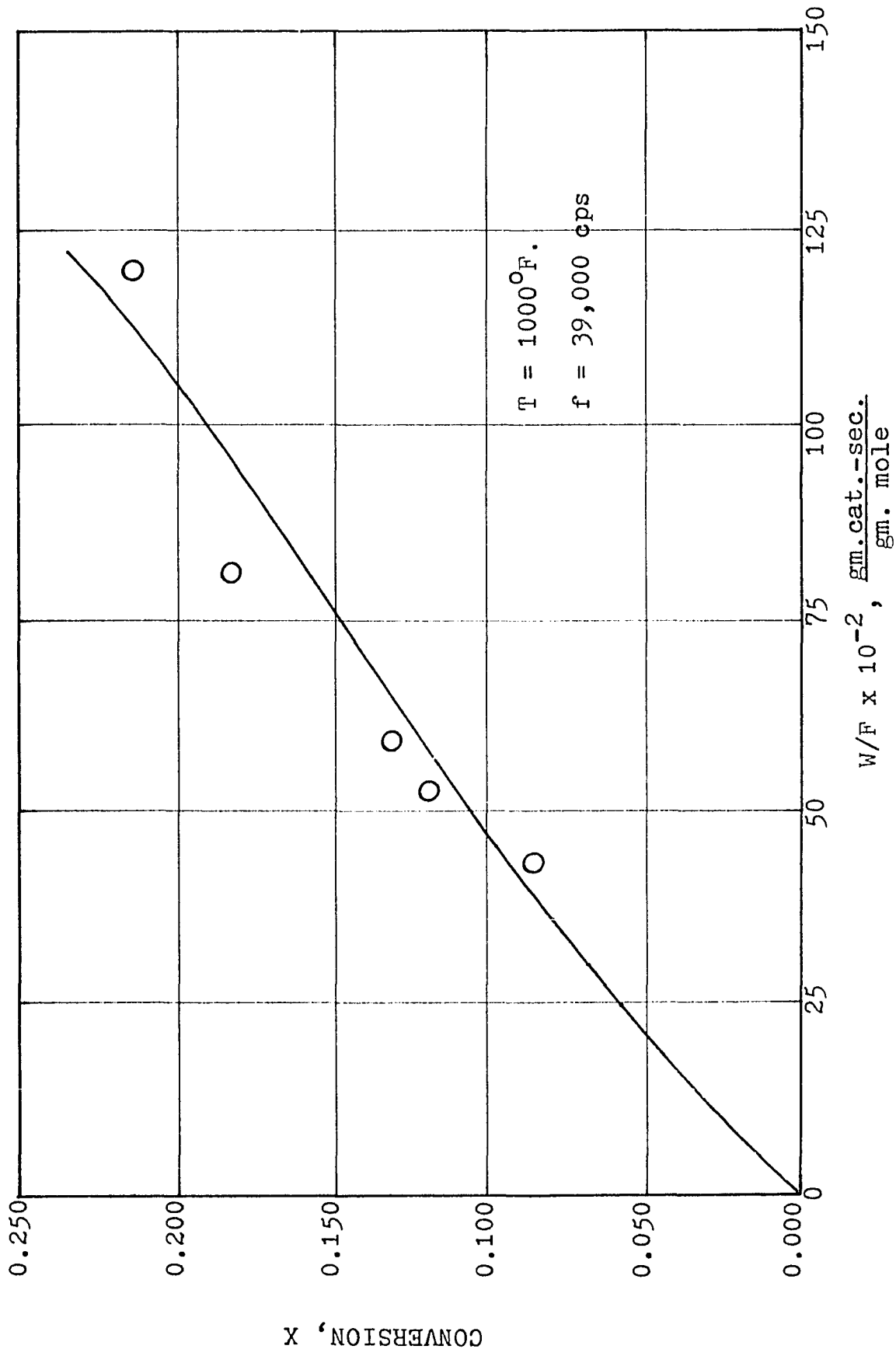

FIGURE 73

APPENDIX IX

SAMPLE ANALYSIS

SAMPLE ANALYSIS

Samples of the reactor effluent were obtained by the following methods:

Gas Sample

The high temperature (650-1050°F.) gaseous effluent is introduced directly into the gas chromatograph via a gas sampling valve. This method proved to be no more accurate than the liquid sample method, even though the sample represents the entire effluent stream.

Liquid Sample

The reactor effluent is partially condensed and subcooled to 70°F. The propylene remains in the gas phase at this temperature and is vented from the system. The remaining liquid phase is injected into the gas chromatograph. Little accuracy is sacrificed by this technique because of the unaccounted for losses of cumene and benzene in the gaseous propylene stream.

The following calculations compare the two sampling techniques, assuming a total cumene feed to the reactor of 100 gm moles and a conversion of 20%.

Gas Sample Analysis (No Losses)

Material Balance

	N_o gm-moles	N_f gm-moles	mole %	M gms./gm-mole	gms.	Wt.%
A	100.0	80.0	66.66	120.19	9,615,20	80.00
R	-	20.0	16.67	78.11	1,562.20	13.00
S	-	20.0	16.67	42.08	841.60	7.00
Total	100.0	120.0	100.0		12,019.00	100.00

Conversion

$$X_A = \frac{120.19(\text{wt.\%R})}{120.19(\text{wt.\%R}) + 78.11(\text{wt.\%A})}$$

$$= \frac{120.19(13.00)}{120.19(13.00) + 78.11(80.00)}$$

$$= \frac{1562.2}{1562.2 + 6248.8} = \frac{1562.2}{7811.0} = 0.2000 \qquad (103)$$

Liquid Sample Analysis (All S Lost, No Other Losses)

Material Balance

	N_o gm-moles	N_f gm-moles	mole %	M gms./gm-mole	gms.	Wt.%
A	100.0	80.0	80.0	120.19	9,615.20	86.02
R	-	20.0	20.0	78.11	1,562.20	13.98
S	-	-	-	42.08	-	-
Total	100.0	100.0	100.0		11,177.40	100.00

Conversion

$$X_A = \frac{120.19(\text{wt.}\%R)}{120.19(\text{wt.}\%R) + 78.11(\text{wt.}\%A)}$$

$$= \frac{120.19(13.98)}{120.19(13.98) + 78.11(86.02)}$$

$$= \frac{1,680.2562}{1,680.2562 + 6,719.0222} = \frac{1,680.2562}{8,399.2784} = 0.2000$$

Liquid Sample Analysis (Actual Losses)

Vapor Pressure at 70°F. (20°C.)

$$\log P_A = 6.92926 - \frac{1206.350}{t+207.202} = 6.92926 - \frac{1206.350}{20+207.202}$$

$$P_A = 3.32 \text{ mm. Hg}$$

$$\log P_R = 6.89745 - \frac{1206.350}{t+220.237} = 6.89745 - \frac{1206.350}{20+220.237}$$

$$P_R = 75.15 \text{ mm. Hg}$$

$$P_S = 9.9 \text{ atm.} = 7,524 \text{ mm. Hg}$$

Condenser Flow Chart (Figure 74)

Overall Material Balance

$$F = L + V \qquad (104)$$

$$120 = L + V$$

FIGURE 74

CONDENSER FLOW CHART

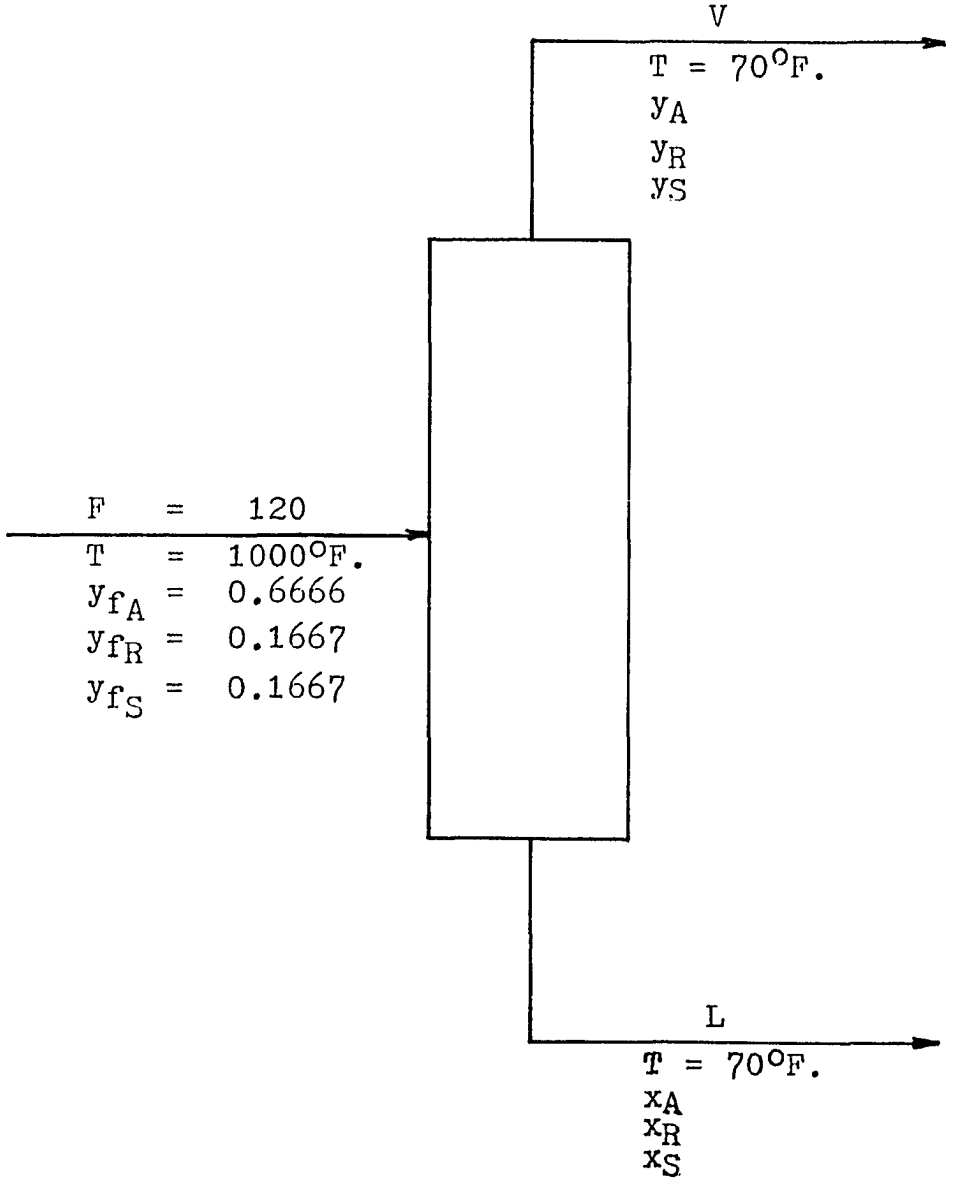

Component Material Balance

$$y_{f_A}F = y_A V + x_A L;\ 80.0 = y_A V + x_A L \tag{105}$$

$$y_{f_R}F = y_R V + x_R L;\ 20.0 = y_R V + x_R L \tag{106}$$

$$y_{f_S}F = y_S V + x_S L;\ 20.0 = y_S V + x_S L \tag{107}$$

Dalton's and Raoult's Laws

$$p_A = y_A \pi = x_A P_A;\ y_A = \frac{x_A P_A}{\pi} \tag{108}$$

$$p_R = y_R \pi = x_R P_R;\ y_R = \frac{x_R P_R}{\pi} \tag{109}$$

$$p_S = y_S \pi = x_R P_S;\ y_S = \frac{x_S P_S}{\pi} \tag{110}$$

Combine Material Balances and Dalton's and Raoult's Laws

$$x_A = \frac{80.0}{L + \frac{P_A}{\pi}(120-L)} = \frac{80.0}{L + \frac{3.32}{760}(120-L)}$$

$$= \frac{80.0}{0.52416 + 0.995632L}$$

$$x_R = \frac{20.0}{L + \frac{P_R}{\pi}(120-L)} = \frac{20.0}{L + \frac{75.15}{760}(120-L)}$$

$$= \frac{20.0}{11.8656 + 0.90112L}$$

$$x_S = \frac{20.0}{L + \frac{P_S}{\pi}(120-L)} = \frac{20.0}{L + \frac{7.524}{760}(120-L)}$$

$$= \frac{20.0}{1,188 - 8.90L}$$

Trial and Error Solution

Let L = 100.0

$$x_A = \frac{80.0}{0.52416 + 99.5632} = \frac{80.0}{100.08736} = 0.7993$$

$$x_R = \frac{20.0}{11.8656 + 90.112} = \frac{20.0}{101.9776} = 0.1961$$

$$x_S = \frac{20.0}{1,188 - 890} = \frac{20.0}{298} = 0.0671$$

$$\overline{1.0625}$$

Let L = 111.0

$$x_A = \frac{80.0}{0.52416 + 110.51515} = \frac{80.0}{111.03931} = 0.7205$$

$$x_R = \frac{20.0}{11.8656 + 100.0243} = \frac{20.0}{111.88992} = 0.1787$$

$$x_S = \frac{20.0}{1,188 - 987.9} = \frac{20.0}{200.1} = 0.1000$$

$$\overline{0.9992}$$

Corrected Mole Fractions

$$x_A = \frac{0.7205}{0.9992} = 0.7211$$

$$x_R = \frac{0.1787}{0.9992} = 0.1788$$

$$x_S = \frac{0.1000}{0.9992} = 0.1001$$

$$\overline{1.0000}$$

Material Balance

	N_o gm-moles	N_f gm-moles	mole %	M gm. / gm moles	gms.	wt.%
A	100.0	80.0421	72.11	120.19	9,620.34	0.8266
R	-	19.8468	17.88	78.11	1,550.23	0.1332
S	-	11.1111	10.01	42.08	467.56	0.0402
Total	100.0	111.0000	100.00		11,638.13	1.0000

Conversion

$$x_A = \frac{120.19(\text{wt.}\%R)}{120.19(\text{wt.}\%R) + 78.11(\text{wt.}\%A)}$$

$$= \frac{120.19(13.32)}{(120.19)(13.32) + 78.11(82.66}$$

$$= \frac{1,600.9308}{1,600.9308 + 6,456.5726}$$

$$= \frac{1,600.9308}{8,057.5034} = 0.1987$$

Error

$$\% \text{ error} = \frac{(0.2000 - 0.1987)(100)}{0.2000}$$

$$= \frac{0.0013(100)}{0.2000} = 0.65\%$$

Sample Calculation from Actual Data

Run No. 11.53

Analysis (Wt. %)

	Liquid Sample				Gas
	Test 1	Test 2	Test 3	Average	Sample
Cumene	90.62	91.35	91.30	91.09	89.11
Benzene	7.62	7.18	7.18	7.32	7.08
Propylene	1.76	1.47	1.52	1.59	3.81
	100.00	100.00	100.00	100.00	100.00

Liquid Sample Conversion

$$x_A = \frac{120.19(7.32)}{120.19(7.32) + 78.11(91.09)} = 11.0\%$$

Gas Sample Conversion

$$x_A = \frac{(120.19)(7.08)}{(120.19)(7.08) + 78.11(89.11)} = 10.9\%$$

APPENDIX X

ULTRASONIC ENGINEERING

ULTRASONIC ENGINEERING

Fundamental Equations

Figure 76 illustrates a schematic representation of the instantaneous position of the gas particles through which a sound wave is travelling. The gas particles are each volume elements of gas containing millions of molecules. The drawing shows the alternate compression and expansion of the gas in the direction of the propagation of the sound wave.

Figure 76 illustrates the sine wave representation of the sound wave.

Sound Wave Equation

$$y = Y\cos\left[\frac{2\pi}{\lambda}(x-Vt)\right] = Y\cos\left[2\pi f\left(t-\frac{x}{V}\right)\right] \qquad (111)$$

$$\lambda\ \frac{cm}{cycle} = \left(V\frac{cm}{sec}\right)\left(T\frac{sec}{cycle}\right) = \frac{V\ \frac{cm}{sec}}{f\frac{cycles}{sec}}$$

$$f = \frac{1}{T}$$

Transverse Velocity

$$v = \frac{dy}{dt} = \frac{d}{dt}\left[Y\cos 2\pi f\left(t-\frac{x}{V}\right)\right] = -Y\sin 2\pi f\left(t-\frac{x}{V}\right)\left[2\pi f\right]$$

$$v = -2\pi f Y\sin 2\pi f\left(t-\frac{x}{V}\right) \qquad (112)$$

FIGURE 75

SCHEMATIC DIAGRAM OF SOUND WAVE

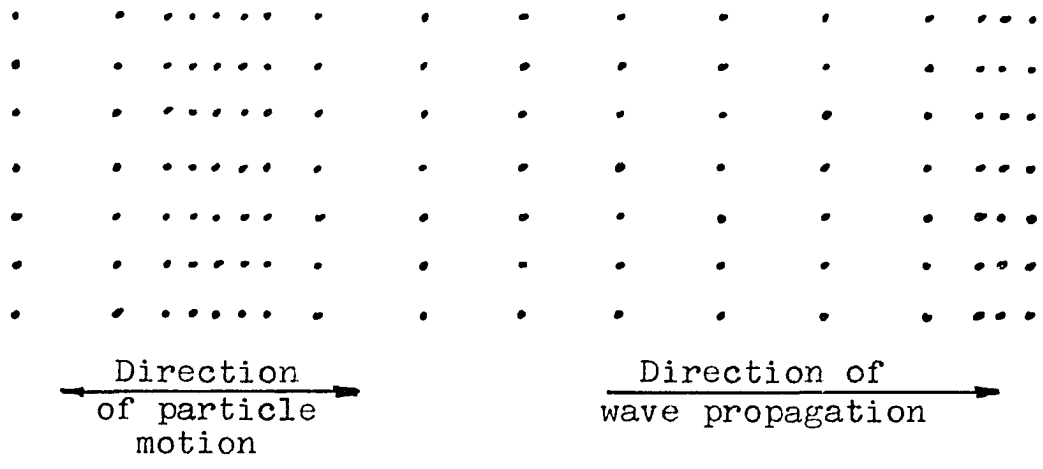

FIGURE 76

SINE WAVE REPRESENTATION OF SOUND WAVE

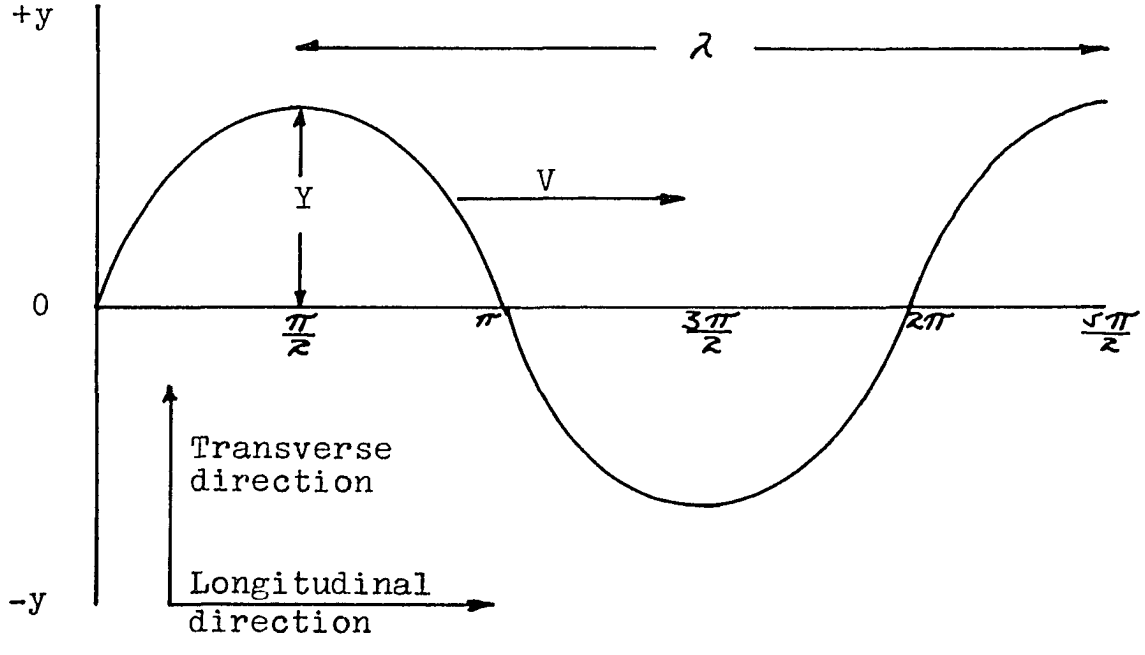

Transverse Acceleration

$$a = \frac{dv}{dt} = \frac{d}{dt}\left[-2\pi f Y \sin 2\pi f\left(t-\frac{x}{V}\right)\right]$$

$$= -2\pi f Y \cos 2\pi f\left(t-\frac{x}{V}\right)\left[2\pi f\right]$$

$$a = -4\pi^2 f^2 Y \cos 2\pi f\left(t-\frac{x}{V}\right) \qquad (113)$$

Velocity of Propagation of Sound Waves in a Gas

Figure 77 illustrates an element of gas in a tube in which there is a longitudinal sound wave. Both the equilibrium and displaced positions are shown.

Newton's Second Law

$$F = ma \qquad (114)$$

$$F_{NET} = \left(p_o + p\ \frac{\text{dynes}}{\text{cm}^2}\right)(A\ \text{cm}^2) - \left(p_o + p + \Delta p\ \frac{\text{dynes}}{\text{cm}^2}\right)(A\ \text{cm}^2)$$

$$= -\Delta pA\ \text{dynes}$$

$$m = \left(\rho_o\ \frac{\text{gms}}{\text{cm}^3}\right)(A\ \text{cm}^2)(\Delta x\ \text{cm}) = \rho_o A \Delta x\ \text{gms.}$$

$$a = \frac{d^2y}{dt^2}\ \frac{\text{cm}}{\text{sec}^2}$$

$$-\Delta pA = \rho_o A \Delta x\ \frac{d^2y}{dt^2}$$

$$\frac{d^2y}{dt^2} = \frac{-\Delta pA}{\rho_o A \Delta x} = -\frac{1}{\rho_o}\ \frac{p}{\Delta x}$$

$$\frac{d^2y}{dt^2} = -\frac{1}{\rho_o}\ \frac{dp}{dx}$$

FIGURE 77

ELEMENT OF GAS IN A TUBE IN WHICH THERE IS A LONGITUDINAL SOUND WAVE

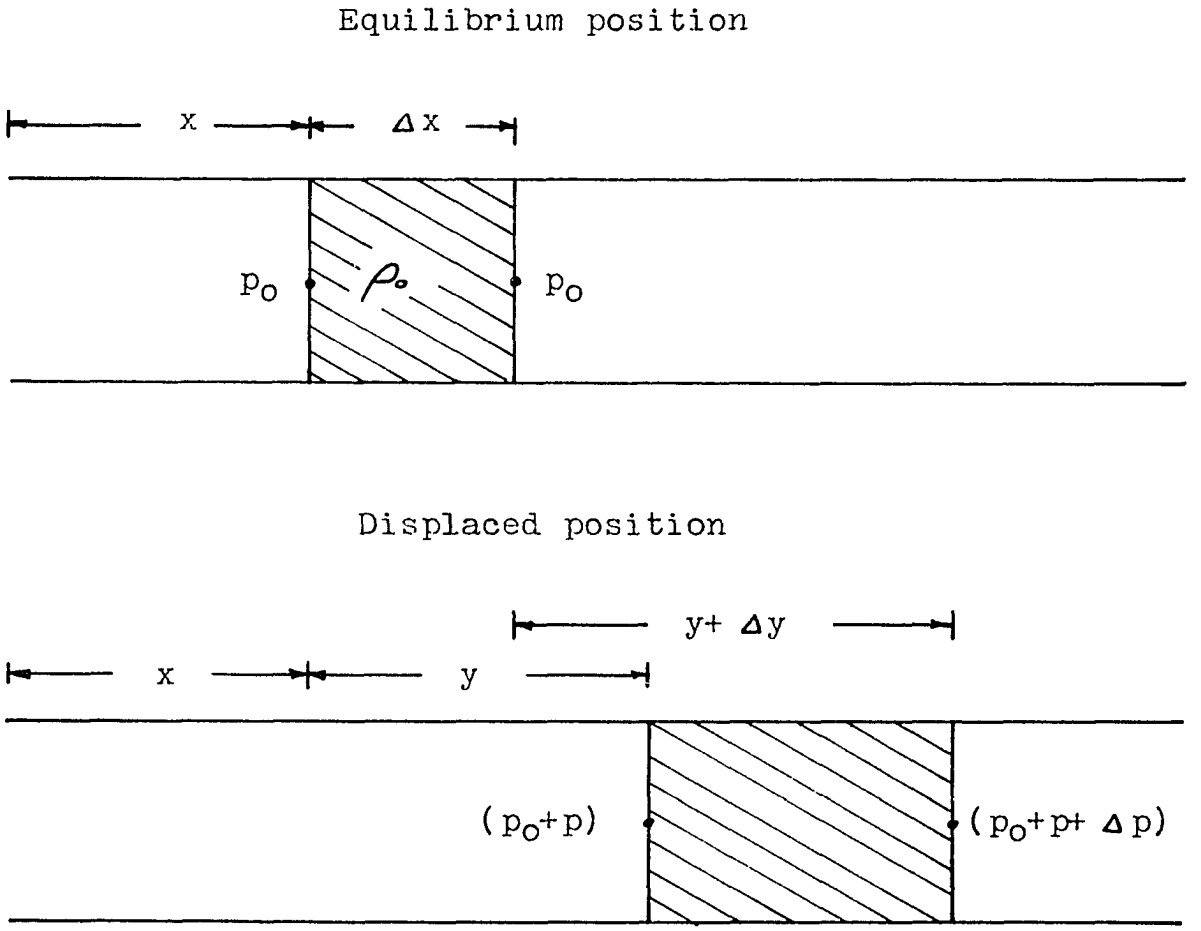

Calculate p

Definition of Compressibility

$$k = -\left[\frac{1}{\text{original volume}}\right]\left[\frac{\text{change in volume}}{\text{change in pressure}}\right]$$

$$= -\frac{1}{v}\frac{dv}{dp} \qquad (115)$$

Original volume $= (A\,cm^2)(\triangle x\ cm) = A\triangle x\ cm^3$

Change in volume

$= (\triangle x+y+\triangle y-y\ cm)(A\ cm^2)-(\triangle x\ cm)(A\ cm^2)$

$= (\triangle x+\triangle y)A - \triangle xA$

$= \triangle yA\ cm^3$

Change in pressure

$$= \frac{(p_o+p)+(p_o+p+\triangle p)}{2} - p_o$$

$$= \frac{2p_o+2p+\triangle p}{2} - p_o$$

$$= p_o+p+\frac{\triangle p}{2}-p_o$$

$$= p\ \frac{dynes}{cm^2}$$

$$k = \left[-\frac{1}{A\triangle x\ cm^3}\right]\left[\frac{\triangle yA\ cm^3}{p\ \frac{dynes}{cm^2}}\right] = -\frac{\triangle y}{p\triangle x}\ \frac{cm^2}{dyne}$$

Rearrange to Obtain p

$$p = \frac{-1}{k}\frac{\triangle y}{\triangle x} = \frac{-1}{k}\frac{dy}{dx}$$

$$\frac{dp}{dx} = \frac{-1}{k}\frac{d^2y}{dx^2}$$

Substitute into Equation for Newton's Second Law

$$\frac{d^2y}{dt^2} = -\frac{1}{\rho_o}\frac{dp}{dx} = -\frac{1}{\rho_o}\left[-\frac{1}{k}\frac{d^2y}{dx^2}\right]$$

$$\frac{\partial^2 y}{\partial t^2} = \frac{1}{\rho_o k}\frac{\partial^2 y}{\partial x^2}$$

Change Variables

Let $y = f(x \pm Vt) = f(u) = f$

$$\frac{\partial y}{\partial x} = \frac{\partial f}{\partial x} = \frac{\partial f}{\partial u} \cdot \frac{\partial u}{\partial x}$$

$$\frac{\partial u}{\partial x} = \frac{\partial (x \pm Vt)}{\partial x} = \frac{\partial x}{\partial x} = 1$$

$$\frac{\partial y}{\partial x} = \frac{\partial f}{\partial u} \cdot 1 = \frac{\partial f}{\partial u}$$

$$\frac{\partial^2 y}{\partial x^2} = \frac{\partial}{\partial x}\left(\frac{\partial y}{\partial x}\right) = \frac{\partial}{\partial x}\left(\frac{\partial f}{\partial u}\right) = \frac{\partial u}{\partial x} \cdot \frac{\partial}{\partial u}\left(\frac{\partial f}{\partial u}\right)$$

$$= (1)\frac{\partial}{\partial u}\left(\frac{\partial f}{\partial u}\right) = \frac{\partial^2 f}{\partial u^2}$$

$$\frac{\partial y}{\partial t} = \frac{\partial f}{\partial t} = \frac{\partial f}{\partial u} \cdot \frac{\partial u}{\partial t}$$

$$\frac{\partial u}{\partial t} = \frac{\partial (x \pm Vt)}{\partial t} = \pm V$$

$$\frac{\partial y}{\partial t} = \frac{\partial f}{\partial u}(\pm V) = \pm V \frac{\partial f}{\partial u}$$

$$\frac{\partial^2 y}{\partial t^2} = \frac{\partial}{\partial t}\left(\frac{\partial y}{\partial t}\right) = \frac{\partial}{\partial t}\left(\pm V \frac{\partial f}{\partial u}\right) = \frac{\partial u}{\partial t} \cdot \frac{\partial}{\partial u}\left(\pm V \frac{\partial f}{\partial u}\right)$$

$$= \pm V \cdot \frac{\partial}{\partial u}\left(\pm V \frac{\partial f}{\partial u}\right) = V^2 \frac{\partial^2 f}{\partial u^2}$$

Substitution

$$V^2 \frac{\partial^2 f}{\partial u^2} = \frac{1}{\rho_o k} \frac{\partial^2 f}{\partial u^2}$$

$$V^2 = \frac{1}{\rho_o k}$$

$$V = \left[\frac{1}{\rho_o k}\right]^{\frac{1}{2}} \tag{116}$$

Adiabatic Compression

Definition

$$pv^{\gamma} = c \tag{117}$$

$$\gamma = \frac{c_P}{c_V}$$

Differentiate

$$v^{\gamma}\, dp + p\gamma v^{\gamma-1} dv = 0$$

$$\frac{dv}{dp} = -\frac{v^{\gamma}}{p\gamma v^{\gamma-1}} = -\frac{v}{p\gamma}$$

Substitute into Compressibility Equation

$$k = -\frac{1}{v}\frac{dv}{dp} = +\frac{1}{v} \cdot \frac{v}{p\gamma} = \frac{1}{p\gamma} \tag{118}$$

Substitution

$$V = \left[\frac{1}{\rho_o k}\right]^{\frac{1}{2}} = \left[\frac{p\gamma}{\rho_o}\right]^{\frac{1}{2}}$$

$$pv = nRT$$

$$p = \frac{nRT}{v}$$

$$\frac{p\ \frac{\text{dynes}}{\text{cm}^2}}{\rho_o\ \frac{\text{gms}}{\text{cm}^3}} = \frac{(R\ \frac{\text{ergs}}{\text{gm mole-}^oK})(1\ \frac{\text{dyne-cm}}{\text{erg}})(T^oK)}{(M\ \frac{\text{gms}}{\text{gm mole}})} = \frac{RT}{M}$$

$$V = \left[\frac{\gamma RT}{M}\right]^{\frac{1}{2}} \qquad (119)$$

Pressure Variations in a Sound Wave

Pressure Equation

$$p = -\frac{1}{k}\frac{dy}{dx} \qquad (120)$$

Sound Wave Equation

$$y = Y\cos\left[\frac{2\pi}{\lambda}(x-Vt)\right] \qquad (121)$$

Differentiate and Combine Equations

$$\frac{dy}{dx} = -Y\sin\left[\frac{2\pi}{\lambda}(x-Vt)\right]\left[\frac{2\pi}{\lambda}\right] = -\frac{2\pi Y}{\lambda}\sin\left[\frac{2\pi}{\lambda}(x-Vt)\right]$$

$$p = \frac{2\pi Y}{k\lambda}\sin\left[\frac{2\pi}{\lambda}(x-Vt)\right]$$

$$V = \left[\frac{1}{\rho_o k}\right]^{\frac{1}{2}}$$

$$V^2 = \frac{1}{\rho_o k}$$

$$k = \frac{1}{\rho_o V^2}$$

$$p = \frac{2\pi\rho_o V^2 Y}{\lambda} \sin\left[\frac{2\pi}{\lambda}(x-Vt)\right]$$

$$p = p_{max}\sin\left[\frac{2\pi}{\lambda}(x-Vt)\right]$$

$$p_{max} = \frac{2\pi\rho_o V^2 Y}{\lambda} = \frac{2\pi\rho_o \gamma RTY}{M\lambda}$$

$$p_{max} = \frac{2\pi\rho_o c_p RTY}{M\lambda c_V}$$

$$p_{max} = 2\pi f Y \rho_o \left[\frac{c_p RT}{c_V M}\right]^{\frac{1}{2}} \qquad (122)$$

Intensity of a Sound Wave

Work Done on System

$$w = -\int_o^p p\,dv \qquad (123)$$

$$k = -\frac{1}{v_o}\frac{dv}{dp}$$

$$dv = kv_o dp$$

$$w = +\int_o^p kv_o p\,dp = kv_o\left[\frac{p^2}{2}\right]_o^p = \tfrac{1}{2} kv_o p^2$$

Energy per Unit Volume

$$\frac{w_{max}}{v_o} = \tfrac{1}{2}kp_{max}^2 \tag{124}$$

Intensity

Definition

$$I = \frac{(\text{energy})}{(\text{unit area})(\text{unit time})} \tag{125}$$

$$I = \frac{(\tfrac{1}{2}kp_{max}^2 \frac{\text{dyne-cm}}{\text{cm}^3})(\text{A cm})(\text{Vdt cm})}{(\text{A cm}^2)(\text{dt sec})}$$

$$= \tfrac{1}{2}kp_{max}^2 \; V \frac{\text{dyne-cm}}{\text{cm}^2\text{-sec}}$$

$$V = \left[\frac{c_P RT}{c_V M}\right]^{\frac{1}{2}}$$

$$k = \frac{1}{\rho_o V^2} = \frac{c_V M}{\rho_o c_P RT}$$

$$k_V = \left[\frac{c_V M}{\rho_o c_P RT}\right]\left[\frac{c_P RT}{c_V M}\right]^{\frac{1}{2}} = \left[\frac{c_V M}{c_P RT}\right]^{\frac{1}{2}} \frac{1}{\rho_o}$$

$$I = \frac{p_{max}^2}{2\rho_o}\left[\frac{c_V M}{c_P RT}\right]^{\frac{1}{2}} \tag{126}$$

FIGURE 78

INTENSITY FLOW CHART

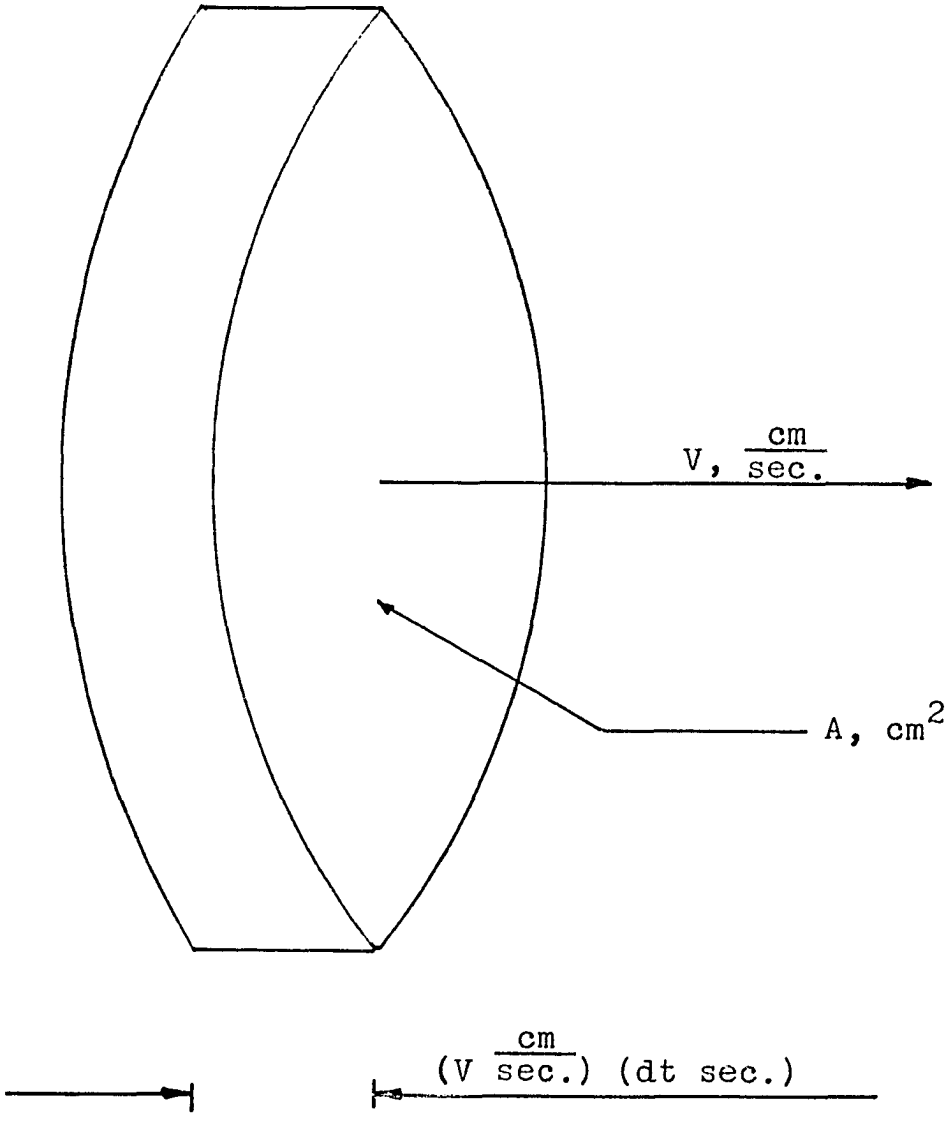

Definition of a Decibel

$$\beta = 10 \log \frac{I}{I_o} \tag{127}$$

β = sound intensity level, decibels

$I_o = 10^{-16} \frac{\text{watts}}{\text{cm}^2}$

$p_{max} = 0.002 \frac{\text{dynes}}{\text{cm}^2}$ at $I_o = 10^{-16} \frac{\text{watts}}{\text{cm}^2}$ in air

Standing Waves

Definition

Standing waves are caused as a result of the reflection of sound waves back from the end of a tube. The total displacement is the sum of the displacements of the original wave and the reflected wave. Whereas, in a travelling wave the amplitude remains constant as the wave form progresses, in a standing wave, the amplitude fluctuates and the wave form remains fixed.

Derivation of Standing Wave Equation

Displacement of Original Wave

$$y_1 = Y\cos\left[\frac{2\pi}{\lambda}(x-Vt)\right] \tag{128}$$

Displacement of Reflected Wave

$$y_2 = -Y\cos\left[\frac{2\pi}{\lambda}(-x-Vt)\right] \tag{129}$$

Total Displacement

$$y = y_1 + y_2 = Y\cos\left[\frac{2\pi}{\lambda}(x-Vt)\right] - Y\cos\left[\frac{2\pi}{\lambda}(-x-Vt)\right]$$

$$= Y\cos\left[\frac{2\pi}{\lambda}(x-Vt)\right] - Y\cos\left[\frac{2\pi}{\lambda}(x+Vt)\right]$$

$$= Y\cos\left[\frac{2\pi}{\lambda}(x-Vt)\right] - \cos\left[\frac{2\pi}{\lambda}(x+Vt)\right]$$

$$\cos(\alpha - \beta) - \cos(\alpha + \beta) = 2\sin\alpha\sin\beta$$

$$y = Y\left\{2\sin\left[\frac{2\pi x}{\lambda}\right]\sin\left[\frac{2\pi Vt}{\lambda}\right]\right\}$$

$$f = \frac{V}{\lambda}$$

$$V = f\lambda$$

$$y = 2Y\sin\left[\frac{2\pi x}{\lambda}\right]\sin\left[\frac{2\pi f\lambda t}{\lambda}\right] = 2Y\sin\left[\frac{2\pi x}{\lambda}\right]\sin\left[2\pi ft\right]$$

$$y = \left[2Y\sin(2\pi ft)\right]\sin\left[\frac{2\pi x}{\lambda}\right]$$

Figure 79 defines the various terms associated with a standing wave.

Fundamental Frequency

$$f_o = \frac{V}{\lambda_o}$$

$$\lambda_o = 4L$$

$$V = \left[\frac{c_p RT}{c_V M}\right]^{\frac{1}{2}}$$

FIGURE 79

SCHEMATIC DRAWING OF A STANDING WAVE

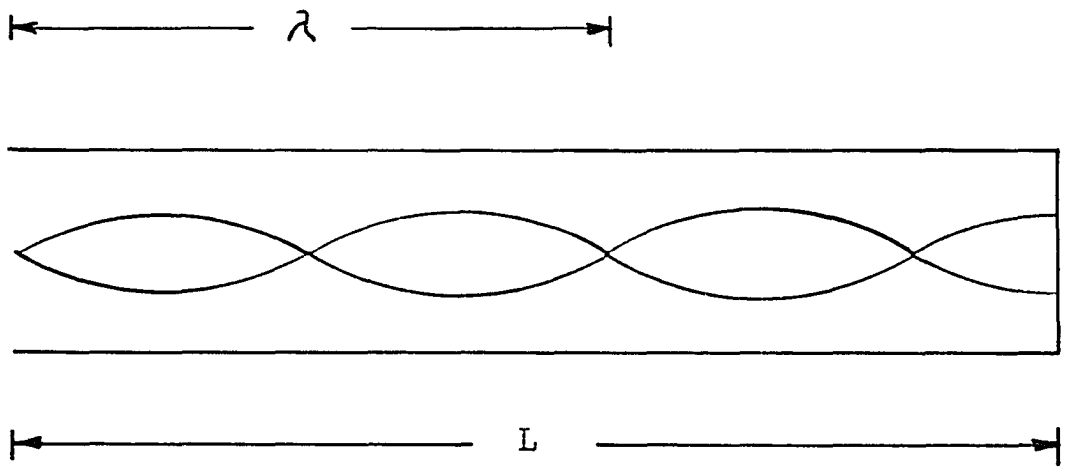

$$f_o = \frac{V}{4L} = \left[\frac{c_pRT}{c_VM}\right]^{\frac{1}{2}} \frac{1}{4L} \qquad (130)$$

"Tuned" Wavelengths and Frequencies

	$4L$	$\frac{4L}{3}$	$\frac{4L}{5}$	$\frac{4L}{n}$
f	$\left[\frac{c_pRT}{c_VM}\right]^{\frac{1}{2}} \frac{1}{4L}$	$\left[\frac{c_pRT}{c_VM}\right]^{\frac{1}{2}} \frac{3}{4L}$	$\left[\frac{c_pRT}{c_VM}\right]^{\frac{1}{2}} \frac{5}{4L}$	$\left[\frac{c_pRT}{c_VM}\right]^{\frac{1}{2}} \frac{n}{4L}$

$n = 1,3,5,7,9,\text{etc.}$

Summary of Ultrasonic Engineering Equations

Sound Wave Equation

$$y = Y\cos\left[\frac{2\pi}{\lambda}(x-Vt)\right] = Y\cos\left[2\pi f(t-\tfrac{x}{V})\right] \qquad (111)$$

$$y_{max} = Y$$

$$\lambda = VT = \frac{V}{f}$$

$$f = \frac{1}{T}$$

Transverse Velocity

$$v = -2\pi fY\sin 2\pi f(t-\tfrac{x}{V}) \qquad (112)$$

$$v_{max} = 2\pi fY \qquad (131)$$

Transverse Acceleration

$$a = -4\pi^2 f^2 Y\cos 2\pi f(t-\tfrac{x}{V}) \qquad (113)$$

$$a_{max} = 4\pi^2 f^2 Y \tag{132}$$

Velocity of Propagation

$$V = \left[\frac{1}{\rho_o k}\right]^{\frac{1}{2}} = \left[\frac{\gamma RT}{M}\right]^{\frac{1}{2}} \tag{119}$$

Acoustic Pressure

$$p = \left[\frac{2\pi\rho_o V^2 Y}{\lambda}\right]\sin\left[\frac{2\pi}{\lambda}(x-Vt)\right] \tag{133}$$

$$p_{max} = \frac{2\pi\rho_o V^2 Y}{\lambda} = \frac{2\pi\rho_o \gamma RTY}{M\lambda} = \frac{2\pi\rho_o c_p RTY}{M\lambda c_V}$$

$$= 2\pi f Y \rho_o \left[\frac{c_p RT}{c_V M}\right]^{\frac{1}{2}} = \left[2\rho_o I\right]^{\frac{1}{2}} \left[\frac{c_p RT}{c_V M}\right]^{\frac{1}{4}} \tag{122}$$

Intensity

$$I = \frac{p_{max}^2}{2\rho_o}\left[\frac{c_V M}{c_p RT}\right]^{\frac{1}{2}} \tag{126}$$

$$\beta = 10 \log \frac{I}{I_o} = 10 \log \frac{I}{10^{-16} \frac{watts}{cm^2}} \tag{127}$$

Amplitude

$$Y = \frac{p_{max}}{2\pi f \rho_o}\left[\frac{c_V M}{c_p RT}\right]^{\frac{1}{2}} \tag{134}$$

Standing Wave Equation

$$y = \left[2Y\sin(2\pi ft)\right] \sin\frac{2\pi x}{\lambda} \qquad (135)$$

"Tuned" Wavelength and Frequencies

$$\lambda = 4L \;,\; \frac{4L}{3} \;,\; \frac{4L}{5} \;,\; \frac{4L}{n}$$

$$f = \left[\frac{cpRT}{c_V M}\right]^{\frac{1}{2}} \frac{1}{4L}, \left[\frac{cpRT}{c_V M}\right]^{\frac{1}{2}} \frac{3}{4L}, \left[\frac{cpRT}{c_V M}\right]^{\frac{1}{2}} \frac{5}{4L}, \left[\frac{cpRT}{c_V M}\right]^{\frac{1}{2}} \frac{n}{4L}$$

$n = 1,3,5,7,9,\text{etc.}$

Typical Values of Wave Characteristics

The following values are calculated at the extreme temperatures employed in this research, 650°F. and 1050°F., and at the two frequencies studied, 26,000 cps and 39,000 cps. Additionally, the calculations are made at the maximum power output of the equipment at each frequency and at one-half that power output.

Power Output

$$\beta = 10 \log \frac{I}{I_o} \qquad (127)$$

β = power output, decibels

= 161 db at 26,000 cps

= 150 db at 39,000 cps

I_o = constant, 10^{-16} $\frac{\text{watts}}{\text{cm}^2}$

I = intensity, $\frac{\text{watts}}{\text{cm}^2}$

At 26,000 cps,

$$\log \frac{I}{I_o} = \frac{\beta}{10} = \frac{161}{10} = 16.1$$

$$\frac{I}{I_o} = 1.259 \times 10^{16}$$

$$I = (1.259 \times 10^{16})(10^{-16}) = 1.259 \frac{\text{watts}}{\text{cm}^2}$$

At 39,000 cps,

$$\log \frac{I}{I_o} = \frac{\beta}{10} = \frac{150}{10} = 15.0$$

$$\frac{I}{I_o} = 10^{15}$$

$$I = (10^{15})(10^{-16}) = 0.100 \frac{\text{watts}}{\text{cm}^2}$$

The following calculations are for a temperature of 650°F., a frequency of 26,000 cps and an acoustical intensity of 1.259 $\frac{\text{watts}}{\text{cm}^2}$.

Acoustic Pressure

$$p_{max} = \left[2\rho_o I\right]^{\frac{1}{2}} \left[\frac{c_p RT}{c_V M}\right]^{\frac{1}{4}} \qquad (122)$$

$$\rho_o = \frac{PM}{RT} = \frac{(1.0 \text{ atm})(120.19 \frac{\text{gms}}{\text{gm mole}})}{(82.06 \frac{\text{cm}^3\text{-atm}}{\text{gm mole } ^\circ\text{K}})(616^\circ\text{K})} = 0.00238 \frac{\text{gms}}{\text{cm}^3}$$

$$I = (1.259 \frac{\text{watts}}{\text{cm}^2})(10^7 \frac{\text{dyne-cm}}{\text{watt-sec}}) = 1.259 \times 10^7 \frac{\text{dynes}}{\text{cm-sec}}$$

$$\frac{c_P}{c_V} = \frac{0.588 \ \frac{cal}{gm\text{-}^oC}}{0.571 \ \frac{cal}{gm\text{-}^oC}} = 1.030$$

$$R = 8.31 \times 10^7 \ \frac{gm\text{-}cm^2}{sec^2\text{-}gm \ mole\text{-}^oK}$$

$$T = 616^oK.$$

$$M = 120.19 \ \frac{gms}{gm\text{-}mole}$$

$$p_{max} = \frac{\left[(2)(0.00238 \ \frac{gms}{cm^3})(1.259 \times 10^8 \ \frac{dynes}{cm\text{-}sec})\right]^{\frac{1}{2}}}{\left[1 \ \frac{gm\text{-}cm}{dyne\text{-}sec^2}\right]^{\frac{1}{2}}} \left[\frac{(1.030)(8.31 \times 10^7 \ \frac{gm\text{-}cm^2}{sec^2\text{-}gm \ mole\text{-}^oK})(616^oK)}{120.19 \ \frac{gms}{gm \ mole}}\right]^{\frac{1}{4}}$$

$$= (59.928 \times 10^4 \ \frac{dyne^2\text{-}sec}{cm^5})^{\frac{1}{2}} (4.3868 \times 10^8 \ \frac{cm^2}{sec^2})^{\frac{1}{4}}$$

$$= (7.741 \times 10^2)(1.447 \times 10^2) \ \frac{dynes}{cm^2}$$

$$= 1.120 \times 10^5 \ \frac{dynes}{cm^2}$$

$$p_{max} = \frac{(1.120 \times 10^5 \ \frac{dynes}{cm^2})(2.2481 \times 10^{-6} \ \frac{lb}{dyne})}{(0.155 \ \frac{in^2}{cm^2})} = 1.62 \ \frac{lb}{in^2}$$

Velocity of Propagation

$$V = \left[\frac{c_p RT}{c_V M}\right]^{\frac{1}{2}} \qquad (119)$$

$$= \left[\frac{(1.030)(8.31 \times 10^7 \ \frac{gm\text{-}cm^2}{sec^2\text{-}gm \ mole\text{-}^oK})(616^oK)}{(120.19 \ \frac{gms}{gm \ mole})}\right]^{\frac{1}{2}}$$

$$V = 20{,}945 \ \frac{cm.}{sec.}$$

Amplitude

$$Y = \frac{p_{max}}{2\pi f \rho_o}\left[\frac{c_V M}{c_p RT}\right]^{\frac{1}{2}} = \frac{p_{max}}{2\pi f \rho_o V} \qquad (134)$$

$$= \frac{(1.120 \times 10^5 \ \frac{dynes}{cm^2})(1 \ \frac{gm\text{-}cm}{dyne\text{-}sec^2})}{(2\pi)(26{,}000 \ \frac{1}{sec})(0.00238 \ \frac{gms}{cm^3})(20{,}945 \ \frac{cm}{sec})}$$

$$Y = 0{,}0138 \text{ cm.}$$

Transverse Velocity

$$v_{max} = 2\pi f Y \qquad (131)$$

$$= 2\pi(26{,}000 \ \frac{1}{sec})(0.0138 \text{ cm})$$

$$v_{max} = 2{,}254 \ \frac{cm.}{sec.}$$

Transverse Acceleration

$$a_{max} = 4\pi^2 f^2 Y = 2\pi f v_{max} \qquad (132)$$

$$= \frac{2\pi(26{,}000 \ \frac{1}{sec})(2.254 \ \frac{cm}{sec})}{(980 \ \frac{cm/sec^2}{g})}$$

$$a_{max} = 375{,}734 \ g$$

The results of similar calculations for temperatures of 650°F. and 1050°F., frequencies of 26,000 cps and 39,000 cps, and power outputs of full power and one-half power are shown on the following Table 11.

TABLE 11

SUMMARY OF TYPICAL WAVE CHARACTERISTICS

T, temperature, $^{o}F.$	650	650	650	650
f, frequency, $\frac{1}{sec}$	26,000	26,000	39,000	39,000
Power output	full	half	full	half
I, intensity, $\frac{watts}{cm^2}$	1.259	0.630	0.100	0.050
ρ_o, gas density, $\frac{gms}{cm^3}$	0.00238	0.00238	0.00238	0.00238
c_p/c_V	1.030	1.030	1.030	1.030
V, velocity of propagation, $\frac{cm}{sec}$	20,945	20,945	20,945	20,945
λ , wavelength, cm.	0.806	0.806	0.537	0.537
p_{max}, acoustic pressure, $\frac{lb}{in^2}$	1.62	1.15	0.46	0.32
Y, amplitude, cm.	0.0138	0.0098	0.0026	0.0018
v_{max}, transverse velocity $\frac{cm}{sec}$	2,254	1,601	637	441
a_{max}, transverse acceleration, g.	375,734	266,881	159,279	110,270

TABLE 11 (continued)

SUMMARY OF TYPICAL WAVE CHARACTERISTICS

T, temperature, $^{o}F.$	1050	1050	1050	1050
f, frequency, $\frac{1}{sec}$	26,000	26,000	39,000	39,000
Power output	full	half	full	half
I, intensity, $\frac{watts}{cm^2}$	1.259	0.630	0.100	0.050
ρ_o, gas density, $\frac{gms}{cm^3}$	0.00175	0.00175	0.00175	0.00175
c_p/c_V	1.024	1.024	1.024	1.024
V, velocity of propagation, $\frac{cm}{sec}$	24,298	24,298	24,298	24,298
λ , wavelength, cm.	0.935	0.935	0.623	0.620
p_{max}, acoustic pressure, $\frac{lb}{in^2}$	1.50	1.06	0.42	0.30
Y, amplitude, cm.	0.0149	0.0105	0.0028	0.0020
v_{max}, transverse velocity, $\frac{cm}{sec}$	2,434	1.715	686	490
a_{max}, transverse acceleration, g.	405,740	285,885	171,531	122,522

Summary of Ultrasonic Engineering Nomenclature

V = velocity of propagation of wave form, $\frac{cm}{sec}$

Y = amplitude, cm.

λ = wave length, $\frac{cm}{cycle}$

t = time, sec.

x = distance traversed by wave form, cm.

y = displacement, cm.

f = frequency, $\frac{cycles}{sec}$

T = period, $\frac{sec}{cycle}$

v = transverse velocity, $\frac{cm}{sec}$

a = transverse acceleration, $\frac{cm}{sec^2}$

g_c = conversion factor, 980 $\frac{dynes}{gm.}$

ρ_o = original gas density, $\frac{gms}{cm^3}$

k = compressibility, $\frac{cm^2}{dyne}$, $\frac{cm\text{-}sec^2}{gm}$ $\left(dyne = \frac{gm\text{-}cm}{sec^2}\right)$

$\gamma = \frac{c_P}{c_V}$

c_P = heat capacity of gas at constant pressure, $\frac{cal}{gm\text{-}^oC}$

c_V = heat capacity of gas at constant volume, $\frac{cal}{gm\text{-}^oC}$

$R = 8.31 \times 10^7 \frac{ergs}{mole\text{-}^oK} = 8.31 \times 10^7 \frac{dyne\text{-}cm}{gm\ mole\text{-}^oK}$

$\left(erg = dyne - cm = \frac{gm\text{-}cm^2}{sec^2}\right)$

T = temperature of gas, ^{o}K.

M = molecular weight of gas, $\frac{gms}{gm\text{-}mole}$

p = pressure, $\frac{dynes}{cm^2}$

p_{max} = maximum pressure caused by sound wave, $\frac{dynes}{cm^2}$

I = intensity, $\frac{erg}{cm^2\text{-}sec}$, $\frac{dyne\text{-}cm}{cm^2\text{-}sec}$ $(10^{-7}\ \frac{watt\text{-}sec}{erg})$

β = sound intensity level, decibels

$I_o = 10^{-16}\ \frac{watts}{cm^2}$

L = reactor length, cm.

n = 1,3,5,7,9,etc.

APPENDIX XI

DESIGN EQUATION FOR

PSEUDO FIRST ORDER REACTION

DESIGN EQUATION FOR PSEUDO FIRST ORDER REACTION

Plug Flow Reactor Design Equation

$$\frac{W}{FA_o} = \int_{X_{A_o}}^{X_{A_f}} \frac{dX_A}{(-r_A)} \qquad (136)$$

W = wt. catalyst, gms.

FA_o = feed rate of A, $\frac{\text{gm moles A}}{\text{sec.}}$

X_{A_o} = initial conversion of A

X_{A_f} = final conversion of A

$(-r_A)$ = reaction rate, $\frac{\text{gm moles A}}{\text{gm cat-sec}}$

Reaction

$$C_6H_5\text{–}CH\text{–}(CH_3)_2 \longrightarrow C_6H_6 + CH_3\text{–}CH{=}CH_2$$

Cumene — Benzene — Propylene

$$A \underset{k'}{\overset{k}{\rightleftharpoons}} R + S$$

Rate Equation

$$(-r_A) = kp_A - k'p_Rp_S \qquad (137)$$

$$p_A = \frac{n_ART}{V} = C_ART$$

$$p_R = \frac{n_RRT}{V} = C_RRT$$

$$p_S = \frac{n_SRT}{V} = C_SRT$$

$$(-r_A) = kRTC_A - k'(RT)^2C_RC_S$$

$(-r_A)$ = reaction rate, $\frac{\text{gm moles A}}{\text{gm cat-sec}}$

p_A, p_R, p_S = partial pressure, atm.

k = forward reaction rate constant for overall reaction, $\frac{\text{gm moles}}{\text{gm cat-atm-sec}}$

k' = reverse reaction rate constant for overall reaction, $\frac{\text{gm moles}}{\text{gm cat-atm}^2\text{-sec}}$

$R = 82.06 \frac{\text{cm}^3\text{-atm}}{\text{gm mole-}^\circ\text{K}}$

$T = {}^\circ K.$

C_A, C_R, C_S = concentration, $\frac{\text{gm moles}}{\text{cm}^3}$

Substitute Rate Equation into Plug Flow Reactor Design Equation

$$\frac{W}{F_{A_o}} = \int_{X_{A_o}}^{X_{A_f}} \frac{dX_A}{kRTC_A - k'(RT)^2C_RC_S} \qquad (138)$$

Assume Pseudo First Order Reversible Reaction

Reaction

$$A \underset{k'_P}{\overset{k_P}{\rightleftharpoons}} R$$

Rate Equation

$$(-r_A) = k_P C_A - k'_P C_R \qquad (139)$$

$$K_P = \frac{k_P}{k'_P} = \frac{C_R}{C_A} = \frac{C_{R_e}}{C_{A_e}}$$

Material Balance

	Inlet	Reactor	Outlet
A	$N_{A_o}=N_{A_o}$	$N_A=N_{A_o}-X_A N_{A_o}$	$N_{A_f}=N_{A_o}-X_{A_f} N_{A_o}$
R	$N_{R_o}=N_{R_o}$	$N_R=N_{R_o}-X_A N_{A_o}$	$N_{R_f}=N_{R_o}+X_{A_f} N_{A_o}$
Total	$N_{A_o}+N_{R_o}$	$N_{A_o}+N_{R_o}$	$N_{A_o}+N_{R_o}$

$$C_A = \frac{N_A}{V} = \frac{N_{A_o}-X_A N_{A_o}}{V} = \frac{N_{A_o}(1-X_A)}{V} = C_{A_o}(1-X_A) = C_{A_o}-C_{A_o}X_A$$

$$C_R = \frac{N_R}{V} = \frac{N_{R_o}+X_A N_{A_o}}{V} = \frac{N_{R_o}}{V} + \frac{N_{A_o}}{V} X_A = C_{R_o} + C_{A_o}X_A$$

Substitution

$$(-r_A) = k_P(C_{A_o}-C_{A_o}X_A) - k'_P(C_{R_o} + C_{A_o}X_A)$$

$$= k_P C_{A_o}(1-X_A) - k'_P C_{A_o}\left[\frac{C_{R_o}}{C_{A_o}} + X_A\right]$$

At Equilibrium

$$k = \frac{k_P}{k'_P} = \frac{C_{R_o} + C_{A_o}X_A}{C_{A_o} - C_{A_o}X_A} = \frac{\frac{C_{R_o}}{C_{A_o}} + X_{A_e}}{1 - X_{A_e}}$$

$$\frac{C_{R_o}}{C_{A_o}} + X_{A_e} = \frac{k_P}{k'_P}(1-X_{A_e})$$

$$\frac{C_{R_o}}{C_{A_o}} = \frac{k_P}{k'_P}(1-X_{A_e}) - X_{A_e}$$

Substitution

$$(-r_A) = k_P C_{A_o}(1-X_A) - k'_P C_{A_o}\left[\frac{k_P}{k'_P}(1-X_{A_e}) - X_{A_e} + X_A\right]$$

$$= k_P C_{A_o} - k_P C_{A_o} X_A - k_P C_{A_o} + k_P C_{A_o} X_{A_e} + k'_P C_{A_o} X_{A_e} - k'_P C_{A_o} X_A$$

$$= k_P(C_{A_o} X_{A_e} - C_{A_o} X_A) + k'_P(C_{A_o} X_{A_e} - C_{A_o} X_A)$$

$$(-r_A) = (k_P + k'_P) C_{A_o}(X_{A_e} - X_A) \qquad (140)$$

Substitute Rate Equation into Plug Flow Reactor Design Equation

$$\frac{W}{F_{A_o}} = \int_{X_{A_o}}^{X_{A_f}} \frac{dX_A}{(k_P + k'_P) C_{A_o}(X_{A_e} - X_A)}$$

Initial rate ($X_A = 0$)

$$r_o = (k_P + k'_P) C_{A_o}(X_{A_e} - X_A) = (k_P + k'_P) C_{A_o} X_{A_e}$$

$$(k_P + k'_P) C_{A_o} = \frac{r_o}{X_{A_e}}$$

$$\frac{W}{F_{A_o}} = \frac{X_{A_e}}{r_o} \int_{X_{A_o}}^{X_{A_f}} \frac{dX_A}{(X_e - X_A)}$$

Integrate

$$\frac{W}{F_{A_o}} = \frac{X_{A_e}}{r_o} \left[-\ln(X_{A_e} - X_A) \right]_{X_{A_o}=0}^{X_{A_f}=X} = \frac{X_{A_e}}{r_o} \left[-\ln\left(\frac{X_{A_e} - X_A}{X_{A_e}}\right) \right]$$

$$= \frac{X_{A_e}}{r_o} \left[-\ln\left(1 - \frac{X_A}{X_{A_e}}\right) \right]$$

$$\frac{W}{F_{A_o}} = \frac{X_{A_e}}{r_o} \ln \left[\frac{1}{1 - \frac{X_A}{X_{A_e}}} \right] \qquad (141)$$

Calculate X_{A_e}

$$K = \frac{\frac{C_{R_o}}{C_{A_o}} + X_{A_e}}{1 - X_{A_e}}$$

$$C_{R_o} = 0$$

$$K = \frac{X_{A_e}}{1 - X_{A_e}}$$

$$X_{A_e} = K - KX_{A_e}$$

$$X_{A_e} = \frac{K}{K + 1}$$

Tabulate Results

T, $^{o}F.$	K, atm.	X_{A_e}
850	2.01	0.626
950	6.21	0.861
1050	15.96	0.942

Plot $\frac{W}{F_{A_o}}$ vs. $\ln\left[\frac{1}{1 - \frac{X_A}{X_{A_e}}}\right]$ as Shown in Figure 80 to Determine r_o

This plot can now be employed to calculate the initial reaction rate, r_o, as a check against the values determined by extrapolation of the reaction rate vs. conversion curves.

FIGURE 80

PSEUDO FIRST ORDER PLOT OF DATA

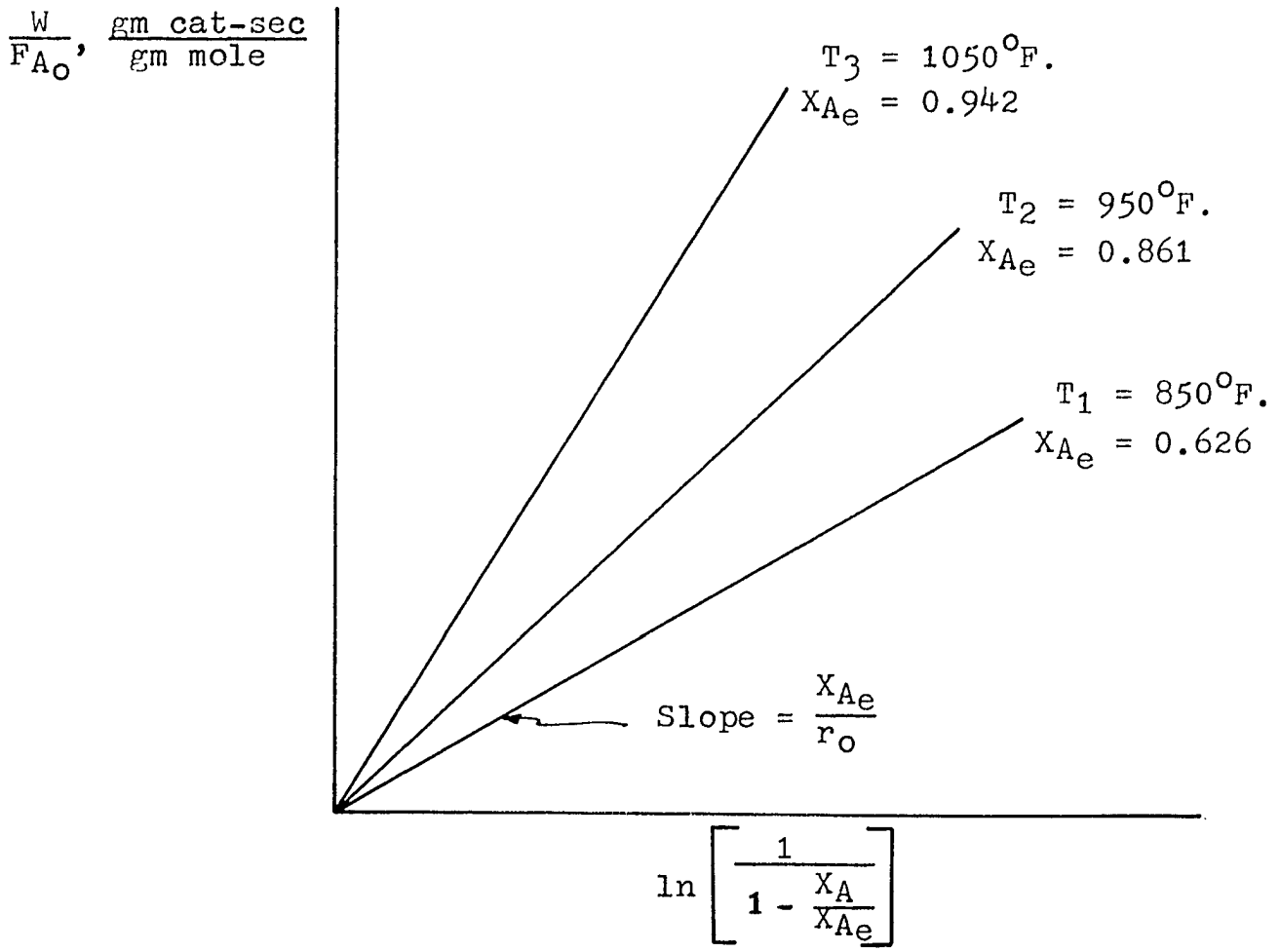

APPENDIX XII

RATIO OF EFFECTIVENESS FACTOR FOR DIFFERENT SIZE CATALYST PARTICLES

RATIO OF EFFECTIVENESS FACTOR FOR DIFFERENT SIZE CATALYST PARTICLES

Reaction Design Equation

$$\frac{W}{F_{A_o}} = \gamma\left[\left(\frac{1}{2\delta} - \frac{1}{2\delta^3}\right)\ln\frac{(1+X_A\delta)}{(1-X_A\delta)} + \frac{X_A}{\delta^2}\right]$$
$$+\beta\left[\frac{1}{2\delta^3}\ln\frac{(1+X_A\delta)}{(1-X_A\delta)} - \frac{1}{2\delta^2}\ln(1-\delta^2X_A^2) - \frac{X_A}{\delta^2}\right] \quad (99)$$

$$\gamma = \frac{1}{\epsilon Lk_2K_A\Pi} + \frac{1}{Lk_2}$$

$$\beta = \frac{2}{\epsilon Lk_2K_A\Pi} + \frac{K_R}{\epsilon Lk_2K_A}$$

$$\delta = \left[1 + \frac{\Pi}{K}\right]^{\frac{1}{2}}$$

At constant conversion, pressure and temperature, δ and X_A are constant and the reaction design equation reduces to the following:

$$\frac{W}{F_{A_o}} = \left[\frac{1}{\epsilon Lk_2K_A\Pi} + \frac{1}{\epsilon Lk_2}\right]C_1 + \left[\frac{2}{\epsilon Lk_2K_A\Pi} + \frac{K_R}{\epsilon Lk\ K_A}\right]C_2$$
$$= \frac{1}{\epsilon}\left\{\left[\frac{1}{Lk_2K_A\Pi} + \frac{1}{Lk_2}\right]C_1 + \left[\frac{2}{Lk_2K_A\Pi} + \frac{K_R}{Lk_2K_A}\right]C_2\right\}$$
$$= \frac{1}{\epsilon}\left[C_3\ C_1 + C_4\ C_2\right]$$
$$= \frac{1}{\epsilon}\ C_5 \quad (142)$$

Ratio of Reciprocal Space Velocity

$$\frac{\left[\frac{W}{FA_o}\right]_1}{\left[\frac{W}{FA_o}\right]_2} = \frac{\frac{C_5}{\epsilon_1}}{\frac{C_5}{\epsilon_2}} = \frac{\epsilon_2}{\epsilon_1} \qquad (143)$$

Plot W/FA_o vs. X_A for Various Size Catalyst Particles as Shown in Figure 81

Plot W/FA_o vs. d_P at Constant X_A and Extrapolate to $d_P = 0$ as Shown in Figure 82

Calculate Effectiveness Factor Employing Example Data

Catalyst No.	d_P cm.	$\frac{W}{FA_o}$, gm cat-sec / gm mole	$= \frac{\left[\frac{W}{FA_o}\right]_0}{\left[\frac{W}{FA_o}\right]}$
0	0	1.1	$\epsilon_0 = \frac{1.1}{1.1} = 1.00$
1	0.045	1.3	$\epsilon_1 = \frac{1.1}{1.3} = 0.85$
2	0.33	5.7	$\epsilon_2 = \frac{1.1}{5.7} = 0.19$
3	0.43	7.6	$\epsilon_3 = \frac{1.1}{7.6} = 0.15$
4	0.53	10.0	$\epsilon_4 = \frac{1.1}{10.0} = 0.11$

FIGURE 81

RECIPROCAL SPACE VELOCITY VS. CONVERSION

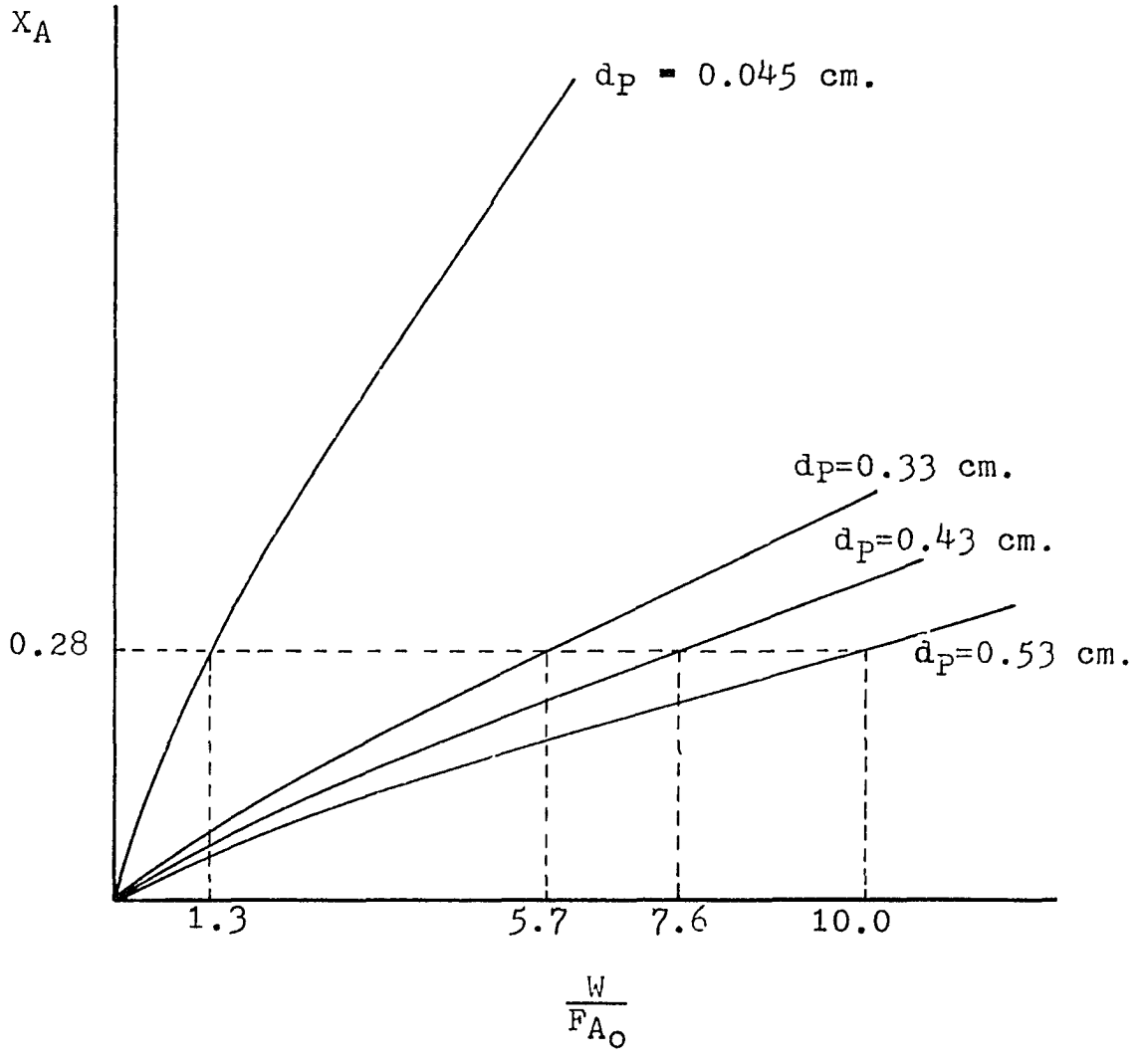

FIGURE 82

RECIPROCAL SPACE VELOCITY VS. CATALYST PARTICLE DIAMETER AT CONSTANT CONVERSION ($X_A = 0.28$)

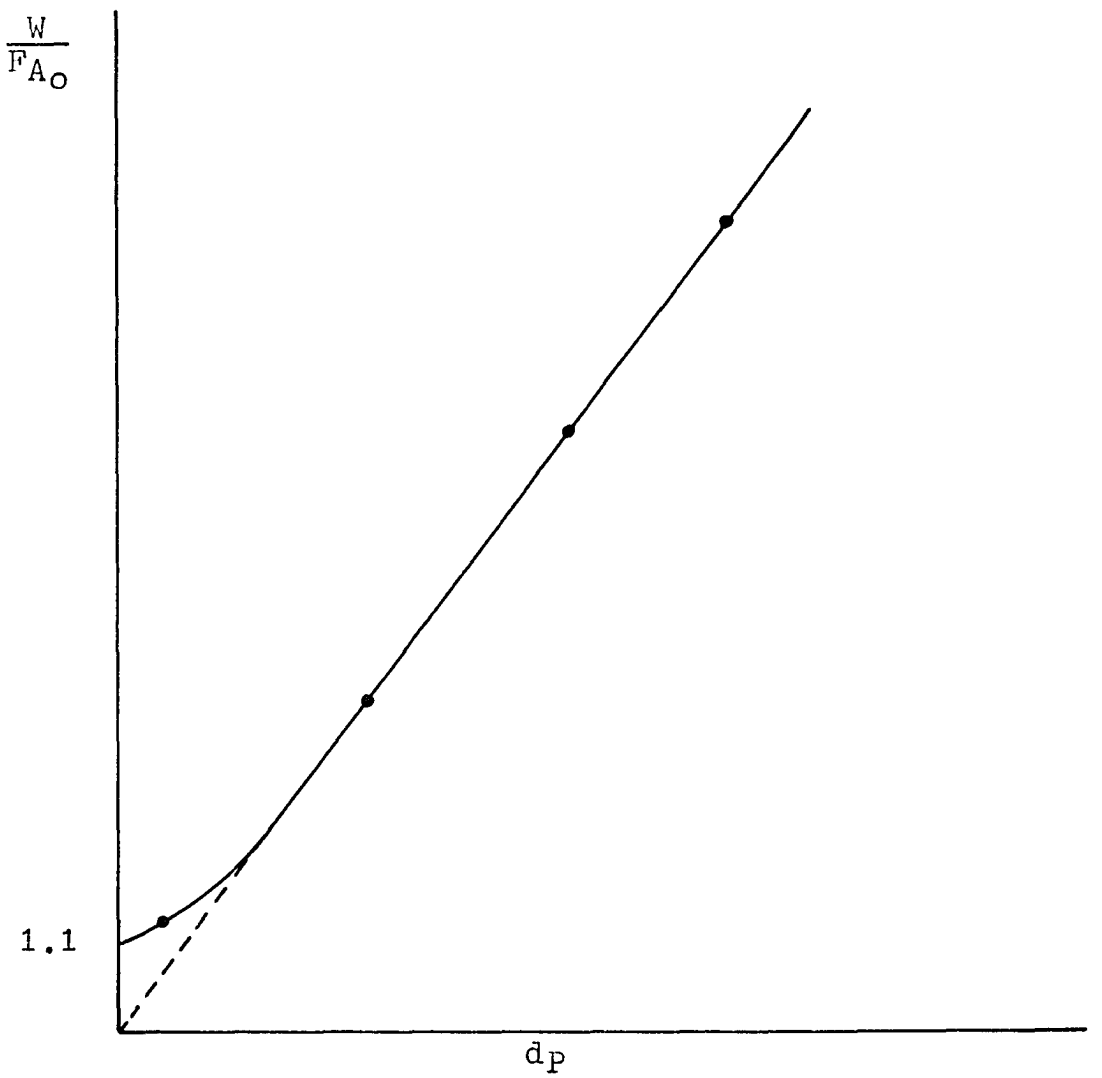

Relationship Between Effectiveness Factor and Catalyst Particle Diameter

Reaction Design Equation

$$\left[\frac{W}{F_{A_o}}\right]_1 = \frac{1}{\epsilon_1} f(X_A) \text{ at constant temperature and pressure} \quad (144)$$

If only the outside surface of the catalyst is effective, then $\epsilon = C_6 a$, where

C_6 = a constant

$$a = \frac{\text{outside surface area of catalyst}}{\text{unit mass}}, \frac{cm^2}{gm}$$

$$= \frac{(4\pi r_p^2 \frac{cm^2}{pellet})}{(\frac{4}{3}\pi r_p^3 \rho_p \frac{gms}{pellet})}$$

$$= \frac{4\pi(\frac{d_p}{2})^2}{\frac{4}{3}\pi(\frac{d_p}{2})^3 \rho_p}$$

$$= \frac{6d_p^2}{d_p^3 \rho_p}$$

$$= \frac{6}{d_p \rho_p}$$

$$= \frac{6C_6}{d_p \rho_p} = \frac{C_7}{d_p}$$

$$d_p = C_7\left[\frac{1}{\epsilon}\right]$$

A plot of d_P vs. $\frac{1}{\epsilon}$ should yield a straight line if this assumption is true as shown in Figure 83.

$$\frac{W}{FA_o} = \frac{1}{\epsilon_1} f(X_A) = \frac{d_{P_1}}{C_7} f(X_A)$$

$$\frac{W}{FA_o d_P} = \frac{1}{C_7} f(X_A) = C_8 f(X_A) \qquad (145)$$

Data for all size catalysts should fall on the curve of $\frac{W}{FA_o d_P}$ vs. X_A.

FIGURE 83

RECIPROCAL EFFECTIVENESS FACTOR VS.
CATALYST PARTICLE DIAMETER

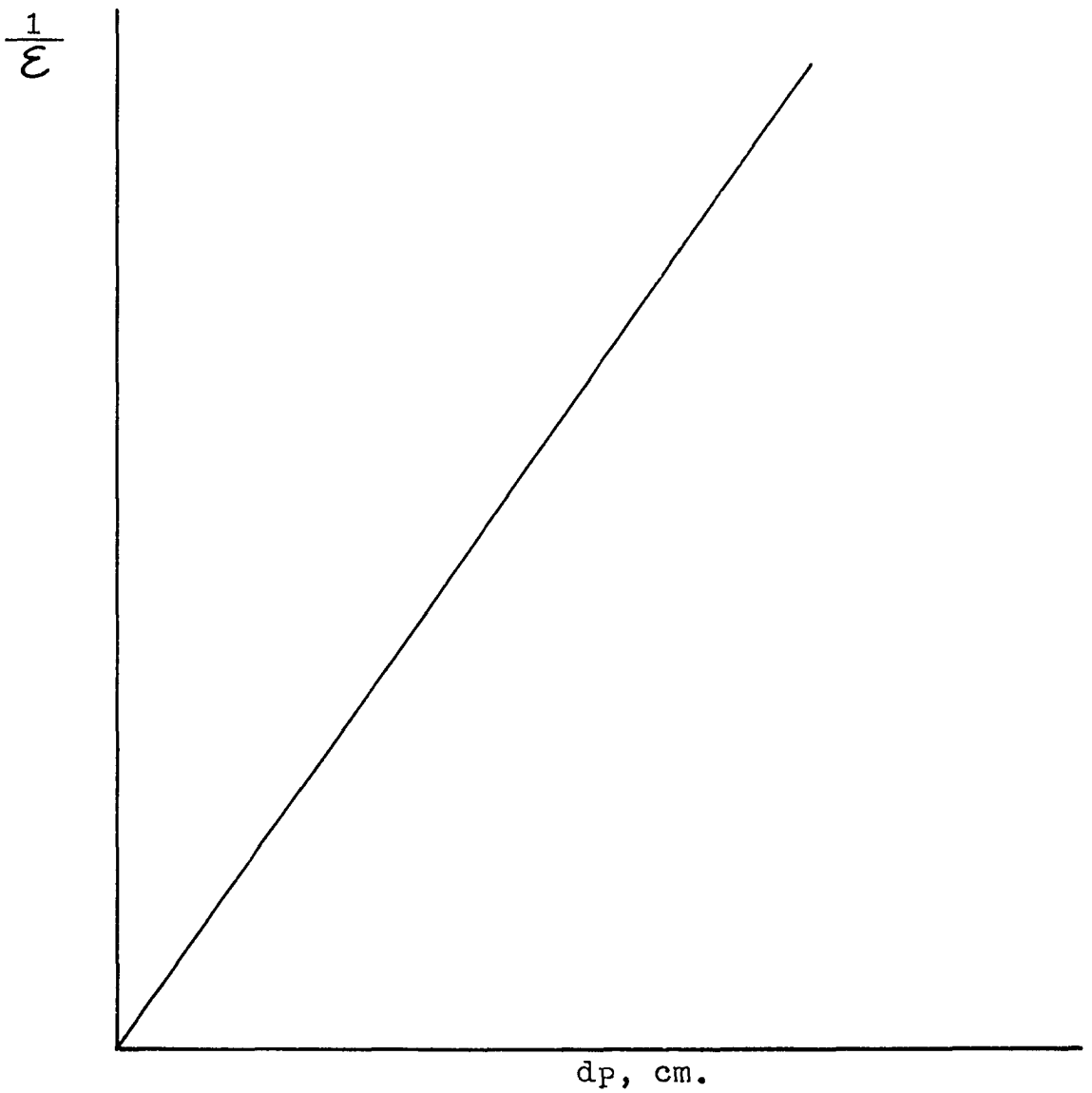

FIGURE 84

CONVERSION VS. $\left[\frac{W}{F_{A_o} d_P}\right]$

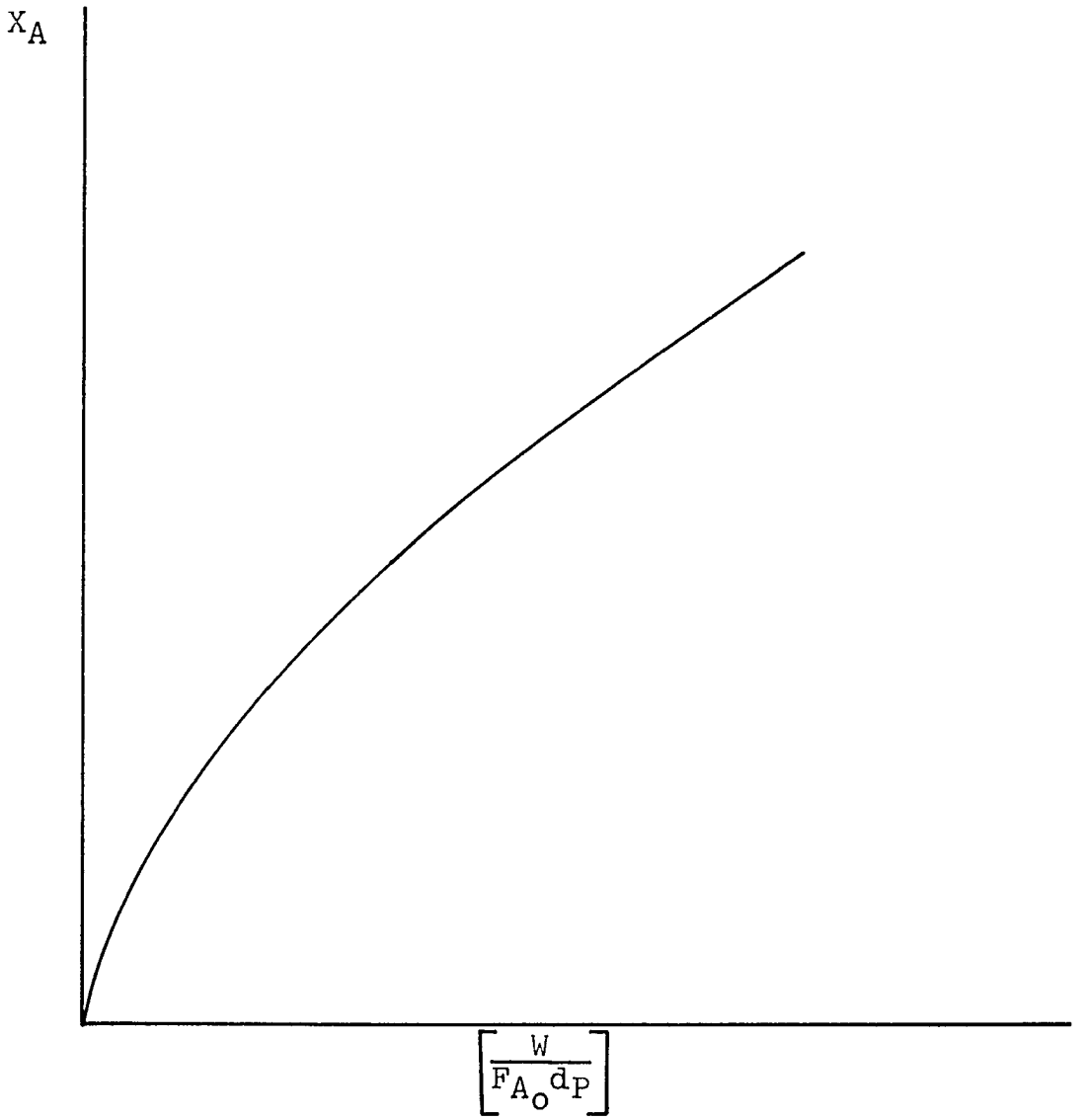

APPENDIX XIII

THE CARBON-OXYGEN REACTION

THE CARBON-OXYGEN REACTION

During several of the initial runs in this study, a problem was encountered with carbonization of the cumene at reaction temperatures of 1000°F. and subsequent plugging of the reactor and fouling of the catalyst. Carbonization was sometimes so severe that it was often very difficult to remove the preheater from the reactor to clean it.

This problem was solved by purging the reactor with air at reaction temperature for 24 hours after each run to burn off the carbon.

The Carbon-Oxygen Reaction Rate Equation

For the reaction

$$C + O_2 \longrightarrow CO_2$$

$$B(S) + A(g) \longrightarrow \text{gaseous product},$$

Parker and Hottell[37] have shown that the rate equation for surface reaction controlling is as follows:

$$-r_B = \frac{4.32 \times 10^{14} C_{A_g}}{T^{\frac{1}{2}}} e^{-\frac{44.000}{RT}} \qquad (146)$$

$r_B = \frac{\text{gm.moles carbon reacted}}{\text{sec-cm}^2}$

$T = {}^{o}K.$

C_{A_g} = concentration of oxygen, $\frac{\text{gm-moles}}{\text{cm}^3}$

$R = 1.98 \frac{\text{cal}}{\text{gm mole-}{}^{o}K}$

Calculation of Rate Constant, k_s

$$k_s = \frac{4.32 \times 10^{14}}{T^{\frac{1}{2}}} \; e^{\frac{-44,000}{RT}}$$

k_s = rate constant, $\frac{cm}{sec}$

$$T^{\frac{1}{2}} = (850^{o}F.)^{\frac{1}{2}} = (727^{o}K)^{\frac{1}{2}} = 27^{o}K^{\frac{1}{2}}$$

$$k_s = \frac{4.32 \times 10^{14}}{27} \; e^{-\frac{44,000 \; \frac{cal}{gm \; mole}}{(1.98 \; \frac{cal}{gm \; mole\text{-}^{o}K})(727^{o}K)}}$$

$$= 0.1598 \times 10^{14} \; e^{-30.6}$$

$$= (0.1598 \times 10^{14})(5.137 \times 10^{-14}) = 0.821 \; \frac{cm}{sec}$$

Calculation of Oxygen Concentration, C_{A_g}

$$C_{A_g} = \frac{(1.0 \text{ atm.})\;(0.21)}{(0.0821 \; \frac{\text{liter-atm.}}{\text{gm mole-}^{o}K})(727^{o}K)(1000 \; \frac{cm^3}{\text{liter}})}$$

$$= 3.52 \times 10^{-6} \; \frac{\text{gm-moles}}{cm^3}$$

Calculation of Reaction Rate

$$-r_B = k_s C_{A_g} = (0.821 \; \frac{cm}{sec})(3.52 \times 10^{-6} \; \frac{\text{gm-moles}}{cm^3})$$

$$= 2.89 \times 10^{-6} \; \frac{\text{gm-moles}}{cm^2\text{-sec}}$$

Calculation of Maximum Weight of Carbon

Assume 5% carbonization at a feed rate of 600 gms./hr. cumene for 30 min.

$$\text{gms. carbon} = \frac{(600\ \frac{\text{gms}}{\text{hr}})(0.05)(0.5\ \text{hrs})(12.011\ \frac{\text{gms}}{\text{gm mole}})}{(120.12\ \frac{\text{gms}}{\text{gm mole}})}$$

$$= 1.5\ \text{gms. carbon}$$

Calculation of Available Surface Area

Reactor

$$S_R = \frac{(0.767\ \text{in})(20.5\ \text{in})}{(2.54\ \frac{\text{cm}}{\text{in}})^2} = 3.26\ \text{cm}^2$$

Preheater

$$S_P = \frac{(0.767\ \text{in})(20.5\ \text{in})}{(2.54\ \frac{\text{cm}}{\text{in}})^2} = 7.66\ \text{cm}^2$$

Catalyst

$$S_C = (13.1\ \frac{\text{cm}^2}{\text{gm}})(5.748\ \text{gms}) = 75.30\ \text{cm}^2$$

Total area = 86.22 cm^2

Required Reaction Time

$$t = \frac{(1.5\ \text{gms})}{(12.011\ \frac{\text{gms}}{\text{gm-mole}})(2.89\text{x}10^{-6}\frac{\text{gm moles}}{\text{cm}^2\text{-sec}})(60\frac{\text{sec}}{\text{min}})(86.22\ \text{cm}^2)}$$

$$= 8.4\ \text{min.}$$

On several occasions, after two 20 minute runs, the reactor was purged at 850°F. for 30 minutes with air. The reactor was subsequently disassembled and found to be essentially free from carbon.

APPENDIX XIV

DATA

DATA

The following Table 12 lists all the data collected in this research. The digits before the decimal point in the Run No. signify a series of runs made at the same temperature. The first or first and second digits after the decimal point signify runs made at the same temperature and feed rate. The last digit after the decimal point signifies the following:

1 - 39,000 cps

2 - 26,000 cps

3 - no ultrasound

A coding system was necessary to avoid confusion since a total of 479 runs were made, involving some 640 samples and 1,920 gas chromatograph analyses.

In every case, a run in the absence of ultrasound was made before and after the application of ultrasound. The analyses reported are the average of six samples, three samples being taken before and three samples after.

The order in which the 39,000 cps and 26,000 cps ultrasonic frequencies were applied were randomly reversed throughout the entire investigation.

Conversions were calculated from liquid samples, but were checked often against gas samples taken directly from the reactor.

Figure 85 illustrates an actual data sheet.

FIGURE 85

DATA SHEET

Run No.	16.1		Reactor Diameter, cm.					0.992
Date	5-1-72		Frequency, cps					39,26
Catalyst, gms.	5.748		Power, watts					25
Bed Height, cm.	10.158		Feed Tank Diameter, in.					1
Time	1225	1245	1330	1350	1410	1430	1450	1510
Tank Height, in.	32.85	32.85	31.05	30.40	29.70	29.00	28.20	-
Rotameter, mm.	-	26	26	26	26	26	26	-
Rota. Feed Rate, gms/hr.	-	25	25	25	25	25	25	-
Tank Feed Rate, gms/hr.	-	-	-	-	-	-	24	-
Heater No. 1	40	40	40	40	40	40	40	40
Heater No. 2	40	40	40	40	40	40	40	40
Heater No. 3	40	40	40	40	40	40	40	40
Heater No. 4 and No. 5	40	40	40	40	40	40	40	40
Hot Oil Heater	110	110	110	110	110	110	110	110
TI-1, °F.	70	70	70	70	70	70	70	70
TI-2, °F.	710	710	710	710	710	710	710	710
TI-3, °F.	750	750	750	750	750	750	750	750
TI-4, °F.	750	750	750	750	750	750	750	750
TI-5, °F.	750	750	750	750	750	750	750	750
TI-6, °F.	750	750	750	750	750	750	750	750
TI-7, °F. (Hot Oil)	350	348	346	348	350	352	354	352
TC-1, °F.	750	750	750	750	750	750	750	750
Ultrasound	off	off	off	off	26	39	off	-
W/F, gm cat-sec/gm mole	-	-	-	-	-	-	102,900	-
Cumene, %	-	-	-	82.66	77.98	76.15	83.16	-
Benzene, %	-	-	-	15.69	20.40	22.23	15.24	
Propylene, %	-	-	-	1.65	1.62	1.62	1.60	-
Conversion, X	-	-	-	22.6	28.7	31.0	22.0	-
Nitrogen Purge	on	off	off	off	off	off	on	off
Air Purge	off	off	off	off	off	off	off	on

TABLE 12

TABULATION OF DATA

Run No.	Catalyst gms.	Bed Ht. cm.	Bed Dia. cm.	Ultrasound cps	Ultrasound watts	Feed Rate gms/hr	W/F gm cat-sec / gm mole	Temp. °F.	X Conversion %
3.11	5.7	10.2	0.992	-	-	194	12,730	850	29.1
3.12	5.7	10.2	0.992	-	-	102	24,200	850	30.9
3.21	5.7	10.2	0.992	-	-	293	8,430	850	15.8
3.22	5.7	10.2	0.992	-	-	387	6,380	850	9.1
3.31	5.7	10.2	0.992	-	-	500	4,930	850	9.8
3.32	5.7	10.2	0.992	-	-	589	4,200	850	3.2
3.41	5.7	10.2	0.992	-	-	99	25,000	950	39.7
3.42	5.7	10.2	0.992	-	-	198	12,480	950	26.5
3.51	5.7	10.2	0.992	-	-	304	8,125	950	19.0
3.52	5.7	10.2	0.992	-	-	387	6,380	950	6.6
3.61	5.7	10.2	0.992	-	-	496	4,980	950	13.5
3.62	5.7	10.2	0.992	-	-	589	4,190	950	4.2
3.71	5.7	10.2	0.992	-	-	97	25,500	1050	51.3
3.72	5.7	10.2	0.992	-	-	194	12,750	1050	32.3
3.81	5.7	10.2	0.992	-	-	302	8,170	1050	23.4
3.82	5.7	10.2	0.992	-	-	407	6,075	1050	17.9
3.91	5.7	10.2	0.992	-	-	511	4,830	1050	14.8
3.92	5.7	10.2	0.992	-	-	600	4,120	1050	9.1
5.11	0.958	1.693	0.992	39,000	25	99	4,180	850	7.86
5.12	0.958	1.693	0.992	26,000	25	99	4,180	850	6.67
5.13	0.958	1.693	0.992	-	-	99	4,180	850	6.20
5.21	0.958	1.693	0.992	39,000	25	193	2,150	850	3.73
5.22	0.958	1.693	0.992	26,000	25	193	2,150	850	3.01
5.23	0.958	1.693	0.992	-	-	193	2,150	850	2.87

TABLE 12 (continued)

TABULATION OF DATA

Run No.	Catalyst gms.	Bed Ht. cm.	Bed Dia. cm.	Ultrasound cps	Ultrasound watts	Feed Rate gms/hr	W/F gm cat-sec / gm mole	Temp. °F.	X Conversion %
5.31	0.958	1.693	0.992	39,000	25	296	1,400	850	2.35
5.32	0.958	1.693	0.992	26,000	25	296	1,400	850	2.15
5.33	0.958	1.693	0.992	-	-	296	1,400	850	1.65
5.41	0.958	1.693	0.992	39,000	25	392	1,158	850	1.32
5.42	0.958	1.693	0.992	26,000	25	392	1,158	850	1.15
5.43	0.958	1.693	0.992	-	-	392	1,158	850	0.763
5.51	0.958	1.693	0.992	39,000	25	501	827	850	0.429
5.52	0.958	1.693	0.992	26,000	25	501	827	850	0.275
5.53	0.958	1.693	0.992	-	-	501	827	850	0.238
5.61	0.958	1.693	0.992	39,000	25	586	707	850	0.816
5.62	0.958	1.693	0.992	26,000	25	586	707	850	0.669
5.63	0.958	1.693	0.992	-	-	586	707	850	0.505
6.11	0.958	1.693	0.992	39,000	25	99	4,180	950	7.02
6.12	0.958	1.693	0.992	26,000	25	99	4,180	950	5.69
6.13	0.958	1.693	0.992	-	-	99	4,180	950	5.30
6.21	0.958	1.693	0.992	39,000	25	192	2,150	950	3.06
6.22	0.958	1.693	0.992	26,000	25	192	2,150	950	3.01
6.23	0.958	1.693	0.992	-	-	192	2,150	950	3.26
6.31	0.958	1.693	0.992	39,000	25	285	1,453	950	2.03
6.32	0.958	1.693	0.992	26,000	25	285	1,453	950	1.80
6.33	0.958	1.693	0.992	-	-	285	1,453	950	1.62
6.41	0.958	1.693	0.992	39,000	25	382	1,083	950	0.734
6.42	0.958	1.693	0.992	26,000	25	382	1,083	950	0.616
6.43	0.958	1.693	0.992	-	-	382	1,083	950	0.671

TABLE 12 (continued)

TABULATION OF DATA

Run No.	Catalyst gms.	Bed Ht. cm.	Bed Dia. cm.	Ultrasound cps	Ultrasound watts	Feed Rate gms/hr	W/F gm cat-sec / gm mole	Temp. °F.	X Conversion %
6.51	0.958	1.693	0.992	39,000	25	491	843	950	0.691
6.52	0.958	1.693	0.992	26,000	25	491	843	950	0.492
6.53	0.958	1.693	0.992	-	-	491	843	950	0.326
6.61	0.958	1.693	0.992	39,000	25	593	698	950	0.277
6.62	0.958	1.693	0.992	26,000	25	593	698	950	0.249
6.63	0.958	1.693	0.992	-	-	593	698	950	0.258
7.11	0.958	1.693	0.992	39,000	25	98	4,225	1050	5.39
7.12	0.958	1.693	0.992	26,000	25	98	4,225	1050	4.01
7.13	0.958	1.693	0.992	-	-	98	4,225	1050	3.98
7.21	0.958	1.693	0.992	39,000	25	211	1,963	1050	2.50
7.22	0.958	1.693	0.992	26,000	25	211	1,963	1050	2.70
7.23	0.958	1.693	0.992	-	-	211	1,963	1050	3.95
8.11	0.958	1.693	0.992	39,000	25	98	4,230	1050	5.97
8.12	0.958	1.693	0.992	26,000	25	98	4,230	1050	5.35
8.13	0.958	1.693	0.992	-	-	98	4,230	1050	5.17
8.21	0.958	1.693	0.992	39,000	25	205	2,020	1050	2.76
8.22	0.958	1.693	0.992	26,000	25	205	2,020	1050	2.21
8.23	0.958	1.693	0.992	-	-	205	2,020	1050	2.32
8.31	0.958	1.693	0.992	39,000	25	304	1,363	1050	1.59
8.32	0.958	1.693	0.992	26,000	25	304	1,363	1050	1.53
8.33	0.958	1.693	0.992	-	-	304	1,363	1050	2.06
9.11	1.916	3.386	0.992	39,000	25	92	8,980	950	16.62
9.12	1.916	3.386	0.992	26,000	25	92	8,980	950	13.56
9.13	1.916	3.386	0.992	-	-	92	8,980	950	12.26

TABLE 12 (continued)

TABULATION OF DATA

Run No.	Catalyst gms.	Bed Ht. cm.	Bed Dia. cm.	Ultrasound cps	Ultrasound watts	Feed Rate gms/hr	W/F gm cat-sec / gm mole	Temp. °F.	X Conversion %
9.21	1.916	3.386	0.992	39,000	25	202	4,090	950	6.33
9.22	1.916	3.386	0.992	26,000	25	202	4,090	950	6.53
9.23	1.916	3.386	0.992	-	-	202	4,090	950	7.00
9.31	1.916	3.386	0.992	39,000	25	306	2,980	950	5.17
9.32	1.916	3.386	0.992	26,000	25	306	2,980	950	4.97
9.33	1.916	3.386	0.992	-	-	306	2,980	950	4.97
9.41	1.916	3.386	0.992	39,000	25	422	1,965	950	3.08
9.42	1.916	3.386	0.992	26,000	25	422	1.965	950	2.59
9.43	1.916	3.386	0.992	-	-	422	1,965	950	2.38
9.51	1.916	3.386	0.992	39,000	25	495	1,673	950	1.54
9.52	1.916	3.386	0.992	26,000	25	497	1,673	950	1.52
9.53	1.916	3.386	0.992	-	-	495	1,673	950	1.41
9.61	1.916	3.386	0.992	39,000	25	606	1,368	950	1.88
9.62	1.916	3.386	0.992	26,000	25	606	1,368	950	1.69
9.63	1.916	3.386	0.992	-	-	606	1,368	950	1.46
10.11	1.916	3.386	0.992	39,000	25	112	7,390	850	6.09
10.12	1.916	3.386	0.992	26,000	25	112	7,390	850	4.79
10.13	1.916	3.386	0.992	-	-	112	7,390	850	5.12
10.21	1.916	3.386	0.992	39,000	25	203	4,080	850	4.30
10.22	1.916	3.386	0.992	26,000	25	203	4,080	850	3.85
10.23	1.916	3.386	0.992	-	-	203	4,080	850	3.57
10.31	1.916	3.386	0.992	39,000	25	310	2,670	850	2.14
10.32	1.916	3.386	0.992	26,000	25	310	2,670	850	2.34
10.33	1.916	3.386	0.992	-	-	310	2,670	850	2.00

TABLE 12 (continued)

TABULATION OF DATA

Run No.	Catalyst gms.	Bed Ht. cm.	Bed Dia. cm.	Ultrasound cps	Ultrasound watts	Feed Rate gms/hr	W/F gm cat-sec / gm mole	Temp. °F.	X Conversion %
10.41	1.916	3.386	0.992	39,000	25	393	2,110	850	1.97
10.42	1.916	3.386	0.992	26,000	25	393	2,110	850	1.67
10.43	1.916	3.386	0.992	-	-	393	2,110	850	1.53
10.51	1.916	3.386	0.992	39,000	25	484	1,714	850	1.29
10.52	1.916	3.386	0.992	26,000	25	484	1,714	850	1.09
10.53	1.916	3.386	0.992	-	-	484	1,714	850	0.840
10.61	1.916	3.386	0.992	39,000	25	609	1,370	850	0.637
10.62	1.916	3.386	0.992	26,000	25	609	1,370	850	0.415
10.63	1.916	3.386	0.992	-	-	609	1,370	850	0.498
11.11	5.748	10.158	0.992	39,000	25	108	23,100	1000	29.3
11.12	5.748	10.158	0.992	26,000	25	108	23,100	1000	26.3
11.13	5.748	10.158	0.992	-	-	108	23,100	1000	24.2
11.21	5.748	10.158	0.992	39,000	25	208	11,950	1000	21.2
11.22	5.748	10.158	0.992	26,000	25	208	11,950	1000	24.1
11.23	5.748	10.158	0.992	-	-	208	11,950	1000	23.6
11.31	5.748	10.158	0.992	39,000	25	302	8,250	1000	17.7
11.32	5.748	10.158	0.992	26,000	25	302	8,250	1000	16.8
11.33	5.748	10.158	0.992	-	-	302	8,250	1000	16.8
11.41	5.748	10.158	0.992	39,000	25	426	5,840	1000	13.0
11.42	5.748	10.158	0.992	26,000	25	426	5,840	1000	12.5
11.43	5.748	10.158	0.992	-	-	426	5,840	1000	13.6
11.51	5.748	10.158	0.992	39,000	25	484	5,150	1000	12.1
11.52	5.748	10.158	0.992	26,000	25	484	5,150	1000	10.6
11.53	5.748	10.158	0.992	-	-	484	5,150	1000	11.0

TABLE 12 (continued)

TABULATION OF DATA

Run No.	Catalyst gms.	Bed Ht. cm.	Bed Dia. cm.	Ultrasound cps	Ultrasound watts	Feed Rate gms/hr	W/F gm cat-sec / gm mole	Temp. °F.	X Conversion %
11.61	5.748	10.158	0.992	39,000	25	593	4,200	1000	8.49
11.62	5.748	10.158	0.992	26,000	25	593	4,200	1000	8.39
11.63	5.748	10.158	0.992	-	-	593	4,200	1000	7.94
12.11	5.478	10.158	0.992	39,000	25	101	24,600	950	27.2
12.12	5.748	10.158	0.992	26,000	25	101	24,600	950	22.9
12.13	5.748	10.158	0.992	-	-	101	24,600	950	22.0
12.21	5.748	10.158	0.992	39,000	25	201	13,400	950	16.1
12.22	5.748	10.158	0.992	26,000	25	201	13,400	950	16.0
12.23	5.748	10.158	0.992	-	-	201	12,400	950	16.0
12.31	5.748	10.158	0.992	39,000	25	321	7,750	950	14.4
12.32	5.748	10.158	0.992	26,000	25	321	7,750	950	12.4
12.33	5.748	10.158	0.992	-	-	321	7,750	950	11.9
12.41	5.748	10.158	0.992	39,000	25	417	5,975	950	10.6
12.42	5.748	10.158	0.992	26,000	25	417	5,975	950	10.1
12.43	5.748	10.158	0.992	-	-	417	5,975	950	9.93
12.51	5.748	10.158	0.992	39,000	25	483	5,150	950	9.32
12.52	5.748	10.158	0.992	26,000	25	483	5,150	950	9.67
12.53	5.748	10.158	0.992	-	-	483	5,150	950	8.97
12.61	5.748	10.158	0.992	39,000	25	589	4,230	950	8.08
12.62	5.748	10.158	0.992	26,000	25	589	4,230	950	8.13
12.63	5.748	10.158	0.992	-	-	589	4,230	950	7.62
13.11	5.748	10.158	0.992	39,000	25	102	24,400	900	13.1
13.12	5.748	10.158	0.992	26,000	25	102	24,400	900	11.8
13.13	5.748	10.158	0.992	-	-	102	24,400	900	12.0
13.21	5.748	10.158	0.992	39,000	25	212	11,730	900	11.6

TABLE 12 (continued)

TABULATION OF DATA

Run No.	Catalyst gms.	Bed Ht. cm.	Bed Dia. cm.	Ultrasound cps	Ultrasound watts	Feed Rate gms/hr	W/F gm cat-sec / gm mole	Temp. °F.	X Conversion %
13.22	5.748	10.158	0.992	26,000	25	212	11,730	900	10.6
13.23	5.748	10.158	0.992	-	-	212	11,730	900	9.88
13.31	5.748	10.158	0.992	39,000	25	331	7,520	900	10.5
13.32	5.748	10.158	0.992	26,000	25	331	7,520	900	9.71
13.33	5.748	10.158	0.992	-	-	331	7,520	900	9.78
13.41	5.748	10.158	0.992	39,000	25	425	5,870	900	7.98
13.42	5.748	10.158	0.992	26,000	25	425	5,870	900	8.37
13.43	5.748	10.158	0.992	-	-	425	5,870	900	8.18
13.51	5.748	10.158	0.992	39,000	25	510	4,880	900	6.73
13.52	5.748	10.158	0.992	26,000	25	510	4,880	900	6.04
13.53	5.748	10.158	0.992	-	-	510	4,880	900	6.64
13.61	5.748	10.158	0.992	39,000	25	639	3,900	900	7.04
13.62	5.748	10.158	0.992	26,000	25	639	3,900	900	5.92
13.63	5.748	10.158	0.992	-	-	639	3,900	900	5.63
14.11	5.748	10.158	0.992	39,000	25	38	65,500	850	30.4
14.12	5.748	10.158	0.992	26,000	25	38	65,500	850	21.3
14.13	5.748	10.158	0.992	-	-	38	65,500	850	20.5
14.21	5.748	10.158	0.992	39,000	25	87	28,600	850	26.7
14.22	5.748	10.158	0.992	26,000	25	87	28,600	850	26.1
14.23	5.748	10.158	0.992	-	-	87	28,600	850	26.5
14.31	5.748	10.158	0.992	39,000	25	103	24,200	850	24.0
14.32	5.748	10.158	0.992	26,000	25	103	24,200	850	21.4
14.33	5.748	10.158	0.992	-	-	103	24,200	850	20.3
14.41	5.748	10.158	0.992	39,000	25	220	11,320	850	15.0
14.42	5.748	10.158	0.992	26,000	25	220	11,320	850	13.9

TABLE 12 (continued)

TABULATION OF DATA

Run No.	Catalyst gms.	Bed Ht. cm.	Bed Dia. cm.	Ultrasound cps	Ultrasound watts	Feed Rate gms/hr	W/F gm cat-sec / gm mole	Temp. °F.	X Conversion %
14.43	5.748	10.158	0.992	-	-	220	11,320	850	12.4
14.51	5.748	10.158	0.992	39,000	25	293	8,480	850	10.3
14.52	5.748	10.158	0.992	26,000	25	293	8,480	850	9.08
14.53	5.748	10.158	0.992	-	-	293	8,480	850	9.20
14.61	5.748	10.158	0.992	39,000	25	388	6,409	850	8.52
14.62	5.748	10.158	0.992	26,000	25	388	6,409	850	6.93
14.63	5.748	10.158	0.992	-	-	388	6,409	850	6.22
14.71	5.748	10.158	0.992	39,000	25	526	4,730	850	5.78
14.72	5.748	10.158	0.992	26,000	25	526	4,730	850	5.58
14.73	5.748	10.158	0.992	-	-	526	4,730	850	5.61
14.81	5.748	10.158	0.992	39,000	25	593	4,200	850	7.47
14.82	5.748	10.158	0.992	26,000	25	593	4,200	850	5.92
14.83	5.748	10.158	0.992	-	-	593	4,200	850	4.51
13.71	5.748	10.158	0.992	39,000	25	25	99,500	900	26.1
13.72	5.748	10.158	0.992	26,000	25	25	99,500	900	22.3
13.73	5.748	10.158	0.992	-	-	25	99,500	900	23.9
13.81	5.748	10.158	0.992	39,000	25	45	54,800	900	28.1
13.82	5.748	10.158	0.992	26,000	25	45	54,800	900	23.6
13.83	5.748	10.158	0.992	-	-	45	54,800	900	21,5
12.71	5.748	10.158	0.992	39,000	25	28	90,500	950	63.3
12.72	5.748	10.158	0.992	26,000	25	28	90,500	950	51.2
12.73	5.748	10.158	0.992	-	-	28	90,500	950	43.2
12.81	5.748	10.158	0.992	39,000	25	32	77,100	950	52.6
12.82	5.748	10.158	0.992	26,000	25	32	77,100	950	44.1
12.83	5.748	10.158	0.992	-	-	32	77,100	950	36.1

TABLE 12 (continued)

TABULATION OF DATA

Run No.	Catalyst gms.	Bed Ht. cm.	Bed Dia. cm.	Ultrasound cps	Ultrasound watts	Feed Rate gms/hr	W/F gm cat-sec / gm mole	Temp. °F.	X Conversion %
15.11	5.748	10.158	0.992	39,000	25	23	111,000	800	57.2
15.12	5.748	10.158	0.992	26,000	25	23	111,000	800	49.3
15.13	5.748	10.158	0.992	-	-	23	111,000	800	48.9
15.21	5.748	10.158	0.992	39,000	25	34	73,300	800	33.9
15.22	5.748	10.158	0.992	26,000	25	34	73,300	800	30.2
15.23	5.748	10.158	0.992	-	-	34	73,300	800	28.9
15.31	5.748	10.158	0.992	39,000	25	103	24,100	800	34.5
15.32	5.748	10.158	0.992	26,000	25	103	24,100	800	27.9
15.33	5.748	10.158	0.992	-	-	103	24,100	800	26.3
15.41	5.748	10.158	0.992	39,000	25	187	13,350	800	20.9
15.42	5.748	10.158	0.992	26,000	25	187	13,350	800	18.2
15.43	5.748	10.158	0.992	-	-	187	13.350	800	15.7
15.51	5.748	10.158	0.992	39,000	25	291	8,570	800	12.0
15.52	5.748	10.158	0.992	26,000	25	291	8,570	800	9.80
15.53	5.748	10.158	0.992	-	-	291	8,570	800	9.34
15.61	5.748	10.158	0.992	39,000	25	391	6,375	800	8.68
15.62	5.748	10.158	0.992	26,000	25	391	6,375	800	7.18
15.63	5.748	10.158	0.992	-	-	391	6,375	800	5.68
15.71	5.748	10.158	0.992	39,000	25	499	5,000	800	7.39
15.72	5.748	10.158	0.992	26,000	25	499	5,000	800	5.66
15.73	5.748	10.158	0.992	-	-	499	5,000	800	4.32
15.81	5.748	10.158	0.992	39,000	25	618	4,030	800	5.56
15.82	5.748	10.158	0.992	26,000	25	618	4,030	800	4.93
15.83	5.748	10.158	0.992	-	-	618	4,030	800	4.07

TABLE 12 (continued)

TABULATION OF DATA

Run No.	Catalyst gms.	Bed Ht. cm.	Bed Dia. cm.	Ultrasound cps	Ultrasound watts	Feed Rate gms/hr	W/F gm cat-sec / gm mole	Temp. °F.	X Conversion %
16.11	5.748	10.158	0.992	39,000	25	24	102,900	750	31.0
16.12	5.748	10.158	0.992	26,000	25	24	102.900	750	28.7
16.13	5.748	10.158	0.992	-	-	24	102,900	750	22.3
16.21	5.748	10.158	0.992	39,000	25	42	59,300	750	31.7
16.22	5.748	10.158	0.992	26,000	25	42	59,300	750	26.5
16.23	5.748	10.158	0.992	-	-	42	59,300	750	26.5
16.31	5.748	10.158	0.992	39,000	25	101	24,600	750	19.4
16.32	5.748	10.158	0.992	26,000	25	101	24,600	750	17.9
16.33	5.748	10.158	0.992	-	-	101	24,600	750	16.7
16.41	5.748	10.158	0.992	39,000	25	196	12,700	750	13.8
16.42	5.748	10.158	0.992	26,000	25	196	12,700	750	7.63
16.43	5.748	10.158	0.992	-	-	196	12,700	750	6.89
16.51	5.748	10.158	0.992	39,000	25	282	8,830	750	9.96
16.52	5.748	10.158	0.992	26,000	25	282	8,830	750	6.77
16.53	5.748	10.158	0.992	-	-	282	8,830	750	5.77
16.61	5.748	10.158	0.992	39,000	25	438	5,680	750	5.80
16.62	5.748	10.158	0.992	26,000	25	438	5,680	750	3.99
16.63	5.748	10.158	0.992	-	-	438	5,680	750	3.51
16.71	5.748	10.158	0.992	39,000	25	511	4,870	750	3.96
16.73	5.748	10.158	0.992	-	-	511	4,870	750	2.52
16.81	5.748	10.158	0.992	39,000	25	600	4,150	750	5.43
16.82	5.748	10.158	0.992	26,000	25	600	4,150	750	2.92
16.83	5.748	10.158	0.992	-	-	600	4,150	750	1.73
17.11	5.748	10.158	0.992	39,000	25	22	113,300	700	25.7
17.12	5.748	10.158	0.992	26,000	25	22	113,300	700	21.1

TABLE 12 (continued)

TABULATION OF DATA

Run No.	Catalyst gms.	Bed Ht. cm.	Bed Dia. cm.	Ultrasound cps	Ultrasound watts	Feed Rate gms/hr	W/F gm cat-sec / gm mole	Temp. °F.	X Conversion %
17.13	5.748	10.158	0.992	-	-	22	113,300	700	19.7
17.21	5.748	10.158	0.992	39,000	25	48	51,300	700	13.7
17.22	5.748	10.158	0.992	26,000	25	48	51.300	700	12.8
17.23	5.748	10.158	0.992	-	-	48	51,300	700	11.7
17.31	5.748	10.158	0.992	39,000	25	104	23,900	700	8.64
17.32	5.748	10.158	0.992	26,000	25	104	23,900	700	7.48
17.33	5.748	10.158	0.992	-	-	104	23,900	700	7.04
17.41	5.748	10.158	0.992	39,000	25	196	12,750	700	6.83
17.42	5.748	10.158	0.992	26,000	25	196	12,750	700	4.83
17.43	5.748	10.158	0.992	-	-	196	12,750	700	4.13
17.51	5.748	10.158	0.992	39,000	25	306	8,125	700	4.55
17.52	5.748	10.158	0.992	26,000	25	306	8,125	700	3.23
17.53	5.748	10.158	0.992	-	-	306	8,125	700	3.11
17.61	5.748	10.158	0.992	39,000	25	411	6,040	700	3.41
17.62	5.748	10.158	0.992	26,000	25	411	6,040	700	2.12
17.63	5.748	10.158	0.992	-	-	411	6,040	700	1.77
17.71	5.748	10.158	0.992	39,000	25	498	5,000	700	2.00
17.72	5.748	10.158	0.992	26,000	25	498	5,000	700	1.36
17.73	5.748	10.158	0.992	-	-	498	5,000	700	1.05
17.81	5.748	10.158	0.992	39,000	25	610	4,080	700	1.74
17.82	5.748	10.158	0.992	26,000	25	610	4,080	700	0.992
17.83	5.748	10.158	0.992	-	-	610	4,080	700	0.871
18.11	5.748	10.158	0.992	39,000	25	24	106,000	650	8.26
18.12	5.748	10.158	0.992	26,000	25	24	106,000	650	6.62
18.13	5.748	10.158	0.992	-	-	24	106,000	650	5.87

TABLE 12 (continued)

TABULATION OF DATA

Run No.	Catalyst gms.	Bed Ht. cm.	Bed Dia. cm.	Ultrasound cps	Ultrasound watts	Feed Rate gms/hr	W/F gm cat-sec / gm mole	Temp. °F.	X Conversion %
18.21	5.748	10.158	0.992	39,000	25	47	53,250	650	2.65
18.22	5.748	10.158	0.992	26,000	25	47	53,250	650	1.87
18.23	5.748	10.158	0.992	-	-	47	53,250	650	1.73
18.31	5.748	10.158	0.992	39,000	25	102	24,400	650	4.08
18.32	5.748	10.158	0.992	26,000	25	102	24,400	650	2.99
18.33	5.748	10.158	0.992	-	-	102	24,400	650	1.96
18.41	5.748	10.158	0.992	39,000	25	203	12,250	650	2.26
18.42	5.748	10.158	0.992	26,000	25	203	12,250	650	1.03
18.43	5.748	10.158	0.992	-	-	203	12,250	650	1.03
18.51	5.748	10.158	0.992	39,000	25	307	8,125	650	0.798
18.52	5.748	10.158	0.992	26,000	25	307	8,125	650	0.483
18.53	5.748	10.158	0.992	-	-	307	8,125	650	0.698
18.61	5.748	10.158	0.992	39,000	25	402	6,190	650	1.66
18.62	5.748	10.158	0.992	26,000	25	402	6,190	650	0.686
18.63	5.748	10.158	0.992	-	-	402	6,190	650	0.418
19.11	5.748	10.158	0.992	39,000	25	31	81,000	650	8.03
19.12	5.748	10.158	0.992	26,000	25	31	81,000	650	5.76
19.13	5.748	10.158	0.992	-	-	31	81,000	650	5.76
19.21	5.748	10.158	0.992	39,000	25	74	33,900	650	2.10
19.22	5.748	10.158	0.992	26,000	25	74	33,900	650	1.20
19.23	5.748	10.158	0.992	-	-	74	33,900	650	0.823
19.31	5.748	10.158	0.992	39,000	25	224	11,110	650	0.493
19.32	5.748	10.158	0.992	26,000	25	224	11,110	650	0.249
19.33	5.748	10.158	0.992	-	-	224	11,110	650	0.229

TABLE 12 (continued)

TABULATION OF DATA

Run No.	Catalyst gms.	Bed Ht. cm.	Bed Dia. cm.	Ultrasound cps	Ultrasound watts	Feed Rate gms/hr	W/F gm cat-sec/gm mole	Temp. °F.	X Conversion %
19.41	5.748	10.158	0.992	39,000	25	330	7,550	650	1.31
19.42	5.748	10.158	0.992	26,000	25	330	7,550	650	0.790
19.43	5.748	10.158	0.992	-	-	330	7,550	650	0.623
18.71	5.748	10.158	0.992	39,000	25	480	5,190	650	0.433
18.72	5.748	10.158	0.992	26,000	25	480	5,190	650	0.175
18.73	5.748	10.158	0.992	-	-	480	5,190	650	0.080
18.81	5.748	10.158	0.992	39,000	25	578	4,320	650	0.371
18.82	5.748	10.158	0.992	26,000	25	578	4,320	650	0.204
18.83	5.748	10.158	0.992	-	-	578	4,310	650	0.214
21.11	5.748	10.158	0.992	39,000	25	32	79,100	900	56.8
21.12	5.748	10.158	0.992	26,000	25	32	79,100	900	46.4
21.13	5.748	10.158	0.992	-	-	32	79,100	900	45.9
21.21	5.748	10.158	0.992	39,000	25	75	33,400	900	37.5
21.22	5.748	10.158	0.992	26,000	25	75	33,400	900	28.9
21.23	5.748	10.158	0.992	-	-	75	33,400	900	26.5
21.31	5.748	10.158	0.992	39,000	25	228	10.930	900	22.0
21.32	5.748	10.158	0.992	26,000	25	228	10,930	900	16.7
21.33	5.748	10.158	0.992	-	-	228	10.930	900	15.7
21.41	5.748	10.158	0.992	39,000	25	245	10,170	900	20.6
21.42	5.748	10.158	0.992	26,000	25	245	10.170	900	16.7
21.43	5.748	10.158	0.992	-	-	245	10,170	900	16.4
21.51	5.748	10.158	0.992	39,000	25	347	7,175	900	17.9
21.52	5.748	10.158	0.992	26,000	25	347	7,175	900	16.0
21.53	5.748	10.158	0.992	-	-	347	7,175	900	17.4

TABLE 12 (continued)

TABULATION OF DATA

Run No.	Catalyst gms.	Bed Ht. cm.	Bed Dia. cm.	Ultrasound cps	Ultrasound watts	Feed Rate gms/hr	W/F gm cat-sec / gm mole	Temp. °F.	X Conversion %
20.11	5.748	10.158	0.992	39,000	25	34	73,250	950	40.8
20.12	5.748	10.158	0.992	26,000	25	34	73,250	950	38.2
20.13	5.748	10.158	0.992	-	-	34	73,250	950	37.8
20.21	5.748	10.158	0.992	39,000	25	50	49,750	950	31.3
20.22	5.748	10.158	0.992	26,000	25	50	49,750	950	31.1
20.23	5.748	10.158	0.992	-	-	50	49,750	950	28.0
20.31	5.748	10.158	0.992	39,000	25	74	33,450	950	23.6
20.32	5.748	10.158	0.992	26,000	25	74	33,450	950	27.9
20.33	5.748	10.158	0.992	-	-	74	33,450	950	22.0
20.41	5.748	10.158	0.992	39,000	25	264	9,425	950	16.9
20.42	5.748	10.158	0.992	26,000	25	264	9,425	950	14.3
20.43	5.748	10.158	0.992	-	-	264	9,425	950	13.9
20.51	5.748	10.158	0.992	39,000	25	352	7,074	950	9.88
20.52	5.748	10.158	0.992	26,000	25	352	7,074	950	9.02
20.53	5.748	10.158	0.992	-	-	352	7,074	950	8.50
23.11	5.748	10.158	0.992	39,000	25	36	69,085	800	35.0
23.12	5.748	10.158	0.992	26,000	25	36	69,085	800	30.3
23.13	5.748	10.158	0.992	-	-	36	69,085	800	29.2
23.21	5.748	10.158	0.992	39,000	25	74	33,609	800	25.5
23.22	5.748	10.158	0.992	26,000	25	74	33,609	800	20.8
20.23	5.748	10.158	0.992	-	-	74	33,609	800	20.2
23.31	5.748	10.158	0.992	39,000	25	231	10,767	800	10.5
23.32	5.748	10.158	0.992	26,000	25	231	10.767	800	7.52
23.33	5.748	10.158	0.992	-	-	231	10,767	800	7.03

TABLE 12 (continued)

TABULATION OF DATA

Run No.	Catalyst gms.	Bed Ht. cm.	Bed Dia. cm.	Ultrasound cps	Ultrasound watts	Feed Rate gms/hr	W/F gm cat-sec gm mole	Temp. °F.	X Conversion %
23.41	5.748	10.158	0.992	39,000	25	262	9,493	800	9.02
23.42	5.748	10.158	0.992	26,000	25	262	9,493	800	6.52
23.43	5.748	10.158	0.992	-	-	262	9,493	800	5.81
23.51	5.748	10.158	0.992	39,000	25	351	7,086	800	7.04
23.52	5.748	10.158	0.992	26,000	25	351	7,086	800	5.01
23.53	5.748	10.158	0.992	-	-	351	7,086	800	4.07
24.11	5.748	10.158	0.992	39,000	25	35	71,086	800	35.0
24.12	5.748	10.158	0.992	26,000	25	35	71,059	750	30.5
24.13	5.748	10.158	0.992	-	-	35	71,059	750	28.7
24.21	5.748	10.158	0.992	39,000	25	76	32,725	750	24.5
24.22	5.748	10.158	0.992	26,000	25	76	32,725	750	20.0
24.23	5.748	10.158	0.992	-	-	76	32,725	750	19.5
24.31	5.748	10.158	0.992	39,000	25	230	10,813	750	10.5
24.32	5.748	10.158	0.992	26,000	25	230	10,813	750	7.52
24.33	5.748	10.158	0.992	-	-	230	10,813	750	7.03
24.41	5.748	10.158	0.992	39,000	25	258	9,640	750	9.71
24.42	5.748	10.158	0.992	26,000	25	258	9,640	750	7.02
24.43	5.748	10.158	0.992	-	-	258	9,640	750	6.06
24.51	5.748	10.158	0.992	39,000	25	353	7,046	750	6.01
24.52	5.748	10.158	0.992	26,000	25	353	7,046	750	4.53
24.53	5.748	10.158	0.992	-	-	353	7,046	750	3.54
25.11	5.748	10.158	0.992	39,000	25	32	77,721	700	18.2
25.12	5.748	10.158	0.992	26,000	25	32	77,721	700	15.0
25.13	5.748	10.158	0.992	-	-	32	77,721	700	13.5

TABLE 12 (continued)

TABULATION OF DATA

Run No.	Catalyst gms.	Bed Ht. cm.	Bed Dia. cm.	Ultrasound cps	Ultrasound watts	Feed Rate gms/hr	W/F gm cat-sec / gm mole	Temp. °F.	X Conversion %
25.21	5.748	10.158	0.992	39,000	25	76	32,725	700	3.75
25.22	5.748	10.158	0.992	26,000	25	76	32,725	700	6.35
25.23	5.748	10.158	0.992	-	-	76	32,725	700	5.60
25.31	5.748	10.158	0.992	39,000	25	229	10,861	700	[illegible]62
25.32	5.748	10.158	0.992	26,000	25	229	10,861	700	3.50
25.33	5.748	10.158	0.992	-	-	229	10,861	700	3.00
25.41	5.748	10.158	0.992	39,000	25	261	9,529	700	4.50
25.42	5.748	10.158	0.992	26,000	25	261	9,529	700	3.49
25.43	5.748	10.158	0.992	-	-	261	9,529	700	2.85
25.51	5.748	10.158	0.992	39,000	25	352	7,066	700	4.01
25.52	5.748	10.158	0.992	26,000	25	352	7,066	700	3.05
25.53	5.748	10.158	0.992	-	-	352	7,066	700	2.65
22.11	5.748	10.158	0.992	39,000	25	25	99,500	850	47.7
22.12	5.748	10.158	0.992	39,000	12.5	25	99,500	850	41.5
22.13	5.748	10.158	0.992	26,000	25	25	99,500	850	40.2
22.14	5.748	10.158	0.992	26,000	12.5	25	99,500	850	39.5
22.15	5.748	10.158	0.992	-	-	25	99,500	850	36.6
22.21	5.748	10.158	0.992	39,000	25	33	75,400	850	39.7
22.22	5.748	10.158	0.992	39,000	12.5	33	75,400	850	34.6
22.23	5.748	10.158	0.992	26,000	25	33	75,400	850	32.2
22.24	5.748	10.158	0.992	26,000	12.5	33	75,400	850	30.0
22.25	5.748	10.158	0.992	-	-	33	75,400	850	28.0
22.31	5.748	10.158	0.992	39,000	25	47	52,800	850	34.4
22.32	5.748	10.158	0.992	39,000	12.5	47	52,800	850	28.0
22.33	5.748	10.158	0.992	26,000	25	47	52,800	850	29.2

TABLE 12 (continued)

TABULATION OF DATA

Run No.	Catalyst gms.	Bed Ht. cm.	Bed Dia. cm.	Ultrasound cps	Ultrasound watts	Feed Rate gms/hr	W/F gm cat-sec/gm mole	Temp. °F.	X Conversion %
22.34	5.748	10.158	0.992	26,000	12.5	47	52,800	850	30.1
22.35	5.748	10.158	0.992	-	-	47	52,800	850	27.5
22.41	5.748	10.158	0.992	39,000	25	73	34,000	850	23.4
22.42	5.748	10.158	0.992	39,000	12.5	73	34,000	850	22.9
22.43	5.748	10.158	0.992	26,000	25	73	34,000	850	23.6
22.44	5.748	10.158	0.992	26,000	12.5	73	34,000	850	21.2
22.45	5.748	10.158	0.992	-	-	73	34,000	850	21.5
22.51	5.748	10.158	0.992	39,000	25	106	23,500	850	30.9
22.52	5.748	10.158	0.992	39,000	12.5	106	23,500	850	25.0
22.53	5.748	10.158	0.992	26,000	25	106	23,500	850	24.9
22.54	5.748	10.158	0.992	26,000	12.5	106	23,500	850	23.3
22.55	5.748	10.158	0.992	-	-	106	23,500	850	21.6
22.61	5.748	10.158	0.992	39,000	25	211	11,800	850	21.4
22.62	5.748	10.158	0.992	39,000	12.5	211	11,800	850	20.8
22.63	5.748	10.158	0.992	26,000	25	211	11,800	850	19.0
22.64	5.748	10.158	0.992	26,000	12.5	211	11,800	850	18.8
22.65	5.748	10.158	0.992	-	-	211	11,800	850	18.3
22.71	5.748	10.158	0.992	39,000	25	237	10,500	850	17.3
22.72	5.748	10.158	0.992	39,000	12.5	237	10,500	850	17.2
22.73	5.748	10.158	0.992	26,000	25	237	10,500	850	16.8
22.74	5.748	10.158	0.992	26,000	12.5	237	10,500	850	17.5
22.75	5.748	10.158	0.992	-	-	237	10,500	850	17.5
22.81	5.748	10.158	0.992	39,000	25	260	9,475	850	16.8
22.82	5.748	10.158	0.992	39,000	12.5	263	9,475	850	16.0
22.83	5.748	10.158	0.992	26,000	25	263	9,475	850	16.0

TABLE 12 (continued)

TABULATION OF DATA

Run No.	Catalyst gms.	Bed Ht. cm.	Bed Dia. cm.	Ultrasound cps	Ultrasound watts	Feed Rate gms/hr	W/F gm cat-sec gm mole	Temp. °F.	X Conversion %
22.84	5.748	10.158	0.992	26,000	12.5	263	9,475	850	16.3
22.85	5.748	10.158	0.992	-	-	263	9,475	850	16.1
22.91	5.748	10.158	0.992	39,000	25	311	8,020	850	14.0
22.92	5.748	10.158	0.992	39,000	12.5	311	8,020	850	15.0
22.93	5.748	10.158	0.992	26,000	25	311	8,020	850	13.6
22.94	5.748	10.158	0.992	26,000	12.5	311	8,020	850	13.0
22.95	5.748	10.158	0.992	-	-	311	8,020	850	12.3
22.101	5.748	10.158	0.992	39,000	25	356	6,990	850	15.2
22.102	5.748	10.158	0.992	39,000	12.5	356	6,990	850	13.8
22.103	5.748	10.158	0.992	26,000	25	356	6,990	850	14.4
22.104	5.748	10.158	0.992	26,000	12.5	356	6,990	850	15.6
22.105	5.748	10.158	0.992	-	-	356	6,990	850	15.0
22.111	5.748	10.158	0.992	39,000	25	405	6,150	850	11.1
22.112	5.748	10.158	0.992	39,000	12.5	405	6,150	850	12.5
22.113	5.748	10.158	0.992	26,000	25	405	6,150	850	11.9
22.114	5.748	10.158	0.992	26,000	12.5	405	6,150	850	11.3
22.115	5.748	10.158	0.992	-	-	405	6,150	850	10.9
22.121	5.748	10.158	0.992	39,000	25	509	4,900	850	9.31
22.122	5.748	10.158	0.992	39,000	12.5	509	4,900	850	9.64
22.123	5.748	10.158	0.992	26,000	25	509	4,900	850	9.96
22.124	5.748	10.158	0.992	26,000	12.5	509	4,900	850	10.4
22.125	5.748	10.158	0.992	-	-	509	4,900	850	11.5
22.131	5.748	10.158	0.992	39,000	25	622	4,010	850	8.90
22.132	5.748	10.158	0.992	39,000	12.5	622	4,010	850	4.21
22.133	5.748	10.158	0.992	26,000	25	622	4,010	850	4.34

TABLE 12 (continued)

TABULATION OF DATA

Run No.	Catalyst gms.	Bed Ht. cm.	Bed Dia. cm.	Ultrasound cps	Ultrasound watts	Feed Rate gms/hr	W/F gm cat-sec / gm mole	Temp. °F.	X Conversion %
22.134	5.748	10.158	0.992	26,000	12.5	622	4,010	850	3.90
22.135	5.748	10.158	0.992	-	-	622	4,010	850	4.21
26.11	5.748	10.158	0.992	39,000	25	38	65,300	850	41.5
26.12	5.748	10.158	0.992	26,000	25	38	65,300	850	35.0
26.13	5.748	10.158	0.992	-	-	38	65,300	850	29.8
27.11	5.748	10.158	0.992	39,000	15	103	24,200	800	16.9
27.12	5.748	10.158	0.992	26,000	25	103	24,200	800	15.5
27.13	5.748	10.158	0.992	-	-	103	24,200	800	16.3
28.11	5.748	10.158	0.992	39,000	25	22	110,400	750	41.3
28.12	5.748	10.158	0.992	26,000	25	22	110,400	750	36.4
28.13	5.748	10.158	0.992	-	-	22	110,400	750	32.5
29.11	5.748	10.158	0.992	39,000	25	103	24,200	650	5.35
29.12	5.748	10.158	0.992	26,000	25	103	24,200	650	4.71
29.13	5.748	10.158	0.992	-	-	103	24,200	650	4.52
30.11	5.748	10.158	0.992	39,000	25	140	17,800	1000	24.4
30.12	5.748	10.158	0.992	26,000	25	140	17,800	1000	23.8
30.13	5.748	10.158	0.992	-	-	140	17,800	1000	22.8
31.11	5.748	10.158	0.992	39,000	25	47	52,750	900	24,7
31.12	5.748	10.158	0.992	26,000	25	47	52,750	900	23.5
31.13	5.748	10.158	0.992	-	-	47	52,750	900	22.7
31.21	5.748	10.158	0.992	39,000	25	23	106,300	900	52.3
31.22	5.748	10.158	0.992	26,000	25	23	106,300	900	46.1
31.23	5.748	10.158	0.992	-	-	23	106,300	900	44.5
32.11	5.748	10.158	0.992	39,000	25	31	81,000	850	44.5
32.12	5.748	10.158	0.992	26,000	25	31	81,000	850	38.5

TABLE 12 (continued)

TABULATION OF DATA

Run No.	Catalyst gms.	Bed Ht. cm.	Bed Dia. cm.	Ultrasound cps	Ultrasound watts	Feed Rate gms/hr	W/F gm cat-sec / gm mole	Temp. °F.	X Conversion %
32.13	5.748	10.158	0.992	-	-	31	81,000	850	33.5
33.11	5.748	10.158	0.992	39,000	25	33	76,200	900	44.9
33.12	5.748	10.158	0.992	26,000	25	33	76,200	900	37.2
33.13	5.748	10.158	0.992	-	-	33	76,200	900	33.4
33.21	5.748	10.158	0.992	39,000	25	25	98,100	900	49.9
33.22	5.748	10.158	0.992	26,000	25	25	98,100	900	44.5
33.23	5.748	10.159	0.992	-	-	25	98,100	900	42.1
34.11	5.748	10.158	0.992	39,000	25	60	41,200	650	5.70
34.12	5.748	10.158	0.992	26,000	25	60	41.200	650	5.11
34.13	5.748	10.158	0.992	-	-	60	41.200	650	4.82
34.21	5.748	10.158	0.992	39,000	25	42	58,800	650	5.88
34.22	5.748	10.158	0.992	26,000	25	42	58,800	650	5.91
34.23	5.748	10.158	0.992	-	-	42	58,800	650	5.42
35.11	5.748	10.158	0.992	39,000	25	25	101,000	800	39.9
35.12	5.748	10.158	0.992	26,000	25	25	101,000	800	37.1
35.13	5.748	10.158	0.992	-	-	25	101,000	800	34.9
35.21	5.748	10.158	0.992	39,000	25	20	124,300	800	43.9
35.22	5.748	10.158	0.992	26,000	25	20	124,300	800	39.6
35.23	5.748	10.150	0.992	-	-	20	124,300	800	38.1
36.13	5.748	10.158	0.992	-	-	125	19,900	900	19.1
36.23	5.748	10.158	0.992	-	-	82	30,100	900	27.6
36.33	5.748	10.158	0.992	-	-	62	39,800	900	34.3
36.43	5.748	10.158	0.992	-	-	41	60,200	900	41.6
36.53	5.748	10.158	0.992	-	-	31	79,900	900	41.2

APPENDIX XV

THERMOCOUPLE CORRECTION

THERMOCOUPLE CORRECTION

The reaction temperature of all runs was controlled by a Leeds & Northrup Speedomax Temperature Controller. The controller maintained the desired temperature by energizing and de-energizing the reactor heaters. The control temperature was sensed by a thermocouple which was inserted in a thermocouple well. The tip of the thermocouple well was located inside the reactor and into the catalyst bed.

Because of the heat conduction from the tip of the thermocouple well to the cooler external end of the well, the temperature at the thermocouple junction will be less than the actual gas temperature passing by the tip. Bird[6] has shown this error to conform to the following equation:

$$\frac{T_1 - T_a}{T_w - T_a} = \frac{1}{\cosh\left[\frac{hL^2}{k\,B}\right]^{\frac{1}{2}}} \qquad (147)$$

T_1 = temperature indicated by thermocouple, 950°F.

T_w = temperature of cool end of thermocouple well, 570°F.

T_a = actual gas temperature, °F.

h = heat transfer coefficient, 120 $\frac{Btu}{hr\text{-}ft\text{-}^oF.}$

L = length of well, 0.708 ft.

k = thermal conductivity of metal, 60 $\frac{\text{Btu}}{\text{hr-ft}^2\text{-}^\circ\text{F.}}$

B = thickness of well, 0.00692 ft.

$$\frac{950 - T_a}{570 - T_a} = \frac{1}{\cosh 12.04} = \frac{1}{163,376} = 0.00000612$$

$$T_a = 950^\circ\text{F.}$$

Therefore, the error is insignificant and the thermocouple does sense the actual gas temperature.

APPENDIX XVI

QUADRATIC REGRESSION EQUATION

QUADRATIC REGRESSION EQUATION

All the data collected at each temperature and frequency are presented herein as plots of conversion versus reciprocal space velocity. The curves best fitting the data were calculated by the quadratic regression method to fit the following equation:

$$X = a + b\left(\frac{W}{F}\right) + c\left(\frac{W}{F}\right)^2 \qquad (21)$$

and,

$$an + b\sum\left(\frac{W}{F}\right) + c\sum\left(\frac{W}{F}\right)^2 = \sum X \qquad (148)$$

$$a\sum\left(\frac{W}{F}\right) + b\sum\left(\frac{W}{F}\right)^2 + c\sum\left(\frac{W}{F}\right)^3 = \sum(X)\left(\frac{W}{F}\right) \qquad (149)$$

$$a\sum\left(\frac{W}{F}\right)^2 + b\sum\left(\frac{W}{F}\right)^3 + c\sum\left(\frac{W}{F}\right)^4 = \sum(X)\left(\frac{W}{F}\right)^2 \qquad (150)$$

where,

n = number of data points.

The resulting three constants for each operating condition are shown in Table 13 and the data and calculated curves are shown in Figures 86 through 111.

The quadratic regression curves were employed only to evaluate conversion at the specific reciprocal space velocities of 20,000, 50,000 and 80,000 $\frac{\text{gm cat-sec.}}{\text{gm mole}}$. The statistical significance of the mass transfer coefficient as a function of temperature as calculated from the conversion versus reciprocal space velocity information obtained from the regression lines was then determined.

TABLE 13

QUADRATIC EQUATION CONSTANTS

Temp. $^{o}F.$	$f_{cps} \times 10^{-3}$	Power	a	$b \times 10^{6}$	$c \times 10^{11}$
650	39	full	-0.000959	1.74	-0.91
650	26	full	-0.00605	1.76	-1.06
650	-	off	-0.00664	1.75	-1.10
700	39	full	0.0309	1.45	0.590
700	26	full	0.0253	0.923	0.790
700	-	off	0.0205	0.958	0.650
750	39	full	0.0231	7.55	-3.74
750	26	full	0.0051	6.66	-3.17
750	-	off	-0.0054	7.00	-3.70
800	39	full	0.0453	5.97	-2.32
800	26	full	0.0308	5.32	-1.93
800	-	off	0.0226	5.41	-2.09
850	39	full	0.0282	9.92	-5.87
850	26	full	0.0252	9.04	-5.76
850	-	off	0.0258	8.40	-5.60
850	39	half	0.0989	5.01	-2.00
850	26	half	0.0974	4.79	-2.03
850	-	off	0.0258	8.40	-5.60
900	39	full	0.0877	5.33	-1.86
900	26	full	0.0789	4.16	-1.13
900	-	off	0.0655	6.26	-3.15
950	39	full	0.0359	7.52	-1.75
950	26	full	0.0256	8.76	-4.30
950	-	off	0.0255	8.12	-4.42
1000	39	full	0.0215	20.3	-39.5
1000	26	full	-0.0224	29.4	-75.2
1000	-	off	-0.0213	29.8	-81.5

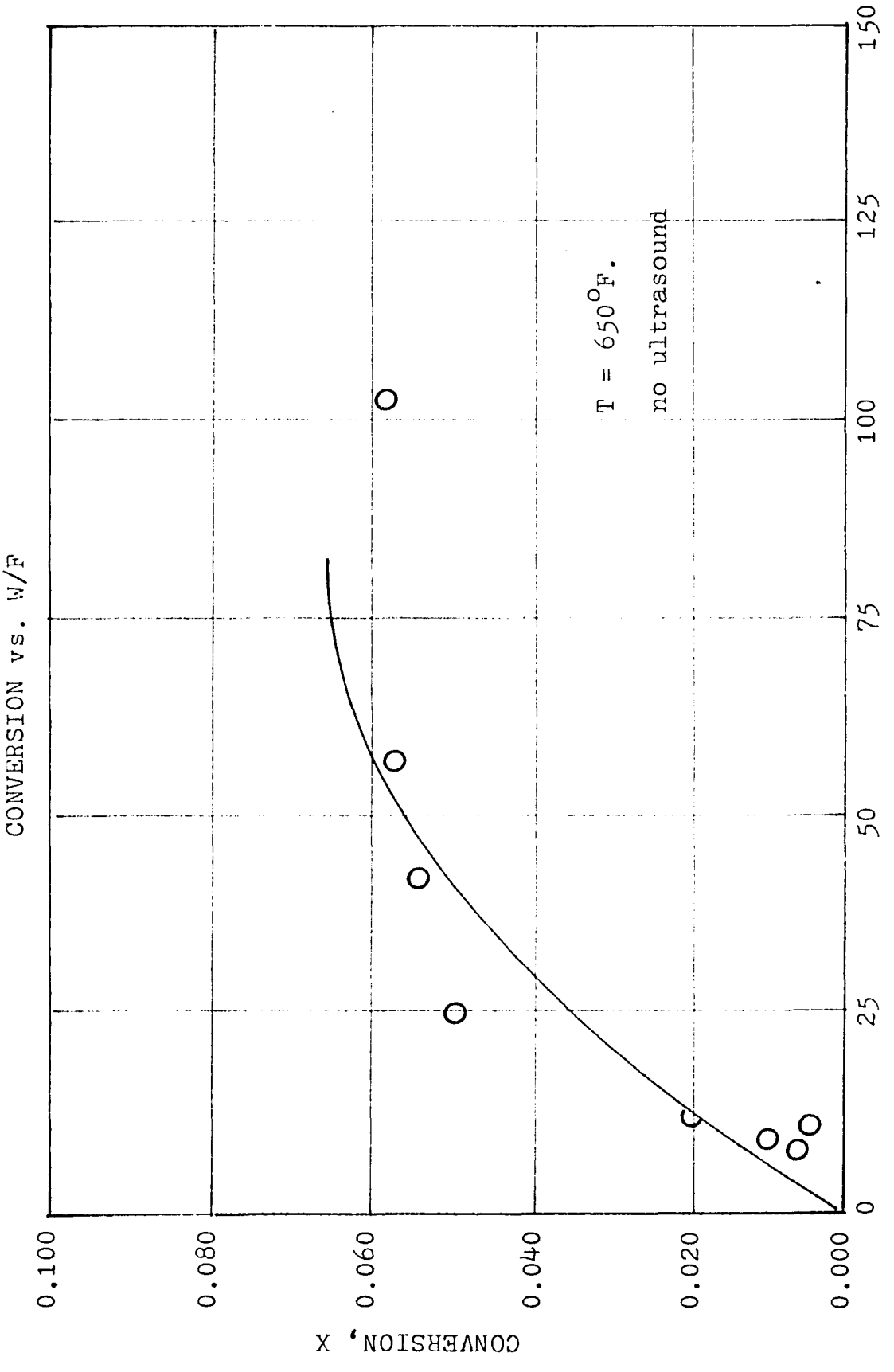

FIGURE 86

FIGURE 87

CONVERSION vs. W/F

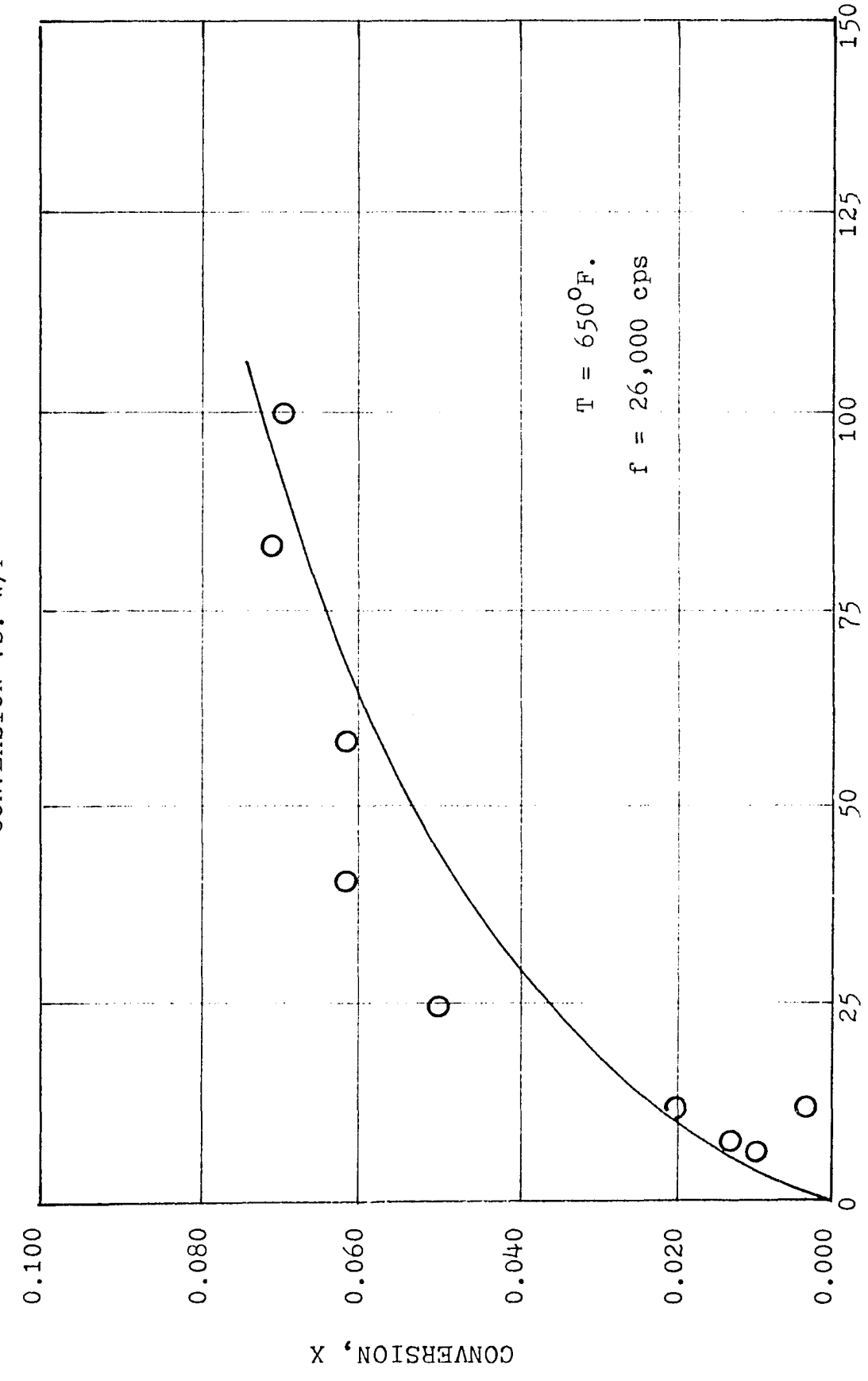

FIGURE 88

CONVERSION vs. W/F

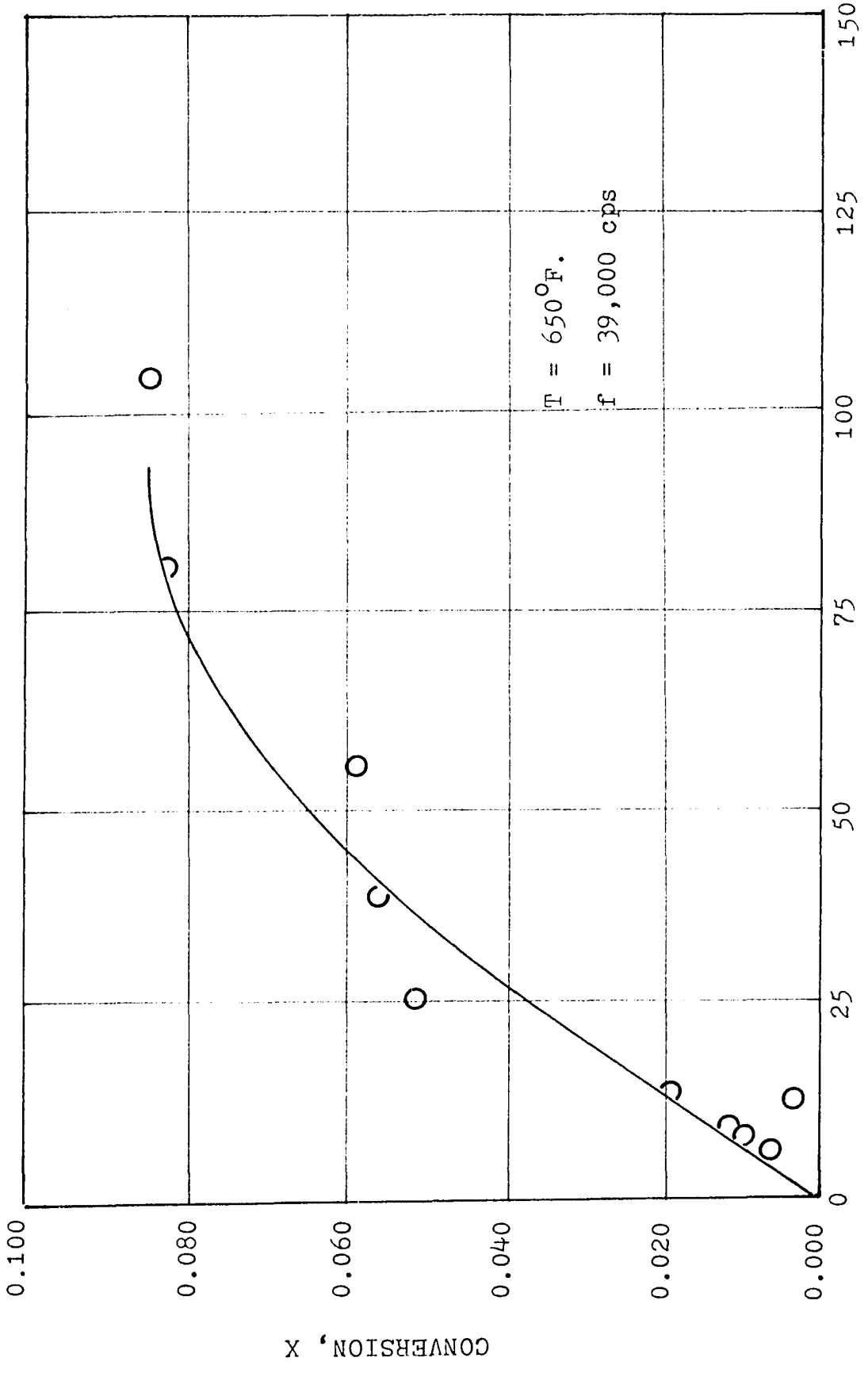

FIGURE 89

CONVERSION vs. W/F

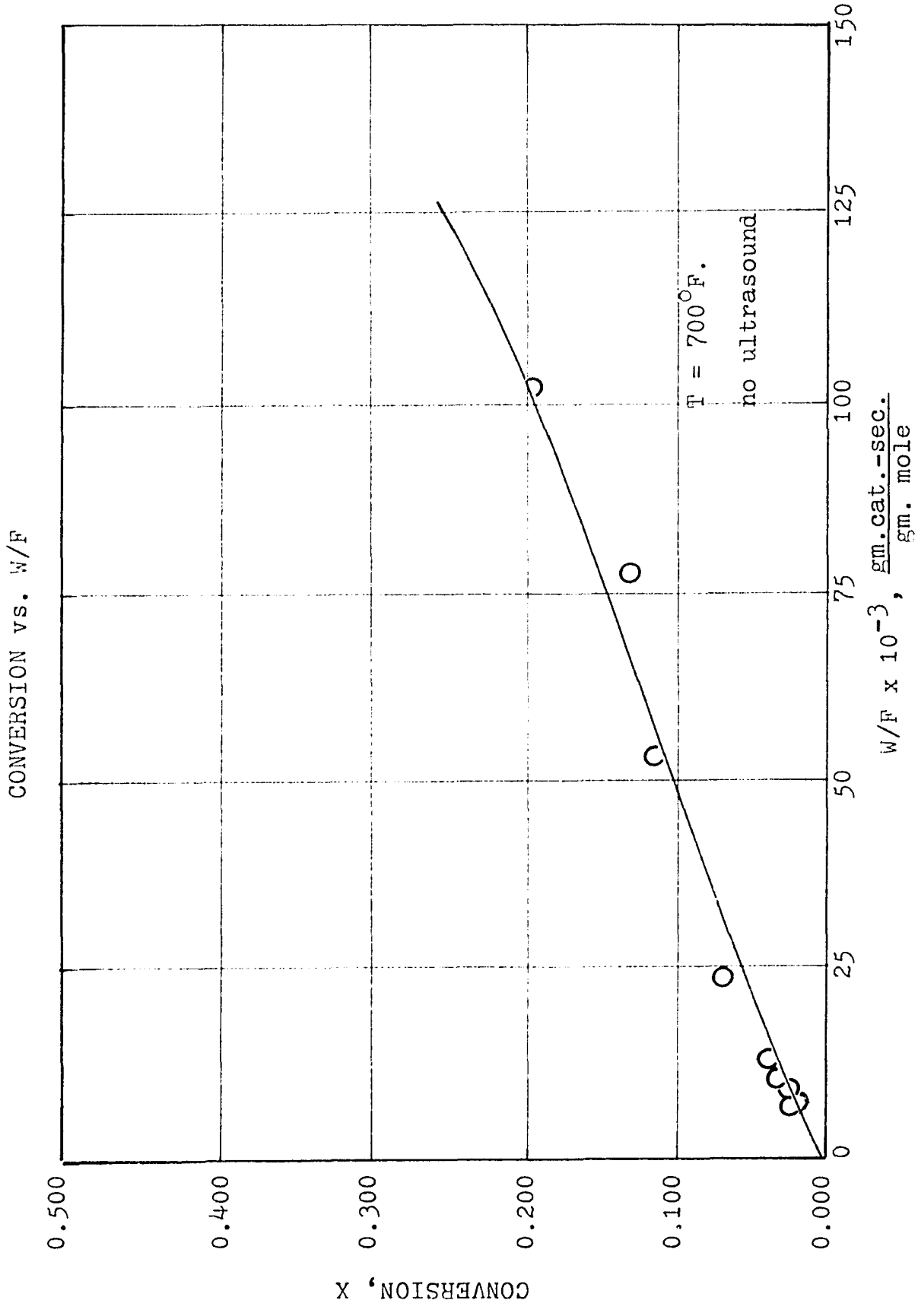

FIGURE 90

CONVERSION vs. W/F

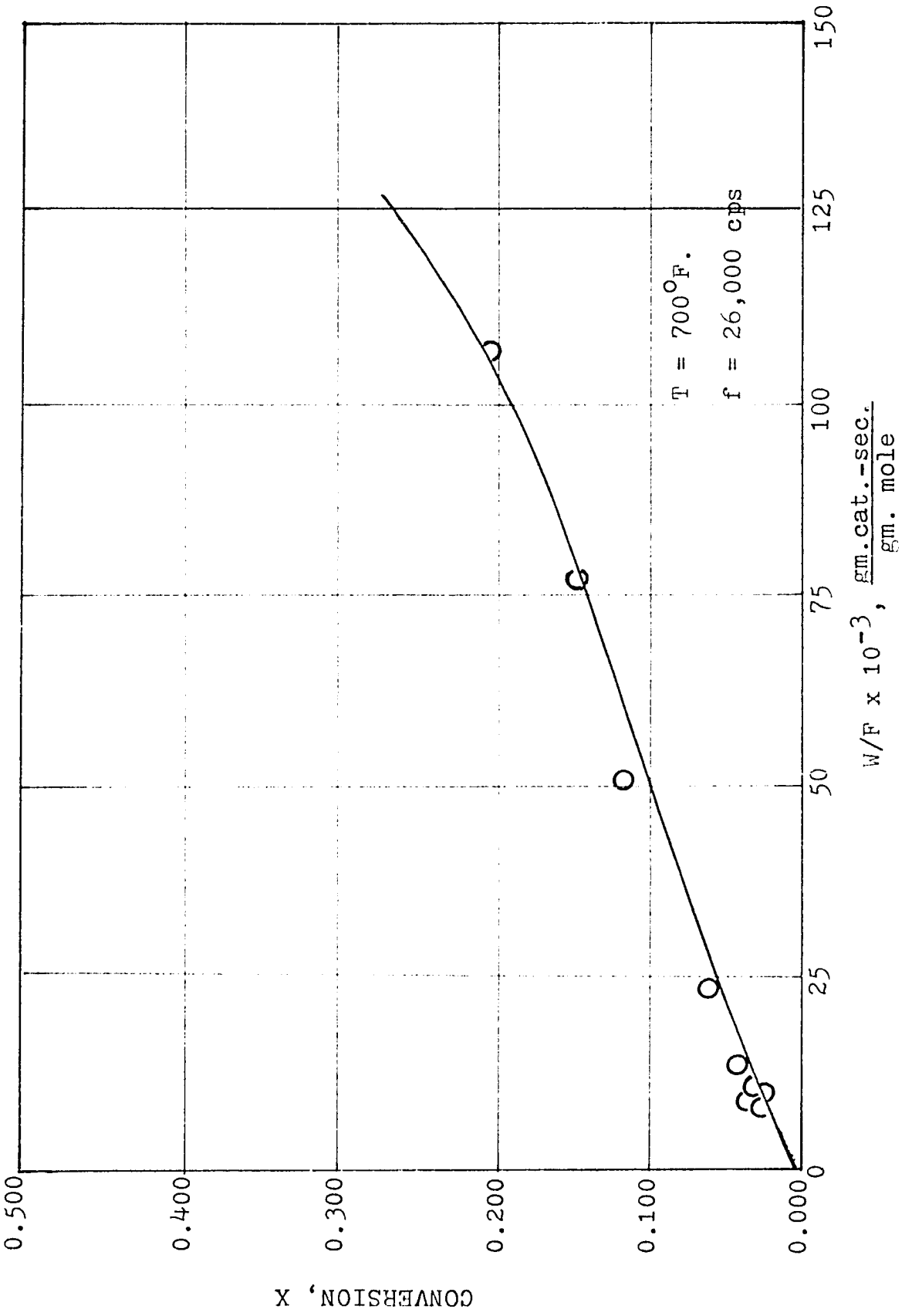

FIGURE 91

CONVERSION vs. W/F

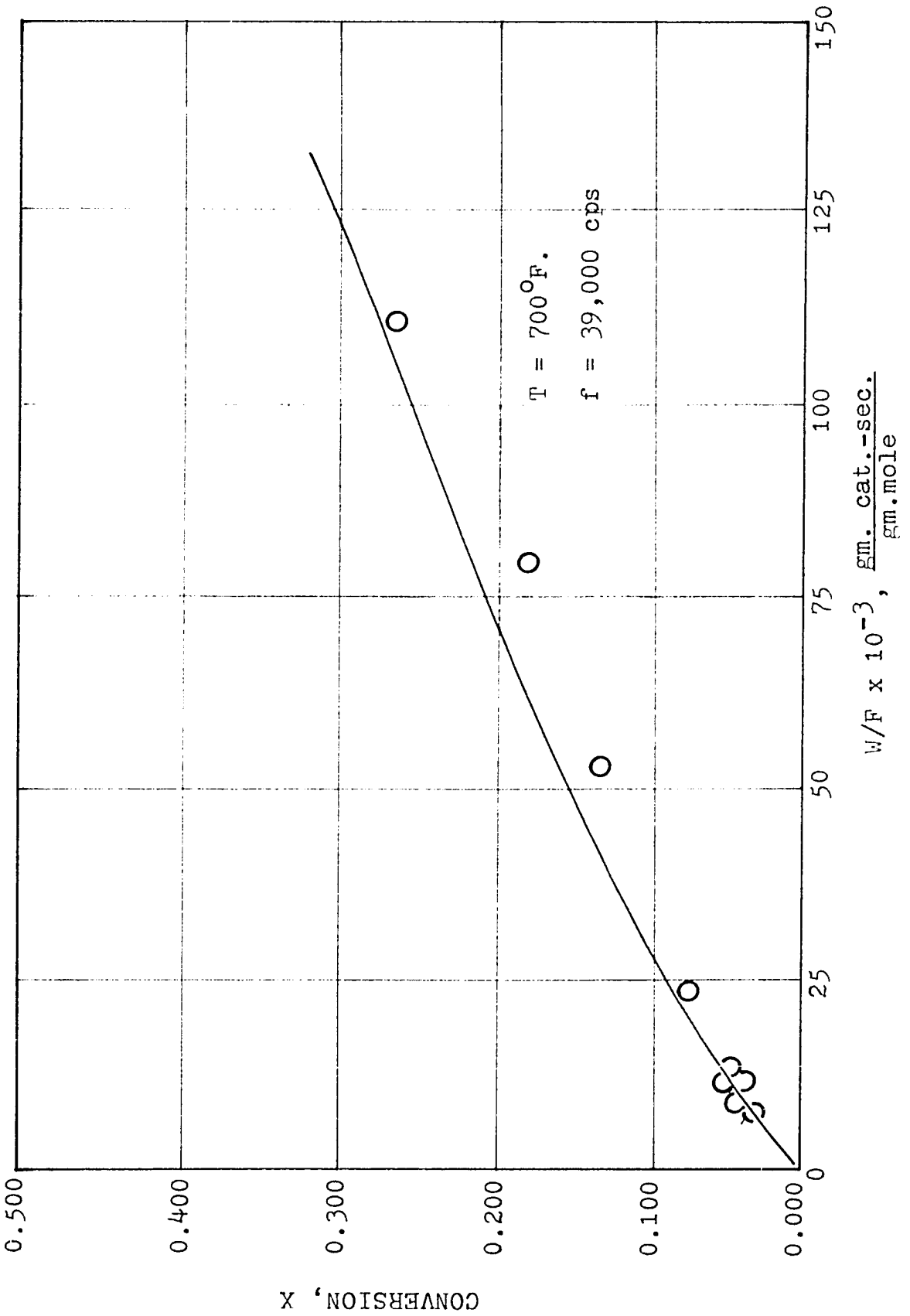

FIGURE 92

CONVERSION vs. W/F

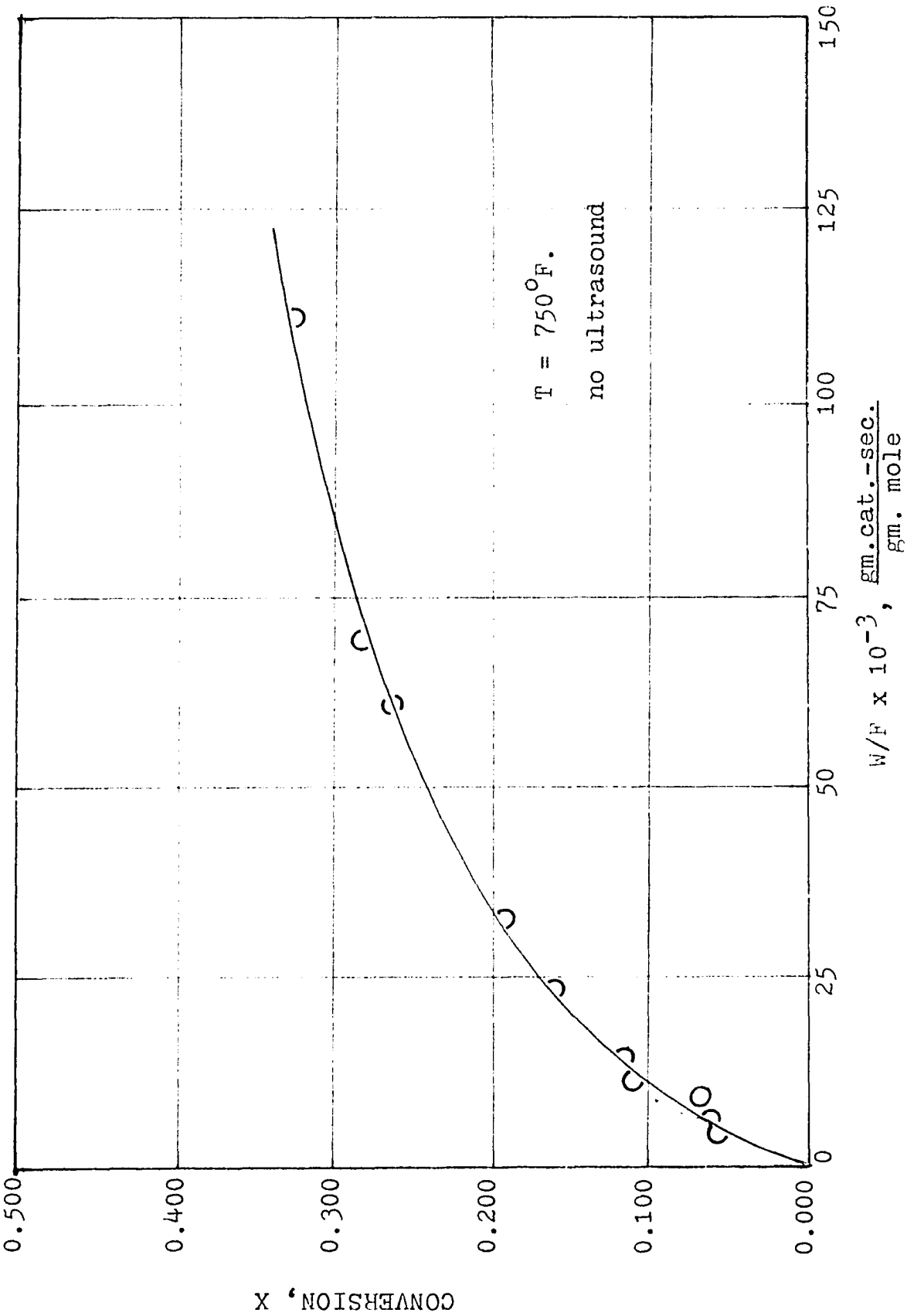

FIGURE 93

CONVERSION vs. W/F

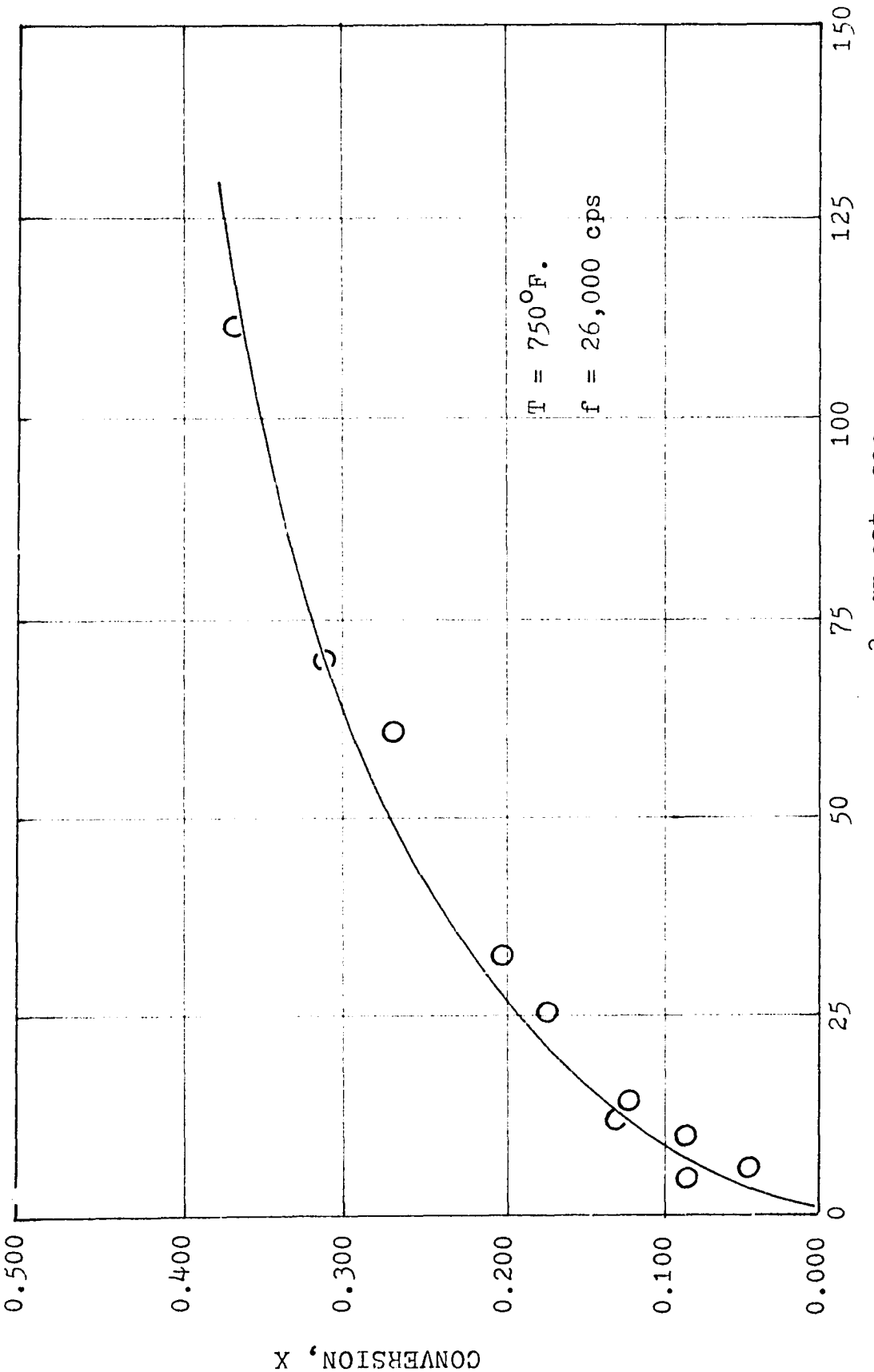

FIGURE 94

CONVERSION vs. W/F

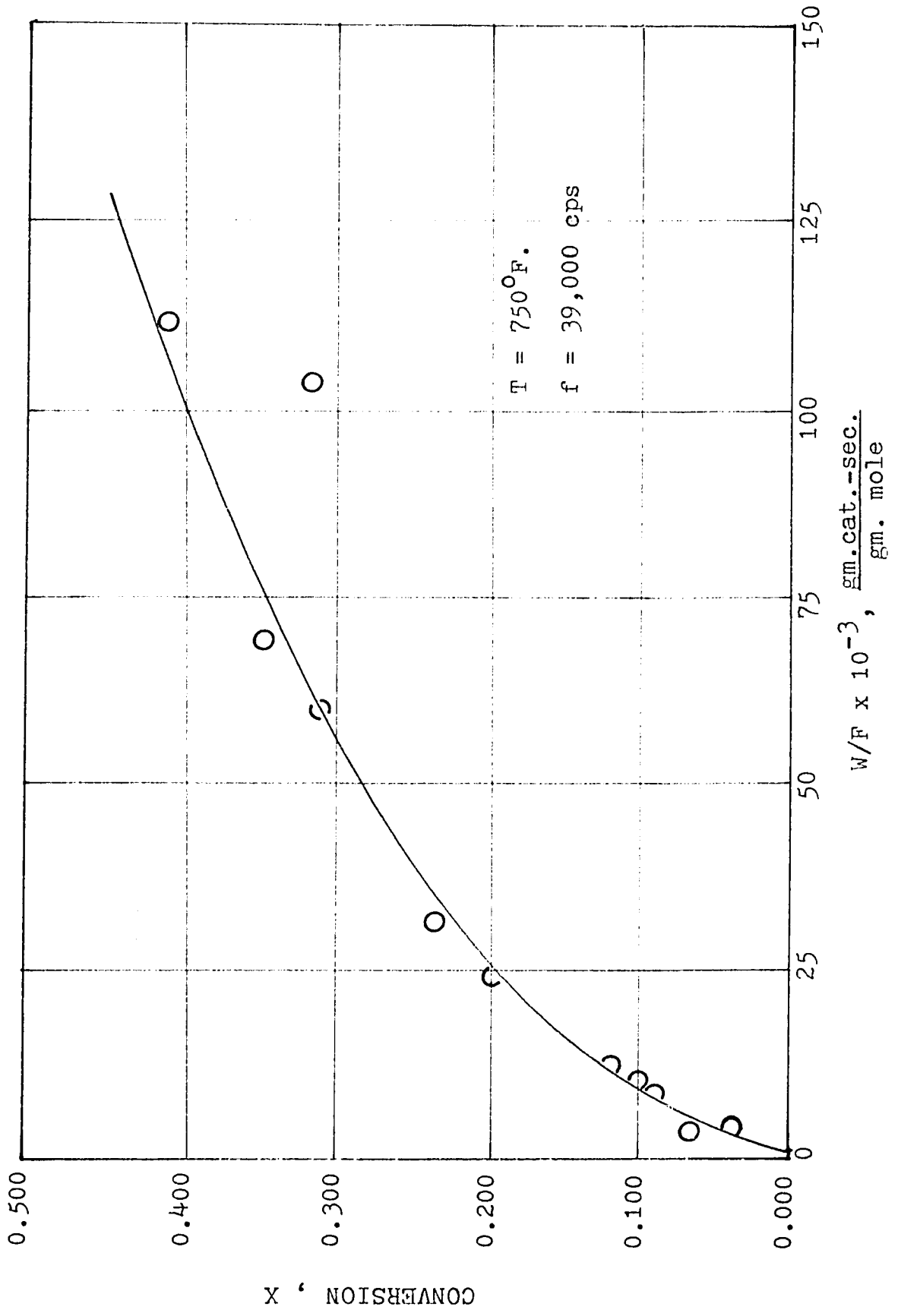

FIGURE 95

CONVERSION vs. W/F

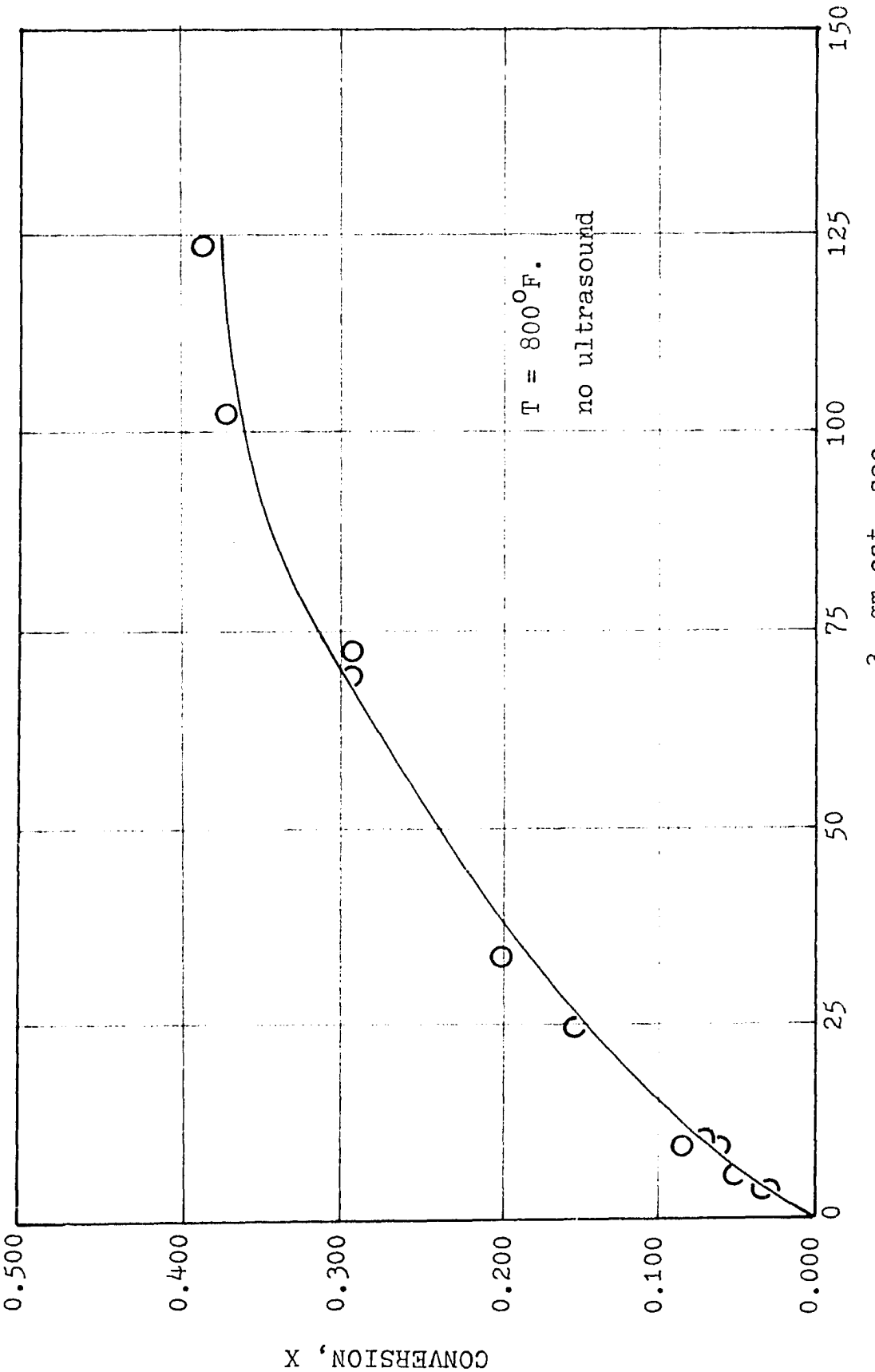

FIGURE 96

CONVERSION vs. W/F

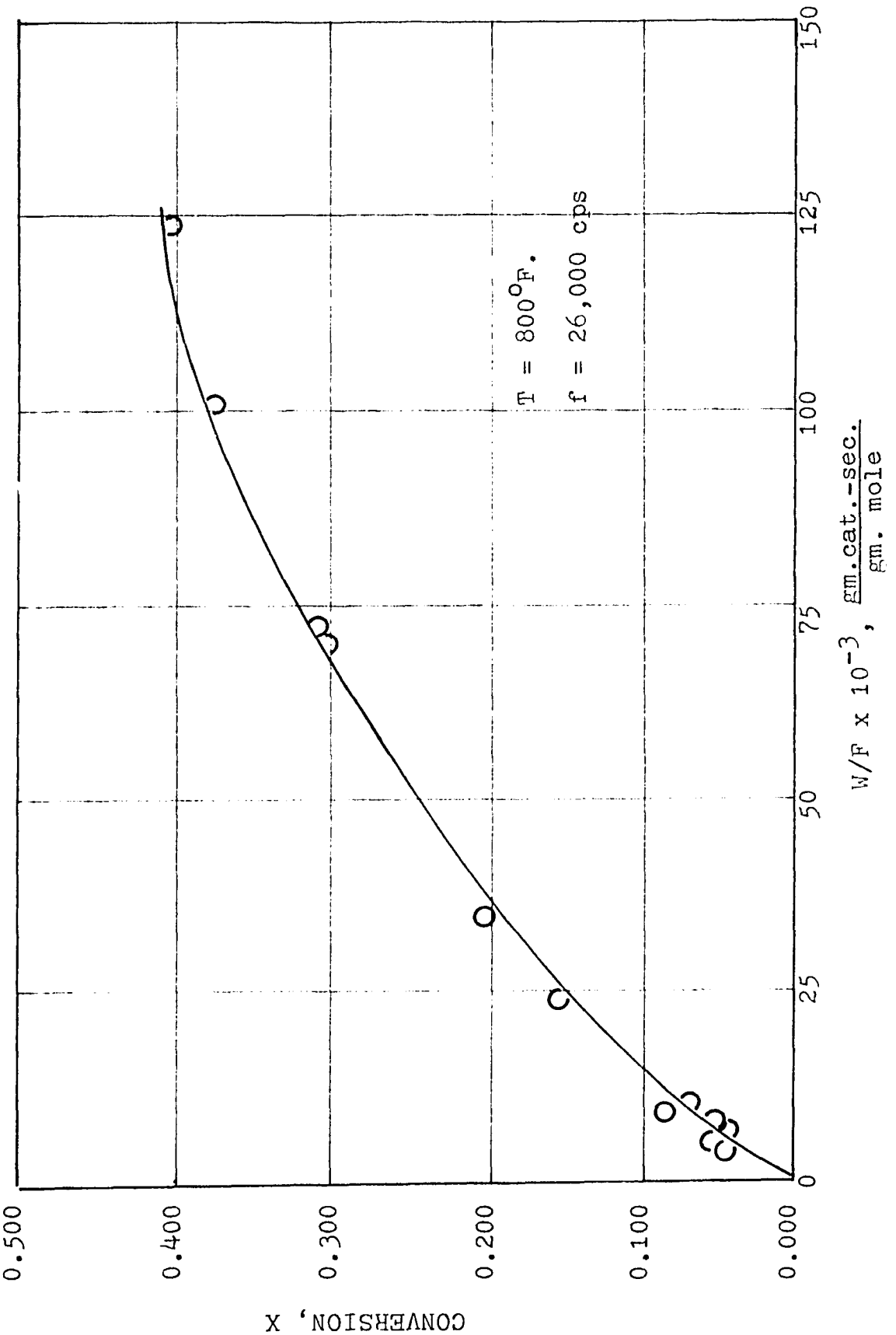

FIGURE 97

CONVERSION vs. W/F

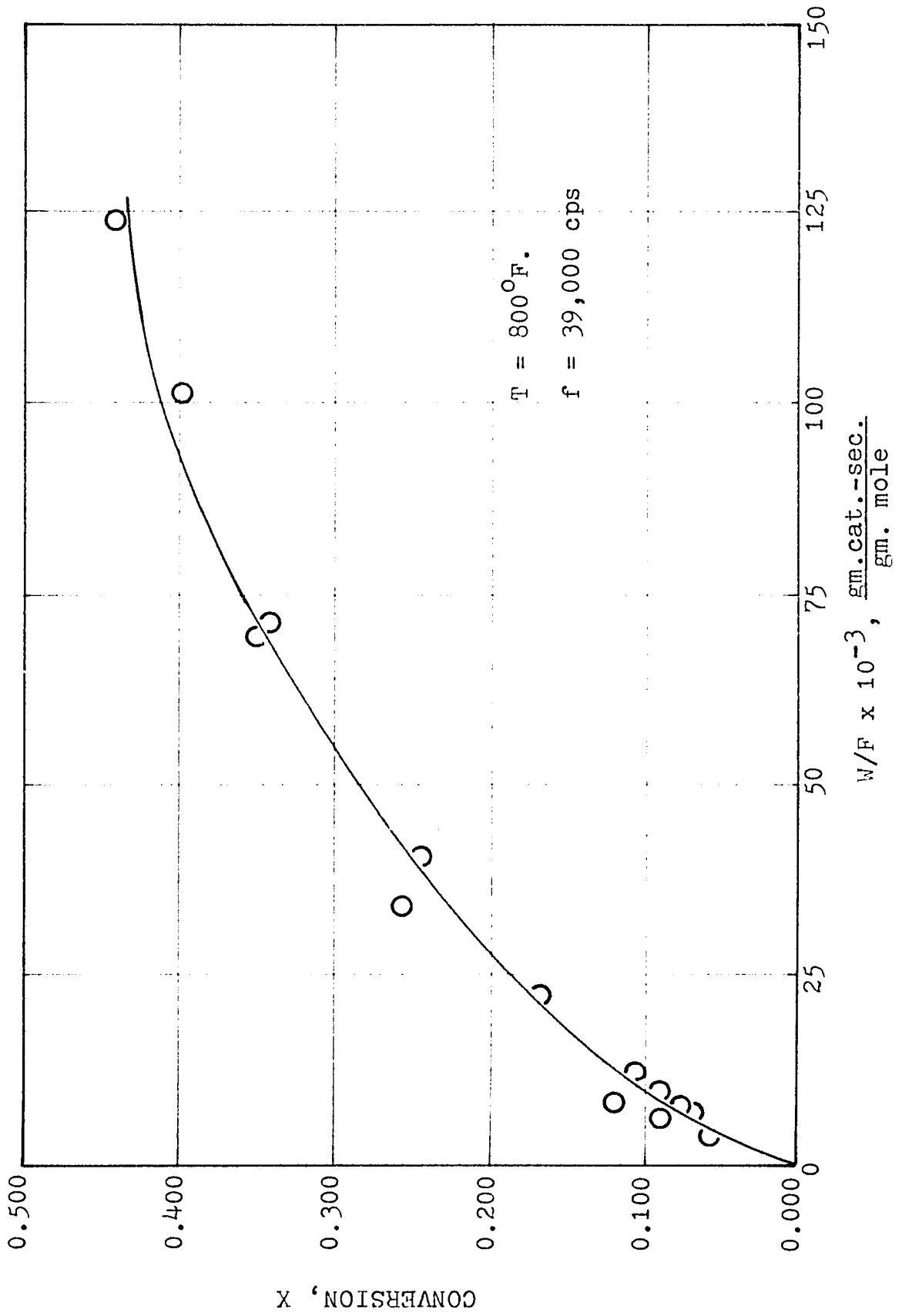

FIGURE 98

CONVERSION vs. W/F

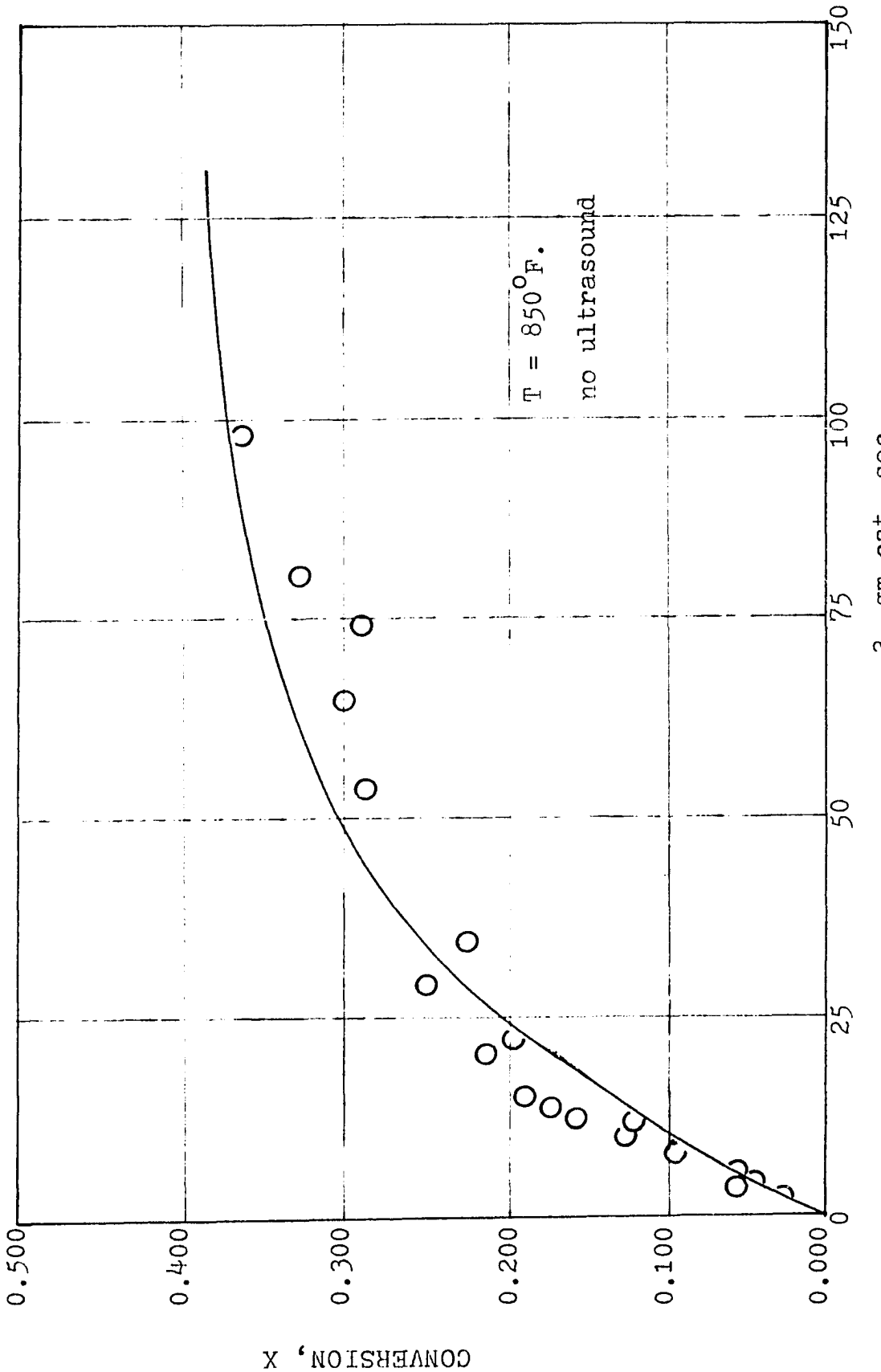

FIGURE 99

CONVERSION vs. W/F

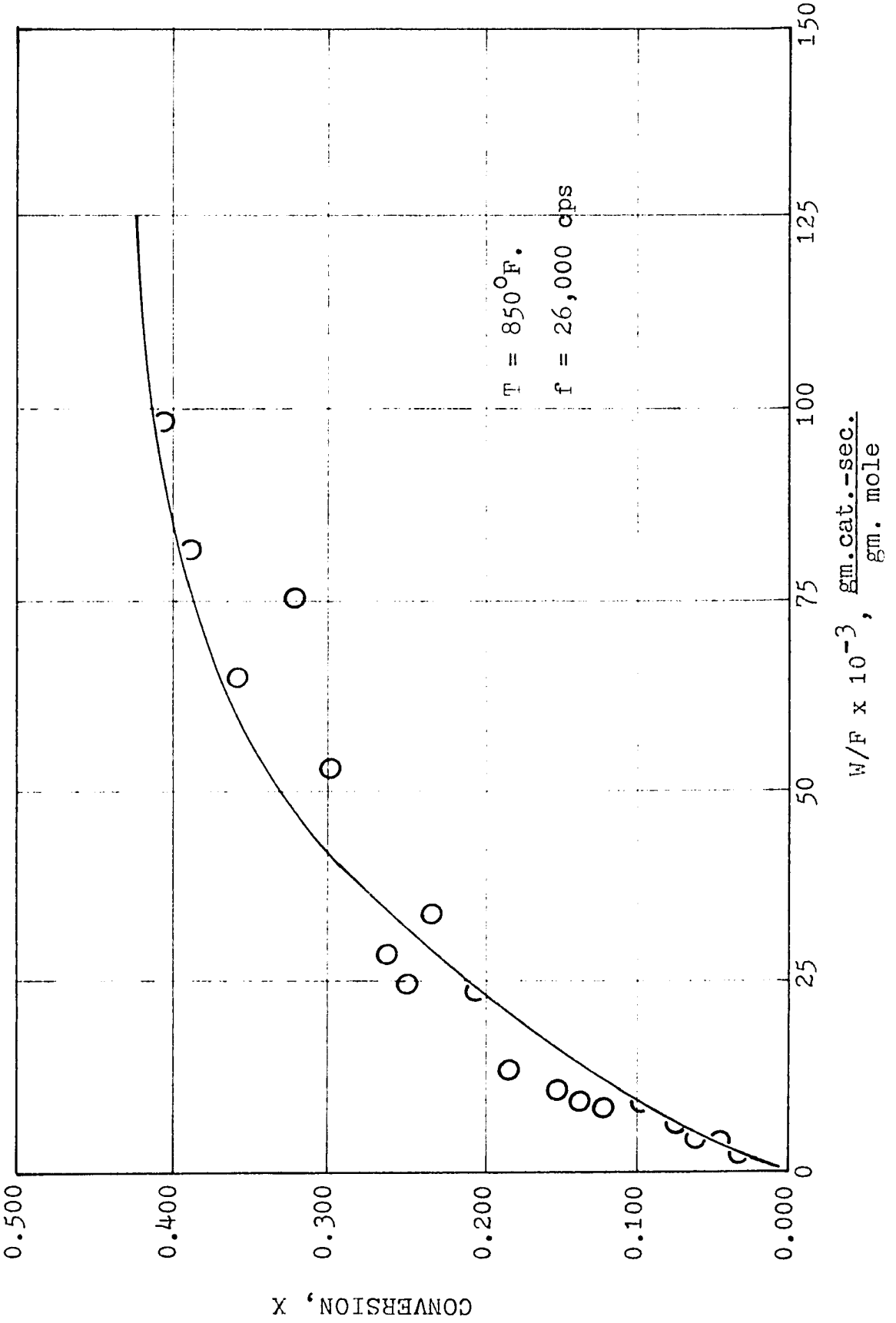

FIGURE 100

CONVERSION vs. W/F

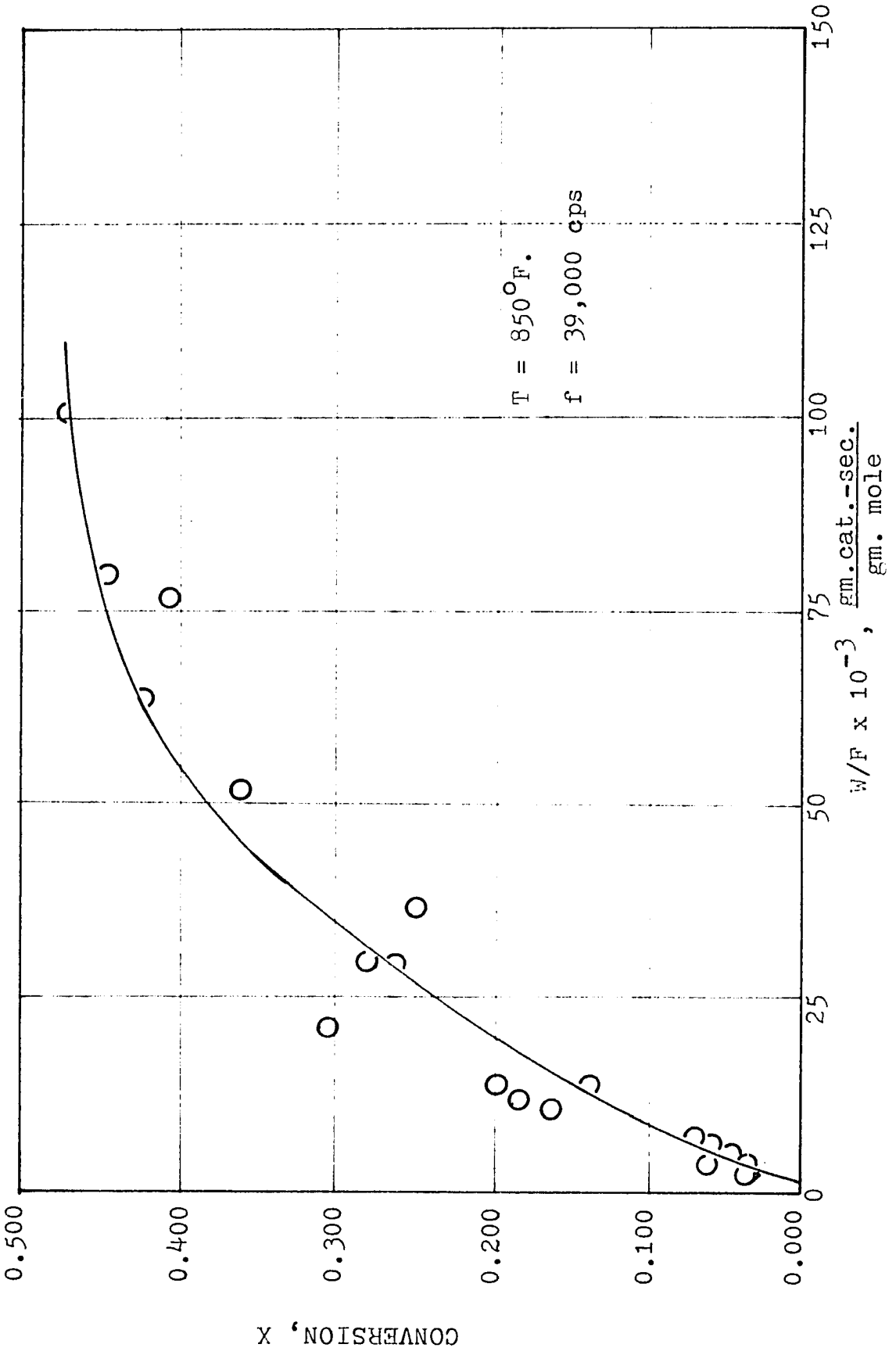

FIGURE 101

CONVERSION vs. W/F

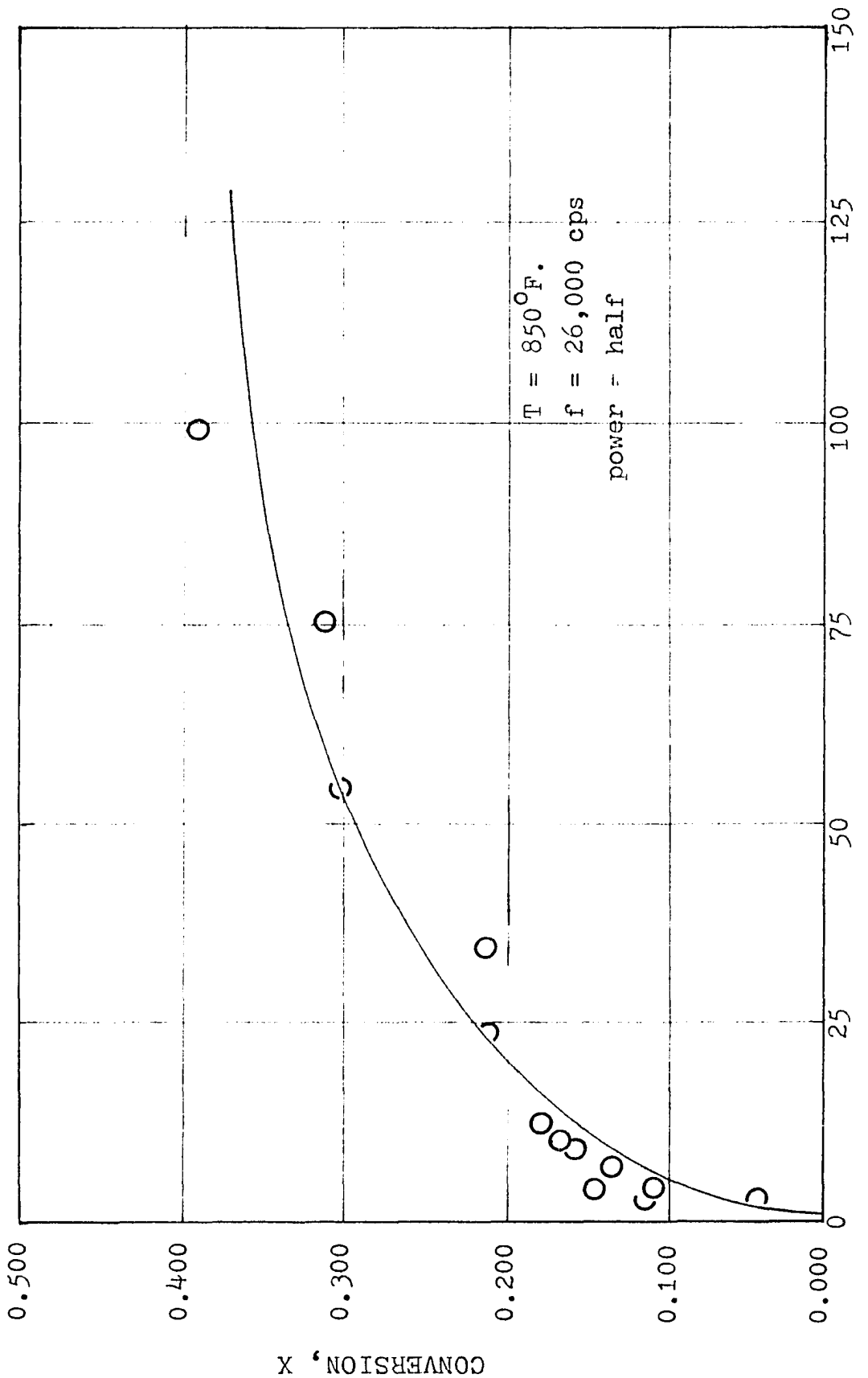

FIGURE 102

CONVERSION vs. W/F

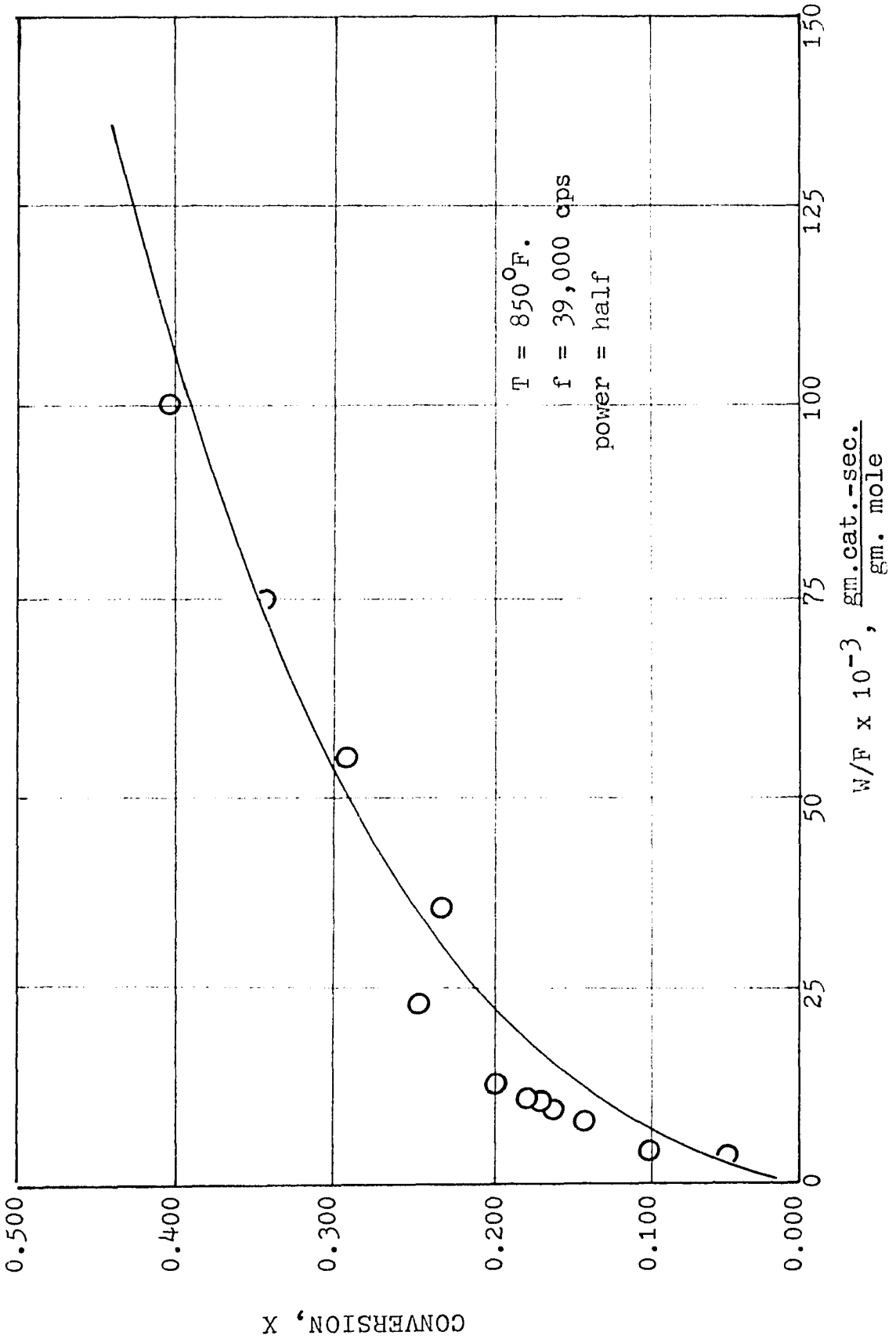

FIGURE 103

CONVERSION vs. W/F

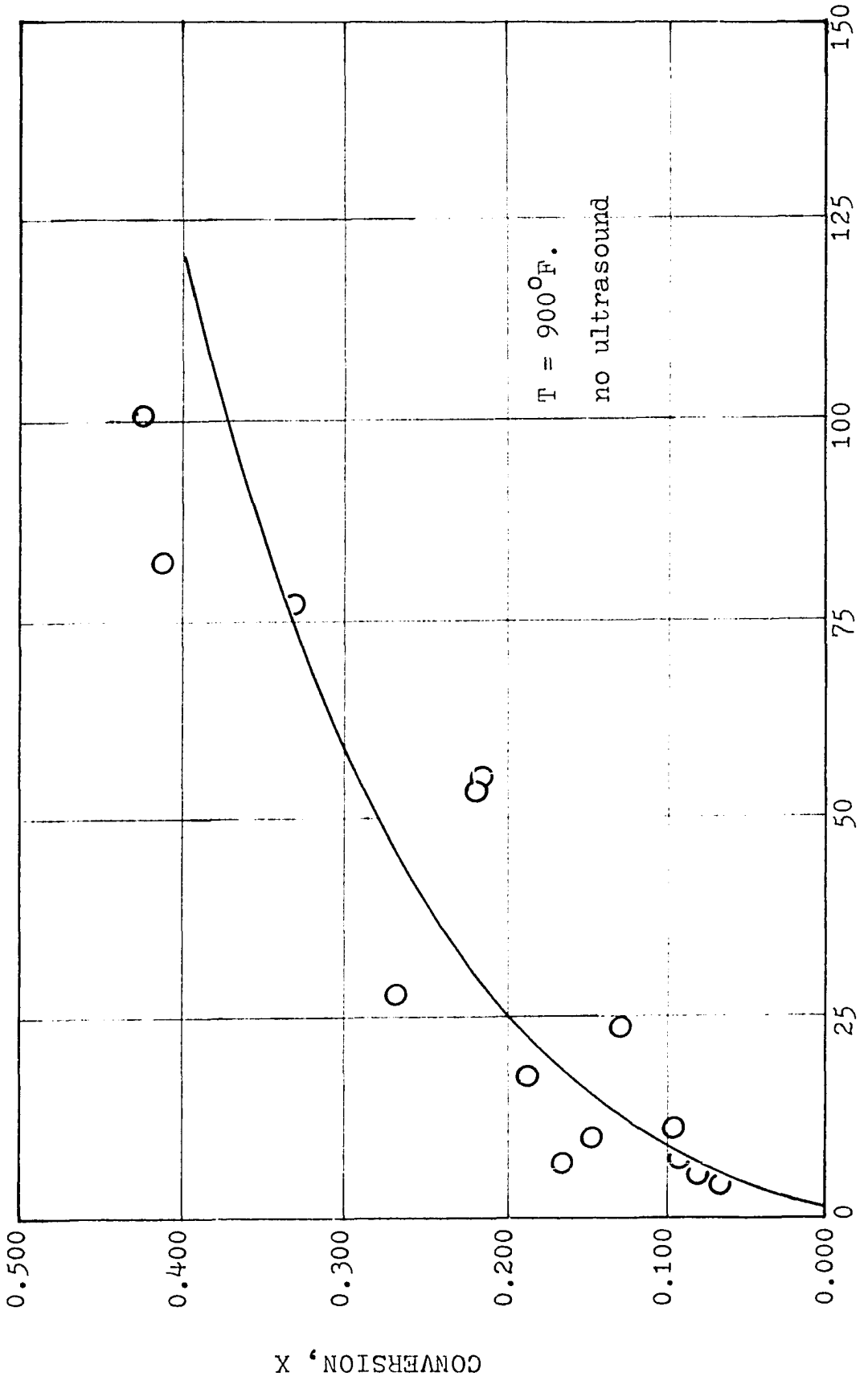

FIGURE 104

CONVERSION vs. W/F

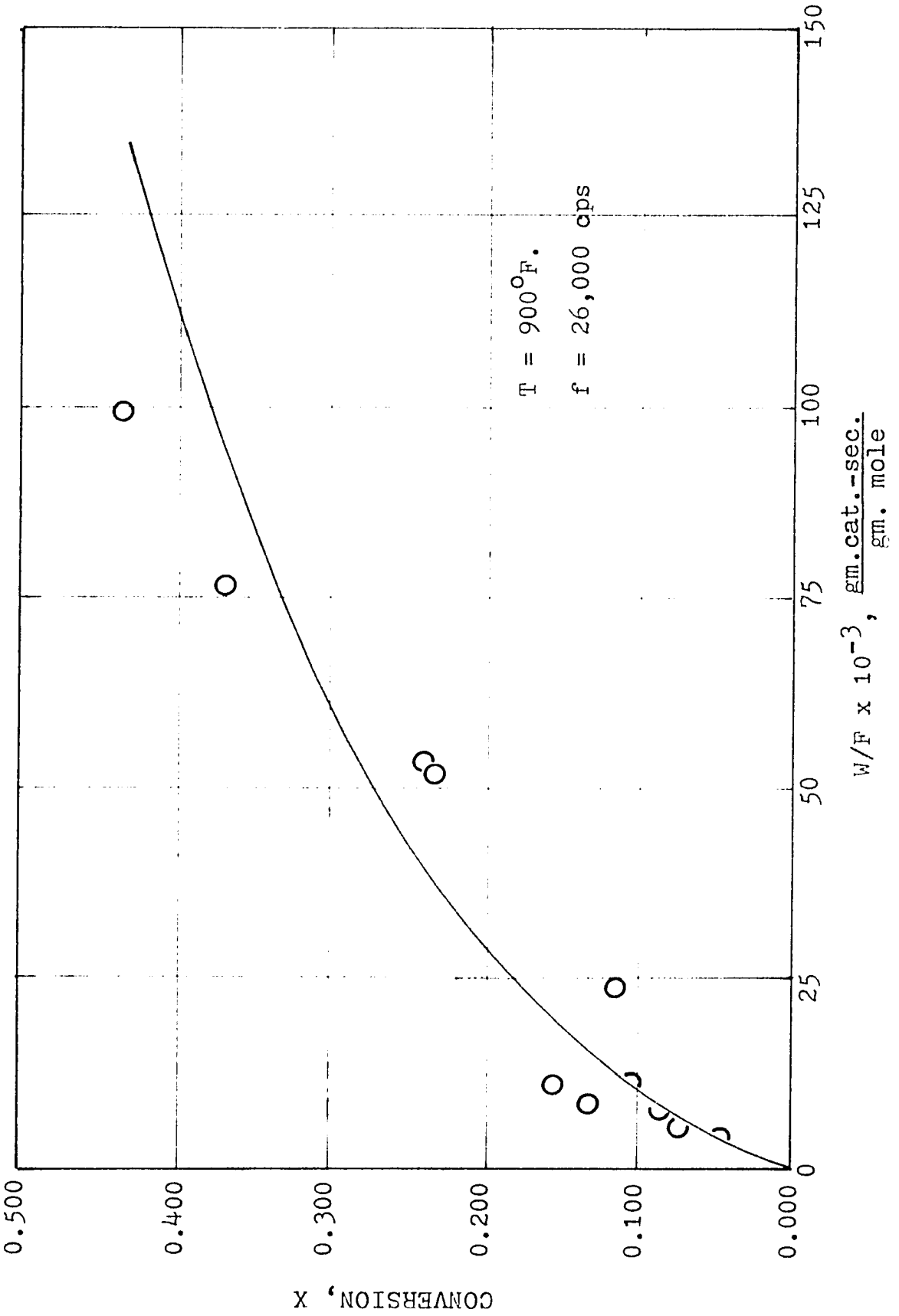

FIGURE 105

CONVERSION vs. W/F

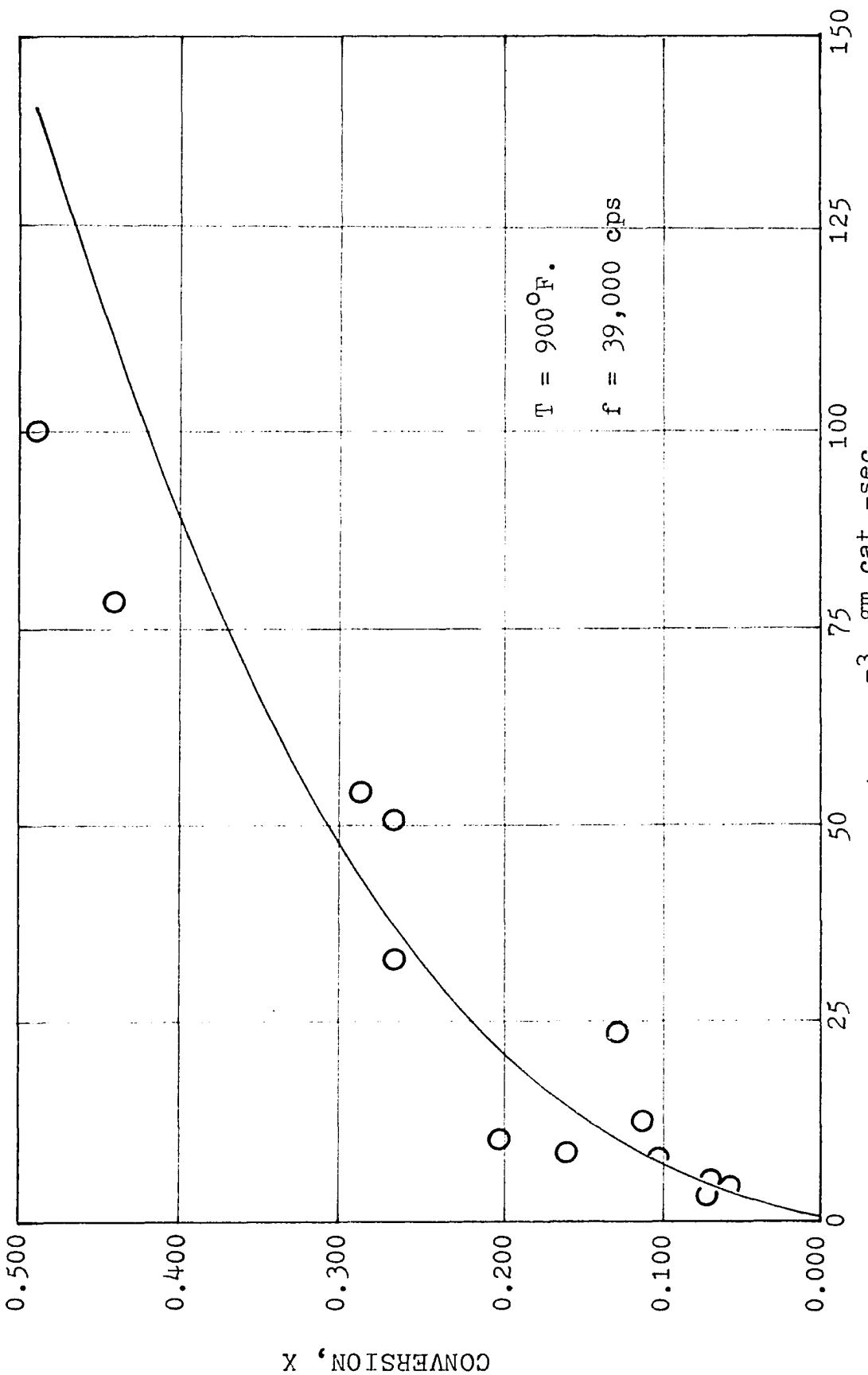

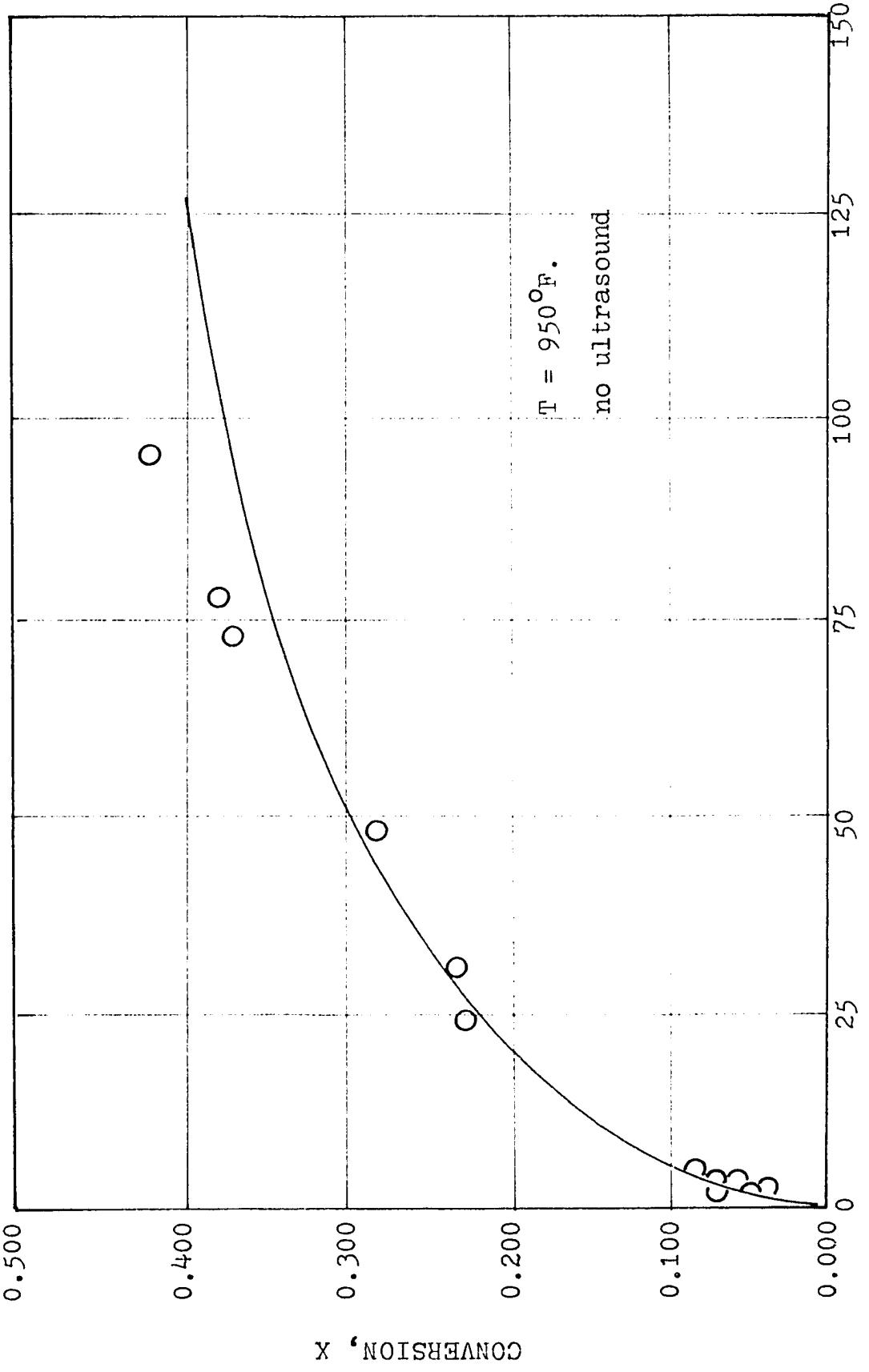

FIGURE 106

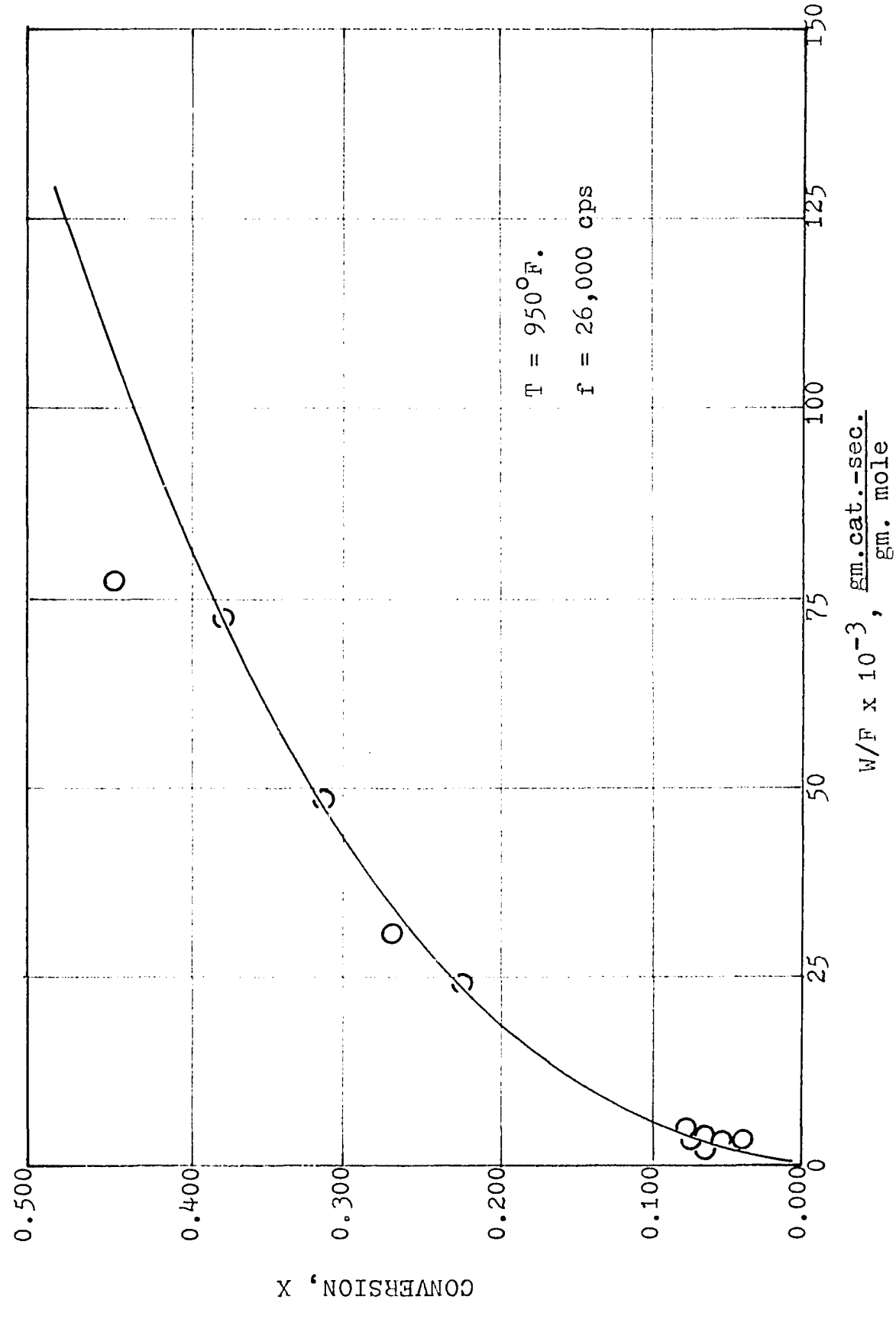

FIGURE 107

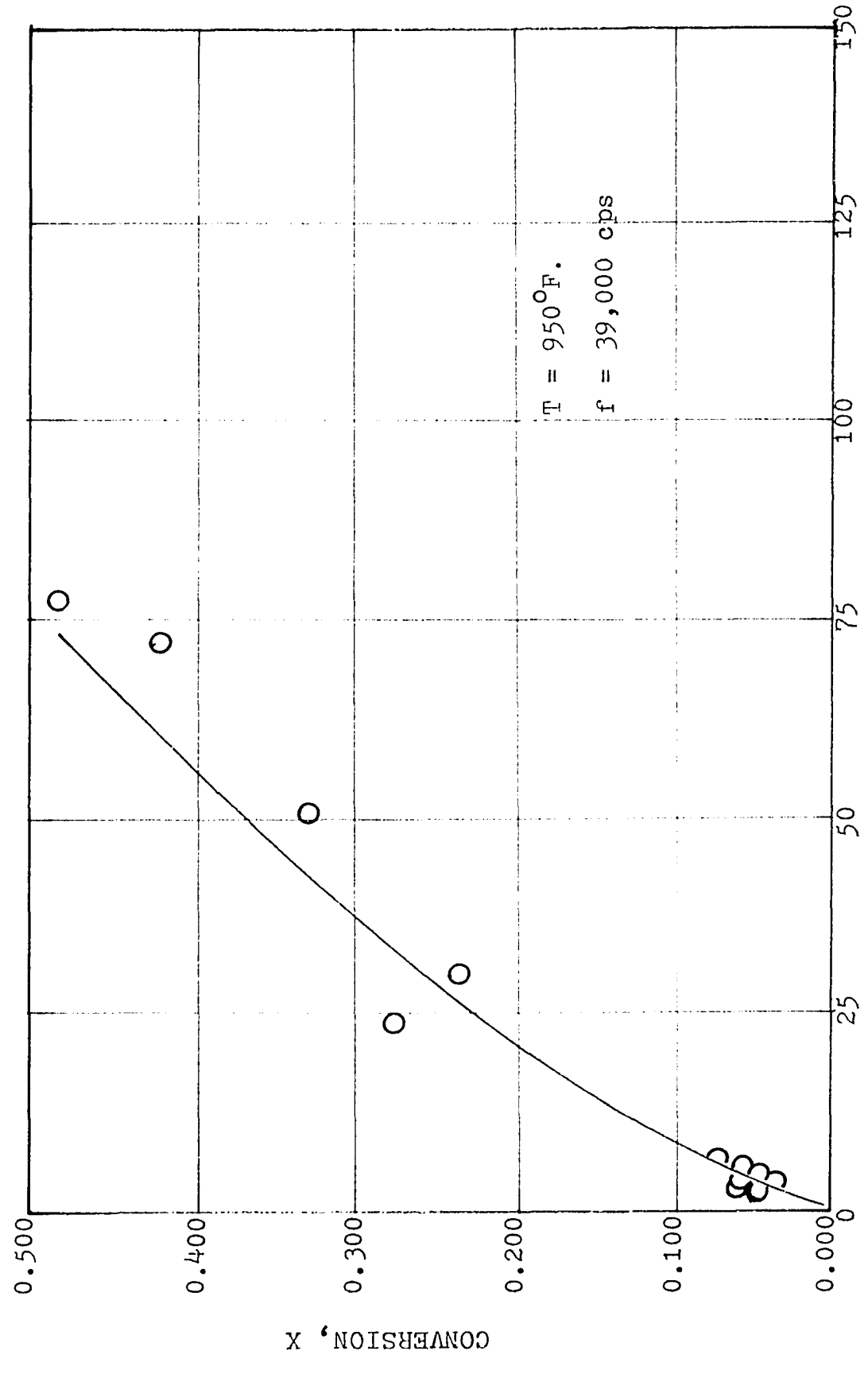

FIGURE 10S

FIGURE 109

CONVERSION vs. W/F

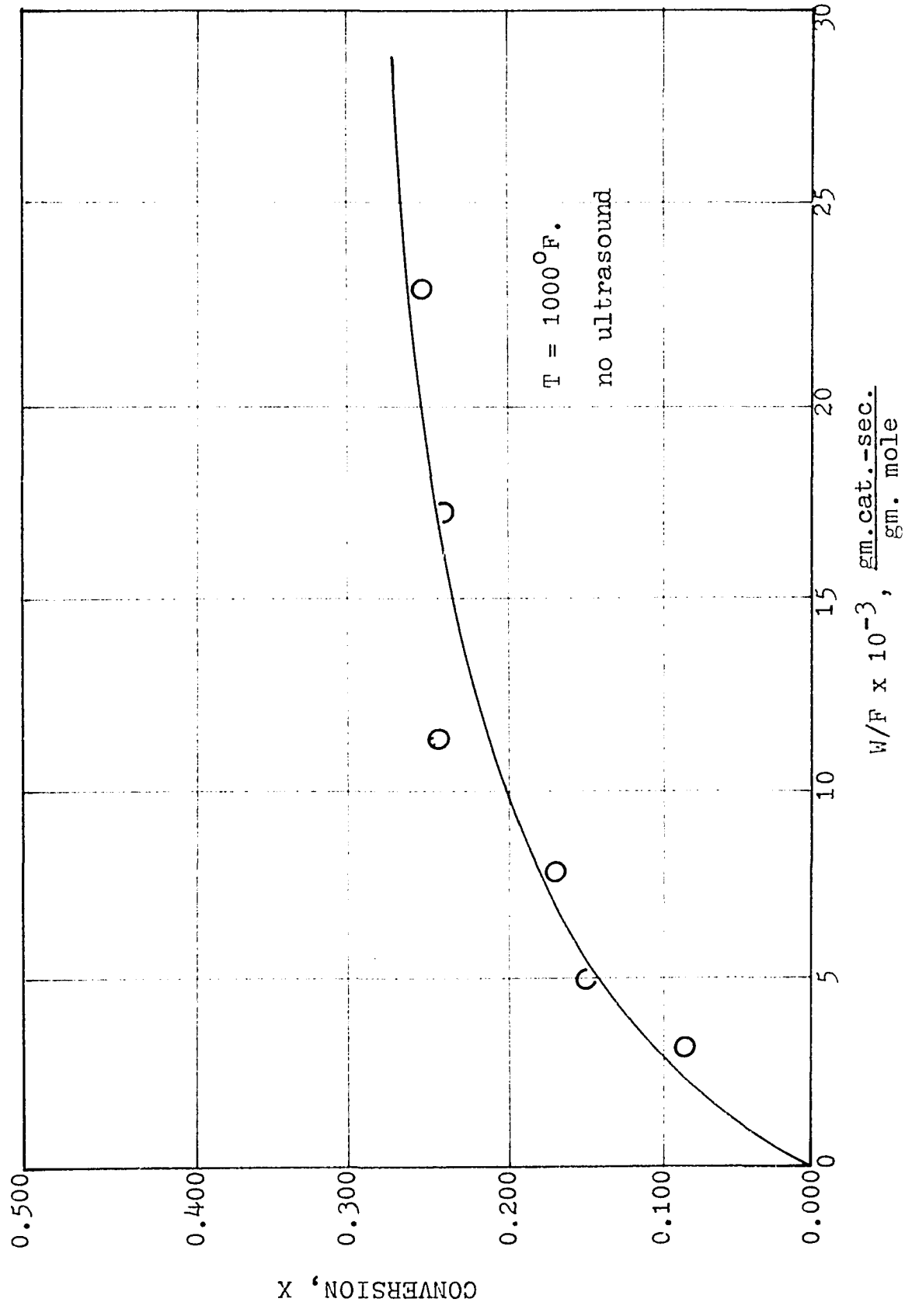

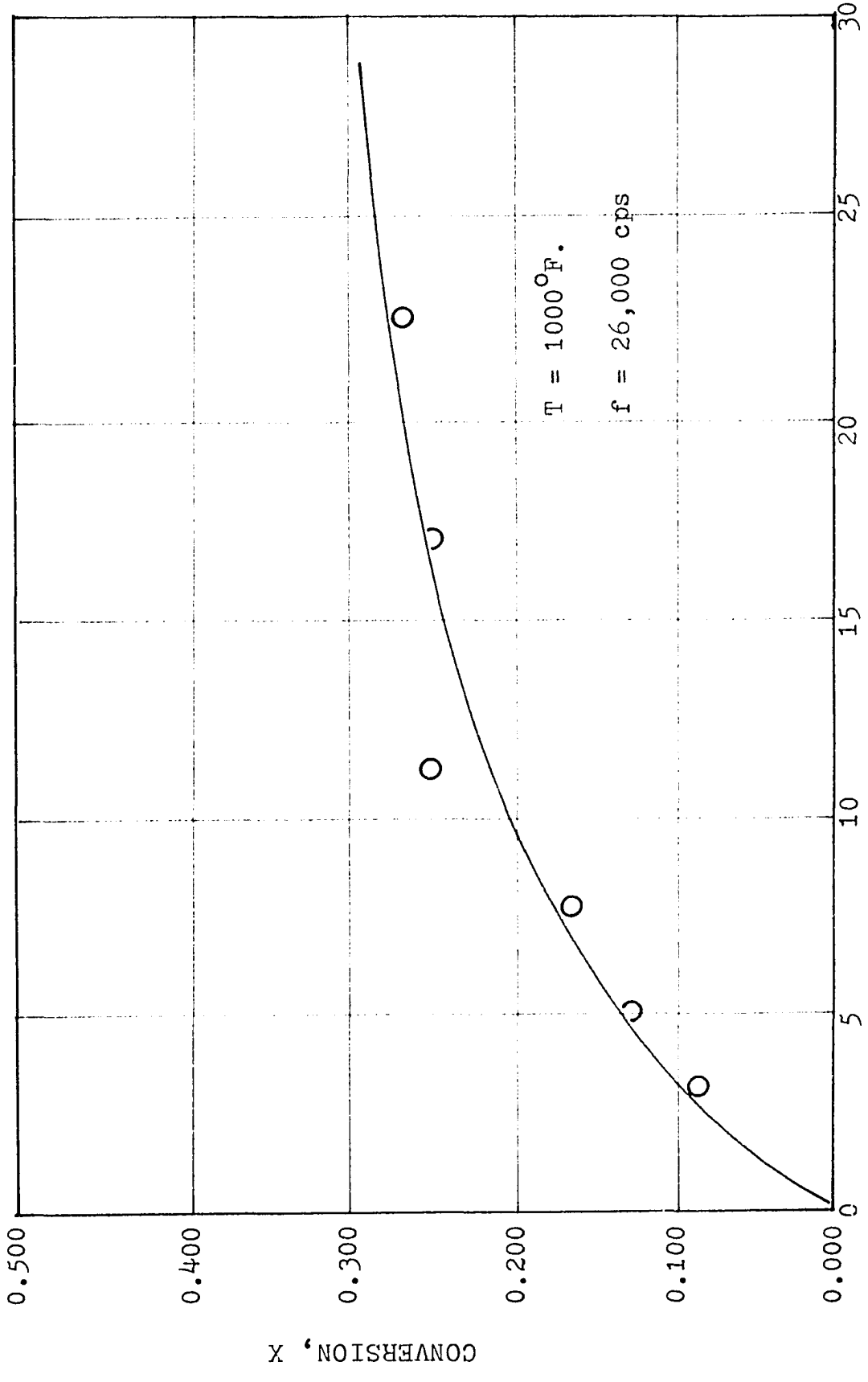

FIGURE 110

FIGURE 111

CONVERSION vs. W/F

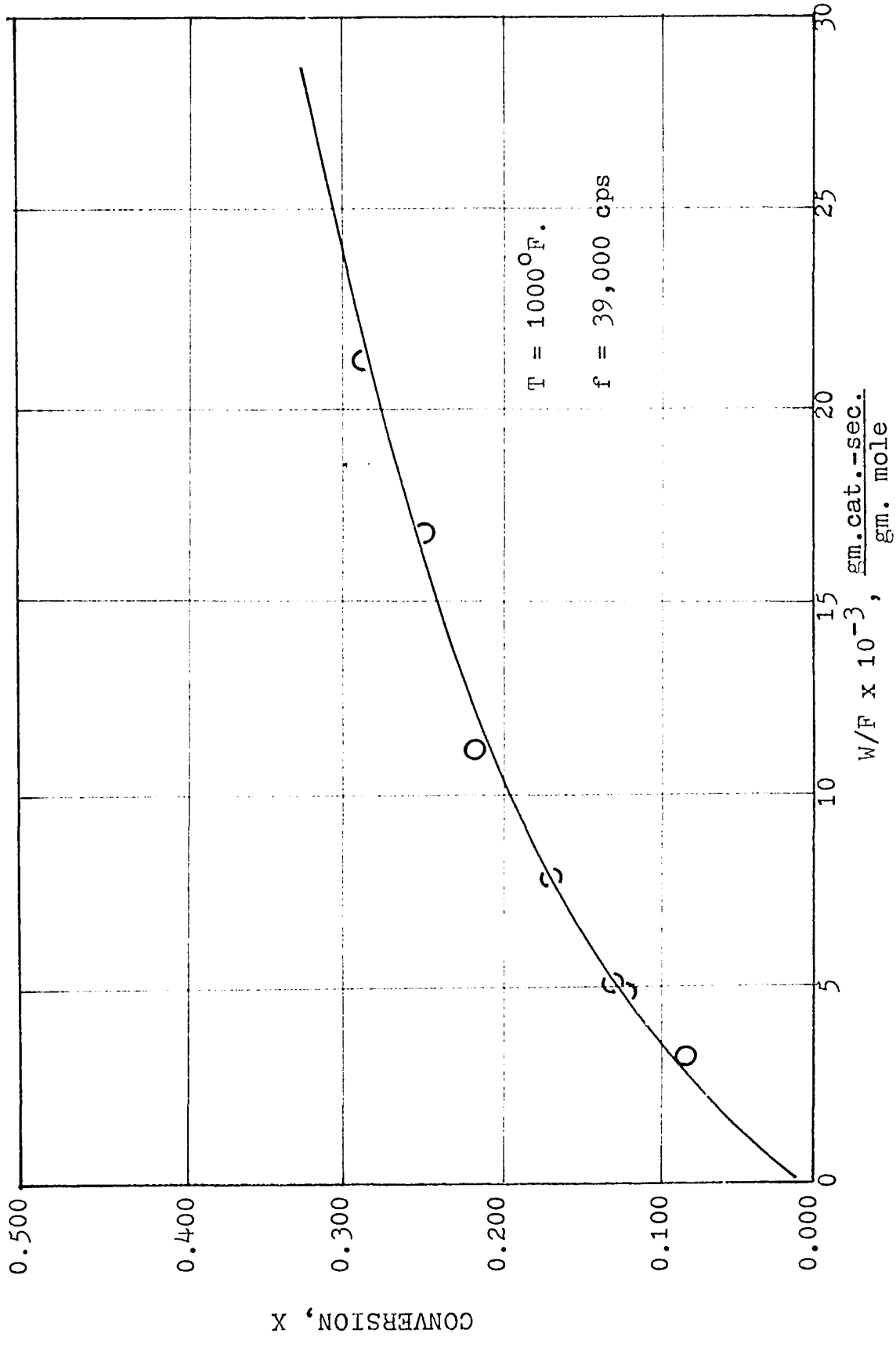

APPENDIX XVII

EVALUATION OF REACTION ACTIVATION ENERGY

EVALUATION OF REACTION ACTIVATION ENERGY

Arrhenius' Law

Arrhenius' Law, which describes the reaction rate constant as a function of the reaction activation energy and temperature is a follows:

$$k = k_o e^{-\frac{E}{RT}} \tag{151}$$

where,

k = reaction rate constant, $\frac{\text{gm moles}}{\text{gm cat-sec}}$

k_o = frequency factor, $\frac{\text{gm moles}}{\text{gm cat-sec}}$

E = activation energy, $\frac{\text{cal}}{\text{gm mole}}$

T = temperature, ^oK.

R = conversion factor, $1.98 \frac{\text{cal}}{\text{gm mole } ^oK.}$

For solid catalyzed reactions, the surface reaction rate corrected for pore diffusion, ϵLk_2, is substituted for k, the reaction rate constant. After this substitution is made, the natural logarithm of the equation is taken in order to obtain a linear function of reciprocal temperature.

$$\epsilon Lk_2 = k_o e^{-\frac{E}{RT}} \tag{152}$$

$$\ln \epsilon Lk_2 = \ln k_o - \frac{E}{RT} \ln e$$

$$= \ln k_o - \frac{E}{RT}$$

$$\ln \epsilon Lk_2 = \left(-\frac{E}{R}\right)\frac{1}{T} + \ln k_o \qquad (153)$$

Calculation of Activation Energy

In the above equation, $-\frac{E}{R}$ is the slope of the straight line obtained when $\ln \epsilon Lk_2$ is plotted against reciprocal temperature.

As shown in Chapter V, the equations for the curves at the frequencies studied are as follows:

no ultrasound: $\log \epsilon Lk_2 = -4812 \frac{1}{T^oR} - 1.141 \qquad (154)$

$$\ln \epsilon Lk_2 = -6157 \frac{1}{T^oK} - 2.628$$

26,000 cps: $\log \epsilon Lk_2 = -4115 \frac{1}{T^oR} - 1.637 \qquad (155)$

$$\ln \epsilon Lk_2 = -5265 \frac{1}{T^oK} - 3.770$$

39,000 cps: $\log \epsilon Lk_2 = -2801 \frac{1}{T^oR} - 2.534 \qquad (156)$

$$\ln \epsilon Lk_2 = -3584 \frac{1}{T^oK} - 5.836$$

The calculation of activation energy, E, from the constants associated with reciprocal temperature obtained from the above equations yield the following results:

no ultrasound: $-\frac{E}{R} = -6.57$; $E = (6157)(1.98)$

$$= 12.1 \frac{\text{kcal}}{\text{gm mole}}$$

26,000 cps.: $-\frac{E}{R} = -5265$; $E = (5265)(1.98)$

$$= 10.4 \frac{\text{kcal}}{\text{gm mole}}$$

39,000 cps: $-\frac{E}{R} = 3584$; $E = (3584)(1.98)$

$= 7.1 \frac{\text{kcal}}{\text{gm mole}}$

Calculation of the Characterization Factor

No ultrasound: $\ln k_o = -2.628$

$k_o = 0.0723 \frac{\text{gm moles}}{\text{gm cat-sec.}}$

26,000 cps: $\ln k_o = -3.770$

$k_o = 0.0231 \frac{\text{gm moles}}{\text{gm cat-sec.}}$

39,000 cps: $\ln k_o = 5.836$

$k_o = 0.00293 \frac{\text{gm moles}}{\text{gm cat-sec.}}$

APPENDIX XVIII

EVALUATION OF INTRINSIC RATE CONSTANT

EVALUATION OF INTRINSIC RATE CONSTANT

In order to plot ϵLk_2 as a function of Kelvin temperature on the same graph as the mass transfer coefficient, k_g, the equations for ϵLk_2 as a function of Rankine temperature must be transformed. The dimensions of ϵLk_2 in these equations are $\frac{gm\ moles}{gm\ cat\text{-}sec}$ which must be transposed to $\frac{cm}{sec}$ to correspond to the dimensions of k_g. This is accomplished by the following calculations:

No Ultrasound

$$\log \epsilon Lk_2 = -4812 \frac{1}{T^oR} - 1.141 \qquad (154)$$

$$k_s = \frac{(\epsilon Lk_2 \frac{gm\ moles}{gm\ cat\text{-}sec})(82.03 \frac{cm^3\text{-}atm}{gm\ mole\text{-}^oK})(T^oK)}{(1\ atm)(13.1 \frac{cm^2}{gm\ cat})}$$

$$T^oR = 1.8^oK$$

$$\log k_s = \log \epsilon Lk_2 + \log T^oK + \log \frac{82.03}{13.1}$$

$$\log k_s = -4812 \frac{1}{1.8T^oK} - 1.141 + \log T^oK + \log 6.2618320$$

$$\log k_s = \frac{-2673.2388}{T^oK} + \log T^oK - 0.3443293 \qquad (157)$$

Frequency = 26,000 cps

$$\log \epsilon Lk_2 = -4115 \frac{1}{T^oR} - 1.637 \qquad (155)$$

$$\log k_s = \frac{-2286.3666}{T^oK} + \log T^oK - 0.8399895 \qquad (158)$$

Frequency = 39,000 cps

$$\log \epsilon Lk_2 = -2801 \frac{1}{T^oK} - 2.534 \qquad (156)$$

$$\log k_s = \frac{-1555.8388}{T^oK} + \log T^oK - 1.7368171 \qquad (159)$$

The values of $\log k_s$ calculated at each temperature and frequency are shown in Table 14. Some of the values of the mass transfer coefficient, k_g, are also indicated in the table.

TABLE 14

INTRINSIC RATE CONSTANT AND MASS TRANSFER COEFFICIENT

T °F.	T °K.	log k_s, $\frac{cm}{sec}$			log k_g, $\frac{cm}{sec}$					
					W/F = 80,000 $\frac{gm\ cat\text{-}sec}{gm\ mole}$			W/F = 20,000 $\frac{gm\ cat\text{-}sec}{gm\ mole}$		
		No Ultra-sound	f = 26,000 cps	f = 39,000 cps	No Ultra-sound	f = 26,000 cps	f = 39,000 cps	No Ultra-sound	f = 26,000 cps	f = 39,000 cps
650	616	-3.89	-3.76	-3.47	-1.62	-1.61	-1.55	-1.58	-1.56	-1.43
700	644	-3.67	-3.58	-3.34						
750	672	-3.49	-3.41	-3.22	-1.52	-1.51	-1.44	-1.41	-1.39	-1.29
800	700	-3.32	-3.26	-3.11						
850	727	-3.16	-3.12	-3.02						
900	755	-3.01	-2.99	-2.92	-1.38	-1.35	-1.27	-1.17	-1.15	-1.08
950	783	-2.86	-2.87	-2.83						
1000	811	-2.73	-2.75	-2.75	-1.29	-1.25	-1.15	-1.01	-0.98	-0.94

APPENDIX XIX

CALCULATION OF MAXIMUM PROBABLE ERROR

CALCULATION OF MAXIMUM PROBABLE ERROR

Reciprocal Space Velocity, W/F_{A_o}

$$d\left(\frac{W}{F_{A_o}}\right) = \frac{F_{A_o}dW - WdF_{A_o}}{F_{A_o}^2} = \frac{dW}{F_{A_o}} - \frac{WdF_{A_o}}{F_{A_o}^2}$$

$$\frac{d\left(\frac{W}{F_{A_o}}\right)}{\frac{W}{F_{A_o}}} = \frac{dW}{W} - \frac{dF_{A_o}}{F_{A_o}}$$

The maximum probable error is the sum of the individual errors. Therefore,

$$\frac{d\left(\frac{W}{F_{A_o}}\right)}{\frac{W}{F_{A_o}}} = \frac{dW}{W} + \frac{dF_{A_o}}{F_{A_o}}$$

For example,

$$W = 5.748 \text{ gms.} \pm 0.001 \text{ gm.}$$

$$F_{A_o} = 200 \frac{\text{gms}}{\text{hr.}} \pm 0.8 \frac{\text{gms}}{\text{hr.}}$$

$$\frac{d\left(\frac{W}{F_{A_o}}\right)}{\frac{W}{F_{A_o}}} = \frac{0.001}{5.748} + \frac{0.8}{200} = 0.0001739 + 0.0040 = 0.00417$$

$$\% \text{ error} = 0.42\%$$

$$W/F_{A_o} = 12,435 \pm 52$$

Conversion, X_A

$$X_A = \frac{120.19R}{120.19R + 78.11A}$$

$$dX_A = \frac{(120.19R+78.11A)(120.19)dR-120.19R(120.19dR+78.11dA)}{(120.19R + 78.11A)^2}$$

$$= \frac{120.19dR}{120.19R+78.11A} - \frac{(120.19)^2RdR}{(120.19R+78.11A)^2} - \frac{(120.19)(78.11)RdA}{(120.19R+78.11dA)^2}$$

$$\frac{dX_A}{X_A} = \frac{dR}{R} + \frac{120.19\ dR}{(120.19R+78.11A)} + \frac{78.11\ dA}{(120.19R+78.11A)}$$

For example,

$$R = 7.32\% \pm 0.12\%$$

$$A = 91.09\% \pm 0.53\%$$

$$\frac{dX_A}{X_A} = \frac{0.12}{7.32} + \frac{120.19(0.12) + 78.11(0.53)}{120.19(7.32) + 78.11(91.09)}$$

$$\% \text{ error} = 2.34\%$$

$$X_A = 11.0\% \pm 0.2\%$$

APPENDIX XX

CALCULATION OF POWER INPUT

CALCULATION OF POWER INPUT

The maximum total power output of the ultrasonic horn employed in this research was 25 watts according to the manufacturers specifications. The power input per mole of reactor feed at the lowest and highest feed rates studied is as follows:

Power Input at Feed Rate of 25 gms./hr.

$$P = \frac{(25 \text{ watts})(1 \frac{\text{Joule}}{\text{watt-sec}})(3600 \frac{\text{sec}}{\text{hr}})(120.19 \frac{\text{gms}}{\text{gm mole}})}{(4.186 \frac{\text{Joules}}{\text{cal}})(25 \frac{\text{gms}}{\text{hr}})(1000 \frac{\text{cal}}{\text{kcal}})}$$

$$= 103.4 \frac{\text{kcal}}{\text{gm-mole}}$$

Power Input at Feed Rate of 600 gms/hr.

$$P = \frac{(25 \text{ watts})(1 \frac{\text{Joule}}{\text{watt-sec}})(3600 \frac{\text{sec}}{\text{hr}})(120.19 \frac{\text{gms}}{\text{gm mole}})}{(4.186 \frac{\text{Joules}}{\text{cal}})(600 \frac{\text{gms}}{\text{hr}})(1000 \frac{\text{cal}}{\text{kcal}})}$$

$$= 4.3 \frac{\text{kcal}}{\text{gm-mole}}$$

APPENDIX XXI

SAMPLE CALCULATION OF THE MASS TRANSFER COEFFICIENT

SAMPLE CALCULATION OF THE MASS TRANSFER COEFFICIENT

The mass transfer coefficient is calculated from the following equation derived in Chapter II and Appendix IV:

$$k_g = \frac{6.26\ X_{A_f}\ T}{(W/F_{A_o})\ln(1 + Y_{A_{LM}})} \qquad (22)$$

Some actual values for the parameters are as follows:

$$W/F_{A_o} = 20{,}000\ \frac{\text{gm cat-sec.}}{\text{gm mole}}$$

$$T = 850^{o}\text{F.} = 727^{o}\text{K.}$$

$$X_{A_f} = 0.171$$

$$X_{A_o} = \frac{1-X_{A_f}}{1+X_{A_f}} = \frac{1-0.171}{1+0.171} = \frac{0.829}{1.171} = 0.708$$

$$Y_{A_{LM}} = \frac{1-X_{A_o}}{\ln 1/X_{A_o}} + \frac{1-0.708}{\ln \frac{1}{0.708}} = \frac{0.292}{\ln 1.412} = 0.845$$

Substitution of the above values into Equation (22) yields the following:

$$k_g = \frac{(6.26)(0.171)(727)}{(20{,}000)\ln(0.845)} = 0.0635\ \frac{\text{cm}}{\text{sec}}$$

APPENDIX XXII

ANALYSIS OF VARIANCE

ANALYSIS OF VARIANCE

The confidence intervals for the coefficients of the linear equations expressing $\log k_g$ as a function of T and $\log \epsilon Lk_2$ as a function of $\frac{1}{T}$ are calculated as illustrated in the following example.

Linear Equation at W/F_o = 80,000 $\frac{\text{gm cat-sec}}{\text{gm mole}}$ and No Ultrasound

$$\log k_g = 0.00169T - 2.66$$

Let $y = \log k_g$

$x = T$

$a = -2.66$

$b = 0.00169$

Calculate S_x and S_y

$$S_x = \left[\frac{n\Sigma x^2 - (\Sigma x)^2}{n(n-1)}\right]^{\frac{1}{2}}$$

$n = 5$ (number of data points)

$x^2 = 2{,}653{,}227$

$(\Sigma x)^2 = (3637)^2 = 13{,}227{,}769$

$$S_x = \left[\frac{(5)(2{,}653{,}227) - 13{,}227{,}769}{5(4)}\right]^{\frac{1}{2}} = 43.798$$

$$S_y = \left[\frac{n\Sigma y^2 - (\Sigma y)^2}{n(n-1)}\right]^{\frac{1}{2}}$$

$n = 5$

$y^2 = 10.336845$

$(\Sigma y)^2 = (-7.18143)^2 = 51.572936$

$$S_y = \left[\frac{5(10.336845)-51.572936}{5(4)}\right]^{\frac{1}{2}} = 0.074595$$

Calculate r

$$r = \frac{bS_x}{S_y} = \frac{(0.00169)(43.798)}{0.074595} = 0.9922729$$

Calculate $S_{y\cdot x}$

$$S_{y\cdot x} = S_y\left[\frac{(n-1)(1-r^2)}{(n-2)}\right]^{\frac{1}{2}} = 0.074595\left[\frac{4(0.0153945)}{3}\right]^{\frac{1}{2}}$$

$$= 0.0010689$$

Calculation of S_a and S_b

$$S_a = S_{y\cdot x}\left[\frac{1}{n} + \frac{\bar{x}^2}{(n-1)S_x^2}\right]^{\frac{1}{2}}$$

$$\bar{x}^2 = \left[\frac{\Sigma x}{n}\right]^2 = \left[\frac{3637}{5}\right]^2 = 529{,}100.76$$

$$S_a = (0.0010689)\left[\frac{1}{5} + \frac{529{,}100.76}{4(43.798)^2}\right]^{\frac{1}{2}} = 0.0088889$$

$$S_b = \frac{S_{y\cdot x}}{(n-1)^{\frac{1}{2}}S_x} = \frac{(0.0010689)}{(4)^{\frac{1}{2}}(43.798)} = 0.0000122$$

Calculate 99% Confidence Interval

$$t_{n-2,} = t_{3,99} = 5.841$$

$$a = -2.66 \pm t_{3,99}S_a = -2.66\pm(5.841)(0.0088889) = -2.66\pm0.05$$

$$b = 0.00169\pm t_{3,99}S_b = 0.00169\pm(5.841)(0.0000122)$$

$$= 0.00169\pm0.00007$$

Calculate 95% Confidence Interval

$$t_{n-2,} = t_{3,95} = 3.182$$

$$a = -2.66 \pm (3.182)(0.0088889) = -2.66 \pm 0.03$$

$$b = 0.00169 \pm (3.182)(0.0000122) = 0.00169 \pm 0.00004$$

Calculate 90% Confidence Interval

$$t_{n-2,} = t_{3,90} = 2.358$$

$$a = -2.66 \pm (2.358)(0.0088889) = -2.66 \pm 0.02$$

$$b = 0.00169 \pm (2.358)(0.0000122) = 0.00169 \pm 0.00003$$

The confidence intervals are similarly calculated for the remaining relationships.

NOMENCLATURE

A = reference to cumene

A = area, cm^2

a = superficial surface area of catalyst, $\frac{cm^2}{gm}$

a = transverse acceleration, $\frac{cm}{sec^2}$

C = total concentration of A + R + S, $\frac{gm\text{-}moles}{cm^3}$

C_A = concentration of cumene, $\frac{gm\text{-}moles}{cm^3}$

C_{A_e} = equilibrium concentration of benzene, $\frac{gm\text{-}moles}{cm^3}$

C_{A_1} = concentration of active sites occupied by A, $\frac{cm^2}{gm\text{-}cat}$

C_{A_s} = concentration of cumene on catalyst surface, $\frac{gm\text{-}moles}{cm^3}$

C_L = total concentration of available active sites, $\frac{cm^2}{gm\ cat}$

C_1 = concentration of unoccupied active sites, $\frac{cm^2}{gm\ cat}$

C_P = heat capacity of gas at constant pressure, $\frac{cal}{gm\text{-}^oC.}$

C_R = concentration of benzene, $\frac{gm\text{-}moles}{cm^3}$

C_{R_e} = equilibrium concentration of benzene, $\frac{gm\ moles}{cm^3}$

C_{R_1} = concentration of active sites occupied by R, $\frac{cm^2}{gm\ cat}$

C_S = concentration of propylene, $\frac{gm\text{-}moles}{cm^3}$

C_{S_1} = concentration of active sites occupied by S, $\frac{cm^2}{gm\ cat}$

C_V = heat capacity of gas at constant volume, $\frac{cal}{gm\text{-}^oC.}$

D_{AB} = diffusivity of A in A + B + S, $\frac{cm^2}{sec}$

D_{AB} = diffusivity of cumene in benzene, $\frac{cm^2}{sec}$

D_{AS} = diffusivity of cumene in propylene, $\frac{cm^2}{sec}$

D_e = effective pore diffusivity, $\frac{cm^2}{sec}$

D_K = Knudsen diffusivity, $\frac{cm^2}{sec}$

D_s = combined diffusivity, $\frac{cm^2}{sec}$

d = average diameter of catalyst pore, cm.

d_p = diameter of catalyst particle, cm.

E = activation energy, $\frac{gm\ cal}{gm\text{-}mole}$

F = feed rate, $\frac{gms}{hr}$

F = force, dynes

F_{A_o} = initial cumene feed rate, $\frac{gm\text{-}moles}{hr.}$ or $\frac{gm\text{-}moles}{sec.}$ (see text)

f = frequency, $\frac{cycles}{sec.}$

G = superficial mass velocity of gas normal to catalyst bed, $\frac{gms}{cm^2\text{-}sec}$

g_c = conversion factor, 980 $\frac{dynes}{gm.}$

h_S = Thiele modulus = $mr_p = r_p \frac{k_s S_v}{D_e}^{\frac{1}{2}}$, dimensionless

I = intensity, $\frac{erg}{cm^2\text{-}sec}$, $\frac{dyne\text{-}cm.}{cm^2\text{-}sec}$ $(10^{-7}\ \frac{watt\text{-}sec}{erg})$

I_o = $10^{-16}\ \frac{watts}{cm^2}$

K = equilibrium constant for overall reaction, atm.

K_2 = equilibrium constant for surface reaction, atm.

K_3 = equilibrium desorption constant for R, atm.

K_A = equilibrium adsorption constant for A, $\frac{1}{\text{atm.}}$

K_R = equilibrium adsorption constant for R, $\frac{1}{\text{atm.}}$

k = forward reaction rate constant for overall reaction, $\frac{\text{gm moles}}{\text{gm cat-atm-sec}}$

k = compressibility, $\frac{\text{cm}^2}{\text{dyne}}$, $\frac{\text{cm-sec}^2}{\text{gm}}$ (dyne = $\frac{\text{gm-cm}}{\text{sec}^2}$)

k' = reverse reaction rate constant for overall reaction, $\frac{\text{gm moles}}{\text{gm cat-atm}^2\text{-sec}}$

k_o = constant, $\frac{\text{cm}}{\text{sec}}$

k_1 = rate constant for adsorption of A, $\frac{\text{gm moles}}{\text{cm}^2\text{-atm-sec}}$

k'_1 = rate constant for desorption of A, $\frac{\text{gm moles}}{\text{cm}^2\text{-sec}}$

k_2 = forward reaction rate constant for surface reaction, $\frac{\text{gm moles}}{\text{cm}^2\text{-sec}}$

k'_2 = reverse reaction rate constant for surface reaction, $\frac{\text{gm moles}}{\text{cm}^2\text{-atm-sec}}$

k_3 = equilibrium desorption constant for R, atm.

k'_3 = rate constant for adsorption of R, $\frac{\text{gm moles}}{\text{cm}^2\text{-atm-sec}}$

$k_g = \frac{D_{AB}}{\delta}$, mass transfer coefficient, $\frac{\text{cm}}{\text{sec}}$

k_P = pseudo first order forward reaction rate constant, $\frac{\text{cm}^3}{\text{gm cat-sec}}$

k'_P = pseudo first order reverse reaction rate constant, $\frac{\text{cm}^3}{\text{gm cat-sec}}$

k_s = forward intrinsic rate constant for surface reaction, $\frac{cm}{sec}$

k'_s = reverse intrinsic rate constant for surface reaction, $\frac{cm^4}{gm\ mole\text{-}sec}$

L = reactor length, cm.

L = total concentration of active sites, $\frac{cm^2}{gm\ cat}$

l = unoccupied active catalyst site, dimensionless

M = molecular weight, $\frac{gms}{gm\ mole}$

m = mass, gms.

N_A = number of moles of A, gm moles

N_{A_o} = initial number of moles of A, gm moles

N_{A_f} = final number of moles of A, gm moles

N_{A_Z} = rate of mass transfer of A in z direction, $\frac{gm\text{-}moles}{cm^2\text{-}sec}$

N_{B_Z} = rate of mass transfer of R + S in z direction, $\frac{gm\ moles}{cm^2\text{-}sec}$

N_T = total number of moles, gm-moles

n = 1,3,5,7,9, etc.

P = vapor pressure, mm. Hg

p = partial pressure, atm.

p = pressure, $\frac{dynes}{cm^2}$

p_c = critical pressure, atm.

p_{max} = maximum pressure caused by sound wave, $\frac{dynes}{cm^2}$

p_T = total pressure, atm.

R = ideal gas constant, 82.06 $\frac{cm^3\text{-}atm}{gm\ mole\text{-}^oK}$.

R = reference to benzene

R = ideal gas constant, 1.987 $\frac{\text{gm-cal}}{\text{gm mole-}^{o}\text{K}}$

R = 8.31 x 10^{7} $\frac{\text{ergs}}{\text{gm mole-}^{o}\text{K}}$, $\frac{\text{dyne-cm.}}{\text{gm mole-}^{o}\text{K}}$

(erg = dyne-cm = $\frac{\text{gm-cm}^2}{\text{sec}^2}$)

R_e = Reynold's number, dimensionless

R_g = ideal gas constant, 8.3 x 10^{7} $\frac{\text{gm-cm}^2}{\text{gm mole-}^{o}\text{K-sec}^2}$

R_{max} = maximum reaction rate, $\frac{\text{gm moles}}{\text{sec.}}$

R_P = rate of diffusion into catalyst pellet, $\frac{\text{gm-moles}}{\text{sec.}}$

r_o = initial rate of reaction, $\frac{\text{gm moles}}{\text{gm cat-sec}}$

r_A = gm moles A diffusing toward catalyst surface per second per gm catalyst, $\frac{\text{gm-moles}}{\text{gm.sec.}}$

$(-r_{A_1})$ = reaction rate, $\frac{\text{gm moles A}}{\text{gm cat-sec}}$

r_e = equivalent radius of pore, cm.

r_P = radius of catalyst particle, cm.

S = reference to propylene

S_{EX} = external surface area of catalyst, cm^2

S_g = total surface area of porous catalyst, $\frac{cm^2}{gm}$

S_v = total surface of porous catalyst = $\rho_P S_g$, $\frac{cm^2}{cm^3}$

T = temperature, ^{o}K.

T = period, $\frac{\text{sec}}{\text{cycle}}$

t = time, sec.

t = temperature, ^{o}C.

T_C = critical temperature, ^{o}C.

V = velocity of propagation of wave form, $\frac{cm}{sec}$

V_b = molar volume at the normal boiling point, $\frac{cm^3}{gm\ mole}$

V_c = critical molar volume, $\frac{cm^3}{gm\text{-}mole}$

V_g = pore volume, $\frac{cm^3}{gm}$

v = transverse velocity, $\frac{cm}{sec}$

v = volume, cm^3

W = weight catalyst, gms.

W = work done on A system dyne-cm, ergs.

W_c = weight of catalyst, gms.

X = distance traversed by wave form, cm.

X_A = conversion of A, dimensionless

X_{Ae} = equilibrium conversion of cumene, dimensionless

X_{Af} = final conversion of A

X_{Ao} = initial conversion of A

Y = mole fraction in gas phase

Y = amplitude, cm.

Y_A = mole fraction of A, dimensionless

Y_{Ab} = mole fraction of A in bulk stream, dimensionless

Y_{ALM} = log mean mole fraction of cumene in the bulk stream dimensionless

Y_{As} = mole fraction of A at catalyst surface, dimensionless

y = displacement, cm.

z = distance in z direction, cm.

β = sound intensity level, decibels

$\gamma = \frac{C_P}{C_V}$

δ = thickness of stagnant gas film between main gas stream and external surface of catalyst, cm.

ε = void fraction in packed catalyst bed, dimensionless

ϵ = catalyst effectiveness factor, dimensionless

ϵ/K = Lennard-Jones parameter, ^{o}K.

θ = catalyst internal void fraction, dimensionless

λ = wave length, $\frac{cm.}{cycle}$

π = total pressure, atm.

ρ = fluid density, $\frac{gms}{cm^3}$

ρ_B = bulk density of catalyst bed, $\frac{gms}{cm^3}$

ρ_o = initial gas density, $\frac{gms}{cm^3}$

ρ_p = catalyst particle density, $\frac{gms}{cm^3}$ of particle volume

ρ_t = true density of solid material in porous catalyst, $\frac{gms}{cm^3}$

σ = Lennard-Jones parameter, $\mathring{A}$

τ = tortuosity factor, dimensionless

μ_c = critical viscosity, $\frac{gm.}{cm\text{-}sec}$

Ω_D = collision integral

LITERATURE REFERENCES

1. Aerstin, F.G., Timmerhaus, K.D., and Fogler, H.S., A.I.Ch.E. Journal, Vol. 13, 1967, p. 453.

2. Arkhangel'skii, M.E., Zh. Fiz. Khim., Volume 43, 1969, pp. 942-945.

3. Belov, B.G., U.S.S.R. Patent No. 226,328, September 5, 1968.

4. Berger, Heinz, German Patent No. 1,279,660, October 10, 1968

5. Bezre, Walid E., Romanovskii, B.V., and Topchieva, K.V., Kinet. Katal., Vol. 9, 1968, pp. 931-934.

6. Bird, R. Byron, Transport Phenomena. New York: John Wiley and Sons, Inc., 1965, pp. 529-531.

7. Boucher, R.M.G., Towey, J.P., and Tobin, C.D., Research and Development, February, 1966.

8. Boucher, R.M.G., British Chemical Engineering, Vol. 15, 1970, pp. 363-367.

9. Brown, Charles Edwin, Effect of Catalyst Particle Size on the Rate of Synthesis of Methyl Alcohol in an Internally-Recycled Difference Reactor, Doctoral Dissertation, University of Connecticut, 1969, 205 pages.

10. Chen, J.M., and Kalback, W.M., Industrial and Engineering Fundamentals, Vol. 6, No. 2, May 1967, pp. 175-178.

11. Christie, Dan Edwin, Intermediate College Mechanics. New York: McGraw-Hill Book Company, Inc., 1952, pp. 424-425.

12. Corrigan, T.E., Garver, J.C., Rase, H.R., and Kirk, R.S., Chemical Engineering Progress, Vol. 49, 1953, pp. 603-610.

13. Currell, Douglas L., Nagy, Stanley S., Journal of the Acoustical Society of America, Vol. 44, No. 5, 1968, pp. 1201-1203.

14. Fedotov, A.M., U.S.S.R. Patent No. 212,900, September 5, 1968.

15. Fogler, S., "Studies in Ultrasonic Reaction Kinetics," Symposium on Selected Papers - Part I, American Institute of Chemical Engineers, November 26,-30, 1967.

16. Fogler, S., Sound and Vibrations, Vol 1, No. 8, August, 1967, pp. 17-21.

17. Fogler, H. Scott, "Sonochemical Engineering," Chemical Engineering Symposium Series, American Institute of Chemical Engineers, Vol. 67, No. 109, 1971.

18. Fogler, H. Scott, Industrial and Engineering Chemical Fundamentals, Vol. 7, No. 3, 1968, pp. 387-396.

19. Fogler, H. Scott, and Barnes, D., Industrial and Engineering Chemical Fundamentals, Vol. 7, No. 2, 1968, pp. 222-226.

20. Fogler, H. Scott, and Lund, K., Journal of the Acoustical Society of America, Vol. 49, No. 114, 1970.

21. Fridman, V.M., Novitskii, B.G., Baklanov, N.M., and Kochetov, A.S., British Patent No. 1,113,128, May 8, 1968, 3 pp.

22. Garver, John, The Kinetics and Mechanism of the Catalytic Cracking of Cumene, Doctoral Dissertation, University of Wisconsin, 1955.

23. Geissler, George, Strahlentherapie, Vol. 136, No. 6, 1968, pp. 761-765.

24. Gindis, A.P., Akust. Ul'trazvuk. Mezhved. Resp. Nauch.-Tekh., Vol. 2, 1966, pp. 102-105.

25. Greensfelder, B.S., Voge, H.H., and Good, G.M., Industrial Engineering Chemistry, Vol. 41, 1949, pp. 2573-2584.

26. Greguss, P., International Chemical Engineering, Vol. 3, No. 2, April, 1963, pp. 280-294.

27. Griffing, V., and Sette, D., Journal of Chemistry and Physics, Vol. 23, No. 503, 1955.

28. Heymach, George J., and Jost, Donald E., Journal of Polymer Science, Part C, No. 25, 1967, pp. 143-145.

29. Hougan, Olaf A., Watson, Kenneth M., and Ragatz, Roland, A., Chemical Process Principals, Part I, Material and Energy Balances. New York: John Wiley and Sons, Inc., 1965.

30. Jones, James B. ,U.S. Patent No. 3,029,766, April 17, 1962, 7 pp.

31. Jones, James B., "Ultrasonically Activated Catalysts for Chemical Reactions," U.S. Patent No. 3,245,892, April 12, 1966, 4 pp.

32. Kessler, Theodore, Sharkey, A.G., and Friedel, R.A., U.S. Bureau of Mines, Report of Investigation No. 7027, 1967, 11 pp.

33. Kokorev, D.T., Malakhov, R.A., Klyucharev, A.E., Morozov, V.A., and Stepanyuk, V.N., Izobret-Prom. Obraztsy Touarnye Znaki, Vol. 45, No. 24, 1968.

34. Kowalska, Eugenia, and Mizera, Jan, Przem. Chem., Vol. 48, No. 4, 1969, pp. 210-212.

35. Kunii, D., and Levenspiel, O., Fluidization Engineering. New York: John Wiley and Sons, Inc., 1969.

36. Lange, Norbert A., Handbook of Chemistry. Sandusky, Ohio: Handbook Publishers, Inc., 1939.

37. Levenspiel, Octave, Chemical Reaction Engineering. New York: John Wiley and Sons, Inc., 1965, pp. 426-475.

38. Levy, M.B., Nature, Vol. 85, No. 4707, January 16, 1960, p. 159.

39. Macarovici, Constantin, Iscrulescu, Virginia T., and Kovasci, Istvan, Rumanian Patent No. 51,305, November, 1968, 4 pp.

40. Makeeva, L.G., Neklyudova, N.I., Vasil'evich, L.V., Dzhagupov, R.G., and Ragozin, Yu S., Vestn. Mosk. Univ., Series II, Vol. 22, No. 3, 1967.

41. Mal'tsev, A.N., Margulis, M.A., Akust. Zh., Vol 14, No. 2, 1968, pp. 295-297.

42. Manu, V., Sasu, C., and Lucretia, Oprei, Rev. Fiz. Chim., Series A, Vol. 3, No. 11, 1966, pp. 405-412.

43. Margulis, M.A., Mal'tsev, A.N., Zh. Fiz. Chim., Vol. 42, No. 6, 1968, pp. 1441-1451.

44. Mario, E., and Gerraughty, R.J., Journal of Pharmaceutical Science, Vol. 54, No. 2, 1965, pp. 321-323.

45. Mason, Warren P., U.S. Government Research Development Report, Vol. 68, No. 11, 1968, pp. 105-106.

46. Mathewson, W.F., and Smith, J.C., Chemical Engineering Progress Symposium Series, Vol. 59, No. 41, 1963.

47. Mezaki, Reiji, and Happel, John, Catalysis Review, Vol. 3, No. 2, 1969, pp. 241-270.

48. Needham, T.E., Jr., and Gerraughty, Robert J., Journal of Pharmaceutical Science, Vol. 58, No. 1, 1969, pp. 62-64.

49. Nosav, V.A., "Soviet Progress in Applied Ultrasonics, Vol. 2," Ultrasonics in the Chemical Industry, Consultant Bureau, New York, 1965, 164 pp.

50. Panchenkov, G.M. and Zhorov, Yu. M., Neftekhimiya, Vol 1, 1961, pp. 172-181.

51. Pansing, W.F. and Malloy, J.B., Chemical Engineering Progress, Vol. 58, No. 12, 1962, pp. 53-54.

52. Paryjczak, Tadeusz and Witekowa, Stanislawa, Zesz. Nauk. Politech. Lodz. Chem., No. 18, 1967, pp. 91-100.

53. Paryjczak, Tadeusz, Wiad. Chem., Vol 23, No. 6, 1969, pp. 377-398.

54. Peacocke, A.R. and Pritchard, N.J., Biopolymers, Vol. 6, No. 4, 1968, pp. 605-623.

55. Perrin, Marcel, Compt. Rend., Vol. 254, 1962, pp. 269-271.

56. Perry, John H., Chemical Engineering Handbook. New York: McGraw-Hill Book Company, 1963.

57. Peterson, E.E., Chemical Reaction Analysis. Englewood Cliff, New Jersey: Prentice-Hall, Inc., 1965

58. Porter, R.S., Journal of Applied Polymer Science, Vol. 11, No. 3, 1967, pp. 335-340

59. Prakash, S., and Pandey, J.D., University of Allahabad Studies, 1965, pp. 23-45.

60. Prakash, Satya, Prasad, B., and Prakash, S., Vijnana Parishad Anusandhan Patrika, Vol. 9, No. 2, 1966, pp. 109-115.

61. Prakash, Sheo and Jain, S.K., Chim. Anal., Vol.50, No. 6, 1968, pp. 321-324.

62. Prakash, Sheo, Pandey, J.D. and Prakash, O.M., Indian Journal of Chemistry, Vol. 6, No. 3, 1968, pp. 143-144.

63. Prater, C.D. and Lago, R.M., Advances in Catalysis, Vol. 8, 1956, pp. 293-339.

64. Rase, H.F. and Kirk, R.S., Chemical Engineering Progress, Vol. 50, 1954, pp. 35-44.

65. Rayleigh, Lord, Phil. Magazine, Vol. 34, No. 94, 1917.

66. Rice, F.A.H. and Veguilla-Berdecia, L.A., Journal of Physical Chemistry, Vol. 71, No. 12, 1967, pp. 3774-3779.

67. Rossini, F.D., Selected Values of Properties of Hydrocarbons, National Bureau of Standards, C461, Washington, D.C., 1947.

68. Saracco, G. and Arzano, F., Chim. Ind., Vol. 50, No. 3, 1968, pp. 314-318.

69. Satterfield, Charles N., Mass Transfer in Heterogeneous Catalysis. Cambridge, Massachusetts: M.I.T. Press, 1970.

70. Satterfield, Charles N., The Role of Diffusion in Catalysis. Massachusetts: Addison-Wesley Publishing Co., Inc., 1963, pp. 31-36.

71. Sears, Francis W., Principals of Physics I. Cambridge 42, Massachusetts: Addison-Wesley Publishing Co., Inc., 1947, pp. 471-527.

72. Sergeeva, K. Ya., Akust. Zh., Vol. 13, No. 1, 1967.

73. Shaw, M.T. and Rodriguez, F., Journal of Applied Polymer Science, Vol. 11, 1967, pp. 991-999.

74. Slaczka, Andrzej, Rocz. Chem., Vol. 42, No. 6, 1968, pp. 1073-1081.

75. Slaczka, Andrzej, International Chemical Engineering, Vol. 9, No. 1, 1969, pp. 63-68.

76. Spozhakina, A.A., Moskovskaya, I.F. and Topchieva, K.V., Kinet. Katal., Vol. 8, No. 3, 1967, pp. 614-619.

77. Stolyarov, E.A., Zh. Prikl. Khim., Vol. 41, No. 10, 1968, pp. 2302-2303.

78. Suess, W., Pharm. Zentraln. Deut., Vol. 106, No. 2, 1967, pp. 96-90.

79. Tabuchi, Daisaku, Mem. Inst. Sci. Ind. Res., Osaka University No. 24, 1967, pp. 21-24.

80. Tabuchi, Daisaku, Mem. Inst. Sci. Ind. Res., Osaka University No. 25, 1968, pp. 29-34.

81. Topchieva, K.V. and Panchenkov, G.M., Doklady Akad. Nauk. U.S.S.R., Vol. 74, 1950, pp. 1109-1112.

82. Topchieva, K.V., Antipina, T.V. and He-Hsiian, L., Kinetika I Kataliz, Vol. 1, 1960, pp. 471-477.

83. Topchieva, K.V., Romanovskii, B.V. and Timoshenko, V.I., Kinetica I Kataliz, Vol. 6, No. 3, 1965, pp. 471-475.

84. Topil'skii, G.S., Egorov, P.A., and Korchagin, L.V., Ukr. Khim. Zh., Vol. 34, No. 8, 1968, pp. 853-856.

85. Tschernitz, J.L., Bornstein, S., Beckmann, R.B. and Hougan, O.A., Transactions of the American Institute of Chemical Engineers, Vol. 42, 1946, pp. 886-903.

86. Tuchel, N., Farmacia, Vol. 15, No. 6, 1967, pp. 341-346.

87. Tuszynski, T.M. and Graydon, W.F., Industrial Engineering Chemical Fundamentals, Vol. 7, No. 3, 1968, pp. 396-400.

88. Villaine, Philippe, Commission of Atomic Energy (France), 1968.

89. Vladar, J., Vladar, L., Sarkany, I. and Tivadar, P., British Patent No. 1,074,099, June 28, 1967, 5 pp.

90. Wagner, Carl, Science Colloq., Vol. 3, 1968, pp. 17-30.

91. Weissler, A., Cooper, H.W. and Snyder, S., Journal of the American Chemical Society, Vol. 72, 1950, p. 1769.

92. Wood, R.W. and Loomis, A.L., London, Edinburgh and Dublin Philosophical Magazine and Journal of Science, Vol. 4, No. 22, 1927, pp. 417-436.

93. Yang, K.H. and Hougan, O.A., Chemical Engineering Progress, No. 46, 1950, pp. 146-157.

94. Zelikman, Y.L., Telezhkin, B.V., and Sadykova, S.K., Sb. Dokl. Nauch.-Tekh. Konf., Sib. Proek. Nauch.-Isled. Inst. Tsvet. Met., No. 1, 1966, pp. 209-216.

95. Zhorov, Yu. M. and Panchenkov, G.M., Tr. Mosk. Inst. Neftekhim I Gas. Prom., No. 37, 1962, pp. 19-23.

96. Zhorov, Yu. M. and Panchenkov, G.M., Tr. Mosk. Inst. Neftekhim I Gas. Prom., No. 37, 1962, pp. 12-18.

97. Zhorov, Yu. M., Poluyanchenko, E.K. and Panchenkov, G.M., Tr. Mosk. Inst. Neftekhim I Gas. Prom., No. 69, 1967, pp. 169-171.

98. Zil'berg, G.A. and Zodboev, D.D., Tr. Vost.-Sib. Tekhnol. Inst., No. 2, Part 1, 1966, pp. 273-283.

99. Burford, Roger L. Statistics: A Computer Approach. Columbus, Ohio: Charles E. Merrill Publishing Company, 1968, pp. 326-327.

100. Von Mises, Richard, Mathematical Theory of Probability and Statistics. New York, New York: Academic Press, 1964, p. 680.

101. Eberly, Paul E. Jr., Kimberlin, Charles, N. Jr., Industrial Engineering Chemistry Product Research Development, 1970, 9(3), pp. 335-40.

102. Romanovski, B.V., Hud Chi Thauh, K., Topchieva, K.V., Piguzova, L.I., Kinet. Katal., Volume 7, No. 5, 1966, pp. 841-9.

VITA

William Lintner, Jr. was born in

in . He received his B.S.Ch.E. from the Massachusetts Institute of Technology in 1953 and his M.S.Ch.E. from Newark College of Engineering in 1965.

The research for his doctoral dissertation was accomplished in the Chemical Engineering Laboratories of the Newark College of Engineering during the period between September, 1969 and November, 1972. Financial assistance for the research was provided by Newark College of Engineering and the du Pont Fellowship which was awarded during 1972.

Mr. Lintner is a member of the American Institute of Plant Engineers and is a licensed Professional Engineer. He is married and has two children.

He is presently a partner in Chemical Systems, Inc., a chemical engineering design and construction firm.